THE BIOMECHANICS OF COMPETITIVE GAIT: SPRINTING, HURDLING, DISTANCE RUNNING AND RACE WALKING

EDITED BY: Brian Hanley, Johnny Padulo and Jean Slawinski
PUBLISHED IN: Frontiers in Sports and Active Living

frontiers Research Topics

frontiers

ISSN 1664-8714
ISBN 978-2-88971-980-8
DOI 10.3389/978-2-88971-980-8

About Frontiers

Frontiers is more than just an open-access publisher of scholarly articles: it is a pioneering approach to the world of academia, radically improving the way scholarly research is managed. The grand vision of Frontiers is a world where all people have an equal opportunity to seek, share and generate knowledge. Frontiers provides immediate and permanent online open access to all its publications, but this alone is not enough to realize our grand goals.

Frontiers Journal Series

The Frontiers Journal Series is a multi-tier and interdisciplinary set of open-access, online journals, promising a paradigm shift from the current review, selection and dissemination processes in academic publishing. All Frontiers journals are driven by researchers for researchers; therefore, they constitute a service to the scholarly community. At the same time, the Frontiers Journal Series operates on a revolutionary invention, the tiered publishing system, initially addressing specific communities of scholars, and gradually climbing up to broader public understanding, thus serving the interests of the lay society, too.

Dedication to Quality

Each Frontiers article is a landmark of the highest quality, thanks to genuinely collaborative interactions between authors and review editors, who include some of the world's best academicians. Research must be certified by peers before entering a stream of knowledge that may eventually reach the public - and shape society; therefore, Frontiers only applies the most rigorous and unbiased reviews.
Frontiers revolutionizes research publishing by freely delivering the most outstanding research, evaluated with no bias from both the academic and social point of view. By applying the most advanced information technologies, Frontiers is catapulting scholarly publishing into a new generation.

What are Frontiers Research Topics?

Frontiers Research Topics are very popular trademarks of the Frontiers Journals Series: they are collections of at least ten articles, all centered on a particular subject. With their unique mix of varied contributions from Original Research to Review Articles, Frontiers Research Topics unify the most influential researchers, the latest key findings and historical advances in a hot research area! Find out more on how to host your own Frontiers Research Topic or contribute to one as an author by contacting the Frontiers Editorial Office: frontiersin.org/about/contact

THE BIOMECHANICS OF COMPETITIVE GAIT: SPRINTING, HURDLING, DISTANCE RUNNING AND RACE WALKING

Topic Editors:
Brian Hanley, Leeds Beckett University, United Kingdom
Johnny Padulo, University of Milan, Italy
Jean Slawinski, Institut national du sport, de l'expertise et de la performance (INSEP), France

Citation: Hanley, B., Padulo, J., Slawinski, J., eds. (2021). The Biomechanics of Competitive Gait: Sprinting, Hurdling, Distance Running and Race Walking. Lausanne: Frontiers Media SA. doi: 10.3389/978-2-88971-980-8

Table of Contents

frontiers in Sports and Active Living

EDITORIAL
published: 11 November 2021
doi: 10.3389/fspor.2021.790934

Editorial: The Biomechanics of Competitive Gait: Sprinting, Hurdling, Distance Running and Race Walking

Brian Hanley[1]*, *Johnny Padulo*[2] *and Jean Slawinski*[3]

[1] *Carnegie School of Sport, Leeds Beckett University, Leeds, United Kingdom,* [2] *Department of Biomedical Sciences for Health, Faculty of Medicine and Surgery, University of Milan, Milan, Italy,* [3] *Institut National du Sport, de l'Expertise et de la Performance (INSEP), Paris, France*

Keywords: track athletics, endurance exercise, sport performance, sport technology, sprint speed

Editorial on the Research Topic

The Biomechanics of Competitive Gait: Sprinting, Hurdling, Distance Running and Race Walking

This Research Topic features each aspect of competitive gait, comprising sprinting, hurdling, distance running, and race walking. Each of these forms of gait has its own biomechanical signature, and the research published was carried out by 31 authors across 11 countries to provide modern, relevant and robust practical applications to athletes, coaches, scientists, and others who are involved in competitive gait at all standards.

One of the best known running events held across the globe is the marathon, with many athletes of all abilities taking part and millions more watching live broadcasts. Performances in the marathon have improved in recent years, with Bermon et al. examining the role of advanced shoe technology on elite athletes' finishing times over the 42.2 km distance, as well as in other distance races. They found a large improvement in running times over the past few years and attributed much of this to the contribution of new shoe design. Another study on the marathon analyzed the differences in performance between athletes who land with a rearfoot strike, and those who land on the midfoot or forefoot (Hanley, Bissas et al.). They found that although there were differences between the biomechanics of athletes with each footstrike pattern, these were quite small and didn't seem to affect overall performance. Hanley, Bissas et al. also examined the effects of fatigue on marathon gait and differences between men and women for the most in-depth study of elite marathon kinematics ever conducted.

Changes in gait with fatigue, this time within a group of middle-distance runners, was also the focus of the study by Möhler et al.. These authors showed that these runners changed their stance time, rather than step frequency or step length, to maintain a constant running speed during treadmill testing. The study went further than previous research by using the analysis of both discrete parameters and time series analysis in 3D, and provided valuable practical applications for coaches. In another treadmill study using 3D data collection methods, Sundström et al. examined how runners adapt their lower-limb movement patterns on downhill slopes. The authors found that runners changed their hip movement as speed increased, but made modifications to knee kinematics when responding to changes in slope. It was observed that running economy was better at moderate speeds than near-race speed on steep downhill slopes ($-10°$), whereas the reverse was true on less-steep declines ($-5°$), and so running downhill in races should be completed at a slower pace to retain metabolic energy. Of course, biomechanists who work in competitive gait are not just concerned with improving performance, but also with reducing the risk of injury. In their study on mild leg length discrepancy, Menez et al. found that orthotic insoles can improve gait symmetry,

Edited and reviewed by:
Jaap Van Dieen,
Vrije Universiteit Amsterdam, Netherlands

***Correspondence:**
Brian Hanley
b.hanley@leedsbeckett.ac.uk

Specialty section:
This article was submitted to Biomechanics and Control of Human Movement, a section of the journal Frontiers in Sports and Active Living

Received: *07 October 2021*
Accepted: *21 October 2021*
Published: *11 November 2021*

Citation:
Hanley B, Padulo J and Slawinski J (2021) Editorial: The Biomechanics of Competitive Gait: Sprinting, Hurdling, Distance Running and Race Walking. Front. Sports Act. Living 3:790934. doi: 10.3389/fspor.2021.790934

particularly in the pelvis and ankle, and reduce immediate pain, which is an important finding for those who could benefit from a relatively straightforward intervention.

Analyzing performance in competition, when athletes are in their most natural setting, is rarely conducted because of the difficulty of obtaining *in-vivo* measurements. For this reason, several methods for calculating or estimating important variables have been developed. For analyzing the 100 m sprint, Seidl et al. reported on a pilot study conducted under field conditions, finding that a method using radio-based position detection obtained valid results for spatiotemporal variables such as step length and step time, and suggested that the development of this approach could allow for valuable measurements in competition. In their study using shoe-worn inertial sensors, Falbriard et al. estimated overground running speed and compared these sensors with Global Navigation Satellite System (GNSS) technology. They took three approaches to extracting the data and found that the limitations of direct estimation of foot velocity and a general linear model could be overcome with a personalized online model. Mercier et al. took a modeling approach to analyzing strategy and optimization of performance in the 10,000 m event by applying a simulation to real athletes' time split data collected at the 2017 IAAF World Championships. By doing so, they were able to show the negative effect of the bends on speed maintenance and how a conservation of anaerobic energy in the middle of the race allows for a faster last lap.

Two of the most technical events in competitive gait are hurdling and race walking. These forms of gait are restricted, in hurdling by the position and height of the 10 barriers, and in race walking by the need to straighten the knee and avoid visible loss of ground contact. This makes the analysis of technique using biomechanical methods highly relevant for understanding how improvements in performance can be achieved. In their study of the world's best hurdlers competing in the 2017 IAAF World Championship finals, Hanley, Walker et al. used high-speed cameras to compare men's and women's techniques. They found that the lower relative hurdle heights in the women's event result in a less demanding task, and mean that the techniques adopted by men and women are not the same. The men's hurdle is so much higher for them relative to their height that it affects their vertical movement to a greater extent and is more disruptive of forward momentum. Gravestock et al. also analyzed men and women in their study of the role of upper body biomechanics in elite race walkers, but they found little difference in how men and women achieve their gait mechanics. Within the group, pelvic girdle movements were very important in optimizing spatiotemporal variables, and other torso movements were made in reaction to the absence of knee flexion during midstance. Gravestock et al. found through their use of electromyography that there was no evidence that muscle strength was important for better race walking, and so they instead recommended the development of resistance to fatigue in this endurance event.

In conclusion, the articles that have contributed to this Research Topic have covered the main areas in competitive gait. We hope that these novel studies will aid those working in this area in developing performance across a range of athletic abilities. These studies will form a basis for future research that should continue to develop our scientific knowledge in this most popular sport.

AUTHOR CONTRIBUTIONS

All authors listed have made a substantial, direct and intellectual contribution to the work, and approved it for publication.

Conflict of Interest: The authors declare that the research was conducted in the absence of any commercial or financial relationships that could be construed as a potential conflict of interest.

Publisher's Note: All claims expressed in this article are solely those of the authors and do not necessarily represent those of their affiliated organizations, or those of the publisher, the editors and the reviewers. Any product that may be evaluated in this article, or claim that may be made by its manufacturer, is not guaranteed or endorsed by the publisher.

frontiers in Sports and Active Living

ORIGINAL RESEARCH
published: 06 August 2020
doi: 10.3389/fspor.2020.00102

Men's and Women's World Championship Marathon Performances and Changes With Fatigue Are Not Explained by Kinematic Differences Between Footstrike Patterns

Brian Hanley[1]*, *Athanassios Bissas*[1,2] *and Stéphane Merlino*[3]

[1] Carnegie School of Sport, Leeds Beckett University, Leeds, United Kingdom, [2] School of Sport and Exercise, University of Gloucestershire, Gloucester, United Kingdom, [3] Development Department, World Athletics, Monte Carlo, Monaco

World-class marathon runners make initial contact with the rearfoot, midfoot or forefoot. This novel study analyzed kinematic similarities and differences between rearfoot and non-rearfoot strikers within the men's and women's 2017 IAAF World Championship marathons across the last two laps. Twenty-eight men and 28 women, equally divided by footstrike pattern, were recorded at 29.5 and 40 km (laps 3 and 4, respectively) using two high-definition cameras (50 Hz). The videos were digitized to derive spatiotemporal and joint kinematic data, with additional footage (120 Hz) used to identify footstrike patterns. There was no difference in running speed, step length or cadence between rearfoot and non-rearfoot strikers during either lap in both races, and these three key variables decreased in athletes of either footstrike pattern to a similar extent between laps. Men slowed more than women between laps, and overall had greater reductions in step length and cadence. Rearfoot strikers landed with their foot farther in front of the center of mass (by 0.02–0.04 m), with non-rearfoot strikers relying more on flight distance for overall step length. Male rearfoot strikers had more extended knees, dorsiflexed ankles and hyperextended shoulders at initial contact than non-rearfoot strikers, whereas female rearfoot strikers had more flexed hips and extended knees at initial contact. Very few differences were found at midstance and toe-off. Rearfoot and non-rearfoot striking techniques were therefore mostly indistinguishable except at initial contact, and any differences that did occur were very small. The spatiotemporal variables that differed between footstrike patterns were not associated with faster running speeds and, ultimately, neither footstrike pattern prevented reductions in running speeds. The only joint angle measured at a specific gait event to change with fatigue was midswing knee flexion angle in men. Coaches should thus note that encouraging marathon runners to convert from rearfoot to non-rearfoot striking is unlikely to provide any performance benefits, and that training the fatigue resistance of key lower limb muscle-tendon units to avoid decreases in step length and cadence are more useful in preventing reductions in speed during the later stages of the race.

Keywords: athletics, endurance, performance, running, videography

OPEN ACCESS

Edited by:
Ryu Nagahara,
National Institute of Fitness and Sports in Kanoya, Japan

Reviewed by:
Steph Forrester,
Loughborough University, United Kingdom
Daniel Castillo,
Universidad Isabel I de Castilla, Spain

***Correspondence:**
Brian Hanley
b.hanley@leedsbeckett.ac.uk

Specialty section:
This article was submitted to Elite Sports and Performance Enhancement, a section of the journal Frontiers in Sports and Active Living

Received: *09 June 2020*
Accepted: *06 July 2020*
Published: *06 August 2020*

Citation:
Hanley B, Bissas A and Merlino S (2020) Men's and Women's World Championship Marathon Performances and Changes With Fatigue Are Not Explained by Kinematic Differences Between Footstrike Patterns. Front. Sports Act. Living 2:102. doi: 10.3389/fspor.2020.00102

INTRODUCTION

The marathon (42.195 km) is the longest running race at major events such as the Olympic Games and World Athletics Championships. The marathon is a particularly difficult event to succeed in because glycogen depletion normally occurs after approximately 30 km (Jeukendrup, 2011) with a consequent increase in energy dependence on lipids (O'Brien et al., 1993). This reliance on a slower source of energy during the late stages of the marathon usually results in considerable deceleration over the last 10–15 km that affects even world-class runners (Hettinga et al., 2019), and is known colloquially as "hitting the wall" (Buman et al., 2009). Previous studies on the effects of fatigue on predominantly non-elite marathon runners showed that decreases in step length, rather than cadence, were responsible for this decrease in speed (Buckalew et al., 1985; Chan-Roper et al., 2012). It is possible that world-class marathon runners have, by contrast, developed strategies in training to cope with or prevent the onset of fatigue. Alongside physiological (Stellingwerff, 2012) and pacing strategies (Deaner et al., 2019), athletes could potentially improve marathon performances by incorporating particular biomechanical principles with regard to running form and technique (Pizzuto et al., 2019), and therefore try to prevent such dramatic changes in speed during competition.

Adopting a particular footstrike pattern is one aspect of technique that could possibly lead to better long-distance running performances. Marathon runners are predominantly rearfoot strikers (RFS) at both world-class (Hanley et al., 2019) and recreational standards (Larson et al., 2011), although the proportion of midfoot strikers and forefoot strikers in a world-class sample was higher than amongst recreational runners (Hanley et al., 2019). Non-rearfoot striking (NRFS), which encompasses both midfoot and forefoot striking, arises from an anterior footstrike position that theoretically stores and releases greater elastic energy in the Achilles tendon and foot arches than RFS (Perl et al., 2012), and is practiced by most athletes competing in the shorter middle-distance events over 800 and 1500 m (Hayes and Caplan, 2012). Contact times were shorter in the faster NRFS athletes (Hayes and Caplan, 2012), and this might be related to how less time spent in contact was similarly associated with faster half-marathon running (Gómez-Molina et al., 2017; Ogueta-Alday et al., 2017). However, its lower incidence amongst elite-standard marathon runners might occur because running economy during RFS is similar to NRFS (Ardigò et al., 1995; Gruber et al., 2013), and because carbohydrate oxidation rates were indeed found to be higher during forefoot striking than RFS (Gruber et al., 2013). Additionally, many marathon runners who are NRFS during the first half of the race change to RFS in the second half (Larson et al., 2011; Hanley et al., 2019), possibly because continuous NRFS requires increased ankle plantarflexor work and can lead to considerable fatigue in the contractile properties of those key leg muscles (Peltonen et al., 2012; Baggaley et al., 2017).

One potential biomechanical advantage of landing with an NRFS pattern is that the foot lands closer to the whole body center of mass (CM), with a theoretical reduction in braking forces during early stance (Lieberman et al., 2015; Moore, 2016). At an equal running speed, this shorter distance from landing foot to CM should result in reduced step lengths and higher cadences in NRFS (Goss and Gross, 2013), and is achieved through greater knee flexion and ankle plantarflexion at initial contact (Almeida et al., 2015). These greater lower limb angles in turn lead to less overstriding in NRFS (i.e., the ankle lands more directly under the knee), with potential benefits including more limb compliance at the ankle and knee (Lieberman, 2014). Such differences in technique have been inferred by coaches to mean that NRFS could provide benefits such as improved performance and reduced injury risk (Abshire and Metzler, 2010; Anderson, 2018), but Williams (2007) reported that a female marathon runner with a forefoot strike experienced injury because the increased knee flexion that compensated for subtalar pronation during stance increased the stress on the Achilles tendon and foot arches. Notably, many previous experimental studies on kinematic differences between RFS and NRFS were conducted for short durations only using treadmills (Goss and Gross, 2013), analyzed men only (Shih et al., 2013), included a barefoot condition that is not normal in competition (Perl et al., 2012) or instructed habitual RFS runners to adopt a non-habitual NRFS pattern (Ardigò et al., 1995). Furthermore, no studies have compared men and women, or athletes of different footstrike patterns, with regard to how their gait kinematics change during the final stages of a world-class marathon, when the race outcome is often decided. Therefore, a novel study that analyzes well-trained men and women running in a fatiguing competition with their natural footstrike patterns and own footwear will provide athletes and coaches with robust evidence of similarities and differences between RFS and NRFS that could inform training practices, such as running drills. Such information could also be used by coaches to decide whether to encourage their athletes to change footstrike pattern, especially with regard to the effects of fatigue during the latter stages of the marathon.

No previous research has examined the spatiotemporal or joint kinematic differences between RFS and NRFS in world-class athletes and, furthermore, neither sex-based differences nor the potential effects of fatigue have been analyzed in competition. The aim of this novel study was to analyze spatiotemporal and joint kinematic variables in male and female marathon RFS and NRFS runners across the last two 10.5-km laps at the 2017 IAAF World Championships. Based on previous research, it was hypothesized that RFS would have longer steps and lower cadences than NRFS, resulting from differences in knee and ankle angles at initial contact. It was also hypothesized that those differences found between RFS and NRFS would be similar for men and women, but that men would have greater absolute magnitudes for spatial values (e.g., flight distance), although not when normalized as a proportion of step length. It was further hypothesized that running speed and associated spatiotemporal variables would decrease between the second-last and last laps because of fatigue, but that any differences between RFS and NRFS would be consistent across the last two laps.

MATERIALS AND METHODS

Research Approval

Data were collected as part of the London 2017 World Championships Biomechanics Research Project. The use of those data for this study was approved by the IAAF (since renamed World Athletics), who own and control the data, and locally through the Leeds Beckett University research ethics procedures.

Participants

Twenty-eight men (39% of the 71 finishers) and 28 women (36% of 78 finishers) were analyzed in their respective races, held on the same day and on the same course. Personal record (PR) and finishing times were obtained from the open-access World Athletics website (World Athletics, 2019, 2020) for competitors in both races. Fifty percent of the 28 athletes analyzed in each race were RFS and 50% were NRFS.

Data Collection

The men's and women's marathon races were held on a course that consisted of four approximately 10.5 km loops, with the remaining distance comprising a section that led from the start/finish line to the beginning of the loop. A section of straight, wide road near the end of the loop was chosen for video capture so that data collection occurred at approximately 29.5 and 40 km. Two stationary Sony NXCAM HXR-NX3 full high-definition digital cameras (Sony, Tokyo, Japan) were placed on one side of the course, approximately 45° and 135° to the plane of motion, respectively. Each camera was approximately 8 m from the path of the runners. The sampling rate for each camera was 50 Hz, the shutter speed was 1/1250 s, and the resolution was 1920 × 1080 px. The reference volume was 7.50 m long, 3.08 m wide and 1.99 m high. The reference poles were placed so that the 3.08 m width coincided with the path taken by all analyzed runners (marked as the shortest possible route with blue paint by the event organizers). The poles were aligned vertically with the use of a spirit level and plumb line with calibration procedures conducted before and after competition. This approach produced a number of non-coplanar control points and facilitated the construction of specific global coordinate systems.

The procedures used to collect data for the analysis of footstrike patterns have been described previously (Hanley et al., 2019). In brief, two Casio Exilim high-speed cameras (Casio, Tokyo, Japan) were positioned approximately 0.30 m above the running surface on tripods with their optical axes perpendicular to the running direction. The sampling rate for each camera was 120 Hz, the shutter speed was 1/1000 s, and the resolution was 640 × 480 px.

Data Analysis

The video files were imported into SIMI Motion (SIMI Motion version 9.2.2, Simi Reality Motion Systems GmbH, Germany) and manually digitized by a single experienced operator to obtain spatiotemporal and kinematic data. An event synchronization technique (synchronization of four critical instants: right initial contact, right toe-off, left initial contact and left toe-off) was applied to synchronize the two-dimensional coordinates from each camera. Digitizing started 10 frames before the beginning of the first identified gait event (i.e., initial contact or toe-off) and completed 10 frames after the same event during the next gait cycle to provide padding during filtering (Smith, 1989); the start of the next gait cycle was digitized to identify the succeeding step and to provide padding. Therefore, for each athlete, one gait cycle was digitized for each of the last two laps. Each file was first digitized frame-by-frame and, upon completion, adjustments were made as necessary using the points-over-frame method (Bahamonde and Stevens, 2006), where each point was tracked through the entire sequence. The magnification tool in SIMI Motion was set at 400% to aid identification of body landmarks. The 3D Direct Linear Transformation algorithm (Abdel-Aziz et al., 2015) was used to reconstruct the three-dimensional coordinates from each camera's x- and y-image coordinates. De Leva's 14-segment body segment parameter model (de Leva, 1996) was used to obtain data for the CM and for several body segments of interest. Occasionally, dropout occurred where joint positions were not visible, and estimations were made by the operator. Two separate approaches were taken for removing noise (Giakas and Baltzopoulos, 1997): a cross-validated quintic spline smoothed the raw data before coordinate calculations, whereas a recursive second-order, low-pass Butterworth digital filter (zero phase-lag) filtered the same raw data and first derivatives were subsequently obtained. The cut-off frequencies were calculated using residual analysis (Winter, 2005) and ranged between 4.0 and 7.5 Hz.

To ensure reliability of the digitizing process on the speed and spatiotemporal data, repeated digitizing (two trials) of one running sequence (a single digitized gait cycle from one lap of one runner) was performed with an intervening period of 48 h. Three statistical methods for assessing reliability were used: 95% limits of agreement (LOA), coefficient of variation (CV) and intraclass correlation coefficient (ICC) (Atkinson and Nevill, 1998). The data for each tested variable were assessed for heteroscedasticity by plotting the standard deviations (SD) against the individual means of the two trials (Atkinson and Nevill, 1998). If the data exhibited heteroscedasticity, a logarithmic transformation of the data ($\log_e$) was performed before the calculation of absolute reliability measures (Bland and Altman, 1986). The LOA (bias ± random error), CV and ICC (3,1) values for CM horizontal speed were 0.000 ± 0.015 m/s, ± 0.13%, and 1.00, respectively; for the right foot horizontal coordinates 0.001 ± 0.003 m, ± 0.04%, and 1.00, respectively; and for the left foot horizontal coordinates 0.001 ± 0.006 m, ± 0.08%, and 1.00, respectively. The results that relate to the most important spatiotemporal variables therefore showed minimal systematic and random errors, and confirmed the high reliability of the digitizing process with regard to the overall group of athletes. In addition, because the hip joint center markers were used to calculate seven angles between them, the effect of misplacing body landmarks was measured by altering both hip joint center markers laterally by one pixel for one man and one woman. The difference in angle magnitudes between the original and altered files was measured and the root mean square difference (RMSD) calculated for one complete gait cycle; the mean RMSD was 0.2° (± 0.1) for both participants.

Footstrike patterns were defined using the foot position at initial contact with the ground using the methods of Hasegawa

et al. (2007) as either: RFS (the heel contacted the ground first without simultaneous contact by the midfoot or forefoot), midfoot striking (the heel and midfoot, or occasionally the entire sole, contacted the ground together) or forefoot striking (the forefoot/front half of the sole contacted the ground first with a clear absence of heel contact). As there were very few forefoot strikers in either race (Hanley et al., 2019), midfoot and forefoot strikers have been combined as NRFS. Half of the athletes analyzed on lap 3 in each race were RFS, and the other half were NRFS (i.e., $N = 14$ of each footstrike pattern). All men analyzed were consistently either RFS or NRFS on both laps, with one of the NRFS men adopting forefoot striking on lap 3 and midfoot striking on lap 4; however, two women switched from NRFS on lap 3 to RFS on lap 4. Of the other women, one of the NRFS was a forefoot striker on both laps.

Descriptions of the variables analyzed in this study are presented in **Table 1**. All these variables were obtained using the 50 Hz cameras and used directly to calculate the values reported. When summed, the foot ahead, foot behind, flight distance and foot movement distances add up to step length; because it was not possible to measure participants' statures, which might have had an effect on spatial values, each of the four distances was also normalized as a proportion (%) of total step length for comparison purposes. Each athlete's knee angular data were interpolated to 101 points using a cubic spline to equalize the length of the gait cycle for presentation in **Figure 1** (these interpolated data were not used to calculate the knee angle results reported). Joint angular data were averaged between left and right sides, rounded to the nearest integer, and have been presented in this study at specific events of the gait cycle, as defined below:

- Initial contact – the first visible instant during stance where the athlete's foot clearly contacted the ground.
- Midstance – the instant during stance where the athlete's foot center of mass was directly below the CM (i.e., in the horizontal anteroposterior direction).
- Midswing (knee angle only): the instant during swing where the athlete's knee was at its most flexed position (i.e., the minimum knee angle).
- Toe-off: the last visible instant during stance before the foot left the ground.

Statistics

Statistical analyses were conducted using SPSS Statistics 26 (IBM SPSS, Inc., Chicago, IL). Normality of data was tested using the Shapiro-Wilk's test. Overall interactions between footstrike patterns, sex and lap were measured using a three-way mixed analysis of variance (ANOVA), with two-way analyses also found. Because each condition consisted of two groups, spatiotemporal, kinematic and performance variables were compared between men and women, and between RFS and NRFS using independent *t*-tests with adjustments made if Levene's test for equality of variances was less than 0.05, whereas within-athlete comparisons between laps were conducted using dependent *t*-tests (Field, 2009). An alpha level of 5% was set for all tests. To control for the number of statistical tests conducted, effect sizes were calculated using Cohen's *d* where differences were found within comparisons (Cohen, 1988) and considered to be either trivial ($d \leq 0.20$), small (0.21 – 0.60), moderate (0.61–1.20), large (1.21–2.00), or very large (2.01–4.00) (Hopkins et al., 2009). Pearson's product moment correlation coefficient (r) was used to find associations separately within each sample of 28 men

TABLE 1 | Variables analyzed in the study and their description.

Variable name	Description
Running speed (km/h)	The mean horizontal speed during a complete gait cycle
Step length (m)	The distance between successive foot contacts from a specific event on the gait cycle on a particular foot (e.g., toe-off) to the equivalent event on the other foot
Cadence (Hz)	Calculated by dividing horizontal speed by step length (Mero and Komi, 1994)
Contact time (s)	The time duration from initial contact to toe-off
Flight time (s)	The time duration from toe-off of one foot to the initial contact of the opposite foot (Padulo et al., 2014)
Flight distance (m)	The distance the CM traveled during flight (from the instant of toe-off on a particular foot to the instant of initial contact on the other foot) (Hunter et al., 2004)
Foot ahead distance (m)	The distance from the center of mass of the landing foot to the CM
Foot behind distance (m)	The distance from the center of mass of the toe-off foot to the CM
Foot movement distance (m)	The distance the foot center of mass moved from its horizontal position at initial contact to toe-off
Overstriding distance (m)	The distance between the horizontal coordinate of the contact leg knee and the ipsilateral ankle, where larger distances indicated that the ankle landed farther in front of the knee
Hip angle (°)	The sagittal plane angle between the trunk and thigh segments (180° in the anatomical standing position)
Knee angle (°)	The sagittal plane angle between the thigh and lower leg segments (180° in the anatomical standing position)
Ankle angle (°)	The sagittal plane angle between the lower leg and foot segments, calculated in a clockwise direction (110° in the anatomical standing position) (Cairns et al., 1986)
Shoulder angle (°)	The sagittal plane angle between the trunk and upper arm (0° in the anatomical standing position; negative values for the shoulder therefore indicated a hyperextended position)
Elbow angle (°)	The sagittal plane angle between the upper arm and forearm (180° in the anatomical standing position)
Pelvic rotation (°)	The transverse plane angle calculated using the left and right hip joint coordinates
Shoulder girdle rotation (°)	The transverse plane angle calculated using the left and right shoulder joint coordinates

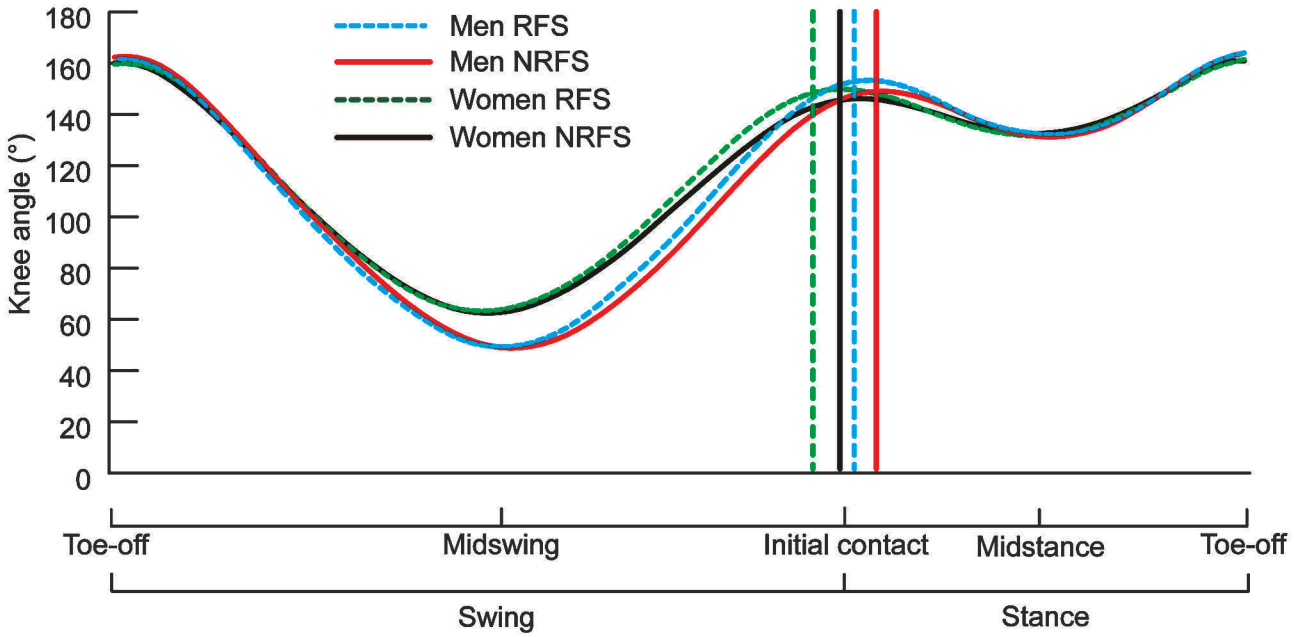

FIGURE 1 | Knee angle during one complete gait cycle for RFS and NRFS in both men's and women's races during lap 3. Results are shown as means, with SD not indicated for any group for clarity (means and SDs are shown in **Tables 4**–**7** for knee angles at initial contact, midstance, toe-off and midswing, respectively). The vertical lines represent the mean initial contact times (as a percentage of the gait cycle) for each group indicated.

and 28 women, and considered to be small (r = 0.10–0.29), moderate (0.30–0.49), large (0.50–0.69) or very large (≥0.70) (Hopkins et al., 2009). Only those correlations that were large or very large were considered significant (in addition to an alpha value < 0.05).

RESULTS

The mean PR times (h:min:s) before competition for the 28 men and 28 women analyzed were 2:11:58 (± 4:42) and 2:31:44 (± 6:24), respectively. The mean finishing time for the men was 2:17:21 (± 5:09), whereas for the women, it was 2:37:29 (± 5:59); two men and three women ran PRs in this particular event. The men had faster PR and finishing times ($p < 0.001$, $d \geq 3.52$). Both men and women had normally distributed finishing times. There was no difference in PR or finishing times between RFS and NRFS in either race, and there was no difference in running speed for the analyzed section between RFS and NRFS during either lap 3 or lap 4 in either race (**Table 2**). There were also no differences for step length or cadence between RFS and NRFS (**Table 2**), although large differences were found for overstriding distance on both laps, as well as differences for foot ahead distance on both laps and foot behind distance for women on lap 4 only (**Table 3**). Given that men are generally taller than women, it was not surprising that absolute distances were greater (**Table 3**), but in proportional terms men relied more on flight distance than women for overall step length (**Table 4**). Between laps 3 and 4, RFS and NRFS men experienced decreases in speed and step length that were large or moderate, whereas the decreases in these variables for women were smaller in general (**Table 2**); there was an interaction found between sex and lap for running speed (p = 0.035), in that men slowed more than women. Similarly, both RFS and NRFS men experienced large increases in contact time between laps, whereas only the NRFS women experienced a small increase (**Table 2**). In terms of components of step length, flight distances decreased between laps 3 and 4 for RFS and NRFS men (moderate effect size) and for NRFS women (small effect size); changes in foot ahead distance were found in RFS men only, although moderate decreases in foot behind distance were found in RFS and NRFS men, with small changes in NRFS women (**Table 3**).

At initial contact, RFS had more extended knees, dorsiflexed ankles and hyperextended shoulders than NRFS in the men's race, whereas in the women's race, RFS had more flexed hips and extended knees than NRFS (**Table 5**); each group's mean knee angle throughout the gait cycle are shown in **Figure 1**. Fewer differences were found between RFS and NRFS in both sexes at midstance and toe-off (**Tables 6**, **7**, respectively), although RFS had more flexed shoulders at toe-off than NRFS in the women's race. There were interactions found between sex and footstrike pattern for hip angle at initial contact, and hip, ankle and shoulder angles at midstance ($p \leq 0.046$). Men had greater pelvic rotation than women, whereas women had greater shoulder girdle rotation (**Table 8**). During midswing, there were no differences in knee flexion angle between RFS and NRFS during either lap in men or women (**Table 8**), but men had lower knee angles during this phase. Indeed, knee flexion angle during

TABLE 2 | Mean ± SD values for key spatiotemporal variables.

	Men			Women		
	RFS	**NRFS**	**All**	**RFS**	**NRFS**	**All**
Speed (km/h)						
Lap 3	17.30 (± 1.32)	17.18 (± 0.87)	17.24 (± 1.10)	14.56 (± 1.03)	14.69 (± 0.95)	14.63** (± 0.98)
Lap 4	15.66[b] (± 1.54)	15.46[c] (± 1.24)	15.56[c] (± 1.38)	13.99[a] (± 1.01)	13.84[b] (± 1.48)	13.92**[b] (± 1.24)
Step length (m)						
Lap 3	1.56 (± 0.10)	1.55 (± 0.10)	1.56 (± 0.10)	1.29 (± 0.10)	1.28 (± 0.11)	1.28** (± 0.10)
Lap 4	1.45[b] (± 0.11)	1.43[b] (± 0.11)	1.44[b] (± 0.11)	1.25[a] (± 0.10)	1.22[a] (± 0.15)	1.24**[a] (± 0.13)
Cadence (Hz)						
Lap 3	3.07 (± 0.12)	3.08 (± 0.15)	3.07 (± 0.13)	3.15 (± 0.15)	3.19 (± 0.20)	3.17* (± 0.17)
Lap 4	3.00[a] (± 0.15)	3.00[a] (± 0.16)	3.00[a] (± 0.15)	3.10[a] (± 0.13)	3.17 (± 0.21)	3.14* (± 0.17)
Contact time (s)						
Lap 3	0.22 (± 0.01)	0.21[†] (± 0.01)	0.22 (± 0.01)	0.24 (± 0.02)	0.22[†] (± 0.01)	0.23* (± 0.02)
Lap 4	0.24[c] (± 0.02)	0.23[c] (± 0.02)	0.23[c] (± 0.02)	0.25 (± 0.02)	0.23[†a] (± 0.02)	0.24[a] (± 0.02)
Flight time (s)						
Lap 3	0.10 (± 0.01)	0.11[†] (± 0.01)	0.11 (± 0.01)	0.08 (± 0.02)	0.09 (± 0.02)	0.09** (± 0.02)
Lap 4	0.10 (± 0.02)	0.11 (± 0.02)	0.10 (± 0.02)	0.08 (± 0.02)	0.09 (± 0.02)	0.08* (± 0.02)

RFS, Rearfoot strikers; NRFS, Non-rearfoot strikers.

[†] *Differences between RFS and NRFS were moderate ($p < 0.05$, $d = 0.61–1.20$).*

* *Differences between men and women were moderate ($p < 0.05$, $d = 0.61–1.20$).*

** *Differences between men and women were large or very large ($p < 0.05$, $d > 1.21$).*

[a] *Differences between laps 3 and 4 were small ($p < 0.05$, $d = 0.21–0.60$).*

[b] *Differences between laps 3 and 4 were moderate ($p < 0.05$, $d = 0.61–1.20$).*

[c] *Differences between laps 3 and 4 were large or very large ($p < 0.05$, $d > 1.21$).*

midswing was the only joint angle to change between laps 3 and 4, increasing in both RFS and NRFS men (no change for women) (**Table 8**). The correlations between the most important spatiotemporal variables, as well as knee flexion because of its change in men from lap 3 to 4, were included in **Table 9**. Knee flexion was strongly correlated with step length and flight distance in both sexes (**Table 9**); no other joint angles consistently correlated with key spatiotemporal variables across laps or sexes, and none found were large. There were very large correlations between speed and step length, but not cadence. Similarly, flight distance was strongly correlated with speed and step length, but not with cadence (**Table 9**). Greater overstriding distances were associated with larger foot ahead distances in both men and women (**Table 9**), but not with speed, step length or cadence.

DISCUSSION

The aim of this study was to analyze spatiotemporal and joint kinematic variables in male and female marathon RFS and NRFS runners across the last two 10.5-km laps at the 2017 IAAF World Championships. The first hypothesis, that RFS would have longer steps and lower cadences than NRFS, was rejected as there were no differences in step length or cadence at the same running speed. Regarding the related hypothesized joint angular differences at initial contact, both NRFS men and women had less knee extension, but whereas the NRFS men had more plantarflexed ankles at initial contact, NRFS the women did not; however, the NRFS women did have less flexed hips. Although the effect of these joint angular differences did not manifest as differences in the two key spatiotemporal variables of step length and cadence, they did result in a greater foot ahead proportion for RFS men and women on both laps, and greater flight distance proportions for NRFS men and women on lap 3. Therefore, given that step length is the same, the main differences in running technique between RFS and NRFS world-class marathon runners are a greater reliance on foot ahead distance in RFS, achieved in both sexes with more extended knees, and that NRFS athletes rely more on flight distance. In theory, a greater foot ahead distance results in more braking forces (Moore, 2016), and although these

TABLE 3 | Mean ± SD values for step length component variables and overstriding distance.

	Men			Women		
	RFS	**NRFS**	**All**	**RFS**	**NRFS**	**All**
Flight distance (m)						
Lap 3	0.60 (± 0.08)	0.64 (± 0.07)	0.62 (± 0.08)	0.42 (± 0.10)	0.47 (± 0.10)	0.44** (± 0.10)
Lap 4	0.52[b] (± 0.10)	0.56[b] (± 0.10)	0.54[b] (± 0.10)	0.39 (± 0.10)	0.43[a] (± 0.11)	0.41**[a] (± 0.11)
Foot ahead (m)						
Lap 3	0.37 (± 0.03)	0.33‡ (± 0.04)	0.35 (± 0.04)	0.32 (± 0.02)	0.30‡ (± 0.03)	0.31** (± 0.03)
Lap 4	0.35[b] (± 0.02)	0.32‡ (± 0.02)	0.33[a] (± 0.03)	0.32 (± 0.03)	0.29† (± 0.03)	0.31* (± 0.03)
Foot behind (m)						
Lap 3	0.47 (± 0.03)	0.47 (± 0.04)	0.47 (± 0.04)	0.43 (± 0.04)	0.42 (± 0.03)	0.43** (± 0.03)
Lap 4	0.45[b] (± 0.03)	0.44[b] (± 0.02)	0.45[b] (± 0.02)	0.43 (± 0.03)	0.41†[a] (± 0.02)	0.42** (± 0.03)
Foot movement (m)						
Lap 3	0.11 (± 0.01)	0.11 (± 0.01)	0.11 (± 0.01)	0.12 (± 0.02)	0.10† (± 0.01)	0.11 (± 0.02)
Lap 4	0.12[b] (± 0.01)	0.11† (± 0.01)	0.12 (± 0.01)	0.11 (± 0.02)	0.10‡ (± 0.01)	0.10* (± 0.02)
Overstriding distance (m)						
Lap 3	0.05 (± 0.02)	0.02‡ (± 0.02)	0.03 (± 0.03)	0.04 (± 0.02)	0.00‡ (± 0.02)	0.02 (± 0.02)
Lap 4	0.04 (± 0.02)	0.01‡ (± 0.01)	0.03 (± 0.02)	0.03 (± 0.02)	0.00‡ (± 0.02)	0.02 (± 0.02)

RFS, Rearfoot strikers; NRFS, Non-rearfoot strikers.
†Differences between RFS and NRFS were moderate ($p < 0.05$, $d = 0.61–1.20$).
‡Differences between RFS and NRFS were large ($p < 0.05$, $d = 0.61–1.20$).
**Differences between men and women were moderate ($p < 0.05$, $d = 0.61–1.20$).*
***Differences between men and women were large or very large ($p < 0.05$, $d > 1.21$).*
[a]Differences between laps 3 and 4 were small ($p < 0.05$, $d = 0.21–0.60$).
[b]Differences between laps 3 and 4 were moderate ($p < 0.05$, $d = 0.61–1.20$).

could not be measured in this study, there were nonetheless no performance differences within these groups. Indeed, it should be noted that NRFS athletes still landed with their foot just over 0.30 m ahead of the CM, and it is possible that the absolute foot ahead differences between RFS and NRFS of 0.02–0.04 m were too small to be meaningful in that regard. Similarly, although RFS athletes of both sexes had greater mean overstriding distances at initial contact, these were only 0.03–0.04 m greater than in NRFS and, given there were no correlations between overstriding distance and the key performance variables of speed, step length and cadence, such differences might have been insufficient for any competitive advantage. Coaches should therefore note that encouraging marathon runners to convert from RFS to NRFS is likely to result in few if any benefits to performance, especially as continuous NRFS can lead to considerable fatigue in the lower limb's contractile properties (Peltonen et al., 2012; Baggaley et al., 2017) and explains why many NRFS to switch to RFS in the later stages of the race (Hanley et al., 2019).

As stated above, running speed is the product of step length and cadence although, within this sample of elite-standard athletes, step length was much more strongly correlated with speed. This does not mean that an appropriately high cadence (>3 Hz) is not important in achieving competitive running speeds, but rather signifies that cadence varied little amongst this relatively homogenous group and thus was not a distinguishing factor for performance. Instead, the importance of step length shows that it is the chief differentiator of marathon running ability, and was strongly correlated with flight distance. Indeed, although step length and flight distance decreased from lap 3 to 4, these variables' association with speed increased on lap 4. A trade-off between longer steps and reduced cadences is normal in running (Heiderscheit et al., 2011), although the negative correlations between foot ahead distance and cadence were small and not indicative of meaningful overstriding in this cohort of well-trained athletes. The movement of the recovery leg during swing was important as those athletes who flexed their knees more had longer steps and flight distances and, in women, faster running speeds. These associations were very large during lap 4 and highlighted the role of the flexed knee during midswing in reducing the energy requirements of the recovery leg (Elliot and

TABLE 4 | Mean ± SD values for step length components expressed as a percentage of total step length.

	Men			Women		
	RFS	**NRFS**	**All**	**RFS**	**NRFS**	**All**
Flight distance (% of total step length)						
Lap 3	38.4 (± 3.1)	41.3† (± 3.5)	39.8 (± 3.6)	32.1 (± 5.8)	36.5† (± 5.0)	34.3* (± 5.8)
Lap 4	35.8[b] (± 4.7)	39.0 (± 4.3)	37.4[a] (± 4.7)	30.8 (± 5.7)	34.6 (± 5.4)	32.7*[a] (± 5.8)
Foot ahead (% of total step length)						
Lap 3	23.9 (± 1.6)	21.4‡ (± 1.6)	22.6 (± 2.0)	25.3 (± 1.5)	23.1† (± 2.5)	24.2* (± 2.3)
Lap 4	24.3 (± 1.8)	22.3† (± 1.6)	23.3 (± 1.9)	25.9 (± 2.3)	23.9† (± 2.4)	24.9* (± 2.5)
Foot behind (% of total step length)						
Lap 3	30.3 (± 1.4)	30.4 (± 2.2)	30.4 (± 1.8)	33.3 (± 3.3)	32.5 (± 2.4)	32.9* (± 2.8)
Lap 4	31.4 (± 2.7)	31.1 (± 2.3)	31.2 (± 2.5)	34.1 (± 2.7)	33.6 (± 3.1)	33.9* (± 2.8)
Foot movement (% of total step length)						
Lap 3	7.3 (± 1.0)	6.9 (± 1.0)	7.1 (± 1.0)	9.2 (± 1.8)	7.8† (± 1.2)	8.5* (± 1.7)
Lap 4	8.6[b] (± 1.2)	7.6†[b] (± 0.9)	8.1[b] (± 1.1)	9.2 (± 1.6)	7.9† (± 1.1)	8.5 (± 1.5)

RFS, Rearfoot strikers; NRFS, Non-rearfoot strikers.
†Differences between RFS and NRFS were moderate ($p < 0.05$, $d = 0.61–1.20$).
‡Differences between RFS and NRFS were large ($p < 0.05$, $d = 0.61–1.20$).
**Differences between men and women were moderate ($p < 0.05$, $d = 0.61–1.20$).*
[a]Differences between laps 3 and 4 were small ($p < 0.05$, $d = 0.21–0.60$).
[b]Differences between laps 3 and 4 were moderate ($p < 0.05$, $d = 0.61–1.20$).

Ackland, 1981) that aids with an improved flight phase (Smith and Hanley, 2013). However, it is possible that increased knee flexion is an outcome of faster running because of the rapid forward movement of the thigh during swing (Mann and Hagy, 1980), rather than a cause of it. Furthermore, it is possible that the increased correlation values for knee flexion on lap 4, as well as those for step length and flight distance, occurred to some extent because of greater ranges in the data during the last lap, itself resulting from a greater separation of athletes because of fatigue.

It was unsurprising that men had greater absolute values for running speed and for those variables influenced by stature, such as step length and its components (apart from foot movement on lap 3). Women had greater cadences than men on both laps, mostly because of shorter flight times, which in turn meant that women relied less on flight distance for total step length. Given its importance to running speed, it was noticeable that the largest absolute sex-based difference for any component of step length was for flight distance (longer by 0.18 and 0.13 m in men on laps 3 and 4, respectively). Women compensated for the smaller contribution of flight distance with longer proportions of foot ahead and foot behind distances on both laps. These small proportional differences were manifested in very few joint angular differences overall, although men had more plantarflexed ankles at initial contact (both laps), midstance (lap 4 only) and toe-off (both laps), and more extended knees at toe-off on both laps. Interestingly, given its strong association with flight distance and step length, knee flexion during midswing was greater in men than women and thus is one of the few technical sex-based differences, although as noted above, this might be an outcome of men's faster running speeds rather than a contributor.

The second hypothesis was that those differences found between RFS and NRFS would be similar for men and women. As mentioned above, there were no differences in step length or cadence in RFS and NRFS for either men or women, although the differences at initial contact in ankle angle between RFS and NRFS amongst men were not found in women, who had different hip flexion magnitudes instead (highlighted by the interaction between sex and footstrike pattern). This sex-based difference in ankle and hip joint angles between footstrike patterns was also found at midstance on lap 4. Additionally, in the men's race, RFS had more hyperextended shoulders at initial contact, whereas in the women's race, RFS had more flexed shoulders at toe-off, indicating that slightly different upper body movements are used by men and women to counterbalance the lower limbs' movements. This point was further demonstrated by how men had greater pelvic rotation and less shoulder girdle rotation than women. Overall, however, any differences (or absence of differences, which were more common) between RFS and NRFS were found in both men and women. These include no differences between midswing knee flexion values between RFS and NRFS. From a technical point of view, this demonstrates that RFS and NRFS techniques are mostly indistinguishable except at

TABLE 5 | Mean ± SD values for joint angles at initial contact.

	Men			Women		
	RFS	**NRFS**	**All**	**RFS**	**NRFS**	**All**
Hip (°)						
Lap 3	143 (± 5)	142 (± 4)	142 (± 4)	143 (± 5)	147† (± 4)	145 (± 5)
Lap 4	144 (± 3)	144 (± 6)	144 (± 5)	143 (± 4)	148† (± 5)	146 (± 5)
Knee (°)						
Lap 3	152 (± 4)	147‡ (± 3)	149 (± 4)	150 (± 5)	147† (± 3)	148 (± 4)
Lap 4	151 (± 4)	147† (± 3)	149 (± 4)	150 (± 4)	147 (± 3)	148 (± 4)
Ankle (°)						
Lap 3	100 (± 4)	104‡ (± 2)	102 (± 4)	97 (± 3)	99 (± 3)	98* (± 3)
Lap 4	101 (± 5)	105† (± 4)	103 (± 5)	98 (± 3)	99 (± 4)	99* (± 4)
Shoulder (°)						
Lap 3	−50 (± 6)	−43‡ (± 5)	−47 (± 6)	−52 (± 7)	−48 (± 7)	−50 (± 7)
Lap 4	−51 (± 5)	−46† (± 6)	−48 (± 6)	−52 (± 6)	−49 (± 8)	−51 (± 7)
Elbow (°)						
Lap 3	70 (± 11)	70 (± 12)	70 (± 11)	65 (± 11)	67 (± 20)	66 (± 16)
Lap 4	68 (± 10)	67 (± 11)	68 (± 10)	65 (± 10)	67 (± 16)	66 (± 13)

There were no significant effects found for laps.
RFS, Rearfoot strikers; NRFS, Non-rearfoot strikers.
† Differences between RFS and NRFS were moderate ($p < 0.05$, $d = 0.61–1.20$).
‡ Differences between RFS and NRFS were large ($p < 0.05$, $d = 0.61–1.20$).
**Differences between men and women were moderate ($p < 0.05$, $d = 0.61–1.20$).*

initial contact, and that differences between the sexes are greater than differences between footstrike patterns. Ultimately, RFS and NRFS have running techniques that are so similar (Ardigò et al., 1995; Gruber et al., 2013), with any differences so small that they are possibly meaningless with regard to effects on performance, that there seems little rationale to encourage marathon runners to run with any footstrike pattern other than what they already do habitually.

The third hypothesis, that running speed and associated spatiotemporal variables would decrease between the second-last and last laps because of fatigue, and that any differences between RFS and NRFS would be consistent across laps, was mostly supported. Speed decreases occurred predominantly in line with reduced step lengths, although the effect sizes were larger in men than women, which might be related to men's greater slowing down between laps 3 and 4. RFS and NRFS athletes in the men's race, and RFS women, had small reductions in cadence also, which resulted from longer contact times. One reason for reduced running speeds is a decline in effectiveness of the stretch-shortening cycle in the muscle-tendon unit (Komi, 2000), which is reflected in a reduction in the storage of elastic energy, leading to fatigue and an increased need for muscular work to maintain a given speed (Nicol et al., 1991). Rather than being able to increase muscular work when fatigued, athletes simply slow and this is largely because they cannot achieve the same step lengths as when unfatigued. A reduction in elastic energy storage is caused partially by an increase in transition time from stretch to shortening (i.e., between braking and push-off phases) (Nicol et al., 1991) and might have occurred in this sample as shown by their longer contact times, although such neuromuscular factors could not be measured in competition. More so than footstrike pattern, distance run (and presumably the fatigue that accrues because of it) was unsurprisingly the main determinant of differences in spatiotemporal variables between laps. Maintaining step length and cadence as close as possible to the magnitudes achieved when running at faster speeds (as on lap 3) avoids decreases in running speed, with the maintenance of a long step length the more decisive of the two. Notwithstanding the need for highly developed cardiovascular and energy systems, being able to achieve this results to some extent from training the fatigue resistance of muscle-tendon units, particularly in the lower limb. The finding in previous research that many NRFS

TABLE 6 | Mean ± SD values for joint angles at midstance.

	Men			Women		
	RFS	**NRFS**	**All**	**RFS**	**NRFS**	**All**
Hip (°)						
Lap 3	151 (± 4)	151 (± 4)	151 (± 4)	150 (± 6)	154 (± 4)	152 (± 5)
Lap 4	153 (± 4)	153 (± 5)	153 (± 4)	150 (± 5)	155† (± 4)	152 (± 5)
Knee (°)						
Lap 3	131 (± 4)	131 (± 4)	131 (± 4)	131 (± 4)	131 (± 3)	131 (± 4)
Lap 4	132 (± 3)	131 (± 4)	132 (± 4)	131 (± 4)	132 (± 3)	131 (± 4)
Ankle (°)						
Lap 3	81 (± 3)	83 (± 3)	82 (± 3)	81 (± 2)	81 (± 2)	81 (± 2)
Lap 4	81 (± 2)	84† (± 2)	83 (± 2)	81 (± 2)	81 (± 1)	81* (± 2)
Shoulder (°)						
Lap 3	−28 (± 5)	−24† (± 5)	−26 (± 5)	−28 (± 4)	−28 (± 7)	−28 (± 6)
Lap 4	−28 (± 5)	−25 (± 4)	−26 (± 5)	−27 (± 5)	−28 (± 5)	−28 (± 5)
Elbow (°)						
Lap 3	73 (± 8)	70 (± 13)	71 (± 10)	71 (± 11)	73 (± 17)	72 (± 14)
Lap 4	72 (± 9)	70 (± 11)	71 (± 10)	70 (± 11)	74 (± 14)	72 (± 12)

There were no significant effects found for laps.
RFS, Rearfoot strikers; NRFS, Non-rearfoot strikers.
† Differences between RFS and NRFS were moderate ($p < 0.05$, $d = 0.61–1.20$).
**Differences between men and women were moderate ($p < 0.05$, $d = 0.61–1.20$).*

marathon runners switch to RFS by the end of the marathon (Larson et al., 2011; Hanley et al., 2019) suggests that many do not have fatigue resistance in the ankle plantarflexors necessary to retain a more anterior striking footstrike pattern (Peltonen et al., 2012; Baggaley et al., 2017).

The largest contributor to shortened step lengths was reduced flight distances (by a mean of 0.08 and 0.03 m in men and women, respectively), whereas no other contributor to step length decreased by more than 0.02 m. Flight distance proportion was one of the few spatiotemporal variables that was not consistently different between RFS and NRFS on both laps; however, most variables did not change between laps (in that they did not differ between RFS and NRFS) and highlights how athletes who have developed either footstrike pattern maintained a consistent technique, despite decreases in speed, step length and cadence. Indeed, there were no changes in stance phase joint angles between laps 3 and 4. However, it was noteworthy that men's minimum knee flexion angles increased during midswing by 5°, a change that has previously been found in a fatiguing 10,000 m race (Elliot and Ackland, 1981), and which might have been a function of reduced running speed (Mann and Hagy, 1980), especially as it did not decrease in women who suffered smaller decreases in speed. Overall, adopting one specific footstrike pattern or the other did not protect against a deterioration of running speed or lead to a change in technique with distance run. Given the few differences between RFS and NRFS on both of the last two laps, that any changes that occurred were similar between both, and that these similarities were quite consistent between men and women, coaches and athletes are advised that there is no strong rationale to change footstrike pattern from what is naturally preferred in either sex.

The main strength of this study was that it was conducted in the highly ecologically valid setting of a major championship race, where the athletes ran using their habitual running style and no intervention was involved. This means that the results found are an accurate reflection of world-class marathon running techniques in the sample studied. However, because there were more RFS runners in both races (Hanley et al., 2019), the 28 athletes who formed the RFS sample were less representative of all RFS competitors than the 28 NRFS athletes were of theirs. Nonetheless, both RFS and NRFS samples within each race were well distributed, as shown by the absence of differences between PR or finishing times. The duration of the competition and the number of athletes competing meant that a sampling rate

TABLE 7 | Mean ± SD values for joint angles at toe-off.

	Men			Women		
	RFS	**NRFS**	**All**	**RFS**	**NRFS**	**All**
Hip (°)						
Lap 3	192 (± 4)	192 (± 4)	192 (± 4)	190 (± 4)	193 (± 4)	191 (± 4)
Lap 4	191 (± 3)	191 (± 4)	191 (± 3)	190 (± 4)	192 (± 3)	191 (± 4)
Knee (°)						
Lap 3	162 (± 4)	163 (± 4)	163 (± 4)	160 (± 4)	160 (± 3)	160* (± 4)
Lap 4	163 (± 3)	162 (± 5)	163 (± 4)	159 (± 4)	161 (± 5)	160* (± 4)
Ankle (°)						
Lap 3	126 (± 6)	128 (± 6)	127 (± 6)	123 (± 6)	124 (± 4)	124* (± 5)
Lap 4	126 (± 6)	128 (± 6)	127 (± 6)	123 (± 5)	125 (± 4)	124* (± 5)
Shoulder (°)						
Lap 3	28 (± 5)	25 (± 6)	27 (± 5)	29 (± 4)	24† (± 6)	27 (± 6)
Lap 4	27 (± 4)	24 (± 4)	26 (± 5)	30 (± 5)	25† (± 5)	27 (± 6)
Elbow (°)						
Lap 3	57 (± 9)	54 (± 10)	55 (± 10)	58 (± 9)	58 (± 16)	58 (± 13)
Lap 4	57 (± 9)	55 (± 10)	56 (± 9)	56 (± 8)	58 (± 12)	57 (± 10)

There were no significant effects found for laps.
RFS, Rearfoot strikers; NRFS, Non-rearfoot strikers.
**Differences between men and women were moderate ($p < 0.05$, $d = 0.61–1.20$).*
† Differences between RFS and NRFS were moderate ($p < 0.05$, $d = 0.61–1.20$).

TABLE 8 | Mean ± SD values for maximum pelvic and shoulder girdle rotation and minimum knee angle (flexion) during midswing.

	Men			Women		
	RFS	**NRFS**	**All**	**RFS**	**NRFS**	**All**
Pelvic rotation (°)						
Lap 3	11 (± 3)	11 (± 4)	11 (± 4)	6 (± 3)	5 (± 2)	5** (± 2)
Lap 4	10 (± 3)	10 (± 5)	10 (± 4)	5 (± 2)	4 (± 2)	5** (± 2)
Shoulder girdle rotation (°)						
Lap 3	15 (± 3)	17 (± 3)	16 (± 3)	19 (± 3)	19 (± 3)	19* (± 3)
Lap 4	16 (± 3)	17 (± 3)	16 (± 3)	19 (± 4)	19 (± 3)	19* (± 3)
Knee angle during midswing (°)						
Lap 3	50 (± 6)	50 (± 6)	50 (± 6)	63 (± 10)	63 (± 11)	63* (± 10)
Lap 4	54[b] (± 6)	55[b] (± 7)	55[b] (± 7)	64 (± 11)	65 (± 12)	65* (± 11)

There were no significant effects found for footstrike pattern.
RFS, Rearfoot strikers; NRFS, Non-rearfoot strikers.
**Differences between men and women were moderate ($p < 0.05$, $d = 0.61–1.20$).*
***Differences between men and women were large or very large ($p < 0.05$, $d > 1.21$).*
[b] Differences between laps 3 and 4 were moderate ($p < 0.05$, $d = 0.61–1.20$).

TABLE 9 | Correlation analysis of key variables in World Championship marathon runners during Laps 3 and 4.

		Step length	Cadence	Foot ahead	Foot behind	Flight distance
Men						
Speed	Lap 3	***r* = 0.76**	$r = 0.35$	$r = 0.41$	***r* = 0.50**	***r* = 0.55**
	Lap 4	***r* = 0.81**	***r* = 0.52**	$r = 0.22$	$r = 0.28$	***r* = 0.74**
Step length	Lap 3		$r = -0.34$	***r* = 0.57**	***r* = 0.65**	***r* = 0.71**
	Lap 4		$r = -0.07$	$r = 0.36$	$r = 0.30$	***r* = 0.90**
Cadence	Lap 3			$r = -0.25$	$r = -0.19$	$r = -0.23$
	Lap 4			$r = -0.19$	$r = 0.02$	$r = -0.04$
Knee flexion	Lap 3	***r* = −0.66**	$r = 0.42$	$r = -0.38$	$r = -0.19$	***r* = −0.59**
	Lap 4	***r* = −0.79**	***r* = 0.50**	$r = -0.27$	$r = -0.19$	***r* = −0.73**
Overstriding distance	Lap 3	$r = 0.44$	$r = -0.07$	***r* = 0.81**	$r = 0.15$	$r = 0.05$
	Lap 4	$r = 0.39$	$r = -0.15$	***r* = 0.83**	$r = 0.09$	$r = 0.12$
Women						
Speed	Lap 3	***r* = 0.73**	$r = 0.14$	$r = 0.29$	$r = 0.07$	***r* = 0.68**
	Lap 4	***r* = 0.83**	$r = 0.07$	$r = 0.44$	$r = 0.30$	***r* = 0.86**
Step length	Lap 3		***r* = −0.57**	$r = 0.38$	$r = 0.37$	***r* = 0.84**
	Lap 4		$r = -0.49$	***r* = 0.53**	***r* = 0.54**	***r* = 0.86**
Cadence	Lap 3			$r = -0.21$	$r = -0.45$	$r = -0.40$
	Lap 4			$r = -0.29$	***r* = −0.50**	$r = -0.38$
Knee flexion	Lap 3	***r* = −0.83**	$r = 0.49$	$r = -0.09$	$r = 0.02$	***r* = −0.88**
	Lap 4	***r* = −0.86**	***r* = 0.52**	$r = -0.34$	$r = -0.27$	***r* = −0.86**
Overstriding	Lap 3	$r = 0.11$	$r = -0.18$	***r* = 0.65**	$r = 0.23$	$r = -0.22$
distance	Lap 4	$r = 0.43$	$r = -0.33$	***r* = 0.70**	***r* = 0.51**	$r = 0.11$

Correlations were significant at $p < 0.05$ and $r \geq 0.50$ (shown in bold).

of 50 Hz was the most suitable for data collection, although the time between frames of 0.02 s means that caution must be taken in particular when considering differences in the temporal values between footstrike patterns, sexes and laps (all values presented were obtained using the original 50 Hz data, rather than from the interpolated data used to create **Figure 1**). Footstrike patterns was treated as a discrete variable, rather than as a continuous one that might be measured using footstrike angle, for example, and this might have prevented more footstrike effects being identified. For this study, the athletes were recorded on all four laps they completed, but only during the last two were athletes spread out enough to enable high-quality analysis; future research could try to analyze athletes at more distances during the marathon to further evaluate the changes that occur with fatigue, and to obtain anthropometric data that could allow for the calculation of spatial variables relative to stature.

CONCLUSIONS

This was the first study to analyze world-class marathon runners of both sexes in competition in comparing the spatiotemporal and joint kinematic differences between RFS and NRFS. The most important finding from all analyses and comparisons was that RFS and NRFS have very similar running techniques, with no differences in step length or cadence at the same running speed. Most joint angles in the upper and lower limbs were the same at key gait events, with most differences occurring at initial contact. This was unsurprising given that what differentiates RFS and NRFS is how the athletes land at initial contact, but even still, the absolute differences in overstriding, flight and foot ahead distances, and ankle, knee and hip joint angles were typically no more than 0.04 m and 5°, respectively. Although this is not meant to imply that RFS and NRFS techniques are identical, there is nonetheless little evidence to support coaching practices that aim to convert an athlete from one footstrike pattern to another. RFS and NRFS athletes of both sexes had similar reductions in speed, step length and cadence between laps 3 and 4, but there were few joint angular changes, showing that individual techniques were not considerably affected by fatigue. In terms of practical applications, coaches should note that the maintenance of a long step length, largely through maintaining a long flight distance, likely arises from training the fatigue resistance of muscle-tendon units, such as the ankle plantarflexors, alongside the development of a marathon runner's cardiovascular and energy systems capabilities.

DATA AVAILABILITY STATEMENT

The datasets presented in this article are not readily available because there is a risk of identifying individual athletes. Requests to access the datasets should be directed to Brian Hanley, b.hanley@leedsbeckett.ac.uk.

ETHICS STATEMENT

The studies involving human participants were reviewed and approved by the Leeds Beckett University Carnegie School of Sport Research Ethics Advisory Group. The patients/participants provided their written informed consent to participate in this study.

AUTHOR CONTRIBUTIONS

BH, AB, and SM conceptualized and designed the study and wrote the manuscript. AB and SM arranged data collection during the World Championships marathon events as Project Director and Project Leader, respectively. BH collected and analyzed the video data. All authors read and approved the final manuscript.

FUNDING

The data collection and initial data analysis were supported by funding provided by the IAAF/World Athletics as part of a wider development/education project; however, the nature of the data is purely descriptive and not associated with any governing body, commercial sector, or product. No funding was provided for the writing of this manuscript. The results of the present study do not constitute endorsement by the World Athletics.

REFERENCES

Abdel-Aziz, Y. I., Karara, H. M., and Hauck, M. (2015). Direct linear transformation from comparator coordinates into space coordinates in close range photogrammetry. *Photogramm. Eng. Remote Sensing* 81, 103–107. doi: 10.14358/PERS.81.2.103

Abshire, D., and Metzler, B. (2010). *Natural Running: The Simple Path to Stronger, Healthier Running*. Boulder, CO: Velo Press.

Almeida, M. O., Davis, I. S., and Lopes, A. D. (2015). Biomechanical differences of foot-strike patterns during running: a systematic review with meta-analysis. *J. Orthop. Sports Phys. Ther.* 45, 738–755. doi: 10.2519/jospt.2015.6019

Anderson, O. (2018). *Running form: How to Run Faster and Prevent Injury*. Champaign, IL: Human Kinetics.

Ardigò, L. P, LaFortuna, C., Minetti, A. E, Mognoni, P., and Saibene, F. (1995). Metabolic and mechanical aspects of foot landing type, forefoot and rearfoot strike, in human running. *Acta Physiol. Scand.* 155, 17–22. doi: 10.1111/j.1748-1716.1995.tb09943.x

Atkinson, G., and Nevill, A. M. (1998). Statistical methods for assessing measurement error (reliability) in variables relevant to sports medicine. *Sports Med.* 26, 217–238. doi: 10.2165/00007256-199826040-00002

Baggaley, M., Willy, R. W, and Meardon, S. A. (2017). Primary and secondary effects of real-time feedback to reduce vertical loading rate during running. *Scand. J. Med. Sci. Sports* 27, 501–507. doi: 10.1111/sms.12670

Bahamonde, R. E., and Stevens, R. R. (2006). "Comparison of two methods of manual digitization on accuracy and time of completion," in *Proceedings of the XXIV International Symposium on Biomechanics in Sports*, eds H. Schwameder, G. Strutzenberger, V. Fastenbauer, S. Lindinger, and E. Müller (Salzburg: Universität Salzburg), 650–653. Retrieved from: https://ojs.ub.uni-konstanz.de/cpa/article/view/207/167 (accessed January 24, 2020).

Bland, J. M., and Altman, D. G. (1986). Statistical methods for assessing agreement between two methods of clinical measurement. *Lancet* 1, 307–310. doi: 10.1016/S0140-6736(86)90837-8

Buckalew, D. P., Barlow, D. A., Fischer, J. W., and Richards, J. G. (1985). Biomechanical profile of elite women marathoners. *Int. J. Sport Biomech.* 1, 330–347. doi: 10.1123/ijsb.1.4.330

Buman, M. P., Brewer, B. W., and Cornelius, A. E. (2009). A discrete-time hazard model of hitting the wall in recreational marathon runners. *Psychol. Sport Exerc.* 10, 662–666. doi: 10.1016/j.psychsport.2009.04.004

Cairns, M. A., Burdette, R. G., Pisciotta, J. C., and Simon, S. R. (1986). A biomechanical analysis of racewalking gait. *Med. Sci. Sports Exerc.* 18, 446–453. doi: 10.1249/00005768-198608000-00015

Chan-Roper, M., Hunter, I., Myrer, J. W., Eggett, D. L., and Seeley, M. K. (2012). Kinematic changes during a marathon for fast and slow runners. *J. Sports Sci. Med.* 11, 77–82.

Cohen, J. (1988). *Statistical Power Analysis for the Behavioural Sciences, 2nd Edn*. Hillsdale, NJ: Lawrence Erlbaum.

de Leva, P. (1996). Adjustments to Zatsiorsky-Seluyanov's segment inertia parameters. *J. Biomech.* 29, 1223–1230. doi: 10.1016/0021-9290(95)00178-6

Deaner, R. O., Addona, V., and Hanley, B. (2019). Risk taking runners slow more in the marathon. *Front. Psychol.* 10:333. doi: 10.3389/fpsyg.2019.00333

Elliot, B., and Ackland, T. (1981). Biomechanical effects of fatigue on 10,000 meter running technique. *Res. Q. Exerc. Sport* 52, 160–166. doi: 10.1080/02701367.1981.10607853

Field, A. P. (2009). *Discovering Statistics Using SPSS, 4th Edn*. London: Sage.

Giakas, G., and Baltzopoulos, V. (1997). A comparison of automatic filtering techniques applied to biomechanical walking data. *J. Biomech.* 30, 847–850. doi: 10.1016/S0021-9290(97)00042-0

Gómez-Molina, J., Ogueta-Alday, A., Camara, J., Stickley, C., Rodríguez-Marroyo, J. A., and García-López, J. (2017). Predictive variables of half-marathon performance for male runners. *J. Sports Sci. Med.* 16, 187–194.

Goss, D. L., and Gross, M. T. (2013). A comparison of negative joint work and vertical ground reaction force loading rates in Chi runners and rearfoot-striking runners. *J. Orthop. Sports Phys. Ther.* 43, 685–692. doi: 10.2519/jospt.2013.4542

Gruber, A. H., Umberger, B. R., Braun, B., and Hamill, J. (2013). Economy and rate of carbohydrate oxidation during running with rearfoot and forefoot running patterns. *J. Appl. Physiol.* 115, 194–201. doi: 10.1152/japplphysiol.01437.2012

Hanley, B., Bissas, A., Merlino, S., and Gruber, A. H. (2019). Most marathon runners at the 2017 IAAF World Championships were rearfoot strikers, and most did not change footstrike pattern. *J. Biomech.* 92, 54–60. doi: 10.1016/j.jbiomech.2019.05.024

Hasegawa, H., Yamauchi, T., and Kraemer, W. J. (2007). Foot strike patterns of runners at the 15-km point during an elite-level half marathon. *J. Strength Cond. Res.* 21, 888–893. doi: 10.1519/00124278-200708000-00040

Hayes, P., and Caplan, N. (2012). Foot strike patterns and ground contact times during high-calibre middle-distance races. *J. Sports Sci.* 30, 1275–1283. doi: 10.1080/02640414.2012.707326

Heiderscheit, B. C., Chumanov, E. S., Michalski, M. P., Wille, C. M., and Ryan, M. B. (2011). Effects of step rate manipulation on joint mechanics during running. *Med. Sci. Sports Exerc.* 43, 296–302. doi: 10.1249/MSS.0b013e3181ebedf4

Hettinga, F. J., Edwards, A. M., and Hanley, B. (2019). The science behind competition and winning in athletics: using world-level competition data to explore pacing and tactics. *Front. Sports Act. Living* 1:11. doi: 10.3389/fspor.2019.00011

Hopkins, W. G., Marshall, S. W., Batterham, A. M., and Hanin, J. (2009). Progressive statistics for studies in sports medicine and exercise science. *Med. Sci. Sports Exerc.* 41, 3–12. doi: 10.1249/MSS.0b013e31818cb278

Hunter, J. P., Marshall, R.N., and McNair, P. J. (2004). Interaction of step length and step rate during sprint running. *Med. Sci. Sports Exerc.* 36, 261–271. doi: 10.1249/01.MSS.0000113664.15777.53

Jeukendrup, A. E. (2011). Nutrition for endurance sports: marathon, triathlon, and road cycling. *J. Sports Sci.* 29, S91–S99. doi: 10.1080/02640414.2011.610348

Komi, P. V. (2000). Stretch-shortening cycle: a powerful model to study normal and fatigued muscle. *J. Biomech.* 33, 1197–1206. doi: 10.1016/S0021-9290(00)00064-6

Larson, P., Higgins, E., Kaminski, J., Decker, T., Preble, J., Lyons, D., et al. (2011). Foot strike patterns of recreational and sub-elite runners in a long-distance road race. *J. Sports Sci.* 29, 1665–1673. doi: 10.1080/02640414.2011.610347

Lieberman, D. E. (2014). Strike type variation among Tarahumara Indians in minimal sandals versus conventional running shoes. *J. Sport Health Sci.* 3, 86–94. doi: 10.1016/j.jshs.2014.03.009

Lieberman, D. E., Warrener, A. G., Wang, J., and Castillo, E. R. (2015). Effects of stride frequency and foot position at landing on braking force, hip torque, impact peak force and the metabolic cost of running in humans. *J. Exp. Biol.* 218, 3406–3414. doi: 10.1242/jeb.125500

Mann, R. A., and Hagy, J. (1980). Biomechanics of walking, running and sprinting. *Am. J. Sports Med.* 8, 345–350. doi: 10.1177/036354658000800510

Mero, A., and Komi, P. V. (1994). EMG, force, and power analysis of sprint-specific strength exercises. *J. Appl. Biomech.* 10, 1–13. doi: 10.1123/jab.10.1.1

Moore, I. S. (2016). Is there an economical running technique? A review of modifiable biomechanical factors affecting running economy. *Sports Med.* 46, 793–807. doi: 10.1007/s40279-016-0474-4

Nicol, C., Komi, P. V., and Marconnet, P. (1991). Fatigue effects of marathon running on neuromuscular performance I. Changes in muscle force and stiffness characteristics. *Scand. J. Med. Sci. Sports* 1, 10–17. doi: 10.1111/j.1600-0838.1991.tb00265.x

O'Brien, M. J., Viguie, C. A., Mazzeo, R. S., and Brooks, G. A. (1993). Carbohydrate dependence during marathon running. *Med. Sci. Sports Exerc.* 25, 1009–1017. doi: 10.1249/00005768-199309000-00007

Ogueta-Alday, A., Morante, J. C., Gómez-Molina, J., and García-López, J. (2017). Similarities and differences among half-marathon runners according to their performance level. *PLoS ONE* 13:e0191688. doi: 10.1371/journal.pone.0191688

Padulo, J., Chamari, K., and Ardigò, L. P. (2014). Walking and running on treadmill: the standard criteria for kinematics studies. *Muscles Ligaments Tendons J.* 4, 159–162. doi: 10.11138/mltj/2014.4.2.159

Peltonen, J., Cronin, N. J., Stenroth, L., Finni, T., and Avela, J. (2012). Achilles tendon stiffness is unchanged after one hour in a marathon. *J. Exp. Biol.* 215, 3665–3671. doi: 10.1242/jeb.068874

Perl, D. P., Daoud, A.I., and Lieberman, D. E. (2012). Effects of footwear and strike type on running economy. *Med. Sci. Sports Exerc.* 44, 1335–1343. doi: 10.1249/MSS.0b013e318247989e

Pizzuto, F., de Oliveira, C. F., Soares, T. S. A., Rago, V., Silva, G., and Oliveira, J. (2019). Relationship between running economy and kinematic parameters in long-distance runners. *J. Strength Cond. Res.* 33, 1921–1928. doi: 10.1519/JSC.0000000000003040

Shih, Y., Lin, K-L., and Shiang, T-Y. (2013). Is the foot striking pattern more important than barefoot or shod conditions in running? *Gait Posture* 38, 490–494. doi: 10.1016/j.gaitpost.2013.01.030

Smith, G. (1989). Padding point extrapolation techniques for the Butterworth digital filter. *J. Biomech.* 22, 967–971. doi: 10.1016/0021-9290(89)90082-1

Smith, L. C., and Hanley, B. (2013). Comparisons between swing phase characteristics of race walkers and distance runners. *Int. J. Exerc. Sci.* 6, 269–277. Available online at: https://digitalcommons.wku.edu/ijes/vol6/iss4/2/

Stellingwerff, T. (2012). Case study: nutrition and training periodization in three elite marathon runners. *Int. J. Sport Nutr. Exerc. Metab.* 22, 392–400. doi: 10.1123/ijsnem.22.5.392

Williams, K. R. (2007). Biomechanical factors contributing to marathon race success. *Sports Med.* 37, 420–423. doi: 10.2165/00007256-200737040-00038

Winter, D. A. (2005). *Biomechanics and Motor Control of Human Movement, 3rd Edn*. Hoboken, NJ: John Wiley & Sons.

World Athletics (2019). *Archive of Past Events*. Available online at: https://www.worldathletics.org/competitions/world-athletics-championships/history (accessed March 17 2020).

World Athletics (2020). *Athletes*. Available online at: https://www.worldathletics.org/athletes-home (accessed March 17 2020).

Conflict of Interest: The authors declare that the research was conducted in the absence of any commercial or financial relationships that could be construed as a potential conflict of interest.

frontiers in Sports and Active Living

ORIGINAL RESEARCH
published: 16 December 2020
doi: 10.3389/fspor.2020.579152

Orthotic Insoles Improve Gait Symmetry and Reduce Immediate Pain in Subjects With Mild Leg Length Discrepancy

Charlotte Menez[1,2]*, *Maxime L'Hermette*[1] and *Jeremy Coquart*[1]

[1] Normandie Univ, UNIROUEN, CETAPS, Rouen, France, [2] Orthodynamica Center, Mathilde Hospital 2, Rouen, France

Background: Mild leg length discrepancy can lead to musculoskeletal disorders; however, the magnitude starting from which leg length discrepancy alters the biomechanics of gait or benefits from treatment interventions is not clear.

Research question: The aim of the current study was to examine the immediate effects of orthotic insoles on gait symmetry and pain on mild leg length discrepancy according to two groups of the leg length discrepancy (i.e., LLD $\leq$ 1 cm vs. LLD $>$ 1 cm).

Methods: Forty-six adults with mild leg length discrepancy were retrospectively included and classified into two groups ($G_{LLD\leq 1cm}$ or $G_{LLD>1cm}$). All subjects underwent routine 3D gait analysis with and without orthotic insoles. The symmetry index was calculated to assess changes in gait symmetry between the right and left limbs. Pain was rated without (in standing) and with the orthotic insoles (after 30 min of use) on a visual analog scale.

Results: There was a significant improvement in the symmetry index of the pelvis in the frontal plane ($p = 0.001$) and the ankle in the sagittal plane ($p = 0.010$) in the stance with the orthotic insoles independent from the group. Pain reduced significantly with the orthotic insoles independently from the group ($p < 0.001$).

Significance: Orthotic insoles significantly improved gait symmetry in the pelvis in the frontal plane and the ankle in the sagittal plane, as well as pain in all subjects (both LLD $\leq$ 1 cm and LLD $>$ 1 cm) suggesting that it may be appropriate to treat even mild leg length discrepancy.

Keywords: leg length inequality, gait analysis, foot orthoses, musculo skeletal diseases, podiatry, walking

OPEN ACCESS

Edited by:
Johnny Padulo,
University of Milan, Italy

Reviewed by:
Claudio Pizzolato,
Griffith University, Australia
Sina David,
Vrije Universiteit
Amsterdam, Netherlands

***Correspondence:**
Charlotte Menez
charlotte.menez@orthodynamica.com

Specialty section:
This article was submitted to Biomechanics and Control of Human Movement, a section of the journal Frontiers in Sports and Active Living

Received: *01 July 2020*
Accepted: *11 November 2020*
Published: *16 December 2020*

Citation:
Menez C, L'Hermette M and Coquart J (2020) Orthotic Insoles Improve Gait Symmetry and Reduce Immediate Pain in Subjects With Mild Leg Length Discrepancy. Front. Sports Act. Living 2:579152. doi: 10.3389/fspor.2020.579152

INTRODUCTION

Leg length discrepancy (LLD) can be either caused by anatomical deformities originating from true differences in the bony structures of the lower limb, or it may be functional, resulting from abnormal lower limb movements (Khamis and Carmeli, 2018). The diagnosis (Brady et al., 2003), classification (Gurney, 2002), and treatment (Campbell et al., 2018) of LLD remain controversial among both researchers and clinicians. Some authors classify discrepancies $\leq$2.0 cm as mild (Moseley, 1996), while others consider discrepancies of up to 3.0 cm as mild (Reid and Smith, 1984; McCaw and Bates, 1991; Gurney, 2002; Brady et al., 2003; Campbell et al., 2018). These classifications are intended to guide practitioners in the treatment of LLD, but there is much

disagreement in the literature as to the magnitude from which LLD requires treatment. It has been suggested that orthotic insoles (OIs), shoe lifts, or other clinical interventions to equalize leg length should be considered for LLD $\geq$ 1.0 cm (White et al., 2004), or even between 0.5 and 1.0 cm (Khamis and Carmeli, 2018). However, other authors are more conservative, suggesting that below 2 cm, no treatment is required (Moseley, 1996).

The lack of consensus regarding the need to treat mild LLD stems from the fact that there is no real agreement as to the biomechanical effects of a mild LLD on lower limb and spinal joints during walking (Friberg, 1982; Kaufman et al., 1996; Goel et al., 1997; Resende et al., 2016; Khamis and Carmeli, 2018). Many studies (Friberg, 1984; Walsh et al., 2000; Seeley et al., 2010; Murray and Azari, 2015; Resende et al., 2016; Tallroth et al., 2017) have reported that even mild LLD can cause lower limb biomechanical disorders. For example, one study (Walsh et al., 2000) found that compensatory strategies and asymmetrical gait occurred from 1.0 cm of LLD induced by foot lifts (from 1 to 5 cm high). Similar results were reported in an earlier study (Kaufman et al., 1996) in which the authors also hypothesized that individuals with even mild LLD use compensatory functional mechanisms to attenuate the effect of the LLD, presumably to minimize displacement of the center of body mass. However, the effect of mild LLD on gait has not been unequivocally demonstrated (Resende et al., 2016; Khamis and Carmeli, 2018).

Mild LLD, including LLD $\leq$ 1 cm, has been associated with an increased risk of knee osteoarthritis (Harvey, 2010) and scoliosis (Specht and De, 1991), both of which are frequently associated with low back pain (Defrin et al., 2005). Mild LLD is therefore frequently treated with the aim of preventing the development of such secondary pathologies. OIs are the most frequently used treatment (Kendall et al., 2014) likely because they are noninvasive, inexpensive, and readily available (Defrin et al., 2005). Despite the widespread use of OI, their impact on gait kinematics (Bandy and Sinning, 1986; Goel et al., 1997; Bangerter et al., 2019) and pain (Defrin et al., 2005; Golightly et al., 2007) has been little studied in subjects with mild anatomical LLD. Recently, Menez et al. (2020) evaluated the effect of OI on gait kinematics and low back pain in subjects with mild LLD. They found that changes in gait symmetry varied and was specific across individuals; however, low back pain decreased in all subjects after the use of OI. However, mild LLD is commonly not treated in patients with low back pain (Junk et al., 1992; Mannello, 1992; Defrin et al., 2005). Moreover, mild LLD is frequently found in the adult population (Junk et al., 1992; Mannello, 1992), and the correction of LLD $\leq$ 1 cm remains insufficiently incorporated into the treatment of low back pain (Junk et al., 1992; Mannello, 1992; Defrin et al., 2005), with many clinicians continuing to overlook the potential impact of mild LLD (Defrin et al., 2005). There is disagreement about the correct treatment and the magnitude of LLD (Gurney, 2002). Indeed, for White et al. (2004), OIs to equalize leg length should be considered in subjects with LLD $\geq$ 1 cm, whereas Khamis and Carmeli (2018) go further, suggesting that even mild LLD between 0.5 and 1 cm should be treated. This recent position of Khamis and Carmeli (2018) is in contradiction with other previous studies suggesting that mild LLD is naturally compensated and should therefore be neglected without any treatment being considered. Apart from the definite interest on pain, the evidence still appears to be limited in terms of kinematics. Therefore, we have searched for additional information to support the interest or not to treat real LLD $\leq$ 1.0 cm.

Studies are therefore needed to clearly identify the magnitude of LLD from which OI improves gait kinematics and/or pain.

It seems that LLD causes asymmetry in the locomotion of the lower limbs, leading to pain, with a disruption of normal biomechanical function. The functional alterations increase biomechanical disorders, asymmetrical gait, low back pain, and/or other pain, and may even promote the development of associated pathologies such as osteoarthritis of the hip or knee. OI is a treatment often used in podiatry to try to reduce biomechanical asymmetries and pain. We hypothesize that OI can reduce the asymmetries and associated pain in subjects with mild and very mild LLD during walking.

The primary aim of this study was therefore to evaluate the immediate effects of OI on gait symmetry and pain according to the degree of mild LLD (i.e., LLD $\leq$ 1 cm vs. LLD $>$ 1 cm $<$ 3 cm). The secondary aim was to analyze the specific effects of OI on lower limb joint kinematics.

MATERIALS AND METHODS

Subjects

This 18-month, retrospective study, included data from consecutive patients with mild LLD followed with a prescription for OI from their General Practitioner. The study was written according to the STrengthening the Reporting of OBservational studies in Epidemiology (STROBE) statement (Von Elm et al., 2014). Data from all patients meeting the following criteria were analyzed retrospectively. Only adults (aged between 18 and 70 years) were included. None previously had correction of their LLD. The diagnosis of mild LLD ($\leq$3.0 cm) was confirmed by a chiropodist using an accepted clinical procedure (Khamis and Carmeli, 2017). The cutoff of 3.0 cm was selected according to Campbell et al. (2018). Subjects were excluded if they were obese (body mass index $\geq$ 30 *kg m^{-2}) or if they had a history of surgery, lower limb injury, or neuromuscular or vascular pathology in the last 6 months (information routinely collected during the clinical examination). Subjects were classified into one of two groups, according to the magnitude of the LLD: $G_{LLD\leq 1cm}$ and $G_{LLD>1cm}$ in line with the studies of Seeley et al. (2010) and Defrin et al. (2005).

All the subjects included had undergone routine care, including biomechanical gait analysis with and without the OI as is the usual procedure in our center.

All procedures performed in this study were in accordance with the ethical standards of the institutional and national research committee and with the 1964 Helsinki declaration

Abbreviations: $G_{LLD\leq 1cm}$, Group Leg Length Discrepancy $\leq$ 1 cm; $G_{LLD>1cm}$, Group Leg Length Discrepancy $>$ 1 cm; LLD, Leg Length Discrepancy; OI, Orthotic Insoles; SI, Symmetry Index; STROBE, STrengthening the Reporting of OBservational studies in Epidemiology.

and its later amendments, and written informed consent was obtained from each subject (Ethical committee number: IRB00012476-2020-15-07-61).

Procedure

The chiropodist performed a clinical examination that included measurement of the LLD, rating of pain, and collection of sociodemographical and anthropometrical data (i.e., sex, age, body mass, height, and body mass index).

LLD was measured using a direct clinical method (mean of two measurements of the distance between the anterior superior iliac spine and the medial malleolus, while lying in a supine position, using a tape measure). This direct method has already been shown to be valid and reliable in comparison with computed tomography scan (Jamaluddin et al., 2011; Neelly et al., 2013). The mean of three measures was used (Beattie et al., 1990). For this study, the intra-tester reproducibility for the measurement with the tape measure was good, with an ICC of 0.809.

Subjects were referred by a physician for causes of acute muscular affection in low back or lower limb. Even if in this study all causes of pain were retained, we were only interested in one pain per subject with LLD (the most painful condition). The origin of the main cause of pain was investigated, and its intensity was assessed using a visual analog scale. Subjects were asked to stand for 5 min (Golightly et al., 2007) and then to rate their immediate pain on a visual analog scale graded from 0 (no pain) to 10 (maximal pain), as proposed by Hayashi et al. (2015). The location of pain was noted for each subject (low back, hip, knee, or ankle). The average of all these pains was calculated without and with the OI.

Gait analysis was then performed using a Qualisys pro-reflex motion analysis system (Qualisys AB®, Göteborg, Sweden) with 10 infrared video cameras at a sampling frequency of 120 Hz. Twenty reflective markers were fixed to the anatomical landmarks: the two most anterior and the two most posterior margins of the iliac spines, the most lateral prominence of the greater trochanter and of the lateral femoral epicondyle, the proximal tip of the head of the fibula, the most anterior border of the tibial tuberosity, the lateral prominence of the lateral malleolus, the Achilles tendon insertion on the calcaneous, and the dorsal margins of the 1st and 5th metatarsal heads, in accordance with Leardini et al. (2007) (**Figure 1**). The same investigator positioned the markers on all subjects. A static calibration was carried out before the gait trials in order to generate a neutrally aligned reference "*IOR lower body*" model with respect to the coordinate system of each segment. Subjects wore their usual shoes without OI, which was necessary because the aim was to put them in a walking condition to which they are accustomed. After 10 min of familiarization with the environment by walking around the room, the subjects were instructed to walk at a self-selected speed along the 15 m walkway. Four trials were recorded, and gait cycles performed in the center 10 m of the walkway were used in the analysis. Each trial consisted of five gait cycles making a total of 20 gait cycles for each subject.

The chiropodist made the OI using a thermoforming process: the OIs were first warmed before being molded using a pillow mold to obtain the foot imprint, as recently described by Menez et al. (2020). The materials used in the OIs were ethinyl vinyl acetate, resin, and polyethylene. Once the OIs were molded, they were further shaped to effectively counteract the effects of the LLD and rebalance the kinematics of walking. The whole procedure took 30 min. They were made according to the therapeutic needs of the subjects, with a heel lift incorporated into the OI of the short leg. The heel lifts were partially corrective of the LLD, to 50%, and were shaped from the calcaneus to the Chopart joint (**Figure 2**). This corrective strategy is used empirically by the pedicurist-chiropodist for all subjects with LLD. At the end of the process, the pedicurist-chiropodist checked the impact of the OI by examining the iliac crest position in the frontal plane while the subject was standing.

FIGURE 1 | Istituti Ortopedici Rizzoli (IOR) lower body marker set—anterior **(A)** and posterior **(B)** views (Leardini et al., 2007).

The subjects then wore the OIs for 30 min during which time they walked within the center (familiarization phase). After this time, the kinematic analysis and pain rating were repeated with the OI.

The 3D displacement of the markers was processed, and kinematic variables were calculated using Visual3D software (C-Motion®, Germantown, United States) with inverse kinematics approach. The anatomical reference frames for each segment were defined according to Cappozzo et al. (1995), consistent with the international recommendations (Wu and Cavanagh, 1995; Wu et al., 2002). Standard coordinate systems (Grood and Suntay, 1983) were attributed to each joint. Joint angles were defined by rotations occurring about the three joint coordinate axes. For the hip and knee joints, flexion/extension was defined as the relative rotation about a fixed medio-lateral axis (Z), internal/external rotation as the relative rotation about a fixed vertical axis (Y), and

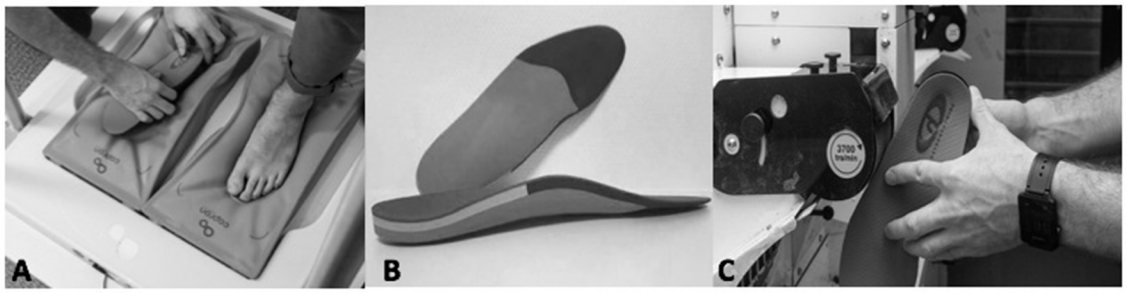

FIGURE 2 | Thermoforming the orthotic insoles **(A)**. Orthotic insoles in ethinyl vinyl acetate, resin, and polyethylene **(B)**. Further shaping the orthotic insoles **(C)**.

abduction/adduction about a "floating" anterior–posterior axis (X). For the ankle joint, these three rotations were defined, respectively, as dorsiflexion/plantarflexion, inversion/eversion, and abduction/adduction. Pelvic tilt (anterior–posterior), rotation, and obliquity (lateral tilt) were calculated using the same convention, with a virtual joint defined between the laboratory global reference frame and the pelvis. In addition to the standard calculation of absolute angles, the offset was calculated by subtracting the corresponding static posture angle from all joint rotations (Leardini et al., 2007).

Total joint range of motion was calculated from peak values (maxima and minima). Then the mean range of motion was calculated from the 20 gait cycles for each joint rotation for each limb. A symmetry index (SI) was calculated using the equation described by Robinson et al. (1987), where:

$$SI = \{(\text{value RJ} - \text{value LJ}) \div [0.5 \times (\text{value RJ} + \text{value LJ})]\} \times 100$$

In this equation, RJ corresponds to the right joint range of motion value and LJ to the left joint range of motion value. The SI yields a percentage value, which in the case of perfect symmetry is equal to 0%.

Statistical Analysis

Data are reported as means ± standard deviations. The normality of the distribution of each variable was verified with a Shapiro–Wilk test, and equality of variances was analyzed with a Levene's test.

A Student independent samples *t*-test or Mann–Whitney *U* test was used to compare the baseline data between groups (i.e., $G_{LLD\leq 1cm}$ vs. $G_{LLD>1cm}$).

A two-way ANOVA with repeated measures was carried out to analyze the effect of the OI on each variable as a function of the group, with the orthosis condition (with/without OI) as the within-subjects factor and the group ($G_{LLD\leq 1cm}$ vs. $G_{LLD>1cm}$) as the between-subjects factor. Separate ANOVAs were carried out for the longer and shorter legs. Sphericity was verified with a Mauchley test, and if it was not met, the significance of the *F*-ratios was adjusted according to the Greenhouse–Geisser procedure or the Huyn–Feldt procedure.

TABLE 1 | Sociodemographic, anthropometric characteristics, and pain ratings of the subjects included in each group.

	$G_{LLD\leq 1cm}$	$G_{LLD>1cm}$
	***n* = 16**	***n* = 30**
Men (%)	43.8%	53.3%
Age (years)	33.4 ± 12.1	35.5 ± 12.4
Body mass (kg)	70.4 ± 13.1	71.6 ± 12.2
Height (m)	1.74 ± 0.10	1.73 ± 0.09
Body mass index (kg m^{-2})	23.2 ± 3.0	23.8 ± 2.7
Leg length discrepancy (mm)	8.3 ± 1.4	15.1 ± 4.0[a]

[a] *Significant difference between groups ($p < 0.001$).*

When significant differences were obtained, a Bonferroni *post-hoc* test was conducted to determine where the differences lay.

Statistical significance was set at $p < 0.05$, and all analyses were performed with Statistica software (version 10.0, Statsoft®, Tulsa, OK, United States).

RESULTS

A total of 46 subjects with anatomic LLD were included in the study (**Table 1**). Sixteen subjects had an LLD ≤ 1.0 cm, and 30 had an LLD between 1.0 and 3.0 cm. In 14 cases, the shorter leg was on the left, and in 32 cases, it was on the right. There were no significant between-group differences for sex ($p = 0.536$), age ($p = 0.585$), body mass ($p = 0.775$), height ($p = 0.787$), body mass index ($p = 0.512$), or pain rating ($p = 0.768$; **Table 1**). All the average normalized kinematic curves for each group ($G_{LLD\leq 1cm}$ and $G_{LLD>1cm}$) without and with orthotic insoles during the gait cycle have been added in the **Supplementary Material**.

Stance Phase

There was a significant effect of the OI on the SI, with an improvement in the symmetry of pelvic motion in the frontal plane ($p = 0.001$) and ankle motion in the sagittal plane ($p = 0.010$; **Table 2**). Although, there was a significant effect of the OI on the hip SI in the frontal plane according to the ANOVA ($p =$

TABLE 2 | Symmetry index (with joint range of motion) between the longer and shorter legs for the sagittal, frontal, and transverse planes for the pelvis, hip, knee, and ankle with or without orthotic insoles (OIs) in both groups during the stance and swing phases.

Phase	Joint	Plane	Without OI		With OI		Orthosis effect (p value)	Group effect (p-value)	Combined effect (p-value)
			$G_{LLD \leq 1cm}$	$G_{LLD > 1cm}$	$G_{LLD \leq 1cm}$	$G_{LLD > 1cm}$			
Stance phase	Pelvis	Sagittal (anterior/posterior tilt)	16.5 ± 14.1	19.9 ± 16.3	15.2 ± 15.2	20.0 ± 16.6	0.803	0.340	0.786
		Frontal (upward/downward tilt)	10.8 ± 8.0	14.4 ± 8.2	7.1 ± 6.0	11.2 ± 7.5	**0.001***	0.085	0.780
		Transverse (internal/external rotation)	5.6 ± 6.1	8.1 ± 7.7	5.6 ± 4.2	8.3 ± 13.3	0.974	0.296	0.949
	Hip	Sagittal (flexion/extension)	4.4 ± 3.6	3.9 ± 2.8	4.9 ± 3.4	3.8 ± 3.1	0.552	0.408	0.345
		Frontal (adduction/abduction)	15.4 ± 9.2	13.4 ± 9.2	10.6 ± 8.1	12.7 ± 10.5	**0.027***	0.992	0.105
		Transverse (internal/external rotation)	25.6 ± 23.5	33.6 ± 25.8	24.6 ± 23.3	29.6 ± 23.9	0.434	0.344	0.633
	Knee	Sagittal (flexion/extension)	8.8 ± 6.1	11.1 ± 8.3	9.8 ± 6.8	11.4 ± 7.1	0.535	0.334	0.718
		Frontal (adduction/abduction)	24.1 ± 13.7	26.5 ± 20.2	22.3 ± 16.9	30.6 ± 22.1	0.699	0.302	0.345
		Transverse (internal/external rotation)	29.2 ± 24.9	27.0 ± 18.0	24.3 ± 24.1	25.6 ± 18.2	0.270	0.936	0.538
	Ankle	Sagittal (dorsiflexion/plantar flexion)	17.3 ± 7.3	18.1 ± 11.5	13.6 ± 9.5	15.2 ± 10.8	**0.010***	0.688	0.719
		Frontal (inversion/eversion)	24.8 ± 16.5	25.4 ± 17.4	26.0 ± 19.1	24.6 ± 16.5	0.934	0.941	0.619
		Transverse (internal/external rotation)	36.8 ± 25.5	30.9 ± 22.2	28.8 ± 22.1	27.8 ± 19.7	0.115	0.564	0.487
Swing phase	Pelvis	Sagittal (anterior/postrior tilt)	27.2 ± 14.8	30.4 ± 24.7	35.7 ± 24.0	29.0 ± 25.2	0.320	0.781	0.168
		Frontal (upward/downward tilt)	19.3 ± 12.5	16.9 ± 10.3	17.4 ± 10.5	13.9 ± 9.7	0.054	0.342	0.646
		Transverse (internal/external rotation)	9.7 ± 7.4	11.1 ± 9.3	10.9 ± 9.0	14.6 ± 19.1	0.248	0.475	0.574
	Hip	Sagittal (flexion/extension)	5.0 ± 3.5	5.0 ± 4.6	5.7 ± 4.5	5.0 ± 3.9	0.469	0.757	0.531
		Frontal (adduction/abduction)	21.4 ± 22.7	22.1 ± 20.4	17.5 ± 17.0	22.2 ± 17.4	0.334	0.634	0.309
		Transverse (internal/external rotation)	34.9 ± 26.4	41.2 ± 30.7	37.3 ± 34.4	37.4 ± 24.8	0.864	0.695	0.419
	Knee	Sagittal (flexion/extension)	3.0 ± 1.6	3.7 ± 2.9	3.2 ± 1.6	3.3 ± 2.7	0.778	0.554	0.351
		Frontal (adduction/abduction)	30.9 ± 23.4	42.1 ± 27.6	31.9 ± 18.9	47.4 ± 35.3	0.509	0.083	0.649
		Transverse (internal/external rotation)	30.3 ± 27.0	29.5 ± 22.5	26.7 ± 21.6	26.6 ± 18.3	0.430	0.934	0.924
	Ankle	Sagittal (dorsiflexion/plantar flexion)	14.4 ± 9.5	15.4 ± 13.4	13.2 ± 9.5	15.5 ± 15.4	0.737	0.657	0.668
		Frontal (inversion/eversion)	33.1 ± 19.9	40.8 ± 31.0	28.4 ± 18.6	35.7 ± 31.1	0.294	0.299	0.968
		Transverse (internal/external rotation)	33.0 ± 28.0	31.1 ± 28.3	31.8 ± 25.9	25.9 ± 23.1	0.183	0.619	0.414

**Significant difference ($p < 0.05$).*

0.027), the Bonferroni *post-hoc* test did not show any significant differences between the conditions ($p = 0.067$).

There was a significant effect of group on the kinematics of several joints. On the side of the longer leg, peak hip adduction was greater ($p = 0.041$), and peak downward lateral pelvic tilt ($p = 0.035$) and peak hip abduction were lower ($p = 0.044$) in the $G_{LLD>1cm}$ (**Table 3**). On the side of the shorter leg, peak upward pelvic tilt (**Figure 3**) was greater ($p = 0.011$), and

TABLE 3 | Peak stance phase angles of the pelvis, hip, knee, and ankle joints for each leg with and without orthotic insoles (OIs) for both groups.

			Without OI		With OI		Orthosis effect (*p*-value)	Group effect (*p*-value)	Combined effect (*p*-value)
			$G_{LLD \leq 1cm}$	$G_{LLD > 1cm}$	$G_{LLD \leq 1cm}$	$G_{LLD > 1cm}$			
Pelvis	Anterior tilt peak	Long	10.2 ± 4.0	10.8 ± 5.7	10.7 ± 3.5	10.9 ± 6.0	0.202	0.803	0.403
		Short	10.2 ± 4.0	10.8 ± 5.6	10.7 ± 3.5	10.9 ± 6.0	0.226	0.798	0.302
	Upward pelvic tilt peak	Long	4.6 ± 1.9	5.8 ± 2.3	4.8 ± 1.8	5.9 ± 2.3	0.417	0.083	0.580
		Short	4.1 ± 1.5	2.5 ± 1.9	4.1 ± 1.7	2.8 ± 2.0	**0.021***	**0.011***	**0.044***
	Internal rotation peak	Long	5.4 ± 2.8	3.7 ± 2.6	5.2 ± 2.7	3.8 ± 2.6	0.716	0.058	0.398
		Short	5.7 ± 2.3	5.5 ± 2.3	6.0 ± 2.5	5.1 ± 2.2	0.820	0.477	**0.011***
	Posterior tilt peak	Long	7.4 ± 4.5	8.6 ± 5.9	8.1 ± 3.9	8.6 ± 6.2	0.239	0.615	0.203
		Short	7.5 ± 4.4	8.5 ± 5.8	8.2 ± 3.9	8.4 ± 6.1	0.182	0.726	0.122
	Downward pelvic tilt peak	Long	−1.3 ± 1.4	−0.1 ± 1.8	−1.5 ± 1.6	−0.5 ± 1.7	**0.003***	**0.035***	0.316
		Short	−2.3 ± 1.7	−3.9 ± 1.9	−2.3 ± 1.5	−3.7 ± 2.0	0.267	**0.012***	0.213
	External rotation peak	Long	−5.3 ± 2.7	−5.2 ± 2.4	−5.6 ± 3.0	−4.8 ± 2.3	0.692	0.592	**0.041***
		Short	−5.0 ± 3.1	−3.7 ± 2.6	−4.9 ± 3.1	−3.7 ± 2.7	0.686	0.14	0.627
Hip	Flexion peak	Long	29.4 ± 4.8	31.5 ± 8.1	30.2 ± 4.5	31.5 ± 8.1	0.325	0.434	0.359
		Short	28.8 ± 5.5	30.5 ± 7.9	30.1 ± 5.1	30.9 ± 8	**0.013***	0.576	0.143
	Extension peak	Long	−8.8 ± 4.8	−8.5 ± 7.0	−8.5 ± 4.9	−8.8 ± 7.3	0.985	0.993	0.48
		Short	−9.7 ± 5.2	−9.9 ± 7.3	−9.1 ± 5.5	−10.1 ± 7.7	0.496	0.795	0.324
	Adduction peak	Long	7.7 ± 3.5	9.9 ± 2.9	7.9 ± 3.8	9.8 ± 2.7	0.612	**0.041***	0.373
		Short	7.2 ± 2.8	5.8 ± 3.5	7.2 ± 2.8	6.1 ± 3.7	0.128	0.221	0.114
	Abduction peak	Long	−0.7 ± 3.3	1.3 ± 2.6	−0.6 ± 3.4	1.0 ± 2.5	0.366	**0.044***	0.08
		Short	−2.3 ± 3.0	−3.0 ± 3.7	−2.1 ± 2.5	−2.6 ± 3.9	**0.046***	0.578	0.343
	Internal rotation peak	Long	5.6 ± 7.9	5.2 ± 7.5	7.3 ± 8.2	4.9 ± 7.6	0.297	0.554	0.136
		Short	6.2 ± 9.4	4.7 ± 7.4	6.0 ± 8.2	4.2 ± 7.7	0.600	0.482	0.829
	External rotation peak	Long	−2.6 ± 7.0	−3.3 ± 7.4	−1.5 ± 6.4	−3.8 ± 7.4	0.644	0.491	0.186
		Short	−2.2 ± 8.2	−5.1 ± 7.7	−2.8 ± 6.7	−5.7 ± 7.5	0.409	0.200	0.911
Knee	Flexion peak	Long	24.8 ± 4.6	23.2 ± 4.5	25.4 ± 5.1	23.5 ± 5.2	0.102	0.247	0.558
		Short	24.2 ± 3.9	22.6 ± 3.9	24.3 ± 3.5	22.5 ± 4.6	0.997	0.164	0.728
	Extension peak	Long	−3.8 ± 3.3	−2.6 ± 4.2	−4.1 ± 3.7	−2.7 ± 4.1	0.434	0.288	0.630
		Short	−4.5 ± 2.7	−3.7 ± 3.6	−4.5 ± 3.6	−3.5 ± 3.7	0.636	0.402	0.772
	Adduction peak	Long	2.9 ± 3.9	2.6 ± 3.7	3.3 ± 4.5	2.6 ± 3.5	0.325	0.671	0.424
		Short	2.7 ± 3.7	2.4 ± 3.9	2.8 ± 3.7	2.3 ± 4.0	0.989	0.699	0.655
	Abduction peak	Long	−1.9 ± 3.6	−2.4 ± 3.6	−1.9 ± 3.8	−2.5 ± 3.2	0.639	0.606	0.744
		Short	−2.5 ± 3.4	−2.2 ± 3.5	−1.8 ± 3.7	−2.8 ± 3.8	0.854	0.066	**0.006***
	Internal rotation peak	Long	−12.1 ± 7.3	−10.4 ± 9.9	−14.0 ± 7.3	−10.3 ± 9.8	0.196	0.315	0.170
		Short	−10.4 ± 8.4	−8.9 ± 7.2	−9.6 ± 7.1	−9.2 ± 8.0	0.745	0.659	0.531
	External rotation peak	Long	−25.3 ± 8.5	−23.7 ± 9.9	−27.4 ± 10.2	−23.3 ± 9.8	0.221	0.335	0.097
		Short	−25.1 ± 9.3	−21.8 ± 8.7	−23.5 ± 8.4	−22.0 ± 9.8	0.442	0.370	0.316
Ankle	Dorsiflexion peak	Long	14.4 ± 4.1	14.7 ± 2.9	13.8 ± 4.0	14.4 ± 3.2	**0.011***	0.708	0.449
		Short	11.3 ± 4.6	12.0 ± 3.6	11.5 ± 4.5	12.6 ± 3.5	**0.028***	0.457	0.277
	Plantar flexion peak	Long	−7.3 ± 4.4	−6.6 ± 2.4	−7.0 ± 4.4	−6.1 ± 2.5	**0.012***	0.416	0.707
		Short	−7.5 ± 4.1	−6.8 ± 3.3	−7.2 ± 4.3	−6.5 ± 3.6	0.187	0.525	0.892
	Inversion peak	Long	12.4 ± 3.7	12 ± 3.5	13.1 ± 3.6	12.3 ± 3.4	**0.018***	0.570	0.365
		Short	14.7 ± 4.8	12.5 ± 3.8	14.7 ± 4.1	12.7 ± 3.7	0.712	0.092	0.760
	Eversion peak	Long	2.6 ± 3.3	2.0 ± 3.1	3.0 ± 3.3	2.9 ± 2.8	**0.001***	0.737	0.193
		Short	3.3 ± 3.2	3.2 ± 3.3	3.2 ± 3.7	3.7 ± 3.2	0.337	0.854	0.168
	Internal rotation peak	Long	−2.9 ± 6.5	−6.8 ± 4.9	−3.4 ± 7.0	−6.5 ± 5.9	0.700	0.054	0.328
		Short	−3.9 ± 4.2	−4.0 ± 5.2	−3.5 ± 4.1	−4.7 ± 5.2	0.542	0.641	**0.023***
	External rotation peak	Long	−8.5 ± 6.5	−11.4 ± 5.1	−8.9 ± 6.4	−11.3 ± 5.9	0.627	0.150	0.455
		Short	−9.6 ± 3.7	−9.1 ± 5.3	−9.2 ± 3.3	−9.5 ± 4.9	0.854	0.938	0.084

**Significant difference ($p < 0.05$).*

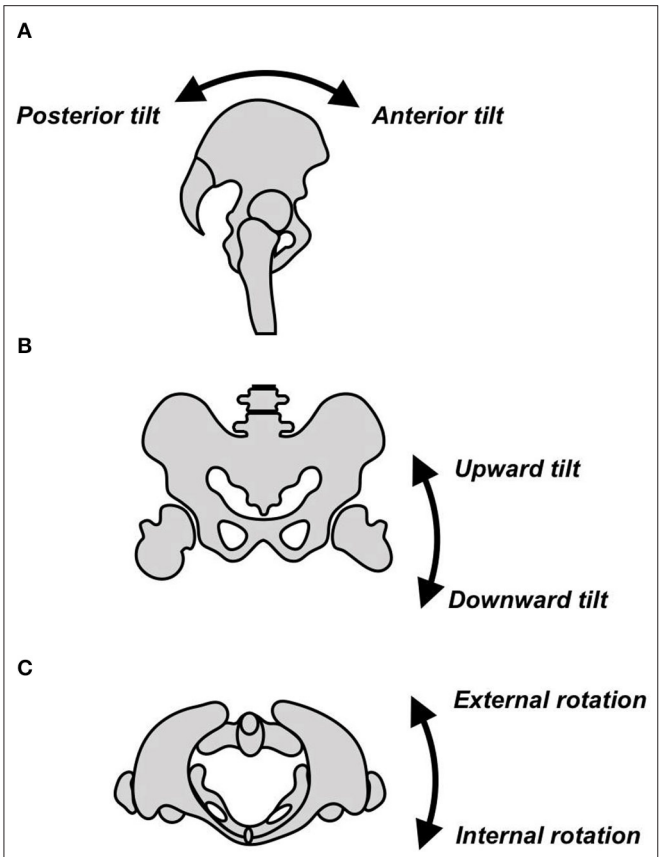

FIGURE 3 | Movement of the pelvis in **(A)** the sagittal plane, **(B)** the frontal plane, and **(C)** the transverse plane.

peak downward lateral pelvic tilt was lower ($p = 0.012$) in the $G_{LLD \leq 1cm}$.

There was a significant effect of OI on the kinematics of several joints. On the side of the longer leg, peak downward lateral pelvic tilt ($p = 0.003$) and peak ankle inversion ($p = 0.018$) were significantly increased with the OI compared to without the OI. Peak ankle eversion ($p = 0.001$), peak ankle dorsiflexion ($p = 0.011$), and peak ankle plantarflexion ($p = 0.012$) were significantly decreased with the OI (**Table 3**). On the side of the shorter leg, peak upward lateral pelvic tilt angle ($p = 0.021$), peak hip flexion angle ($p = 0.013$), and peak ankle dorsiflexion angle ($p = 0.028$) were significantly increased, and peak hip abduction angle ($p = 0.046$) was significantly decreased with the OI.

Although the ANOVA showed an interaction between OI and group for the shorter leg for peak ankle internal rotation ($p = 0.023$) and peak knee abduction ($p = 0.006$), the Bonferroni *post-hoc* test indicated there were no significant differences between these factors. There was a significant interaction between OI and group for peak upward pelvic tilt on the side of the shorter leg: the Bonferroni *post-hoc* test indicated that without the OI, peak upward pelvic tilt was greater in the $G_{LLD \leq 1cm}$ ($p = 0.044$) than the $G_{LLD > 1cm}$.

There was a significant interaction between OI and group for peak upward pelvic tilt: the Bonferroni *post-hoc* test indicated that with the OI, peak upward pelvic tilt increased significantly in the $G_{LLD > 1cm}$ ($p = 0.04$), compared to without the OI.

Swing Phase

There was a significant effect of group on the SI for several joints. On the side of the longer leg, peak upward pelvic tilt and peak hip adduction angle ($p = 0.007$) were significantly lower in the $G_{LLD \leq 1cm}$ ($p = 0.009$), and downward lateral pelvic tilt was greater ($p = 0.013$; **Table 4**). On the side of the shorter leg, peak external pelvic rotation was significantly greater in the $G_{LLD \leq 1cm}$ ($p = 0.014$).

There was a significant effect of OI on the kinematics of several joints. On the side of the longer leg, peak upward pelvic tilt ($p = 0.001$), peak knee flexion decreased ($p = 0.003$), and peak downward pelvic tilt ($p = 0.013$) increased significantly with the OI (**Table 4**).

On the side of the shorter leg, there was a significant increase in peak ankle dorsiflexion ($p < 0.001$).

Pain

There was a significant effect of OI on pain ($p < 0.001$). The pain reduced from 5.9 ± 1.8 to 1.7 ± 2.1 in $G_{LLD \leq 1cm}$ and from 5.7 ± 2.6 to 2.0 ± 2.5 in $G_{LLD > 1cm}$. There was no group effect ($p = 0.929$) (**Table 5**).

DISCUSSION

The aim of this study was to evaluate the immediate effect of OI on gait kinematics and pain in subjects with mild LLD according to two groups of the leg length discrepancy.

The results of this study demonstrated that gait symmetry improved with the OI, particularly at the pelvis (frontal plane) and ankle (sagittal plane) during the stance phase of gait, with no between-group differences. Moreover, there was a significant reduction in pain with the OI (with no between-group differences). The kinematic results support the findings of a number of studies that showed that even mild LLD can alter the kinematics of gait and cause pain (Perttunen et al., 2004; Defrin et al., 2005; Golightly et al., 2007; Seeley et al., 2010; Khamis and Carmeli, 2018). The results of this study add to this body of knowledge by showing that even LLD < 1 cm can alter symmetry and cause pain, and that both symmetry and pain can be improved with OI.

The results of this study confirm previous findings that deviations of pelvic motion in the frontal plane are common in LLD (Giles, 1981; Giles and Taylor, 1982; Walsh et al., 2000; Golightly et al., 2007; Jamaluddin et al., 2011; Resende et al., 2016). There was a significant increase in peak pelvic downward lateral tilt on the side of the longer leg with the OI, and a concomitant increase in peak upward lateral tilt on the side of the shorter leg ($p = 0.021$) in both groups with the OI. Similar results have previously been found with the use of OI in subjects with moderate and severe LLD (Bangerter et al., 2019). The present results showed that OIs have a similar effect in mild LLD $\leq$ 1 and >1 cm. The increase in ankle dorsiflexion on the

TABLE 4 | Peak swing phase angles of the pelvis, hip, knee, and ankle joints for each leg with and without orthotic insoles (OI) for both groups.

			Without OI		With OI		Orthosis effect (*p*-value)	Group effect (*p*-value)	Combined effect (*p*-value)
			$G_{LLD \leq 1cm}$	$G_{LLD > 1cm}$	$G_{LLD \leq 1cm}$	$G_{LLD > 1cm}$			
Pelvis	Anterior tilt peak	Long	9.9 ± 4.0	10.5 ± 5.6	10.4 ± 3.5	10.5 ± 5.9	0.295	0.826	0.242
		Short	9.8 ± 4.2	10.6 ± 5.7	10.4 ± 3.6	10.6 ± 6.1	0.209	0.767	0.294
	Upward pelvic tilt peak	Long	0.7 ± 1.3	2.1 ± 1.6	0.5 ± 1.5	1.7 ± 1.6	**0.001***	**0.009***	0.175
		Short	−0.6 ± 1.7	−1.7 ± 2.0	−0.6 ± 1.7	−1.6 ± 2.0	0.418	0.077	0.654
	Internal rotation peak	Long	4.3 ± 3.0	3.0 ± 2.8	4.3 ± 3.1	3.0 ± 3.0	0.983	0.168	0.87
		Short	4.6 ± 2.7	4.5 ± 2.3	4.8 ± 3.0	4.2 ± 2.3	0.473	0.615	0.101
	Posterior tilt peak	Long	7.5 ± 4.5	8.4 ± 5.7	8.2 ± 4.0	8.4 ± 6.1	0.255	0.758	0.177
		Short	7.4 ± 4.4	8.7 ± 5.9	8.1 ± 3.9	8.7 ± 6.2	0.212	0.579	0.165
	Downward pelvic tilt peak	Long	−4.0 ± 1.5	−2.5 ± 1.9	−4.1 ± 1.7	−2.8 ± 2.0	**0.013***	**0.013***	0.127
		Short	−4.6 ± 1.9	−5.8 ± 2.3	−4.7 ± 1.7	−5.9 ± 2.3	0.502	0.073	0.672
	External rotation peak	Long	−5.4 ± 2.3	−5.0 ± 2.3	−5.5 ± 2.4	−4.7 ± 2.2	0.469	0.459	0.173
		Short	−5.1 ± 2.4	−3.2 ± 2.2	−4.9 ± 2.5	−3.2 ± 2.2	0.617	**0.014***	0.425
Hip	Flexion peak	Long	31.6 ± 5.1	33.7 ± 7.3	31.8 ± 4.9	33.4 ± 7.5	0.890	0.367	0.515
		Short	30.4 ± 5.9	32.1 ± 7.7	31.3 ± 5.2	32.5 ± 8	0.092	0.521	0.435
	Extension peak	Long	−5.8 ± 4.7	−5.7 ± 6.6	−5.2 ± 4.6	−5.8 ± 6.9	0.461	0.897	0.355
		Short	−6.3 ± 5.5	−6.6 ± 7.2	−5.7 ± 5.4	−6.7 ± 7.5	0.567	0.765	0.312
	Adduction peak	Long	1.1 ± 3.3	3.9 ± 2.6	1.2 ± 3.7	3.6 ± 2.5	0.363	**0.007***	0.163
		Short	−0.1 ± 2.7	−0.6 ± 3.6	0.0 ± 2.3	−0.4 ± 3.8	0.092	0.673	0.34
	Abduction peak	Long	−4.7 ± 3.4	−2.7 ± 2.6	−4.4 ± 3.4	−2.8 ± 2.6	0.720	0.051	0.089
		Short	−5.6 ± 2.6	−6.5 ± 3.4	−5.4 ± 2.1	−6.3 ± 3.5	0.091	0.350	0.582
	Internal rotation peak	Long	5.5 ± 7.4	4.6 ± 7.6	6.7 ± 7.6	4.1 ± 7.5	0.651	0.438	0.179
		Short	5.1 ± 8.9	3.5 ± 7.0	5.1 ± 7.5	2.8 ± 7.4	0.614	0.374	0.609
	External rotation peak	Long	−2.5 ± 6.8	−3.0 ± 7.3	−1.2 ± 6.2	−3.7 ± 7.4	0.603	0.482	0.124
		Short	−2.0 ± 8.3	−4.4 ± 7.6	−2.2 ± 7.0	−5.1 ± 7.3	0.478	0.243	0.691
Knee	Flexion peak	Long	65.0 ± 3.3	65.0 ± 4.4	63.9 ± 3.1	64.4 ± 4.5	**0.003***	0.834	0.319
		Short	62.7 ± 3.4	63.0 ± 4.2	62.0 ± 3.3	63.0 ± 4.3	0.256	0.594	0.24
	Extension peak	Long	−3.6 ± 3.6	−2.7 ± 4.3	−4.1 ± 4.0	−2.8 ± 4.1	0.193	0.369	0.425
		Short	−4.6 ± 3.4	−3.5 ± 3.9	−4.6 ± 3.7	−3.4 ± 3.9	0.688	0.308	0.644
	Adduction peak	Long	6.7 ± 5.6	6.2 ± 5.5	7.4 ± 6.5	5.7 ± 5.3	0.828	0.505	0.262
		Short	5.8 ± 5.3	5.3 ± 4.9	5.5 ± 4.9	4.6 ± 4.6	0.314	0.635	0.636
	Abduction peak	Long	−2.8 ± 3.7	−2.9 ± 4.1	−2.3 ± 4.3	−2.9 ± 3.6	0.286	0.783	0.249
		Short	−3.7 ± 2.8	−3.0 ± 4.3	−2.9 ± 2.8	−3.4 ± 4.3	0.528	0.913	0.162
	Internal rotation peak	Long	−16.6 ± 6.2	−15.3 ± 9.2	−18.3 ± 7.6	−15.3 ± 8.9	0.218	0.400	0.176
		Short	−15.1 ± 8.2	−12.7 ± 7.1	−14.5 ± 7.9	−13.0 ± 8.2	0.794	0.394	0.587
	External rotation peak	Long	−28.6 ± 9.1	−26.7 ± 9.1	−30.3 ± 10.2	−26.7 ± 8.5	0.233	0.319	0.199
		Short	−26.5 ± 8.9	−24.0 ± 7.8	−25.4 ± 8.3	−24.7 ± 8.1	0.831	0.522	0.217
Ankle	Dorsiflexion peak	Long	3.2 ± 4.9	3.8 ± 3.8	2.7 ± 4.6	4.0 ± 4.2	0.523	0.449	0.207
		Short	0.9 ± 4.2	2.5 ± 3.3	2.0 ± 3.6	3.6 ± 2.9	**0.001***	0.124	0.886
	Plantar flexion peak	Long	−18.2 ± 7.9	−16.1 ± 5.1	−18.4 ± 7.3	−16.5 ± 5.5	0.367	0.291	0.869
		Short	−21.4 ± 8.4	−18.2 ± 6.1	−20.9 ± 7.8	−17.5 ± 6.2	0.092	0.120	0.706
	Inversion peak	Long	12.4 ± 3.9	11.7 ± 3.4	13.0 ± 4.0	11.8 ± 3.6	0.068	0.390	0.251
		Short	14.8 ± 4.9	12.4 ± 3.8	15.0 ± 4.0	12.7 ± 3.5	0.402	0.056	0.891
	Eversion peak	Long	4.8 ± 3.6	5.4 ± 4.4	5.1 ± 4.1	5.7 ± 4.2	0.324	0.660	0.87
		Short	6.4 ± 4.2	6.2 ± 3.8	6.6 ± 4.5	6.1 ± 3.4	0.896	0.793	0.557
	Internal rotation peak	Long	−2.4 ± 7.9	−6.1 ± 5.1	−3.1 ± 7.7	−6.1 ± 6.1	0.350	0.092	0.360
		Short	−3.0 ± 5.0	−3.2 ± 5.6	−2.9 ± 5.0	−3.7 ± 5.5	0.359	0.768	0.299
	External rotation peak	Long	−14.5 ± 7.5	−16.1 ± 6.0	−15.4 ± 7.5	−16.3 ± 6.8	0.119	0.559	0.336
		Short	−13.1 ± 5.5	−13.3 ± 6.0	−13.2 ± 5.0	−13.6 ± 6.0	0.330	0.877	0.665

**Significant difference ($p < 0.05$).*

TABLE 5 | Localization of pain of the subjects included in each group.

	$G_{LLD \leq 1cm}$		$G_{LLD > 1cm}$	
	$n = 16$		$n = 30$	
Low back pain	9		17	
Hip pain	4		3	
Knee pain	3		4	
Ankle pain	0		6	
	$G_{LLD \leq 1cm}$		$G_{LLD > 1cm}$	
	Without OI	**With OI**	**Without OI**	**With OI**
Visual analog scale scores	5.9 ± 1.8	1.7 ± 2.1	5.7 ± 2.6	2.0 ± 2.5

longer leg (Walsh et al., 2000; Resende et al., 2016) and the increase in the plantar flexion on the shorter leg during stance phase are also in line with the results of previous studies (Song et al., 1997; Walsh et al., 2000; Aiona et al., 2015; Resende et al., 2016). The results of the present study showed that use of an OI significantly increased peak dorsiflexion in the shorter leg and decreased both peak dorsiflexion and peak plantar flexion in the longer leg (independently from the group). These changes likely contributed to the improvement in ankle gait symmetry shown by the SI. The kinematic alterations found at the pelvis (frontal plane) and ankle (sagittal plane) during gait without the OI are typical compensatory strategies that functionally lengthen the shorter limb and shorten the longer limb (Resende et al., 2016). The findings of the present study indicate that the OI reduced the need for such strategies.

The results of several studies in the literature contrast with those of the present study: some studies found no effect of an OI on joint kinematics during gait in mild LLD (Bandy and Sinning, 1986; Goel et al., 1997), although effects were found for moderate and severe LLD (Bangerter et al., 2019). These different results could be due to differences in the study methodologies. First, the sample sizes in both the studies by Bandy and Sinning (1986) and Goel et al. (1997) were smaller than that of the present study, and they may have been underpowered. The studies also analyzed different variables and used different types of LLD correction: Bandy and Sinning (1986) used a heel lift, while Goel et al. (1997) used a shoe lift. Although Bandy and Sinning (1986) found that the heel lift seemed to bring about more symmetrical movement, another study (Khamis and Carmeli, 2017) found that a heel lift was insufficient to affect the entire stance phase of the gait cycle.

The positive effect of the OI on symmetry found in the present study for both mild and very mild LLD was further supported by the significant reduction in pain: use of the OI immediately and significantly reduced pain in both groups, with no between-group differences. These results are clinically important since the biomechanical, postural, and functional changes caused by LLD have been shown to alter joint angles (Gurney, 2002; Campbell et al., 2018), leading to low back pain, scoliosis, pelvic and sacral misalignments, hip and knee osteoarthritis, and even stress fractures of the lower limbs (Gurney, 2002; Kendall et al., 2014; Campbell et al., 2018; Beeck et al., 2019). The reduction of pelvic obliquity with the OI likely reduced muscle overactivity (Mannello, 1992) and the distribution forces on the spinal joints, thus reducing pain (Defrin et al., 2005; Golightly et al., 2007) and potentially reducing the development of pathology in the long-term (Giles, 1981; Giles and Taylor, 1982; Cummings et al., 1993). LLD has been implicated in hip and knee pain due to inadequate distribution of mechanical loads (McCaw and Bates, 1991; McWilliams et al., 2013). Indeed, LLD results in excessive and uneven loading on the hip and/or knee and also on the mobile segments of the lumbar belt (Murray and Azari, 2015). Improvement of the gait symmetry of the pelvis in the frontal plane and of the ankle in the sagittal plane could improve the distribution of mechanical loads throughout the lower limb and thus significantly reduce associated pain. These results are in line with the current literature, which shows that OI can reduce pain in subjects with mild LLD (Defrin et al., 2005; Golightly et al., 2007; Menez et al., 2020). In addition, as reported by Defrin et al. (2005) who evaluated only the effect of insoles on low back pain, very mild LLD can be the source of pain, and the shoe inserts can be a suitable therapeutic solution to reduce pain. Longitudinal studies are now required to determine the long-term effect of OI on chronic pain.

As found in a previous study (Resende et al., 2016), peak hip flexion was increased, and peak hip abduction was decreased on the side of the shorter leg during stance without the OI. Although these deviations were reduced with the OI, the SI did not change for these joints in either group, suggesting that the use of the OI was insufficient to correct them. This was also the case for ankle inversion–eversion during stance on the side of the longer leg, as well as the deviations found in pelvic, knee, and ankle motion during swing phase (**Table 4**). Several factors could explain the lack of normalization of these kinematic parameters with the OI. First, it is possible that the trim magnitude of the OI was too low (the correction applied was 50% of the magnitude of the LLD). Clinically, it may be worthwhile to carry out repeated kinematic analyses with OI of different magnitudes until all joint kinematics become symmetrical left–right. Second, and more likely, the compensatory strategies for the LLD were well-established in these individuals with anatomical LLD, and it is thus unsurprising that their strategies could not be changed in a single session of walking with OI. Moreover, the compensatory biomechanical strategies used by subjects with LLD are complex (Menez et al., 2020). Further studies are required to assess the longer-term effects of OI on gait kinematics.

The present study adds to the current body of literature on LLD by providing more extensive kinematic data. Together, these results confirm that even mild LLD alters gait kinematics.

However, new studies are essential to continue to optimize the management of subjects in the field of podiatry. These future studies will need to consider some of the limitations identified throughout this work. This study was not a randomized controlled trial, and neither the examiner nor the participants were blinded that can lead to a placebo effect of OI for pain assessment. For pain analysis, we have adapted to the field conditions using a visual analog scale. In the clinical and research field, the visual analog scale is widely used and accepted (Hayashi et al., 2015). We have tried to limit the potential bias that comes

with the subjective declaration of the visual analog scale by asking subjects to be as truthful as possible in their evaluations. Future trials should be blinded to reduce this potential bias. On the other hand, more precise questionnaires should be implemented in order to situate and define pain more accurately, as some previous studies have done (Defrin et al., 2005; Golightly et al., 2007). For the SI, we can observe (**Table 2**) that some SIs are higher for the $G_{LLD \leq 1cm}$ than for the $G_{LLD>1cm}$ (especially in the transverse plane). A limitation of the SI is the potential for artificial inflation. This inflation can occur when the observed variables have small changes that can lead to large changes in the SI (Cabral et al., 2016). Finally, it would be interesting to highlight other aspects of motion analysis that could complete and explain some of our results. Indeed, with a kinetic approach, Aiona et al. (2015) and Song et al. (1997) put forward a more important mechanical work of the long leg, therefore possibly a more important articular, muscular, and tendinous work, which was confirmed by Perttunen et al. (2004). In future studies, it would be interesting to supplement the kinematic data with kinetic variables coupled with electromyographic analysis to refine the understanding of the effect of OI on changes in the biomechanics of locomotion.

CONCLUSION

This study contributes to a better understanding of the effect of OI on gait kinematics observed in subjects with mild LLD. OI immediately significantly improved the articular symmetry of the pelvis in the frontal plane and of the ankle in the sagittal plane, regardless of the height of LLD (i.e., LLD $\leq$ 1 cm vs. LLD $>$ 1 cm $<$ 3 cm). In addition, our study confirms that OI significantly reduces pain in subjects with mild LLD. Therefore, we can recommend treatment of mild LLD with OI, even when LLD $\leq$ 1 cm. This study contributes to a better understanding of the effect of OI on gait kinematics in subjects with mild LLD and provides valuable information for clinicians. Nevertheless, future studies could complement this research and shed new light on this research subject.

DATA AVAILABILITY STATEMENT

The raw data supporting the conclusions of this article will be made available by the authors, without undue reservation.

ETHICS STATEMENT

Ethical review and approval was not required for the study on human participants in accordance with the local legislation and institutional requirements. The patients/participants provided their written informed consent to participate in this study.

AUTHOR CONTRIBUTIONS

All of the named authors meet the criteria for authorship. CM was the principal investigator. He co-designed the study, over-saw the project, contributed to the interpretation of the data, revised the study report for intellectual content, and approved the version to be published. JC co-designed the study, contributed to the interpretation of the data, coordinate the project, contributed to the drafting of the manuscript, revised it for intellectual content, and approved the version to be published. ML'H co-designed the study, coordinated the project, revised the report for intellectual content, and approved the version to be published.

FUNDING

This study was funded as a Ph.D. grant by the French National Association of Research and Technology (grant CIFRE n°2016/1120) and Normandie Univ, UNIROUEN, CETAPS, 76000 Rouen, France.

SUPPLEMENTARY MATERIAL

The Supplementary Material for this article can be found online at: https://www.frontiersin.org/articles/10.3389/fspor.2020.579152/full#supplementary-material

REFERENCES

Aiona, M., Do, K. P., Emara, K., Dorociak, R., and Pierce, R. (2015). Gait patterns in children with limb length discrepancy. *J. Pediatr. Orthop.* 35, 280–284. doi: 10.1097/BPO.0000000000000262

Bandy, W. D., and Sinning, W. E. (1986). Kinematic effects of heel lift use to correct lower limb length differences. *J. Orthop. Sports Phys. Ther.* 7, 173–179. doi: 10.2519/jospt.1986.7.4.173

Bangerter, C., Romkes, J., Lorenzetti, S., Krieg, A. H., Hasler, C. -C., Brunner, R., et al. (2019). What are the biomechanical consequences of a structural leg length discrepancy on the adolescent spine during walking? *Gait Posture* 68, 506–513. doi: 10.1016/j.gaitpost.2018.12.040

Beattie, P., Isaacson, K., Riddle, D. L., and Rothstein, J. M. (1990). Validity of derived measurements of leg-length differences obtained by use of a tape measure. *Phys. Ther.* 70, 150–157. doi: 10.1093/ptj/70.3.150

Beeck, A., Quack, V., Rath, B., Wild, M., Michalik, R., Schenker, H., et al. (2019). Dynamic evaluation of simulated leg length inequalities and their effects on the musculoskeletal apparatus. *Gait Posture* 67, 71–76. doi: 10.1016/j.gaitpost.2018.09.022

Brady, R. J., Dean, J. B., Skinner, T. M., and Gross, T. M. (2003). Limb length inequality: clinical implications for assessment and intervention. *J. Orthop. Sports Phys. Ther.* 33, 221–234. doi: 10.2519/jospt.2003.33.5.221

Cabral, S., Resende, R. A., Clansey, A. C., Deluzio, K. J., Selbie, W. S., and Veloso, A. P. (2016). A global gait asymmetry index. *J. Appl. Biomech.* 32, 171–177. doi: 10.1123/jab.2015-0114

Campbell, T. M., Ghaedi, B. B., Ghogomu, E. T., and Welch, V. (2018). Shoe lifts for leg length discrepancy in adults with common painful musculoskeletal conditions: a systematic review of the literature. *Arch. Phys. Med. Rehabil.* 99:981–993.e2. doi: 10.1016/j.apmr.2017.10.027

Cappozzo, A., Catani, F., Della Croce, U., and Leardini, A. (1995). Position and orientation in space of bones during movement: anatomical frame definition and determination. *Clin Biomech.* 10, 171–178. doi: 10.1016/0268-0033(95)91394-T

Cummings, G., Scholz, J. P., and Barnes, K. (1993). The effect of imposed leg length difference on pelvic bone symmetry. *Spine* 18, 368-373. doi: 10.1097/00007632-199303000-00012

Defrin, R., Benyamin, S. B., Aldubi, R. D., and Pick, C. G. (2005). Conservative correction of leg-length discrepancies of 10mm or less for the relief

of chronic low back pain. *Arch. Phys. Med. Rehabil.* 86, 2075-2080. doi: 10.1016/j.apmr.2005.06.012

Friberg, O. (1982). Leg length asymmetry in stress fractures. A clinical and radiological study. *J. Sports Med. Phys. Fitness* 22, 485–488.

Friberg, O. (1984). Leg length inequality and low back pain. *Lancet* 324:1039. doi: 10.1016/S0140-6736(84)91135-8

Giles, L. G. F. (1981). Lumbosacral facetal "joint angles" associated with leg length inequality. *Rheumatology* 20, 233–238. doi: 10.1093/rheumatology/20.4.233

Giles, L. G. F., and Taylor, J. R. (1982). Lumbar spine structural changes associated with leg length inequality. *Spine* 7, 159–162. doi: 10.1097/00007632-198203000-00011

Goel, A., Loudon, J., Nazare, A., Rondinelli, R., and Hassanein, K. (1997). Joint moments in minor limb length discrepancy: a pilot study. *Am. J. Orthop.* 26, 852–856.

Golightly, Y. M., Tate, J. J., Burns, C. B., and Gross, M. T. (2007). Changes in pain and disability secondary to shoe lift intervention in subjects with limb length inequality and chronic low back pain: a preliminary report. *J. Orthop. Sports Phys. Ther.* 37, 380–388. doi: 10.2519/jospt.2007.2429

Grood, E. S., and Suntay, W. J. (1983). A joint coordinate system for the clinical description of three-dimensional motions: application to the knee. *J. Biomech. Eng.* 105, 136–144. doi: 10.1115/1.3138397

Gurney, B. (2002). Leg length discrepancy. *Gait Posture* 15, 195–206. doi: 10.1016/S0966-6362(01)00148-5

Harvey, W. F. (2010). Association of leg-length inequality with knee osteoarthritis: a cohort study. *Ann. Intern. Med.* 152, 287–295. doi: 10.7326/0003-4819-152-5-201003020-00006

Hayashi, K., Ikemoto, T., Ueno, T., Arai, Y.-C. P., Shimo, K., Nishihara, M., et al. (2015). Regional differences of repeatability on visual analogue scale with experimental mechanical pain stimuli. *Neurosci. Lett.* 585:67–71. doi: 10.1016/j.neulet.2014.11.032

Jamaluddin, S., Sulaiman, A. R., Kamarul Imran, M., Juhara, H., Ezane, M. A., and Nordin, S. (2011). Reliability and accuracy of the tape measurement method with a nearest reading of 5 Mm in the assessment of leg length discrepancy. *Singapore Med. J.* 52, 681–684.

Junk, S., Terjesen, T., Rossvoll, I., and Bra°ten, M. (1992). Leg length inequality measured by ultrasound and clinical methods. *Eur. J. Radiol.* 14, 185–188. doi: 10.1016/0720-048X(92)90083-L

Kaufman, K. R., Miller, L. S., and Sutherland, D. H. (1996). Gait asymmetry in patients with limb-length inequality. *J. Pediatr. Orthop.* 16, 144–150. doi: 10.1097/01241398-199603000-00002

Kendall, J. C., Bird, A. R., and Azari, M. F. (2014). Foot posture, leg length discrepancy and low back pain - Their relationship and clinical management using foot orthoses - an overview. *Foot* 24, 75-80. doi: 10.1016/j.foot.2014.03.004

Khamis, S., and Carmeli, E. (2017). Relationship and significance of gait deviations associated with limb length discrepancy: a systematic review. *Gait Posture* 57, 115–123. doi: 10.1016/j.gaitpost.2017.05.028

Khamis, S., and Carmeli, E. (2018). The effect of simulated leg length discrepancy on lower limb biomechanics during gait. *Gait Posture* 61, 73–80. doi: 10.1016/j.gaitpost.2017.12.024

Leardini, A., Sawacha, Z., Paolini, G., Ingrosso, S., Nativo, R., and Benedetti, M. G. (2007). A new anatomically based protocol for gait analysis in children. *Gait Posture* 26, 560–571. doi: 10.1016/j.gaitpost.2006.12.018

Mannello, D. M. (1992). Leg length inequality. *J. Manipulative Physiol. Ther.* 15, 576–590.

McCaw, S. T., and Bates, B. T. (1991). Biomechanical implications of mild leg length inequality. *Br. J. Sports Med.* 25, 10–13. doi: 10.1136/bjsm.25.1.10

McWilliams, A. B., Grainger, A. J., O'Connor, P. J., Redmond, A. C., Stewart, T. D., and Stone, M. H. (2013). A review of symptomatic leg length inequality following total hip arthroplasty. *HIP Int.* 23, 6–14. doi: 10.5301/HIP.2013.10631

Menez, C., Coquart, J., Dodelin, D., Tourny, C., and L'Hermette, M. (2020). Effects of orthotic insoles on gait kinematics and low back pain in subjects with mild leg length discrepancy: a pilot study. *J. Am. Podiatr. Med. Assoc.* doi: 10.7547/18-093. [Epub ahead of print].

Moseley, C. F. (1996). *Leg Length Discrepancy and Angular Deformity of the Lower Limbs. Lovell and Winter's Pediatric Orthopedics*. 4th edn. Philadelphia, PA: Lippincott-Raven, 849–901.

Murray, K. J., and Azari, M. F. (2015). Leg length discrepancy and osteoarthritis in the knee, hip and lumbar spine. *J. Can. Chiropr. Assoc.* 59, 226–237.

Neelly, K., Wallmann, H. W., and Backus, C. J. (2013). Validity of measuring leg length with a tape measure compared to a computed tomography scan. *Physiother. Theory Pract.* 29, 487–492. doi: 10.3109/09593985.2012.755589

Perttunen, J. R., Anttila, E., Södergård, J., Merikanto, J., and Komi, P. V. (2004). Gait asymmetry in patients with limb length discrepancy. *Scand. J. Med. Sci. Sports* 14, 49–56. doi: 10.1111/j.1600-0838.2003.00307.x

Reid, D. C., and Smith, B. (1984). Leg length inequality: a review of etiology and management. *Physiother Canada* 36, 177–182.

Resende, R. A., Kirkwood, R. N., Deluzio, K. J., Cabral, S., and Fonseca, S. T. (2016). Biomechanical strategies implemented to compensate for mild leg length discrepancy during gait. *Gait Posture* 46:147–153. doi: 10.1016/j.gaitpost.2016.03.012

Robinson, R. O., Herzog, W., and Nigg, B. M. (1987). Use of force platform variables to quantify the effects of chiropractic manipulation on gait symmetry. *J. Manipulative Physiol. Ther* 10, 172–176.

Seeley, M. K., Umberger, B. R., Clasey, J. L., and Shapiro, R. (2010). The relation between mild leg-length inequality and able-bodied gait asymmetry. *J. Sports Sci. Med.* 9, 572–579.

Song, K. M., Halliday, S. E., and Little, D. G. (1997). The effect of limb-length discrepancy on gait. *J. Bone Joint Surg.* 79:1690–1698. doi: 10.2106/00004623-199711000-00011

Specht, D. L., and De, K. B. (1991). Anatomical leg length inequality, scoliosis and lordotic curve in unselected clinic patients. *J. Manipulative Physiol. Ther* 14, 368–375.

Tallroth, K., Ristolainen, L., and Manninen, M. (2017). Is a long leg a risk for hip or knee osteoarthritis? *Acta Orthop.* 88, 512–515. doi: 10.1080/17453674.2017.1348066

Von Elm, E., Altman, D. G., Egger, M., Pocock, S. J., Gøtzsche, P. C., Vandenbroucke, J. P., et al. (2014). The Strengthening the Reporting of Observational Studies in Epidemiology (STROBE) Statement: guidelines for reporting observational studies. *Int. J. Surg.* 12, 1495–1499. doi: 10.1016/j.ijsu.2014.07.013

Walsh, M., Connolly, P., Jenkinson, A., and O'Brien, T. (2000). Leg length discrepancy - an experimental study of compensatory changes in three dimensions using gait analysis. *Gait Posture* 12, 156–161. doi: 10.1016/S0966-6362(00)00067-9

White, S. C., Gilchrist, L. A., and Wilk, B. E. (2004). Asymmetric limb loading with true or simulated leg-length differences. *Clin. Orthop. Relat. Res.* 421, 287–292. doi: 10.1097/01.blo.0000119460.33630.6d

Wu, G., and Cavanagh, P. R. (1995). ISB recommendations for standardization in the reporting of kinematic data. *J. Biomech.* 28, 1257–1261. doi: 10.1016/0021-9290(95)00017-C

Wu, G., Siegler, S., Allard, P., Kirtley, C., Leardini, A., Rosenbaum, D., et al. (2002). ISB recommendation on definitions of joint coordinate system of various joints for the reporting of human joint motion-Part I: ankle, hip, and spine. *J. Biomech.* 35, 543–548. doi: 10.1016/S0021-9290(01)00222-6

Conflict of Interest: The authors declare that the research was conducted in the absence of any commercial or financial relationships that could be construed as a potential conflict of interest.

frontiers in Sports and Active Living

ORIGINAL RESEARCH
published: 20 January 2021
doi: 10.3389/fspor.2020.636428

A Model for World-Class 10,000 m Running Performances: Strategy and Optimization

Quentin Mercier[1], *Amandine Aftalion*[1] *and Brian Hanley*[2]*

[1] Centre d'Analyse et de Mathématique Sociales, CNRS UMR-8557, Ecole des Hautes Etudes en Sciences Sociales, Paris, France, [2] Carnegie School of Sport, Leeds Beckett University, Leeds, United Kingdom

The distribution of energetic resources in world-class distance running is a key aspect of performance, with athletes relying on aerobic and anaerobic metabolism to greater extents during different parts of the race. The purpose of this study is to model 10,000 m championship performances to enable a deeper understanding of the factors affecting running speed and, given that more than half the race is run on curves, to establish the effect of the bends on performance. Because a limitation of time split data is that they are typically averaged over 100-m or 1,000-m segments, we simulate two 10,000 m runners' performances and thus get access to their instantaneous speed, propulsive force and anaerobic energy. The numerical simulations provide information on the factors that affect performance, and we precisely see the effect of parameters that influence race strategy, fatigue, and the ability to speed up and deal with bends. In particular, a lower anaerobic capacity leads to an inability to accelerate at the end of the race, and which can accrue because of a reliance on anaerobic energy to maintain pace in an athlete of inferior running economy. We also see that a runner with a worse running economy is less able to speed up on the straights and that, in general, the bends are run slower than the straights, most likely because bend running at the same pace would increase energy expenditure. Notwithstanding a recommendation for adopting the accepted practices of improving aerobic and anaerobic metabolism through appropriate training methods, coaches are advised to note that athletes who avoid mid-race surges can improve their endspurt, which are the differentiating element in closely contested championship races.

Keywords: athletics, coaching, pacing, race tactics, track and field

OPEN ACCESS

Edited by:
François Billaut,
Laval University, Canada

Reviewed by:
Dominic Micklewright,
University of Essex, United Kingdom
Beat Knechtle,
University Hospital Zurich, Switzerland

***Correspondence:**
Brian Hanley
b.hanley@leedsbeckett.ac.uk

Specialty section:
This article was submitted to Elite Sports and Performance Enhancement, a section of the journal Frontiers in Sports and Active Living

Received: *01 December 2020*
Accepted: *21 December 2020*
Published: *20 January 2021*

Citation:
Mercier Q, Aftalion A and Hanley B (2021) A Model for World-Class 10,000 m Running Performances: Strategy and Optimization. Front. Sports Act. Living 2:636428. doi: 10.3389/fspor.2020.636428

INTRODUCTION

The 10,000 m race is the longest track event held as part of the Olympic Games and World Athletics Championships. As an endurance event, the distribution of energetic resources is of prime importance in achieving one's best finishing time, which is theoretically most likely to be achieved with an even pacing profile as seen in cycling time trials (Padilla et al., 2000). Indeed, the world record for the men's 10,000 m running event was recently set not only with the aid of specially-prepared pacemakers but also with a lighting system, the Wavelight pacing technology, which was programmed to show the even pace of the previous record (World Athletics, 2020a). However, championship racing, where the primary aim of the world's best athletes is to win, regardless of finishing time, features much more variable pacing that reflects tactical decision-making

(Casado et al., 2020a). Even when world-class athletes do not run at their maximum sustainable speed in racing, the stresses on their physiological systems still come at a considerable energetic cost. Some of the most important factors that affect performance in distance running are oxygen uptake (VO_2), particularly relative to an individual's maximal oxygen update (Jones et al., 2020), running economy (Lucia et al., 2008) and anaerobic reserve, which is reflected most clearly in the faster speeds experienced during the endspurt (Billat et al., 2003). Most of a 10,000 m race is run at a pace below the critical speed, which is the speed above which finite, predominantly non-oxidative exercise is performed (Burnley and Jones, 2010). In a sense, the objective of a successful pacing strategy is to deplete all possible energy stores (whether by aerobic or anaerobic metabolism) by the end of the race, but not too early that catastrophic deceleration occurs (Foster et al., 2004; Thiel et al., 2012). Hettinga et al. (2019) used 100-m split data to show that Olympic and World Championship 10,000 m male athletes continually changed pace throughout the race, with the best athletes able to achieve higher speeds than the rest of the field from 8,000 m onward. However, no physiological measures were possible in their analysis and contributing factors such as VO_2 are instead estimated for field-based exercise using mathematical analyses (Péronnet and Thibault, 1989). A novel study that models the effects of the factors that affect performance in the 10,000 m will therefore improve our understanding of what differentiates better performances and inform coaches of appropriate training practices.

The 10,000 m track race comprises 50 straight sections and 50 bends, although the length of the bend and the straight are not equal; in fact, on a standard track, the bends are 116 m long and the straights are 84 m long (World Athletics, 2019a). That the straight part of the track is shorter can be seen from the way in which the 100 m sprint race has its start line on an extension from the rest of the track. The effect of running on bends has been analyzed for short distance races (Quinn, 2009; Ohnuma et al., 2018; Aftalion and Martinon, 2019; Churchill et al., 2019; Aftalion and Trélat, 2020), but never for the 10,000 m, despite the potential impact of 50 bends on running performance. Many 10,000 m competitors in major championships are unused to running such long-distance races over multiple laps, as they instead mostly compete in shorter track races, on roads, or in cross country events. Indeed, in the 2017 World Championships men's 10,000 final, one of the competitors had never run that distance on the track before, having qualified for the championships as one of the top 15 finishers in that year's World Cross Country Championships (Hanley et al., 2018). Notwithstanding that athletes might run the bends effectively slower than the straights because of taking a racing line away from the inside kerb, the centrifugal forces and reduced horizontal propulsion experienced during bend running might also affect the speeds attained, as in sprinting (Judson et al., 2019). To maintain constant metabolic energy expenditure, athletes must run slower on the bends; by the same token, if they wish to maintain an even pace, they must increase energy expenditure (Taboga and Kram, 2019). A tactical decision to run wide on the bends in an Olympic 5,000 m final was shown to affect the medal positions (Jones and Whipp, 2002), and so our study that includes analysis of the effects of bends in the longer 10,000 m race will be useful to athletes and coaches in establishing whether bend running is a skill that requires development in training for that event.

To date, studies on pacing in the 10,000 m event have relied on 1,000-m split times (Filipas et al., 2018) or 100-m split times (Thiel et al., 2012; Hettinga et al., 2019), and have shown that changes in pace occur regularly during championship racing, especially during the final 1,000 m. Indeed, achieving a high finishing position in 10,000 m racing is associated with the ability to produce or withstand high pace variability, and more so with the capability of producing a fast final endspurt (Renfree et al., 2020). However, even the higher-resolution data used in previous research are restricted to mean speeds over 100-m distances that could hide some interesting pacing phenomena and prevent a fuller understanding of instantaneous speed and its changes. In the present study, instead of using statistical analyses of 100-m mean speeds, we choose to analyze a select sample of athletes individually and fit a mathematical model that closely resembles their pacing profiles. This process gives access to the instantaneous speed and thus helps us explain the physiological parameters that influence race strategy, fatigue, or the ability to speed up, particularly at the end of the race. Using a deterministic model means that for each race and each athlete, new specific computations are involved, and so in this study we focus on a single race. Furthermore, because the process adopted is a deterministic model, rather than a statistical model or experiment, we do not present a hypothesis. The aim of this study is to model 10,000 m world-class racing performances to allow for a deeper understanding of the factors that affect running speed and to establish the effect of the bends on performance.

MATERIALS AND METHODS

Split time data for each 100-m segment of the men's 10,000 m final at the 2017 IAAF World Championships were obtained from Hanley et al. (2018). Athlete finishing times and personal best times (PBs) (min:s) were also obtained from that report. The race start-time temperature was 20°C and the humidity was 64% (Hanley et al., 2018). To calculate mean speed (m/s) from the running split data, we divide each 100-m distance by time taken. We fit a mathematical model onto the 100-m mean speed data from the race winner (finishing time: 26:49.51) so that realistic constraints are applied that allow insights into the relative effects of different physiological characteristics. We also use the 100-m mean speed data from the 6th-place finisher for our models (finishing time: 26:57.77), based on similarities in these two athletes' racing conditions. For example, the 6th-place runner started on a similar part of the stagger (22nd athlete from the inside) to the winner (20th athlete from the inside), and so there was little or no difference in the effect of the first bend between these two athletes.

The 100-m split mean data for the winner's speed and 6th-place runner's speed are shown in **Figure 1**. The two athletes were never more than 3.23 s apart (∼19 m apart, based on the mean running speed for each 100-m segment), except during the last

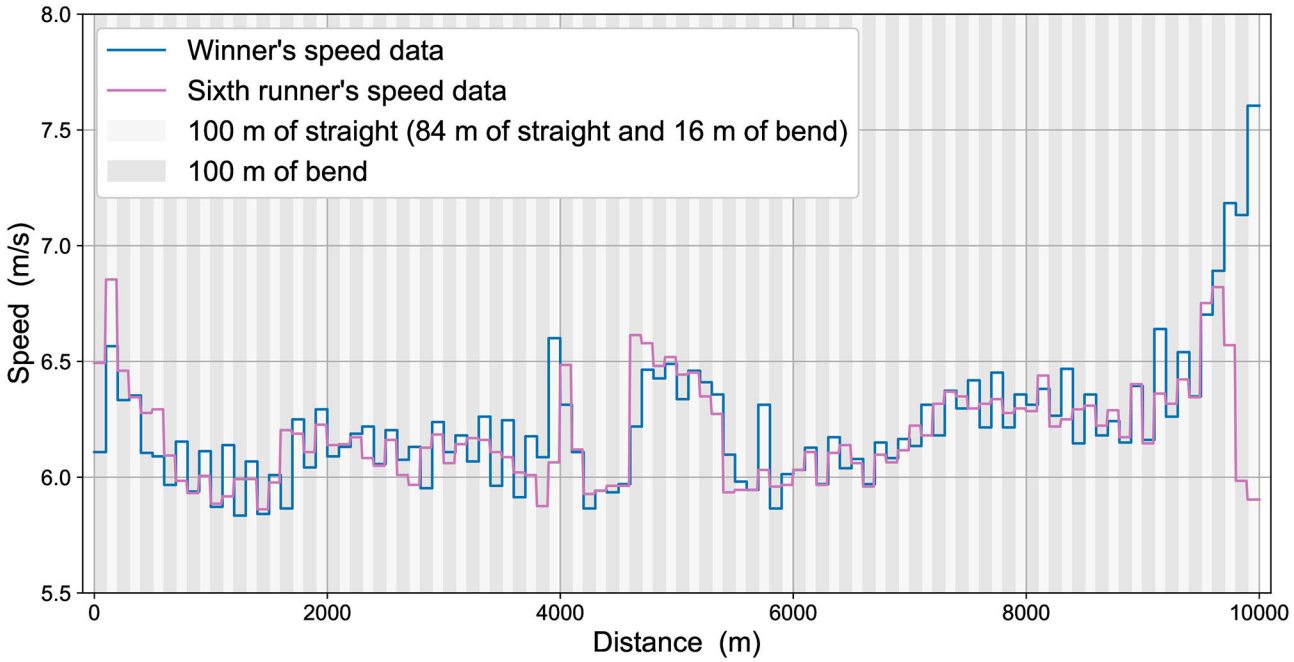

FIGURE 1 | The race data for the winner's speed (blue line) and 6th-place runner's speed (pink line).

lap where the winner was 4.47 s ahead (∼29 m apart) with 100 m remaining, and finished the race 8.26 s ahead (∼56 m apart). The mean absolute difference between them during the first 9,600 m was 1.39 s (±0.97 s), equivalent to about 9 m apart. The winner's PB before the competition was 26:46.57, slightly quicker than the 6th-place athlete's PB of 26:52.65. These athletes had the quickest and fourth-quickest PBs of all starters before the race. Both athletes undertook a strong acceleration at the very beginning of the race and at its end, with the middle part not at a constant speed, but included some tactical elements, in that running pace was elevated between ∼4,000 and 6,000 m (**Figure 1**). Whereas, the race winner generally increased pace throughout the last 1000 m, and whose last 100-m segment was his quickest of all, the 6th-place athlete could follow this increased pace until about 9,600 m only, after which his pace decreased so considerably that his last 100-m was one of his slowest. With considerations of these different tactical approaches at different stages of the race, our aim is to understand the effect of the physiology, mechanics and optimization of effort on these different sections of the race.

Description of the Track

The 2017 World Championship 10,000 m final was run on a standard athletics track 400 m long, made up of straights of 84 m and half circles of radius 36.5 m, acknowledging that the length of the track (in the inside lane) is measured 0.30 m from the kerb, so that the curvature of the track is either zero (in the straights) or 1/36.5 (in the bends) (World Athletics, 2019a). 10,000 m races begin on the first bend using a staggered start, and then the 116-m length of the bends and the 84-m length of the straights alternate. Because the split time data used were recorded every 100 m, the data corresponding to the straights therefore actually include 16 m of bend running.

Deterministic Model

The aim of this study is to model 10,000 m world-class racing performances to allow for a deeper understanding of the factors that affect running speed. Rather than using statistical analyses of mean data over 100-m or 1,000-m segments, we want to fit a model to replicate actual athletes' data so that instantaneous speeds can be calculated.

The model (Aftalion and Bonnans, 2014; Aftalion, 2017; Aftalion and Martinon, 2019; Aftalion and Trélat, 2020) yields an optimal control problem based on a system of coupled ordinary differential equations for the instantaneous speed $v(s)$, the propulsive force per unit of mass $f(s)$, and the anaerobic energy $e(s)$, where s is the distance from start. The system relies on Newton's second law of motion and the energy balance that takes into account the aerobic contribution VO_2, the anaerobic contribution $e(s)$ and the power developed by the propulsive force. Simulations require numerical values for the athletes' parameters. Based on previous research on the world's best athletes and the proportion of maximal oxygen uptake that occurs in elite-standard 10,000 m running, we assume VO_{2max} is 85 mL/kg/min and, in a championship race (rather than a more evenly paced world record), that the athletes run at roughly 85% of this value (Péronnet and Thibault, 1989; Joyner, 1991; Saltin et al., 1995; Billat et al., 2003; Lucia et al., 2008). The other key physiological parameters that influence pacing are:

- the maximal propulsive force per unit of mass f_M,

- the global friction coefficient τ that encompasses all kinds of friction, both from joint and track. In total, $f_M\ \tau$ is the maximal speed,
- the maximal decrease rate and increase rate of the propulsive force, which is related to motor control: an athlete cannot stop or start his effort instantaneously, but needs some time or distance to do so. This is what our control parameters u_- and u_+ provide,
- the total anaerobic energy or maximal accumulated oxygen deficit e^0,
- the VO_2 profile as a function of distance. This is a curve $\sigma(s)$ where s is the relative distance from the start but in fact, in the model, it is a curve $\sigma(e(s))$ where $e(s)$ is the remaining anaerobic energy. We refer the reader to Aftalion (2017), Aftalion and Martinon (2019), Aftalion and Trélat (2020) for more details on the model.

These parameters e^0, u_-, u_+, f_M, τ and the function σ are not measured for each athlete but are estimated through a computation to fit the data. More precisely, they are identified for a specific race and athlete (i.e., the winner and 6th-place finisher in the 10,000 m final in 2017). For fixed values of the parameters, the optimal control problem is solved using Bocop, an open license software developed by Inria-Saclay France (Bonnans et al., 2014). In total, we minimize the error between a single optimization simulation and data for a wide range of parameters to identify those that best match the data.

A crucial piece of information to be included in our model is the centrifugal force on the bends: it does not act as such in the equation of motion but limits the propulsive force $f(s)$ through a constraint that yields a decrease in the effective propulsive force on the bends:

$$f(s)^2 + \frac{v(s)^4}{R(s)^2} \leq f_M^2$$

where $R(s)$ is the radius of curvature at distance s from the start and f_M is the maximal force that the runner can exert.

Because competition officials do not record wind speeds for races longer than 200 m (World Athletics, 2019b), no precise wind data were available for the 10,000 m final. Given the wind reading was +0.3 m/s in the preceding race (World Athletics, 2020b) (the last heat in the first round of the men's 100 m), we considered the effect of wind to be negligible in terms of its effects on the runners' speed or strategy for the 10,000 m final. Concerning our model, it is not an issue to include any wind effects (Pritchard, 1993; Quinn, 2003), even allowing for the bends, provided there are precise data on wind speed and direction for the duration of the race (which is not presently the case for championship races). The wind adds an extra friction term in the law of motion; this term depends on air density (and therefore altitude), on the frontal area of the athlete in the direction of the wind (which changes during the race with wind direction) and the drag coefficient. Thus, the wind effect can be included in the equations, but for a 10,000 m event it is not going to affect performance because neither running speed nor wind speed are fast enough.

RESULTS

The Winner's Race

From the winner's speed data every 100 m, we identify the physiological parameters of this athlete and therefore we are able to compute his optimal speed. We show the instantaneous speed because it allows us to see the variations better. To compute the mean speed, we want to match the split data, therefore we compute the time T_k for the k^{th} segment of 100 m, which is:

$$T_k = \int_{100(k-1)}^{100k} \frac{1}{v(x)} dx.$$

Thus, the mean speed for the k^{th} segment is $v_k = 100/T_k$.

In **Figure 2**, we plot the winner's speed data (in blue) alongside the mean speed found from the simulation (orange), whereas in **Figure 3**, we add the instantaneous speed (green) to the simulated mean speed. On the instantaneous speed figure, we can observe that the instantaneous variations are much bigger on the bends (the gray vertical bands) than what we can surmise from the mean values. We also plot the simulated maximal propulsive force (**Figure 4**) to see how effort is organized during the race. **Figure 5** provides the evolution of the anaerobic energy; we see that the consumption of anaerobic energy is more pronounced at the very beginning of the race and from 6,800 m for the final acceleration, ending with effective exhaustion of anaerobic reserve. The speed bounds are illustrated in **Figure 6** where the strategic part can be seen clearly by the tightness of the bounds between ∼4,000 and 6,000 m.

Effect of the Parameters

We analyze numerically the effect of the physiological parameters. In **Figure 7**, we compare the winner's mean speed (in orange) with a simulation where the anaerobic energy is decreased by 5% (black), with the most noticeable effects occurring between about 4,800 and 5,400 m and from 9,600 m until the race finish. We subsequently select in our simulations an imaginary runner with a higher running economy (i.e., higher cost of running) (Lucia et al., 2008) and adjust his parameters to fit the 6th-place runner in the race. In **Figure 8**, we plot the mean speed data for the 6th-place runner (in pink), together with the simulated mean speed (orange), whereas in **Figure 9**, we plot the instantaneous speed (green). We see that the effect of these parameters is to strongly influence the strategic part of the race in the middle section and the final acceleration (or deceleration) at the end of the race.

DISCUSSION

Using the model, we can evaluate what factors influence race strategy, such as the ability to speed up during the endspurt. The simulation reproduces the main parts of the winner's race well (**Figure 3**): a strong acceleration at the beginning, followed by a cruising speed that is a little slower, a strategic acceleration between 4,000 and 6,000 m, then a slowing down to a slower speed before an acceleration starting at 7,000 m and a very quick last lap. The occurrence of a mid-race surge in speed is not

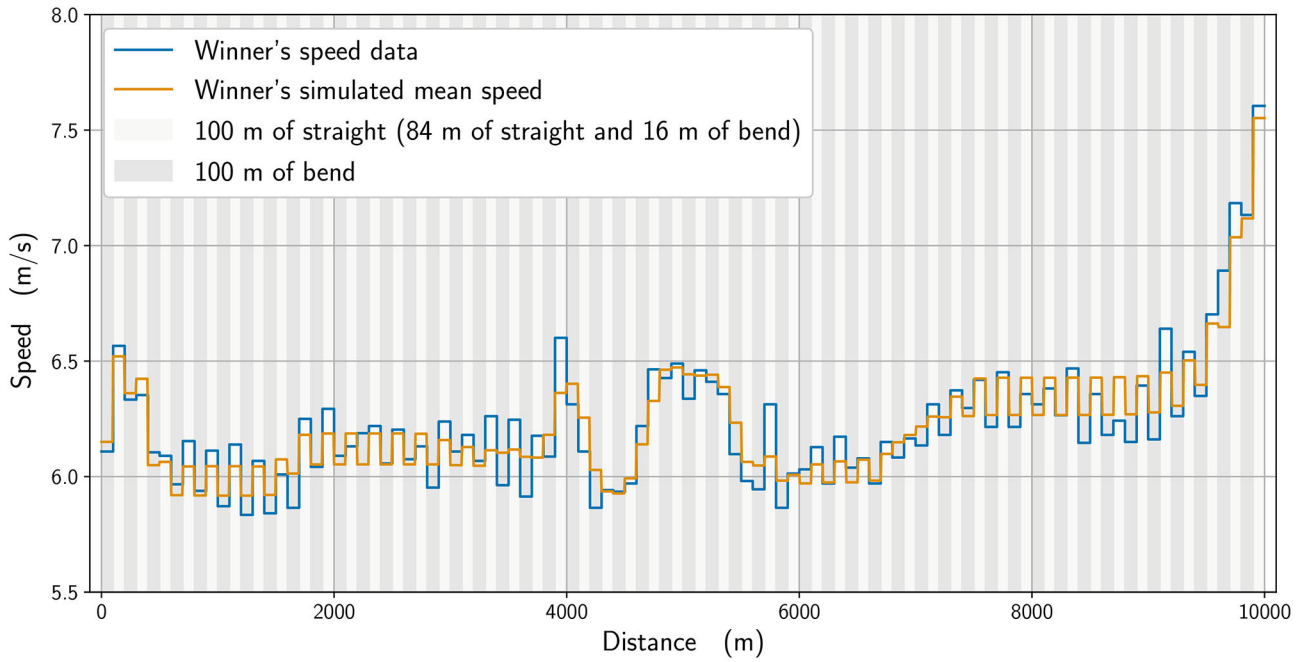

FIGURE 2 | The winner's mean speed data (blue line) with final time t_{data} = 26:49.51 and the simulated mean speed (orange line) with final time t_{simu} = 26:48.92.

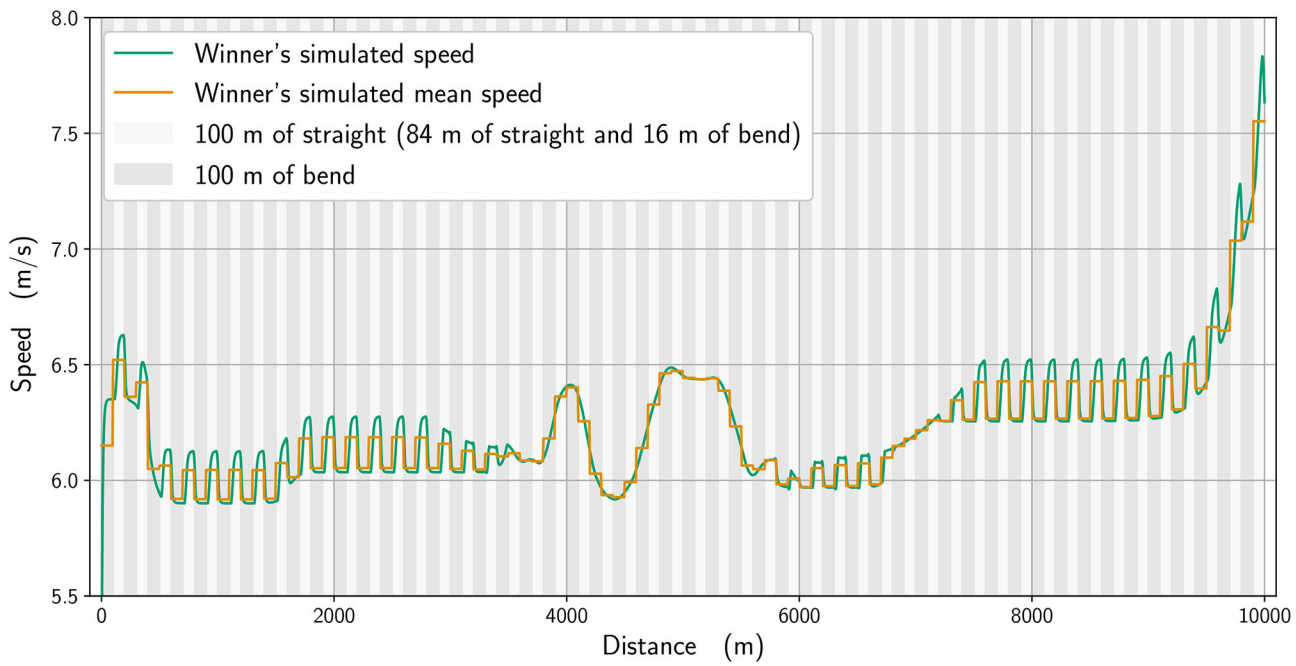

FIGURE 3 | The simulated speed (green line) and its mean every 100 m (orange).

unusual and was inferred to be a tactic used by the winner of the men's 10,000 m Olympic final in 2008 to increase the homeostatic disturbance in his opponents and effectively force them to choose a slower pace or risk dropping out (de Koning et al., 2011).

The 10,000 m race in this study was one that featured frequently observed aspects of racing, in that athletes did not implement an even pace strategy that would potentially result in better times, but instead adopted typical championship tactics

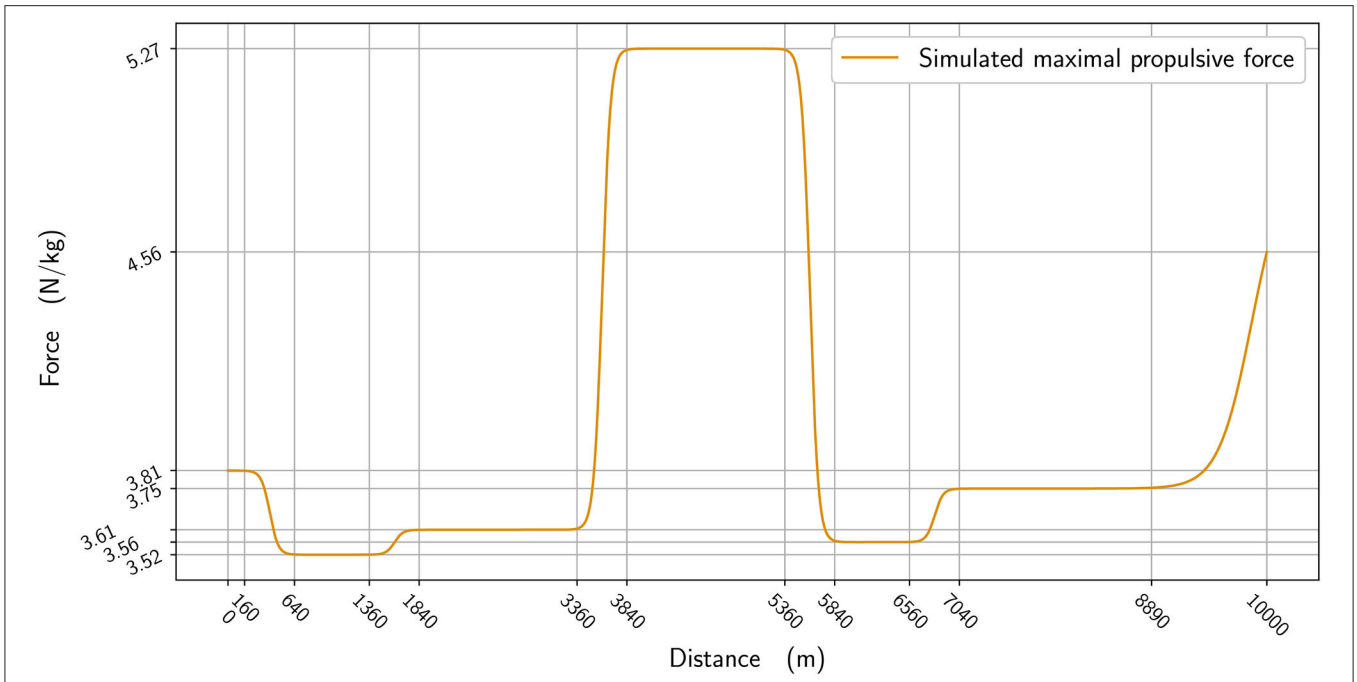

FIGURE 4 | The maximal propulsive force per kg vs. distance.

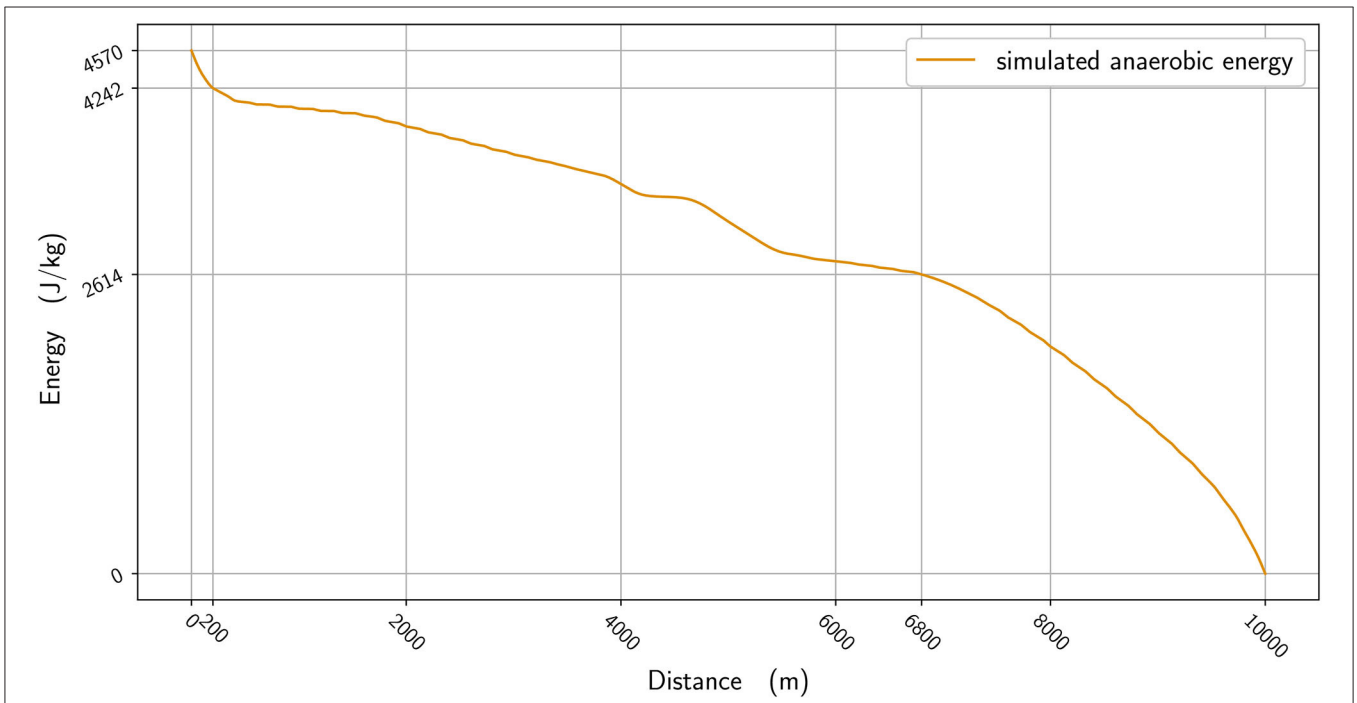

FIGURE 5 | The anaerobic energy per kg vs. distance.

such as varied pace and a fast endspurt. The closeness of the athletes with one lap remaining and, indeed, the narrow winning margin (0.43 s) meant that the winner needed to draw upon all remaining anaerobic reserves during the sprint finish. We see that the anaerobic energy reserve is used more in the sections of the race where a strong acceleration and propulsive force is required: at the very beginning; at around 4,000 m to speed up; and at the end (starting from 6,500 m) (**Figure 5**). Reasoning that

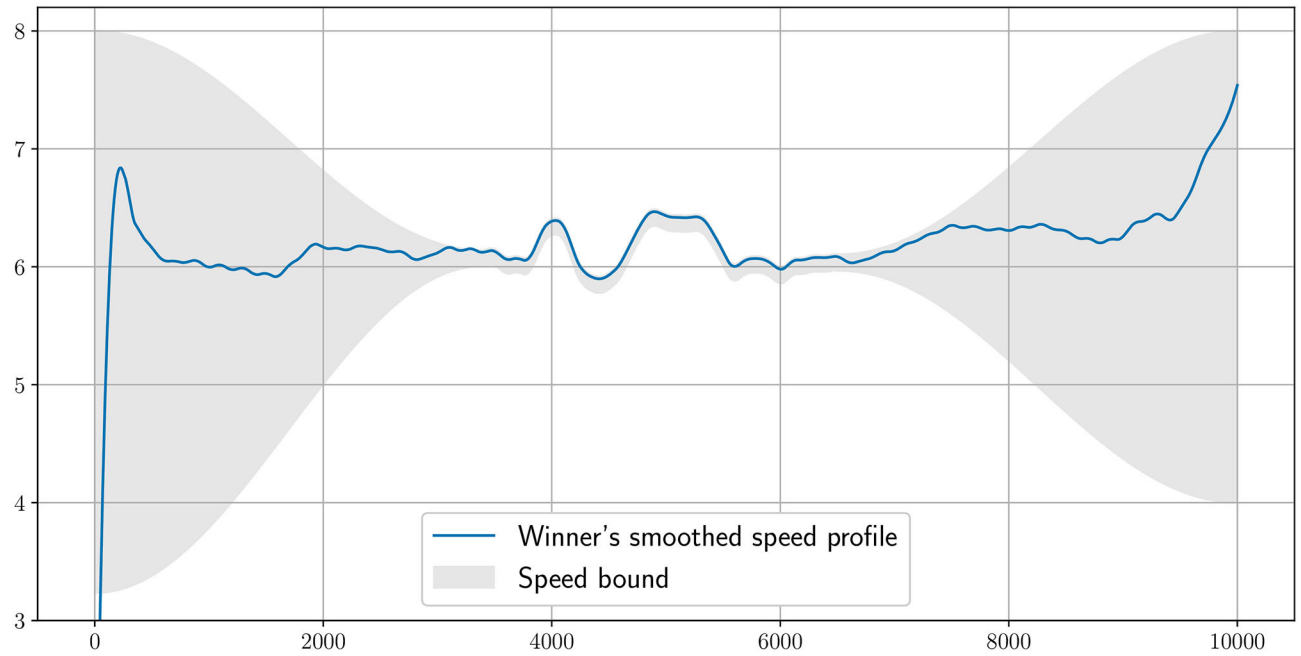

FIGURE 6 | The speed bounds imposed in the simulation around the smoothed winner's speed profile. The speed has to be in the gray area. When the bounds are tight, this is to impose a strategic speed.

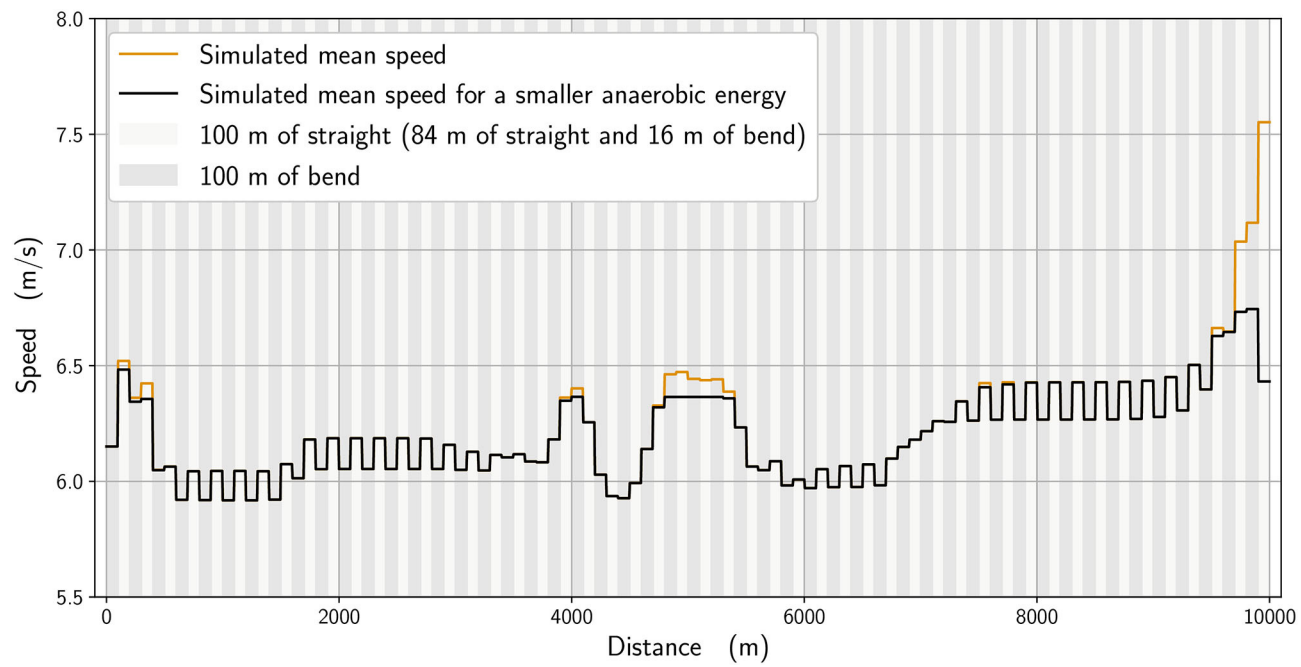

FIGURE 7 | Simulated mean speed for the winner t_{simu} = 26:48.92 (orange line), and with 5% less energy (black line) t_{less} = 26:54.25, $\Delta t = 5.33$ s.

the athletes finishing in the top positions in this race would have similar aerobic capacities, difference in anaerobic physiology can ultimately decide the final race positions. For the part of our analysis where we reduce the simulated winner's anaerobic energy by 5%, we see that the new optimal race has a start that is slightly slower, with an acceleration in the middle of the race that is smaller and, most important of all, a lack of ability to speed up at the end (**Figure 7**). If ever this hypothetical runner tried

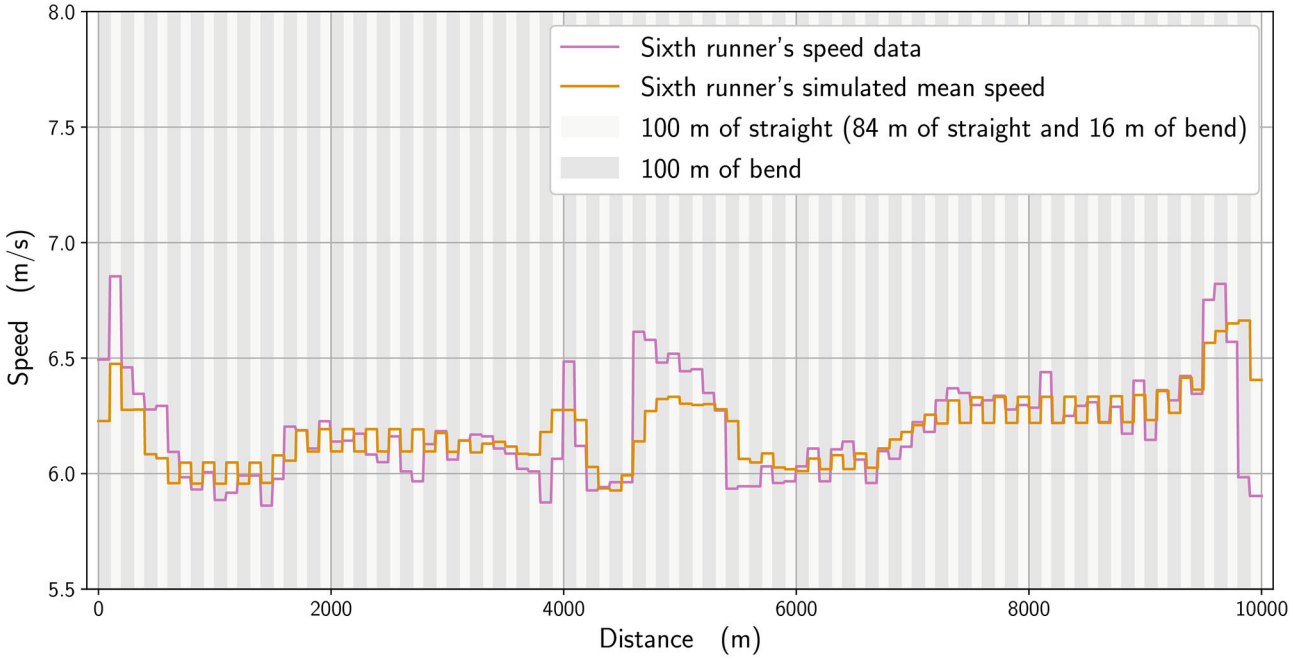

FIGURE 8 | Simulated mean speed for a runner with a higher running economy (orange line) compared with the mean speed for the 6th-place runner (pink line). t_{R6} = 26:57.92, t_{simu} = 26:57.41.

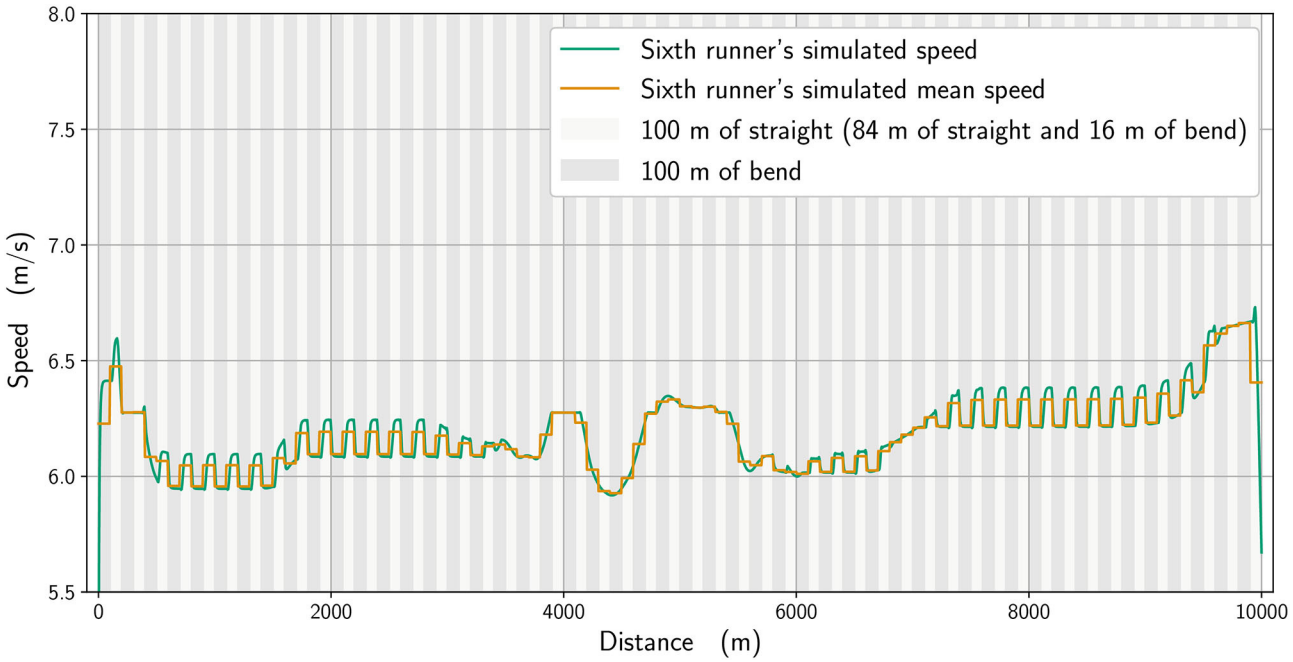

FIGURE 9 | Simulated mean speed (orange line) and instantaneous speed for a runner with a higher running economy (green line).

to speed up as much as the simulated winner at the beginning, then his pace would slow even more at the end. Coaches should therefore note the importance of developing sufficient anaerobic physiology in training, which is generally already understood but, more importantly, that athletes who are likely to be less well anaerobically trained should avoid the surges of increased speed that occur in the earlier stages of the race. These short surges are often deliberately used by athletes to challenge the physiological

responses of their rivals (Thompson, 2007) and the model shows mathematically why this approach can work. By maintaining a more even pace throughout the race, any anaerobic energy that would be used up in these surges can be retained until the endspurt. In addition, an athlete who runs with a low "cruising" speed depletes their anaerobic energy less and enhances their capacity for a fast endspurt; this tactic can be seen in those distance runners with a fast sprint finish who try to deliberately slow the pace from the front, and is another strategy for coaches to consider training for.

There is an effect of bend running on speed, in that the modeled data (calculated to closely replicate the winner and 6th-place athletes' pacing profiles) indicate that the straights are run faster than the bends. This shows that an even pace is never truly achieved in 10,000 m racing, even during the more steady state phases of the race, e.g., between 1,000 and 3,000 m. Athletes do not immediately slow from a straight to a bend, not least because the 100-m straight sections themselves include 16 m of bend, and so the simulated speeds (**Figures 3**, **9**) reflect the gradual decrease in pace on each bend and increase on the straights. To some extent, slower running speeds on the bends are not unexpected given the decrease in horizontal propulsion, and support previous assumptions by Taboga and Kram (2019) from their models of bend running. In any case, coaches should note that leg asymmetry is not uncommon during bend running, with the outer, right leg being more effective at force production (Judson et al., 2019). This means that a certain amount of preparatory training is required before competing in a 10,000 m track race (which comprises 5,800 m of bend running in total) to ensure both legs are effective in producing horizontal impulse and to avoid asymmetry-related injuries (Hamill et al., 1987). However, in the strategic parts between 4,000 and 6,000 m and near the end, when there is noticeable acceleration, the effect of the bend is less pronounced. We notice that for the 6th-place runner (**Figure 9**), the speed variation on the bends is not as great as for the winner: because he has a higher running economy, he cannot vary his speed as much in the straights after the bends. Moreover, he is unable to speed up at the end of the race as this inferior running economy means that maintaining a pace close to the winner relies more on anaerobic sources, which are then no longer available during the endspurt. In addition, a higher running economy reduces the ability to vary his speed once on the straight and restricts his tactical options more so than the athlete with lower running economy. Given that running economy could be the critical factor determining race performance (Lucia et al., 2008), it is undoubtedly a key factor for coaches to emphasize in training regimens (Midgley et al., 2007). It is reasonable to expect that psychological factors, such as demotivation caused by being out of the medal positions on the last lap, could have had an effect on the pacing profile of lower finishing runners. One strength of our model is the potential to include various psychological factors, either related to interactions between runners (Aftalion and Martinon, 2019), or motivation (or lack of motivation) using the cost-benefit model of Le Bouc et al. (2016). However, the difficulty of modeling these for a 10,000 m race is that the computations are very time-consuming and so for the moment we have not included these aspects. Nevertheless, for the 6th-place runner, we do not believe that reduced motivation or a decision to slow down explains the decrease in speed on the last lap because those finishing in the top eight have the incentive of prize money, and also because his speed decrease perfectly fits an energy reduction.

The advantage of using a modeling approach is that it allows us to manipulate the variables involved to assess the effect of changes in those variables, and thus the main strength of this study is how it accounts for the effect of each parameter individually and can be predictive. For example, by reducing anaerobic energy availability in our model we could see the reduced capacity for a fast endspurt or the need to avoid earlier intermittent surges of faster running. Being able to describe instantaneous speed for the whole race means we can account for more realistic changes in pace that using mean splits (over each 100 m) does not allow. One simple example is how the model allows us to show the rapid increase in speed from 0 m/s at the very start of the race, but more usefully means it is possible to see more clearly the effect of running the bends. In this study, we were interested in modeling championship performances, where tactics play a key role and where winning a medal is more important than the time achieved *per se*. Whereas, only a very few athletes can ever hope to set a world record (and planned attempts tend to require considerable race management on behalf of the organizers), championship running offers more athletes the chance to win a medal or achieve a high finishing position. A weakness of the modeling approach taken are that the computations for each race and runner are considerably time-consuming, and large-scale analyses of athletes and any possible interactions between them are costly. The results of this study show that coaches of ambitious athletes should consider training programs that emphasize both the ability to maintain a consistent pace for most of the race (e.g., through tempo runs) and the capability of increasing pace with no undue stress during tactical increases in speed and the endspurt (e.g., through short interval training) (Casado et al., 2020b). Further developments in athlete pace measurements that could provide higher resolution speed data (more frequently than each 100 m) will lead to better understanding, modeling and predictions that can assist coaches with race preparation. The implications for future research are therefore that how this knowledge allows an athlete to adapt a strategy against a runner whose weakness or parameters are known could be tested; indeed, the practical applications of this study include the ability for coaches to adapt race strategy based on knowledge of how energy reserves are used, as well as highlighting the importance of becoming proficient at bend running.

CONCLUSIONS

Based on 100-m time splits for a 10,000 m race, we perform simulations to understand the role of the physiology, efforts and tactics, and what is essential to win a race. We have seen that a

runner with a low running economy can speed up in the middle of the race and maintain a strong pace that will not impact his ability to speed up considerably at the end. On the other hand, a runner with a higher running economy or with a lower anaerobic reserve, or where higher running economy is compensated for with anaerobic energy, can follow most of the race but loses the ability to speed up at the end. We also observe that runners with better running economy have the ability to vary more their speed between the bends and straights, leading to a better time per lap, and overall race performance. Although it is well-established that physiological factors like running economy and anaerobic energy are important in elite-standard endurance running, we show for the first time how athletes who are more limited in these aspects can reduce the impact by adopting race tactics such as even pace running until the final acceleration phase. In addition, there is a clear effect of the bends on running speeds, and athletes are advised to spend some time in preparation for 10,000 m races to familiarize themselves with bend running at race speeds.

DATA AVAILABILITY STATEMENT

The raw data supporting the conclusions of this article will be made available by the authors, without undue reservation.

AUTHOR CONTRIBUTIONS

AA, BH, and QM conceptualized and designed the study. AA and BH wrote the manuscript. AA and QM conducted the data analyses and created the figures. All authors read and approved the final manuscript.

FUNDING

The authors acknowledge support from the LabEx AMIES (ANR-10-LABX-0002-01) of Université Grenoble Alpes, within the program Investissements d'Avenir (ANR-15-IDEX-0002) operated by the French National Research Agency (ANR).

REFERENCES

Aftalion, A. (2017). How to run 100 meters. *SIAM J. Appl. Math*. 77, 1320–1334. doi: 10.1137/16M1081919

Aftalion, A., and Bonnans, J. F. (2014). Optimization of running strategies based on anaerobic energy and variations of velocity. *SIAM J. Appl. Math*. 74, 1615–1636. doi: 10.1137/130932697

Aftalion, A., and Martinon, P. (2019). Optimizing running a race on a curved track. *PLoS ONE* 14:e0221572. doi: 10.1371/journal.pone.0221572

Aftalion, A., and Trélat, E. (2020). How to build a new athletic track to break records. *R. Soc. Open Sci*. 7:200007. doi: 10.1098/rsos.200007

Billat, V., Lepretre, P. M., Heugas, A. M., Laurence, M. H., Salim, D., and Koralsztein, J. P. (2003). Training and bioenergetic characteristics in elite male and female Kenyan runners. *Med. Sci. Sports Exerc*. 35, 297–304. doi: 10.1249/01.MSS.0000053556.59992.A9

Bonnans, J. F., Giorgi, D., Grelard, V., Maindrault, S., and Martinon, P. (2014). *BOCOP—A Toolbox for Optimal Control Problems*. Available online at: http://bocop.org (accessed November 24, 2020).

Burnley, M., and Jones, A. M. (2010). 'Traditional' perspectives can explain the sprint finish. In: Comments on Point:Counterpoint: Afferent feedback from fatigued locomotor muscles is/is not an important determinant of endurance exercise performance. *J Appl. Physiol*. 108, 458–468. doi: 10.1152/japplphysiol.01388.2009

Casado, A., Hanley, B., Jiménez-Reyes, P., and Renfree, A. (2020a). Pacing profiles and tactical behaviors of elite runners. *J. Sport Health Sci*. doi: 10.1016/j.jshs.2020.06.011. [Epub ahead of print].

Casado, A., Hanley, B., and Ruiz-Pérez, L. M. (2020b). Deliberate practice in training differentiates the best Kenyan and Spanish long-distance runners. *Eur. J. Sport Sci*. 20, 887–895. doi: 10.1080/17461391.2019.1694077

Churchill, S. M., Trewartha, G., and Salo, A. I. (2019). Bend sprinting performance: new insights into the effect of running lane. *Sports Biomech*. 18, 437–447. doi: 10.1080/14763141.2018.1427279

de Koning, J. J., Foster, C., Bakkum, A., Kloppenburg, S., Thiel, C., Joseph, T., et al. (2011). Regulation of pacing strategy during athletic competition. *PLoS ONE* 6:e15863. doi: 10.1371/journal.pone.0015863

Filipas, L., La Torre, A., and Hanley, B. (2018). Pacing profiles of Olympic and IAAF World Championship long-distance runners. *J. Strength Cond. Res*. doi: 10.1519/JSC.0000000000002873. [Epub ahead of print].

Foster, C., de Koning, J. J., Hettinga, F., Lampen, J., Dodge, C., Bobbert, M., et al. (2004). Effect of competitive distance on energy expenditure during simulated competition. *Int. J. Sports Med*. 25, 198–204. doi: 10.1055/s-2003-45260

Hamill, J., Murphy, M., and Sussman, D. (1987). The effects of track turns on lower extremity function. *Int. J. Sport. Biomech*. 3, 276–286. doi: 10.1123/ijsb.3.3.276

Hanley, B., Bissas, A., and Merlino, S. (2018). "Biomechanical report for the IAAF World Championships London 2017: 10,000 m men's," in *2017 IAAF World Championships Biomechanics Research Project, July 2018* (London). Monte Carlo: IAAF. Available online at: https://www.worldathletics.org/about-iaaf/documents/research-centre (accessed November 24, 2020).

Hettinga, F. J., Edwards, A. M., and Hanley, B. (2019). The science behind competition and winning in athletics: using world-level competition data to explore pacing and tactics. *Front. Sports Act. Living* 1:11. doi: 10.3389/fspor.2019.00011

Jones, A. M., Kirby, B. S., Clark, I. E., Rice, H. M., Fulkerson, E., Wylie, L. J., et al. (2020). Physiological demands of running at 2-hour marathon race pace. *J Appl. Physiol*. doi: 10.1152/japplphysiol.00647.2020. [Epub ahead of print].

Jones, A. M., and Whipp, B. J. (2002). Bioenergetic constraints on tactical decision making in middle distance running. *Br. J. Sports Med*. 36, 102–104. doi: 10.1136/bjsm.36.2.102

Joyner, M. J. (1991). Modeling: optimal marathon performance on the basis of physiological factors. *J. Appl. Physiol*. 70, 683–687. doi: 10.1152/jappl.1991.70.2.683

Judson, L. J., Churchill, S. M., Barnes, A., Stone, J. A., Brookes, I. G., and Wheat, J. (2019). Horizontal force production and multi-segment foot kinematics during the acceleration phase of bend sprinting. *Scand. J. Med. Sci. Sports* 29, 1563–1571. doi: 10.1111/sms.13486

Le Bouc, R., Rigoux, L., Schmidt, L., Degos, B., Welter, M. L., Vidailhet, M., et al. (2016). Computational dissection of dopamine motor and motivational functions in humans. *J. Neurosci*. 36, 6623–6633. doi: 10.1523/JNEUROSCI.3078-15.2016

Lucia, A., Oliván, J., Bravo, J., Gonzalez-Freire, M., and Foster, C. (2008). The key to top-level endurance running performance: a unique example. *Br. J. Sports Med*. 44, 172–174. doi: 10.1136/bjsm.2007.040725

Midgley, A. W., McNaughton, L. R., and Jones, A. M. (2007). Training to enhance the physiological determinants of long-distance running performance. *Sports Med*. 37, 857–880. doi: 10.2165/00007256-200737100-00003

Ohnuma, H., Tachi, M., Kumano, A., and Hirano, Y. (2018). How to maintain maximal straight path running speed on a curved path in sprint events. *J. Hum. Kinet*. 62, 23–31. doi: 10.1515/hukin-2017-0175

Padilla, S., Mujika, I., Angulo, F., and Goiriena, J. J. (2000). Scientific approach to the 1-h cycling world record: a case study. *J. Appl. Physiol*. 89, 1522–1527. doi: 10.1152/jappl.2000.89.4.1522

Péronnet, F., and Thibault, G. (1989). Mathematical analysis of running performance and world running records. *J. Appl. Physiol*. 67, 453–465. doi: 10.1152/jappl.1989.67.1.453

Pritchard, W. G. (1993). Mathematical models of running. *SIAM Rev*. 35, 359–379. doi: 10.1137/1035088

Quinn, M. D. (2003). The effects of wind and altitude in the 200-m sprint. *J. Appl. Biomech.* 19, 49–59. doi: 10.1123/jab.19.1.49

Quinn, M. D. (2009). The effect of track geometry on 200- and 400-m sprint running performance. *J. Sports Sci.* 27, 19–25. doi: 10.1080/02640410802392707

Renfree, A., Casado, A., Pellejero, G., and Hanley, B. (2020). More pace variation and pack formation in successful world-class 10,000-m runners than in less successful competitors. *Int. J. Sports Physiol. Perform.* 15, 1369–1376. doi: 10.1123/ijspp.2019-0852

Saltin, B., Larsen, H., Terrados, N., Bangsbo, J., Bak, T., Kim, C. K., et al. (1995). Aerobic exercise capacity at sea level and at altitude in Kenyan boys, junior and senior runners compared with Scandinavian runners. *Scand. J. Med. Sci. Sports* 5, 209–221. doi: 10.1111/j.1600-0838.1995.tb00037.x

Taboga, P., and Kram, R. (2019). Modelling the effect of curves on distance running performance. *PeerJ* 7:e8222. doi: 10.7717/peerj.8222

Thiel, C., Foster, C., Banzer, W., and de Koning, J. (2012). Pacing in Olympic track races: competitive tactics versus best performance strategy. *J. Sports Sci.* 30, 1107–1115. doi: 10.1080/02640414.2012.701759

Thompson, P. J. L. (2007). Perspectives on coaching pace skill in distance running: a commentary. *Int. J. Sports Sci. Coach.* 2, 219–221. doi: 10.1260/174795407782233128

World Athletics (2019a). *Track and Field Facilities Manual.* Monte Carlo: World Athletics.

World Athletics (2019b). *C2.1—Technical Rules*. Monte Carlo: World Athletics.

World Athletics (2020a). *Details of Cheptegei's 10,000m World Record Assault Revealed*. Available online at: https://www.worldathletics.org/news/news/cheptegei-10000-wr-assault-valencia-details (accessed November 17, 2020).

World Athletics (2020b). *Results—100 metres Men Heats*. Available online at: https://www.worldathletics.org/competitions/world-athletics-championships/iaaf-world-championships-london-2017-7093740/results/men/100-metres/heats/result (accessed December 17, 2020).

Conflict of Interest: The authors declare that the research was conducted in the absence of any commercial or financial relationships that could be construed as a potential conflict of interest.

frontiers in Sports and Active Living

ORIGINAL RESEARCH
published: 17 February 2021
doi: 10.3389/fspor.2021.634258

Fatigue-Related Changes in Spatiotemporal Parameters, Joint Kinematics and Leg Stiffness in Expert Runners During a Middle-Distance Run

Felix Möhler, Cagla Fadillioglu and Thorsten Stein*

BioMotion Center, Institute of Sports and Sports Science (IfSS), Karlsruhe Institute of Technology, Karlsruhe, Germany

OPEN ACCESS

Edited by:
Jean Slawinski,
Institut national du sport, de l'expertise et de la performance (INSEP), France

Reviewed by:
Yaodong Gu,
Ningbo University, China
Chris Napier,
Simon Fraser University, Canada
Giorgos Paradisis,
National and Kapodistrian University of Athens, Greece

****Correspondence:***
Felix Möhler
felix.moehler@kit.edu

Specialty section:
This article was submitted to Elite Sports and Performance Enhancement, a section of the journal Frontiers in Sports and Active Living

Received: *27 November 2020*
Accepted: *22 January 2021*
Published: *17 February 2021*

Citation:
Möhler F, Fadillioglu C and Stein T (2021) Fatigue-Related Changes in Spatiotemporal Parameters, Joint Kinematics and Leg Stiffness in Expert Runners During a Middle-Distance Run. Front. Sports Act. Living 3:634258. doi: 10.3389/fspor.2021.634258

Fatigue with its underlying mechanisms and effects is a broadly discussed topic and an important phenomenon, particularly in endurance sports. Although several studies have already shown a variety of changes in running kinematics with fatigue, few of them have analyzed competitive runners and even fewer have focused on middle-distance running. Furthermore, the studies investigating fatigue-related changes have mostly reported the results in terms of discrete parameters [e.g., range of motion (RoM)] in the frontal or sagittal plane, and therefore potentially overlooked effects occurring in subphases of the gait cycle or in the transverse plane. On this basis, the goal of the present study was to analyze the effects of exhaustive middle-distance running on expert runners by means of both discrete parameters and time series analysis in 3D. In this study, 13 runners ran on a treadmill to voluntary exhaustion at their individually determined fatigue speeds which was held constant during the measurements. Kinematic data were collected by means of a 3D motion capture system. Spatiotemporal and stiffness parameters as well as the RoM of joints and of center of mass (CoM) within the stance and flight phases were calculated. Independent *t*-tests were performed to investigate any changes in means and coefficients of variation (CV) of these parameters between the rested (PRE) and fatigued (POST) state. Statistical parametric mapping method was applied on the time series data of the joints and the CoM. Results from this exploratory study revealed that during a middle-distance run, expert runners change their stance time, rather than their step frequency or step length in order to maintain the constant running speed as long as possible. Increased upper body movements occurred to counteract the increased angular moment of the lower body possibly due to longer stance times. These findings provide insights into adaptation strategies of expert runners during a fatiguing middle-distance run and may serve a valuable information particularly for comparisons with other group of runners (e.g., females or non-athletes) as well with other conditions (e.g., non-constant speed or interval training), and might be useful for the definition of training goals (e.g., functional core training).

Keywords: locomotion, endurance, treadmill, middle-distance, SPM, range of motion, 3D movement analysis

INTRODUCTION

Fatigue is a complex phenomenon that develops during both high- and low-intensity exercise, and its origin depends on the intensity and duration of exercise (Millet and Lepers, 2004). Fatigue is therefore inherent in endurance sports, for example in running. Several studies have shown that fatigue causes changes in running kinematics (Winter et al., 2017; Kim et al., 2018), which in turn may decrease performance and increase injury risk (Hreljac et al., 2000). Deeper understanding of fatigue-related changes is therefore essential for optimization of training loads or prevention of injuries.

Most previous studies investigated the influence of fatigue during long-distance runs (>3,000 m or an equivalent time) (Winter et al., 2017; Kim et al., 2018; García-Pinillos et al., 2020; Willwacher et al., 2020), and only a few analyzed biomechanical alterations of competitive-level runners under exhaustive effort. Sanno et al. (2018) compared competitive with recreational runners over a 10 km run and found an increased knee flexion at touchdown in both groups as well as increases in maximal knee flexion and decreases in plantar flexion at toe off in the recreational runners (Sanno et al., 2018). Willwacher et al. (2020) observed kinematic adaptations in both recreational and competitive runners during a 10 km treadmill run in the non-sagittal planes. They reported changes between the pre- and post-fatigue state, particularly in hip adduction, ankle eversion and in knee valgus angle, although they did not consider spatiotemporal parameters or changes in the sagittal plane. García-Pinillos et al. (2020) analyzed spatiotemporal parameters and stiffness changes in trained male endurance runners during a 60 min treadmill run, but did not include any results concerning joint kinematics in their study. They reported an increased contact time and step variability as well as decreased flight time and leg stiffness in fatigued runners.

To date, only a limited number of studies have examined kinematic alterations related to fatigue over middle-distance runs (≤3,000 m or an equivalent time). Rabita et al. (2013) evaluated the changes in spring-mass behavior of runners during an effort with a mean time to exhaustion of 5:53 min. They reported decreased leg stiffness and altered spatiotemporal parameters, although they did not include joint kinematics in their analysis. Derrick et al. (2002) examined kinematic adjustments and their influences on shock attenuation potential during an exhaustive run (average time 15:42 min) of recreational runners by means of mobile sensors, and suggested that kinematic adaptations may lead to increased metabolic cost. A recent study by García-Pinillos et al. (2019) analyzed kinematic adaptations during two high-intensity interval programs using a high-speed camera, and reported no changes in the spatiotemporal and kinematic variables studied. In another study examining joint angle alterations and changes in shock absorption capacity after a brief exhaustive run, no significant differences between pre- and post-fatigue states were found (Abt et al., 2011). Maas et al. (2018) analyzed both experienced and novice runners during a run to exhaustion during a 3,200 m time trial pace using a 3D motion capture system. They reported increases in pelvic tilt, pelvic range of motion (RoM) and knee abduction as well as decreases in hip adduction and ankle plantar flexion. Furthermore, they showed that novice runners exhibit larger kinematic adjustments than experienced runners. Another group of researchers also analyzed novice runners in comparison to experienced runners focusing on stride-to-stride variability (Mo and Chow, 2018a) and coordination variability (Mo and Chow, 2018b) for prolonged treadmill run at anaerobic threshold speed. They reported that novice and experienced runners differ from each other particularly in terms of both stride-to-stride and coordination variability.

Several studies only analyzed motion in 1D or 2D (Winter et al., 2017; Kim et al., 2018), which could limit the scope of the results. As suggested by Willwacher et al. (2020), fatigue may cause alterations in non-sagittal planes. Therefore, analyses should comprise all of the relevant and anatomically-possible degrees of freedom. In addition, including upper body kinematics could improve the explanatory value of results, since upper body rotation has been found to increase with fatigue in long distance runs and was hypothesized to be detrimental for performance and to increase injury risk (Strohrmann et al., 2012). In addition, García-Pinillos et al. (2020) argued that robust conclusions regarding coordination, injury prevention and sports performance depend not only the mean values of spatiotemporal parameters but also their variability, which in their study was operationalized as the coefficient of variation. They reported increased variability with fatigue, whereas Hanley and Tucker (2018) found only moderate changes in variability between successive testing distances in their study. Variability of movement patterns is all in all an important and widely discussed topic in a wide range of disciplines, among others in sports biomechanics, since it helps to understand adaptation strategies as well as flexibility of the motor system in movement production (Meardon et al., 2011; Mo and Chow, 2018a,b). In addition, movement variability is speed-dependent (Meardon et al., 2011), so different running distances may lead to different variability characteristics since running speed changes with running distance. Similarly, the expertise of the runners is a factor influencing movement variability. Accordingly, different groups of participants as well as different study designs may provide different results (Mo and Chow, 2018a,b).

Stiffness is another important biomechanical parameter in analyzes of running gait because of its close relationship to injuries and performance (Butler et al., 2003) as well as to fatigue (Rabita et al., 2013; García-Pinillos et al., 2020), however a clear consensus regarding the relationship between these parameters is still lacking. Butler et al. (2003) reported that increased stiffness may be beneficial to sports performance and decreased stiffness may be associated with soft tissue injuries. On the other hand, Lorimer and Hume (2016) concluded that high lower body stiffness may be associated with Achilles tendon injuries, particularly in association with training on surfaces with low stiffness properties. All in all, leg and vertical stiffness might be an important aspect for performance as well as for injury prevention (Pappas et al., 2015).

In summary, existing studies have used a multitude of fatigue protocols, measurement devices, and dependent variables with participants from a broad range of expertise levels. Accordingly,

there is no consensus about the effects of fatigue on the biomechanics of middle-distance running. The goal of the present study was to analyze the possible effects of fatigue on spatiotemporal parameters, leg and vertical stiffness, 3D joint kinematics as well as the center of mass (CoM) trajectory during a middle-distance run by expert runners. In addition, this study aimed to conduct an explorative analysis of entire time series data by means of statistical parametric mapping (SPM) and important discrete parameters (spatiotemporal parameters and RoM). The presented results may provide informative data concerning biomechanical adaptations of competitive-level runners during an exhaustive middle-distance run and may be useful for future research particularly for comparisons with different expertise levels (e.g., non-athletes) or other running distances.

MATERIALS AND METHODS

Data Set

Data from a previously published study (Möhler et al., 2019) were re-analyzed. The participants were 13 male runners (age: 23.5 ± 3.6 years, BMI: 20.6 ± 1.7 kg/m^2). Inclusion criteria were a 10 km record below 35 min (32:59 ± 01:19 min), a minimum mileage von 50 km/week during the 8 weeks preceding the measurement and an active membership in a running club for at least 2 years (7.2 ± 3.2 years). Exclusion criteria were pain in the lower limbs or recent injuries. All participants provided written informed consent. The study was approved by the ethics committee of the Karlsruhe Institute of Technology. Each participant came to the laboratory on two different days 1 week apart. The tests were performed on a motorized treadmill (h/p/cosmos Saturn, Nussdorf-Traunstein, Germany). For safety reasons, subject wore a safety harness which was connected to an emergency stop. During the first visit, their individual fatigue speed was determined during an incremental lactate threshold test. The test started at 8 km/h, the duration per step was 3 min, there were 30 s of rest between the steps and the increment between the steps was 2 km/h. The individual fatigue speed was determined on the basis of lactate values and by means of the critical power concept developed by Monod and Scherrer (1965). The fatigue speed was defined as the speed that runners were potentially able to run for 10 min at most. This speed was at 110% of their speed at 4 mmol/l lactate (19.27 ± 0.72 km/h). During the second visit, the actual measurement was performed. At first, a standardized treadmill familiarization [6 min of walking, 6 min of running (Matsas et al., 2000; Lavcanska et al., 2005)] was performed. Afterwards, participants ran at their individually determined fatigue speed until voluntary exhaustion, which was reached after 4:06 ± 0:52 min (1.34 ± 0.27 km). Exhaustion was confirmed by a Borg-scale rating (Borg, 1982) of 19.6 ± 0.65. Participants wore their own running shoes. During running, 41 marker trajectories were captured by 11 infrared cameras at a recording frequency of 200 Hz (Vicon Motion Systems; Oxford Metrics Group, Oxford, UK). A total of 19 strides were captured at the beginning of the run (PRE measurement, non-fatigued state) and 19 strides immediately before exhaustion (POST measurement, fatigued state).

Data Processing

Data were preprocessed using Vicon Nexus software V1.8.5 (Vicon Motion Systems Ltd., UK). All subsequent data processing operations were performed with MATLAB R2020a (MathWorks, Natick, MA, USA). To obtain joint angles, an inverse kinematics calculation was conducted using a modified version of the full-body model Dynamicus (ALASKA) (Härtel and Hermsdorf, 2006). Foot strikes were identified using the vertical speed of the foot markers whereas toe-off was identified using the vertical acceleration (Leitch et al., 2011).

Duration of stance (time between right foot strike and right toe off), duration of flight (right toe off to left foot strike), and stride frequency (right foot strikes per second) were analyzed as spatiotemporal parameters in order to generally characterize the running kinematics of our participants. Vertical stiffness and leg stiffness were also included in the analyses because these parameters may change under neuromuscular fatigue (Dutto and Smith, 2002; García-Pinillos et al., 2020) and therefore be helpful to understand the general adaptation patterns in presence of fatigue, especially in relation to the spatiotemporal changes. Since the measurements were performed on a non-instrumented treadmill, the stiffness parameters were estimated based on kinematic data as suggested by Morin et al. (2005), who showed the validity of this method. For both spatiotemporal and stiffness parameters, the coefficient of variation (CV) was calculated alongside the mean and standard deviation. The CV was included because it may reveal changes in the stability of the coordination pattern (Jordan et al., 2009). Furthermore, there are some studies indicating a relationship between step variability and injuries (Meardon et al., 2011) as well as endurance performance (Nakayama et al., 2010).

Joint kinematics were analyzed for the lower extremities (ankle, knee, and hip joints) and torso (lumbar spine and thoracic spine joints) in the sagittal (S), frontal (F), and transversal (T) planes to incorporate all important degrees of freedom and constraints. Time series data of joints were analyzed by means of SPM because it has been suggested to be superior to over-simplified discrete parameter analyses by being capable of identifying field regions which co-vary significantly with the experimental design (Pataky et al., 2013). As well as analysis of the entire time series, RoM was calculated as the difference between the maximum and the minimum joint angle for both stance (right foot strike to right toe off) and flight phase (right toe off to left foot strike). The RoM results could be helpful for understanding adaptations to fatigue, particularly in terms of injuries, because it literally manifests the limits of motions. Increases in RoM may indicate a higher risk of soft tissue damages because of potentially increased strains in these tissues. Similarly, analysis of the CoM was accomplished by considering both the time series and the RoM.

Statistics

For the spatiotemporal parameters and the RoM, the 19 PRE strides and the 19 POST strides were averaged for each participant for statistical analysis. The PRE and POST averages were compared using paired *t*-tests and Cohen's *d* was calculated as a measure of effect size. Normality distribution was verified

using the Shapiro-Wilk-test. For all statistical tests, the level of significance was set *a priori* to $p = 0.05$. Cohen's d was classified as the following: $d < 0.5$ small effect, $0.5 < d < 0.8$ medium effect and $d > 0.8$ large effect (Cohen, 1992). The joint angle time series were time-normalized and compared using statistical non-parametric mapping (www.spm1d.org) due to non-normal distribution. All analyses were performed for the right side assuming that both legs would fatigue at a similar rate (Pappas et al., 2015).

RESULTS

Spatiotemporal Parameters and Their Variability

Aiming at investigating spatiotemporal characteristics both in PRE and POST, stance time, time of flight, stride frequency, and their variability across multiple strides were estimated. The results are represented in **Table 1**. Analysis of the spatiotemporal parameters revealed a significantly higher stance time (PRE: 0.16 s, POST: 0.17 s, $p < 0.001$, $d = 3.016$) and shorter time of flight (PRE: 0.33 s, POST: 0.31 s, $p < 0.001$, $d = 2.077$). The CV of the spatiotemporal parameters did not show any significant changes (**Table 1**).

Vertical and Leg Stiffness and Their Variability

Vertical and leg stiffness were included in order to be able to explain changes in spatiotemporal parameters with respect to changes in stiffness, because stiffness is thought to exert a major effect on various athletic variables related to running kinematics (Brughelli and Cronin, 2008). In the POST, both the leg and the vertical stiffness decreased significantly with high effect sizes (PRE_{leg}: 12.40 kN/m, $POST_{leg}$: 10.56 kN/m, $p < 0.001$, $d = 1.856$; $PRE_{vertical}$: 20.55 kN/m, $POST_{vertical}$: 18.01 kN/m, $p < 0.001$, $d = 1.701$), which were in accordance with increased stance times. The CV of both stiffness parameters also decreased significantly with medium effect sizes indicating a less variable stiffness over strides in POST (PRE_{leg}: 0.08, $POST_{leg}$: 0.07, $p = 0.047$, $d = 0.613$; $PRE_{vertical}$: 0.08, $POST_{vertical}$: 0.06, $p = 0.045$, $d = 0.619$) (**Table 1**).

Analyses of Range of Motion

In the stance phase, the RoM predominantly increased with fatigue (**Table 2**). Both at the ankle and at the knee joint, RoM increased significantly in the sagittal plane with a high effect size (Ankle PRE_S: 51.15°, $POST_S$: 53.55°, $p < 0.001$, $d = 1.23$; Knee PRE_S: 37.81°, $POST_S$: 40.97°, $p < 0.001$, $d = 1.451$). The remaining joints, namely the hip (PRE_S: 53.55°, $POST_S$: 56.87°, $p < 0.001$, $d = 2.200$; PRE_F: 17.10°, $POST_F$: 18.82°, $p < 0.001$, $d = 1.282$; PRE_T: 9.39°, $POST_T$: 11.86°, $p < 0.001$, $d = 1.442$), the lumbar spine (PRE_F: 8.10°, $POST_F$ 10.05°, $p < 0.001$, $d = 1.513$, PRE_T: 3.78°, $POST_T$: 4.54°, $p < 0.001$, $d = 2.568$) and the thoracic spine (PRE_S: 5.45°, $POST_S$: 5.93°, $p = 0.009$, $d = 0.863$; PRE_F: 12.82°, $POST_F$: 14.89°, $p < 0.001$, $d = 2.989$; PRE_T: 18.71°, $POST_T$: 22.51°, $p < 0.001$, $d = 1.728$), showed significantly increased RoM with a high effect size in all three planes, except for the lumbar spine in the sagittal plane. Generally speaking, runners showed a tendency toward more joint motion especially in the sagittal plane. The RoM of the CoM increased significantly in the medio-lateral direction ($PRE_{medio-lateral}$: 4.60°, $POST_{medio-lateral}$: 5.11°, $p = 0.039$, $d = 0.641$), but decreased in the vertical direction ($PRE_{vertical}$: 61.85°, $POST_{vertical}$: 60.11°, $p = 0.043$, $d = 0.627$) with medium effect sizes. This means that runners moved more from side-to-side but less up-and-down.

In the flight phase, a smaller number of significant changes were detected compared to the stance phase. The RoM of the hip joint decreased significantly in the sagittal plane with a high effect size (PRE: 22.96°, POST: 20.75°, $p = 0.001$, $d = 1.155$), whereas those of the lumbar (PRE: 1.03°, POST: 1.28°, $p < 0.001$, $d = 1.210$) and the thoracic (PRE: 9.85°, POST°: 10.56, $p = 0.025$, $d = 0.710$) spine increased in the transverse plane. The effect sizes were high and medium, respectively, which means that upper body rotation increased. The RoM of the CoM decreased in the vertical direction with a high

TABLE 1 | Spatiotemporal parameters, vertical, and leg stiffness together with corresponding coefficients of variation (CV) shown as mean ± standard deviation.

	PRE	POST	*P*	*d*
Stance time [s]	**0.16 ± 0.02**	**0.17 ± 0.02**	**< 0.001**	**3.016**
Time of flight [s]	**0.33 ± 0.04**	**0.31 ± 0.03**	**< 0.001**	**2.077**
Stride frequency [1/s]	1.53 ± 0.07	1.54 ± 0.07	0.120	0.464
Vertical stiffness [kN/m]	**20.55 ± 3.98**	**18.01 ± 4.56**	**< 0.001**	**1.701**
Leg stiffness [kN/m]	**12.40 ± 2.62**	**10.56 ± 2.90**	**< 0.001**	**1.856**
Coefficients of variation				
Stance time	0.03 ± 0.01	0.03 ± 0.01	0.175	0.399
Time of flight	0.02 ± 0.01	0.01 ± 0.07	0.069	0.555
Stride frequency	0.01 ± 0.00	0.01 ± 0.00	0.230	0.351
Vertical stiffness	**0.08 ± 0.02**	**0.06 ± 0.02**	**0.045**	**0.619**
Leg stiffness	**0.08 ± 0.03**	**0.07 ± 0.02**	**0.047**	**0.613**

p-values as calculated by the dependent t-test and Cohen's d as effect sizes are given. Significant differences are highlighted in bold ($p < 0.05$). Cohen's d effect sizes of <0.50, 0.5–0.8, and >0.8 indicate small, medium, and large effects, respectively.

TABLE 2 | Range of motion of joints in degrees (°) and of the CoM in mm are shown as mean ± standard deviation for stance and flight phases separately.

	PRE	POST	*p*	*d*
Stance phase				
Ankle—S [°]	**51.15 ± 4.38**	**53.55 ± 4.37**	**< 0.001**	**1.230**
Ankle—F [°]	17.32 ± 5.31	17.53 ± 5.36	0.568	0.163
Ankle—T [°]	11.11 ± 2.21	10.61 ± 2.41	0.363	0.262
Knee—S [°]	**37.81 ± 5.23**	**40.97 ± 6.12**	**< 0.001**	**1.451**
Knee—F [°]	4.54 ± 3.54	4.78 ± 3.52	0.580	0.158
Knee—T [°]	7.16 ± 2.68	7.12 ± 3.35	0.953	0.017
Hip—S [°]	**53.33 ± 5.53**	**56.87 ± 6.24**	**< 0.001**	**2.200**
Hip—F [°]	**17.10 ± 3.60**	**18.82 ± 3.58**	**< 0.001**	**1.282**
Hip—T [°]	**9.39 ± 5.05**	**11.86 ± 5.35**	**< 0.001**	**1.442**
Lumbar Spine—S [°]	12.13 ± 1.98	12.86 ± 2.47	0.088	0.514
Lumbar Spine—F [°]	**8.10 ± 0.86**	**10.05 ± 1.12**	**< 0.001**	**1.513**
Lumbar Spine—T [°]	**3.78 ± 0.54**	**4.54 ± 0.68**	**< 0.001**	**2.568**
Thoracic Spine—S [°]	**5.45 ± 0.78**	**5.93 ± 1.01**	**0.009**	**0.863**
Thoracic Spine—F [°]	**12.82 ± 1.25**	**14.89 ± 1.34**	**< 0.001**	**2.989**
Thoracic Spine—T [°]	**18.71 ± 4.10**	**22.51 ± 22.51**	**< 0.001**	**1.728**
COM ant-post [mm]	13.42 ± 1.62	14.14 ± 2.66	0.213	0.365
COM med-lat [mm]	**4.60 ± 1.36**	**5.11 ± 1.61**	**0.039**	**0.641**
COM vertical [mm]	**61.85 ± 6.87**	**60.11 ± 6.25**	**0.043**	**0.627**
Flight phase				
Ankle—S [°]	13.03 ± 4.17	11.44 ± 4.42	0.059	0.579
Ankle—F [°]	5.17 ± 3.08	5.67 ± 2.44	0.223	0.356
Ankle—T [°]	6.54 ± 3.00	6.39 ± 3.35	0.751	0.090
Knee—S [°]	99.52 ± 10.62	96.65 ± 11.63	0.057	0.583
Knee—F [°]	7.44 ± 3.96	8.16 ± 4.21	0.224	0.355
Knee—T [°]	11.48 ± 8.00	13.12 ± 6.55	0.065	0.564
Hip—S [°]	**22.96 ± 6.14**	**20.75 ± 5.21**	**0.001**	**1.155**
Hip—F [°]	8.85 ± 2.20	8.91 ± 1.43	0.877	0.044
Hip—T [°]	10.55 ± 4.22	10.94 ± 4.87	0.524	0.182
Lumbar spine—S [°]	11.03 ± 2.40	11.19 ± 2.36	0.584	0.156
Lumbar spine—F [°]	4.68 ± 1.33	4.33 ± 1.26	0.190	0.385
Lumbar spine—T [°]	**1.03 ± 0.45**	**1.28 ± 0.47**	**< 0.001**	**1.210**
Thoracic spine—S [°]	4.75 ± 0.97	4.94 ± 1.01	0.117	0.468
Thoracic spine—F [°]	1.99 ± 0.72	2.12 ± 1.11	0.424	0.230
Thoracic spine—T [°]	**9.85 ± 3.25**	**10.56 ± 3.31**	**0.025**	**0.710**
COM ant-post [mm]	13.71 ± 2.78	12.94 ± 3.24	0.163	0.412
COM med-lat [mm]	8.60 ± 3.10	8.15 ± 2.34	0.428	0.227
COM vertical [mm]	**51.88 ± 14.76**	**46.92 ± 11.76**	**0.002**	**1.075**

p-values as calculated by the dependent t-test and Cohen's d as effect sizes are also given. Significant differences ($p < 0.05$) are highlighted in bold. Cohen's d effect sizes of <0.50, 0.5–0.8, and >0.8 indicate small, medium, and large effects, respectively. S, F, and T signifies the sagittal, the frontal, and the transversal plane, respectively.

effect size (PRE: 51.88°, POST: 46.92°, $p = 0.002$, $d = 1.075$) but no significant changes were detected in the other planes (**Table 2**), which means that runners moved less up-and-down during flight.

In summary, the results revealed predominantly greater motion in the sagittal plane for the lower limbs and increased upper body motion especially in the transverse plane. Furthermore, the CoM showed less up-and-down-movement.

Time Series Analyses of Joint and CoM Movements

To prevent any over-simplification, the joint angle data were further analyzed by means of SPM. The trajectories of five joints as well as the CoM in all three planes are represented in **Figure 1**.

The SPM analysis (**Figure 1**) revealed a significantly higher plantarflexion of the ankle around right foot strike in the POST, as well as an increase in dorsiflexion and pronation prior to right foot strike. In the flight phase, the ankle was less plantarflexed and less supinated in the POST.

The knee joint showed more flexion particularly during swing and around right toe-off, whereas it was less flexed before the right foot strike in the POST. In the remaining planes, there were no significant differences except for a change with a short duration in the transverse plane.

The hip joint was less flexed around right foot strike, and more flexed after right toe-off, in the POST. There were several significant differences between the PRE and the POST in the frontal plane of the hip joint. The hip joint was more abducted in the middle of the right stance phase and in the beginning of the right flight phase. Contrarily, it was more adducted in the middle of the left stance phase as well as in the middle of the left flight phase.

The two joints representing trunk movement, in the lumbar and in the thoracic spine, showed less flexion in the sagittal plane, indicating a predominantly increased backwards tilt of the trunk in the POST. In the frontal plane, both the lumbar and the thoracic spine were more tilted to the left before left toe-off. After left toe-off, these areas were more tilted to the right and after right toe-off the thoracic spine was more tilted to the left. In the transverse plane, runners rotated to the right after left toe-off and rotated to the left after right toe-off. This occurred at both the lumbar and the thoracic spine joints, which overall indicates an increased rotation in the upper body.

During almost the entire gait cycle, the position of the CoM was lower in the POST compared to the PRE. In the remaining two directions, anterio-posterior and medio-lateral, there were not any significant changes.

DISCUSSION

This study is one of the first to investigate the effects of fatigue on expert runners during an exhaustive middle-distance run. The analysis was performed in 3D and entire time series were considered in the analysis by means of SPM. The results indicated that fatigue affects the spatiotemporal parameters, stiffness, CoM trajectories and joint kinematics throughout the gait cycle.

Spatiotemporal Parameters and Their Variability

Between the PRE and POST, stride frequency fluctuated between 1.53 and 1.54 Hz (∼92 strides per min). Since the speed was fixed during the fatigue protocol and the stride frequency did not change, the step length had to remain unchanged because speed is the multiplication of stride frequency with stride length. Since stride frequency did not change from PRE to POST, one

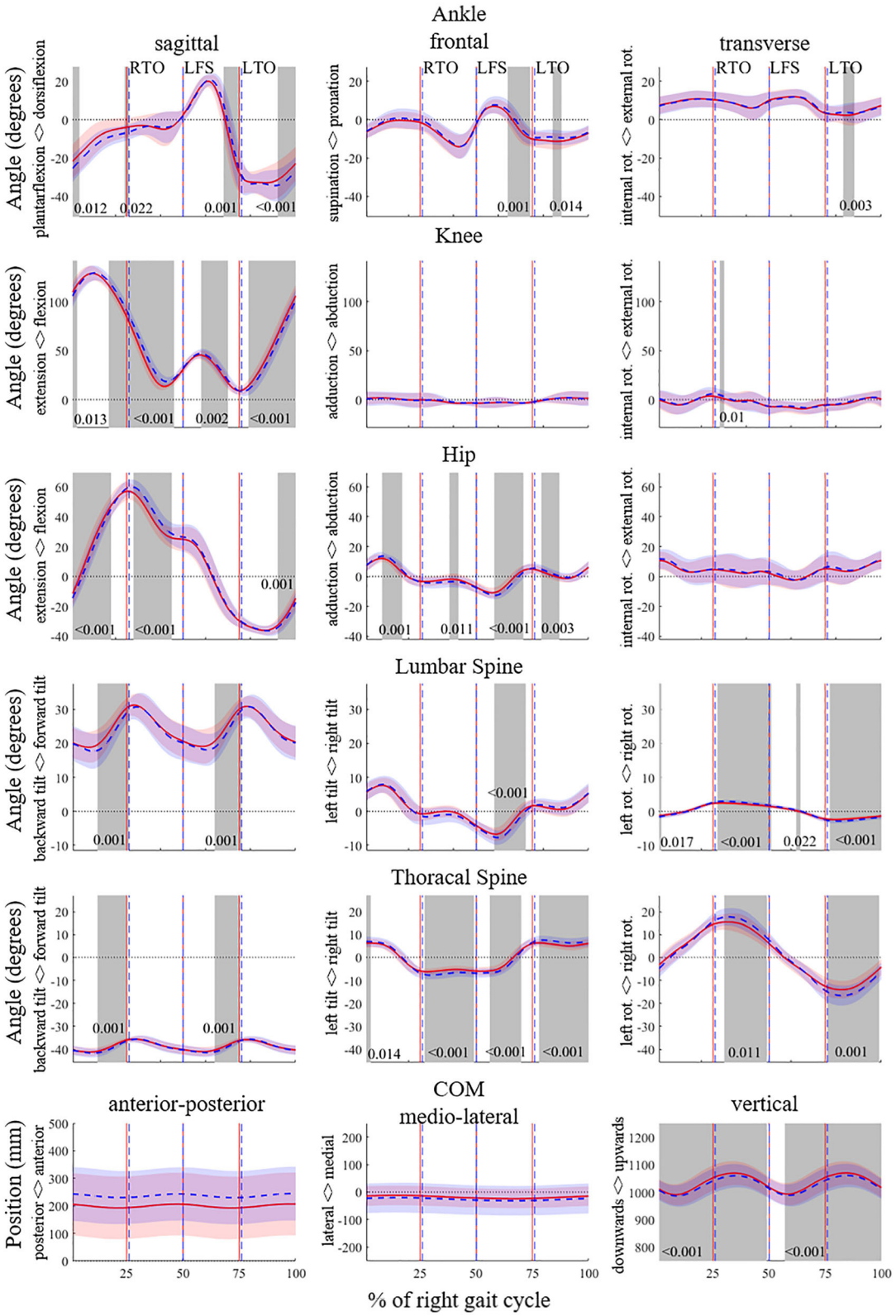

FIGURE 1 | SPM analyses for the angles of the ankle, knee, hip, lumbar spine and thoracic spine in degrees, and of the trajectory of the center of mass (CoM) in mm for the entire running gait cycle of the right leg (from right foot strike to right foot strike) in 3D. The PRE and POST time series data are shown in red and blue, respectively. Significant differences ($p < 0.05$) are highlighted with gray areas and corresponding p-values are given. RTO signifies right toe off; LFS, left foot strike; LTO, left toe-off.

could assume that trained runners choose a stride frequency and a step length associated with the lowest energy cost and try to keep them up (Williams and Cavanagh, 1987; Hunter and Smith, 2007). The stride frequency chosen by the athletes in the present study (∼92 strides per min) was slightly higher than reported by Hunter and Smith (∼86–87 strides per min) who analyzed changes with fatigue during a 1 h high-intensity run. This increase might be due to the higher running velocity (Fletcher and Macintosh, 2017). Even though stride frequency was the same in PRE and POST, contact time increased which was compensated by a decreased flight time.

Vertical and Leg Stiffness and Their Variability

The results show that fatigued runners have a decreased leg and vertical stiffness in the POST, which leads to a longer contact time and shorter flight times. These results are in line with other studies (Dutto and Smith, 2002; Rabita et al., 2011, 2013; García-Pinillos et al., 2020). These decreases in stiffness may be explained by the reduced effectiveness of the stretch-shortening cycle and may possibly increase energy cost, which ultimately would decrease running performance (Hayes and Caplan, 2012; Pappas et al., 2014). The CV of both vertical and leg stiffness decreased with fatigue, which means that stiffness varied more from stride to stride in PRE compared to POST. In a study investigating relationships between coordinative variability and overuse injury (Hamill et al., 2012), a higher variability of a coordinative structure was related to a healthier state of athletes. However, a causal relationship between injury and variability was not yet found. Dutto and Smith (2002) also reported that the relationship between injury mechanisms and shifts in stiffness remained unclear.

Analyses of Range of Motion

Increases in RoM were observed, mainly during the stance phase, which was also reported by Maas et al. (2018). In the ankle, knee, and hip joints, RoM in the sagittal plane increased with fatigue. Since the running speed was fixed by the treadmill, the horizontal mechanical power that each runner had to generate remained unchanged during the entire run. Accordingly, it may be assumed that a tradeoff between mechanical torque and angular displacement has been maintained during the run (Günther and Blickhan, 2002). Consequently, increased angular displacement, which manifests itself as increases in RoM in this case, may be explained by decreased torques at joints, probably due to decreased muscle forces occurring with fatigue (Hanon et al., 2005).

At the hip, the lumbar spine and the thoracic spine, the RoM increased in the frontal and transverse planes. These changes are possibly due to a fatigued core musculature causing difficulties in stabilizing the trunk (Koblbauer et al., 2014), and may be considered to be counterproductive since they do not produce any effective contribution to forward propulsion. On the other hand, increased upper body motion may also be a result of motor control system which tries to compensate increased lower body angular moment by increasing the upper body moment in the reverse direction (For more details see Section "Time Series Analyses of Joint and CoM Movements"). During stance, the CoM showed more movement in the medio-lateral direction and less movement in the vertical direction; this is also in line with the decreased stiffness discussed earlier in Section "Spatiotemporal Parameters and Their Variability."

Time Series Analyses of Joint and CoM Movements

The SPM showed that the ankle was less plantarflexed and supinated during flight. This is in accordance with Mizrahi et al. (2000), who found a decreased activity of the tibialis anterior and hypothesized that this led to a pendant toe. The difference in both knee and hip flexion looks like a time shift in the signal: in the POST, the knee flexion curve is behind the PRE curve, which might be caused by the longer stance phase. There was an increased level of movement in the upper body in the POST. Runners leaned more to the side, which is in accordance with the increased medio-lateral CoM movement during stance (for more details see Section "Vertical and Leg Stiffness and Their Variability"). Additionally, an increased upper body rotation was detected, which means there was an increase in movements which do not support forward propulsion. This was probably due to a decrease in trunk stability and possibly led to a decrease in running efficiency.

The SPM showed that many joint movements are affected, not only around initial contact and toe off but also in other phases of the running gait cycle. This finding is an indicator that the studies whose results are limited to discrete parameters may be missing some important aspects due to over-simplified treatments, as also mentioned by Pataky et al. (2013).

The significant changes between PRE and POST in the lower body mainly occurred in the sagittal plane, whereas the changes in the upper body were distributed in all three planes. Sagittal plane dominance within the changes in the lower body movements can be explained by the fact that forward propulsion is mainly associated with the extensions of hip, knee, and ankle joints. Increased level of lower body joint extensions leads to an increased lower body angular moment in vertical direction (i.e., moment due to rotation around the axis parallel to the direction of gravity). These increased rotational moments are counteracted by increased upper body moments around the this same axis, which is predominantly done by increasing upper body rotation (Hinrichs, 1987). Ultimately, the total moment of the body around the vertical direction approaches zero, so that the runners can sustain an optimum level of horizontal speed. Significant differences in CoM trajectories were only seen in the vertical direction, indicating that the angular moments in the lower and upper body were balanced such that CoM trajectories related to rotation in vertical direction remained unchanged. These findings may be transferred into practical usage as an indicator for the importance of functional core training. A properly functioning tradeoff mechanism between upper and lower body would optimize the horizontal speed, therefore the performance of the runners as well (Hinrichs, 1987). Any weakness or lack of sufficient coordination in the core muscles may potentially decrease the movement efficiency or increase the injury risk.

Main focus of a proper core training should therefore be on the training of movements and positions, rather than just single muscles without considering their synergic behaviors within the complete body (Fredericson and Moore, 2005).

Limitations and Outlook

There are some limitations of the present study that need to be mentioned. First, the use of a treadmill ensured a constant speed and thus enabled investigation of the effects of fatigue in isolation. However, one has to keep in mind that varying speed is a strategy which would be employed by runners when running overground. Besides, it should be noted that although the parameters estimated during treadmill running are comparable to those measured during overground running, they are not equivalent (Van Hooren et al., 2020). Since all participants underwent standardized treadmill familiarization, we can assume that participants had a stable running style. Second, the sample size could have been larger, although it is not easy to recruit a large sample of high-level runners. By using the results found in this exploratory study, subsequent studies may be able to formulate targeted hypotheses concerning the effects of fatigue on running performance or risk of injury. Third, participants of this study were chosen based on their 10 km performance, whereas fatigue protocol was considerably shorter (1.34 ± 0.27 km). This contrast may be considered as a limiting factor. However, even if it would have been preferable to select runners based on their 1,500 or 3,000 m performance, the goal of this study was to analyze fatigue-related changes during a middle-distance run of experienced runners.

CONCLUSION

Despite the number of studies conducted, there is still no clear consensus on how running patterns change in a fatigued state. Compared to long-distance running, middle-distance running has been less frequently studied until now. In this study, the fatigue changes in expert runners during a middle-distance run were investigated in a highly standardized laboratory study by analyzing not only discrete parameters but also time series in 3D. Ultimately, an extensive picture of running in a fatigued state was presented.

The key findings from this study highlight that expert runners increase stance time and decrease time of flight, but keep both the step frequency and the step length constant. Concerning kinematics, increased upper body movements became apparent with fatigue, which may be transferred into the field as an indicator for the importance of functional core training (e.g., total body trainings focusing on core strength) in middle-distance runners. In the fatigued state runners increased their stance time, which led to increased lower body angular moments. These moments were counteracted by increased upper body rotation. The presented results may be used in future research or for practical uptake, particularly when designing training programs (e.g., integrating proper kind of functional core training).

DATA AVAILABILITY STATEMENT

The data analyzed in this study is subject to the following licenses/restrictions: The raw data supporting the conclusions of this article will be made available by the authors, without undue reservation. Requests to access these datasets should be directed to felix.moehler@hotmail.de.

ETHICS STATEMENT

The studies involving human participants were reviewed and approved by the ethics committee of the Karlsruhe Institute of Technology. The patients/participants provided their written informed consent to participate in this study.

AUTHOR CONTRIBUTIONS

FM and TS were involved in the design of the study. FM carried out all data collection and data analysis. All authors were involved in the interpretation and discussion of the results. FM took the lead in writing the manuscript. All authors provided critical feedback and contributed to the final manuscript.

FUNDING

This research did not receive any specific grant from funding agencies in the public, commercial, or not-for-profit sectors. We acknowledge support by the KIT-Publication Fund of the Karlsruhe Institute of Technology.

REFERENCES

Abt, J., Sell, T., Chu, Y., Lovalekar, M., Burdett, R., and Lephart, S. (2011). Running kinematics and shock absorption do not change after brief exhaustive running. *J. Strength Cond. Res.* 25, 1479–1485. doi: 10.1519/JSC.0b013e3181ddfcf8

Borg, G. A. (1982). Psychophysical bases of perceived exertion. *Med. Sci. Sports Exerc.* 14, 377–381. doi: 10.1249/00005768-198205000-00012

Brughelli, M., and Cronin, J. (2008). A review of research on the mechanical stiffness in running and jumping: methodology and implications. *Scand. J. Med. Sci. Sport.* 18, 417–426. doi: 10.1111/j.1600-0838.2008.00769.x

Butler, R. J., Crowell, H. P., and Davis, I. M. C. (2003). Lower extremity stiffness: implications for performance and injury. *Clin. Biomech.* 18, 511–517. doi: 10.1016/S0268-0033(03)00071-8

Cohen, J. (1992). A power primer. *Psychol. Bull.* 112, 155–159. doi: 10.1037/0033-2909.112.1.155

Derrick, T. R., Dereu, D., and Mclean, S. P. (2002). Impacts and kinematic adjustments during an exhaustive run. *Med. Sci. Sports Exerc.* 34, 998–1002. doi: 10.1097/00005768-200206000-00015

Dutto, D. J., and Smith, G. A. (2002). Changes in spring-mass characteristics during treadmill running to exhaustion/Changements des caracteristiques de raideur des jambes lors d' une course d' effort sur tapis roulant. *Med. Sci. Sport. Exerc.* 34, 1324–1331. doi: 10.1097/00005768-200208000-00014

Fletcher, J., and Macintosh, B. (2017). Running economy from a muscle energetics perspective. *Front. Physiol.* 8:433. doi: 10.3389/fphys.2017.00433

Fredericson, M., and Moore, T. (2005). Muscular balance, core stability, and injury prevention for middle- and long-distance runners. *Phys. Med. Rehabil. Clin. N. Am.* 16, 669–689. doi: 10.1016/j.pmr.2005.03.001

García-Pinillos, F., Cartón-Llorente, A., Jaén-Carrillo, D., Delgado-Floody, P., Carrasco-Alarcón, V., Martínez, C., et al. (2020). Does fatigue alter step

characteristics and stiffness during running? *Gait Posture* 76, 259–263. doi: 10.1016/j.gaitpost.2019.12.018

García-Pinillos, F., Molina-Molina, A., Párraga-Montilla, J. A., and Latorre-Román, P. A. (2019). Kinematic alterations after two high-intensity intermittent training protocols in endurance runners. *J. Sport Heal. Sci.* 8, 442–449. doi: 10.1016/j.jshs.2016.11.003

Günther, M., and Blickhan, R. (2002). Joint stiffness of the ankle and the knee in running. *J. Biomech.* 35, 1459–1474. doi: 10.1016/S0021-9290(02)00183-5

Hamill, J., Palmer, C., and Van Emmerik, R. E. A. (2012). Coordinative variability and overuse injury. *Sport. Med. Arthrosc. Rehabil. Ther. Technol.* 4:45. doi: 10.1186/1758-2555-4-45

Hanley, B., and Tucker, C. B. (2018). Gait variability and symmetry remain consistent during high-intensity 10,000 m treadmill running. *J. Biomech.* 79, 129–134. doi: 10.1016/j.jbiomech.2018.08.008

Hanon, C., Thépaut-Mathieu, C., and Vandewalle, H. (2005). Determination of muscular fatigue in elite runners. *Eur. J. Appl. Physiol.* 94, 118–125. doi: 10.1007/s00421-004-1276-1

Härtel, T., and Hermsdorf, H. (2006). Biomechanical modelling and simulation of human body by means of DYNAMICUS. *J. Biomech.* 39:549. doi: 10.1016/S0021-9290(06)85262-0

Hayes, P., and Caplan, N. (2012). Foot strike patterns and ground contact times during high-calibre middle-distance races. *J. Sports Sci.* 30, 1275–1283. doi: 10.1080/02640414.2012.707326

Hinrichs, R. N. (1987). Upper extremity function in running. II: angular momentum considerations. *Int. J. Sport Biomech.* 3, 242–263. doi: 10.1123/ijsb.3.3.242

Hreljac, A., Marshall, R. N., and Hume, P. A. (2000). Evaluation of lower extremity overuse injury potential in runners. *Med. Sci. Sports Exerc.* 32, 1635–1641. doi: 10.1097/00005768-200009000-00018

Hunter, I., and Smith, G. (2007). Preferred and optimal stride frequency, stiffness and economy: changes with fatigue during a 1-h high-intensity run. *Eur. J. Appl. Physiol.* 100, 653–661. doi: 10.1007/s00421-007-0456-1

Jordan, K., Challis, J. H., Cusumano, J. P., and Newell, K. M. (2009). Stability and the time-dependent structure of gait variability in walking and running. *Hum. Mov. Sci.* 28, 113–128. doi: 10.1016/j.humov.2008.09.001

Kim, H. K., Mirjalili, S. A., and Fernandez, J. (2018). Gait kinetics, kinematics, spatiotemporal and foot plantar pressure alteration in response to long-distance running: systematic review. *Hum. Mov. Sci.* 57, 342–356. doi: 10.1016/j.humov.2017.09.012

Koblbauer, I. F., van Schooten, K. S., Verhagen, E. A., and van Dieën, J. H. (2014). Kinematic changes during running-induced fatigue and relations with core endurance in novice runners. *J. Sci. Med. Sport* 17, 419–424. doi: 10.1016/j.jsams.2013.05.013

Lavcanska, V., Taylor, N. F., and Schache, A. G. (2005). Familiarization to treadmill running in young unimpaired adults. *Hum. Mov. Sci.* 24, 544–557. doi: 10.1016/j.humov.2005.08.001

Leitch, J., Stebbins, J., Paolini, G., and Zavatsky, A. B. (2011). Identifying gait events without a force plate during running: a comparison of methods. *Gait Posture* 33, 130–132. doi: 10.1016/j.gaitpost.2010.06.009

Lorimer, A. V., and Hume, P. A. (2016). Stiffness as a risk factor for achilles tendon injury in running athletes. *Sport. Med.* 46, 1921–1938. doi: 10.1007/s40279-016-0526-9

Maas, E., De Bie, J., Vanfleteren, R., Hoogkamer, W., and Vanwanseele, B. (2018). Novice runners show greater changes in kinematics with fatigue compared with competitive runners. *Sport. Biomech.* 17, 350–360. doi: 10.1080/14763141.2017.1347193

Matsas, A., Taylor, N., and McBurney, H. (2000). Knee joint kinematics from familiarised treadmill walking can be generalised to overground walking in young unimpaired subjects. *Gait Posture* 11, 46–53. doi: 10.1016/S0966-6362(99)00048-X

Meardon, S. A., Hamill, J., and Derrick, T. R. (2011). Running injury and stride time variability over a prolonged run. *Gait Posture* 33, 36–40. doi: 10.1016/j.gaitpost.2010.09.020

Millet, G., and Lepers, R. (2004). Alterations of neuromuscular function after prolonged running, cycling and skiing exercises. *Sport. Med.* 34, 105–116. doi: 10.2165/00007256-200434020-00004

Mizrahi, J., Verbitsky, O., and Isakov, E. (2000). Fatigue-related loading imbalance on the shank in running: a possible factor in stress fractures. *Ann. Biomed. Eng.* 28, 463–469. doi: 10.1114/1.284

Mo, S., and Chow, D. H. K. (2018a). Differences in lower-limb coordination and coordination variability between novice and experienced runners during a prolonged treadmill run at anaerobic threshold speed. *J. Sports Sci.* 37, 1021–1028. doi: 10.1080/02640414.2018.1539294

Mo, S., and Chow, D. H. K. (2018b). Stride-to-stride variability and complexity between novice and experienced runners during a prolonged run at anaerobic threshold speed. *Gait Posture* 64, 7–11. doi: 10.1016/j.gaitpost.2018.05.021

Möhler, F., Ringhof, S., Debertin, D., and Stein, T. (2019). Influence of fatigue on running coordination: a UCM analysis with a geometric 2D model and a subject-specific anthropometric 3D model. *Hum. Mov. Sci.* 66, 133–141. doi: 10.1016/j.humov.2019.03.016

Monod, H., and Scherrer, J. (1965). The work capacity of a synergic muscular group. *Ergonomics* 8, 329–338. doi: 10.1080/00140136508930810

Morin, J.-B., Dalleau, G., Kyröläinen, H., Jeannin, T., and Belli, A. (2005). A simple method for measuring stiffness during running. *J. Appl. Biomech.* 21, 167–180. doi: 10.1123/jab.21.2.167

Nakayama, Y., Kudo, K., and Ohtsuki, T. (2010). Variability and fluctuation in running gait cycle of trained runners and non-runners. *Gait Posture* 31, 331–335. doi: 10.1016/j.gaitpost.2009.12.003

Pappas, P., Paradisis, G., Tsolakis, C., Smirniotou, A., and Morin, J.-B. (2014). Reliabilities of leg and vertical stiffness during treadmill running. *Sport. Biomech.* 13, 391–399. doi: 10.1080/14763141.2014.981853

Pappas, P., Paradisis, G., and Vagenas, G. (2015). Leg and vertical stiffness (a)symmetry between dominant and non-dominant legs in young male runners. *Hum. Mov. Sci.* 40, 273–283. doi: 10.1016/j.humov.2015.01.005

Pataky, T. C., Robinson, M. A., and Vanrenterghem, J. (2013). Vector field statistical analysis of kinematic and force trajectories. *J. Biomech.* 46, 2394–2401. doi: 10.1016/j.jbiomech.2013.07.031

Rabita, G., Couturier, A., Dorel, S., Hausswirth, C., and Le Meur, Y. (2013). Changes in spring-mass behavior and muscle activity during an exhaustive run at VO2max. *J. Biomech.* 46, 2011–2017. doi: 10.1016/j.jbiomech.2013.06.011

Rabita, G., Slawinski, J., Girard, O., Bignet, F., and Hausswirth, C. (2011). Spring-mass behavior during exhaustive run at constant velocity in elite triathletes. *Med. Sci. Sports Exerc.* 43, 685–692. doi: 10.1249/MSS.0b013e3181fb3793

Sanno, M., Willwacher, S., Epro, G., and Brüggemann, G.-P. (2018). Positive work contribution shifts from distal to proximal joints during a prolonged run. *Med. Sci. Sport. Exerc.* 50, 2507–2517. doi: 10.1249/MSS.0000000000001707

Strohrmann, C., Harms, H., Kappeler-Setz, C., and Tröster, G. (2012). Monitoring kinematic changes with fatigue in running using body-worn sensors. *IEEE Trans. Inf. Technol. Biomed.* 16, 983–990. doi: 10.1109/TITB.2012.2201950

Van Hooren, B., Fuller, J. T., Buckley, J. D., Miller, J. R., Sewell, K., Rao, G., et al. (2020). Is motorized treadmill running biomechanically comparable to overground running? A systematic review and meta-analysis of cross-over studies. *Sport. Med.* 50, 785–813. doi: 10.1007/s40279-019-01237-z

Williams, K. R., and Cavanagh, P. R. (1987). Relationship between distance running mechanics, running economy, and performance. *J. Appl. Physiol.* 63, 1236–1245. doi: 10.1152/jappl.1987.63.3.1236

Willwacher, S., Sanno, M., and Brüggemann, G.-P. (2020). Fatigue matters: an intense 10 km run alters frontal and transverse plane joint kinematics in competitive and recreational adult runners. *Gait Posture* 76, 277–283. doi: 10.1016/j.gaitpost.2019.11.016

Winter, S., Gordon, S., and Watt, K. (2017). Effects of fatigue on kinematics and kinetics during overground running: a systematic review. *J. Sports Med. Phys. Fitness* 57, 887−899. doi: 10.23736/S0022-4707.16.06339-8

Conflict of Interest: The authors declare that the research was conducted in the absence of any commercial or financial relationships that could be construed as a potential conflict of interest.

frontiers in Sports and Active Living

ORIGINAL RESEARCH
published: 18 March 2021
doi: 10.3389/fspor.2021.585809

Running Speed Estimation Using Shoe-Worn Inertial Sensors: Direct Integration, Linear, and Personalized Model

Mathieu Falbriard, Abolfazl Soltani and Kamiar Aminian*

Laboratory of Movement Analysis and Measurement, École Polytechnique Fédérale de Lausanne, Lausanne, Switzerland

The overground speed is a key component of running analysis. Today, most speed estimation wearable systems are based on GNSS technology. However, these devices can suffer from sparse communication with the satellites and have a high-power consumption. In this study, we propose three different approaches to estimate the overground speed in running based on foot-worn inertial sensors and compare the results against a reference GNSS system. First, a method is proposed by direct strapdown integration of the foot acceleration. Second, a feature-based linear model and finally a personalized online-model based on the recursive least squares' method were devised. We also evaluated the performance differences between two sets of features; one automatically selected set (i.e., optimized) and a set of features based on the existing literature. The data set of this study was recorded in a real-world setting, with 33 healthy individuals running at low, preferred, and high speed. The direct estimation of the running speed achieved an inter-subject mean ± STD accuracy of 0.08 ± 0.1 m/s and a precision of 0.16 ± 0.04 m/s. In comparison, the best feature-based linear model achieved 0.00 ± 0.11 m/s accuracy and 0.11 ± 0.05 m/s precision, while the personalized model obtained a 0.00 ± 0.01 m/s accuracy and 0.09 ± 0.06 m/s precision. The results of this study suggest that (1) the direct estimation of the velocity of the foot are biased, and the error is affected by the overground velocity and the slope; (2) the main limitation of a general linear model is the relatively high inter-subject variance of the bias, which reflects the intrinsic differences in gait patterns among individuals; (3) this inter-subject variance can be nulled using a personalized model.

Keywords: IMUs, speed, running, overground, linear prediction, personalization

OPEN ACCESS

Edited by:
Jean Slawinski,
Institut national du sport, de l'expertise et de la performance (INSEP), France

Reviewed by:
Qingguo Li,
Queen's University, Canada
Janez Podobnik,
University of Ljubljana, Slovenia

****Correspondence:***
Mathieu Falbriard
mathieu.falbriard@epfl.ch

Specialty section:
This article was submitted to Elite Sports and Performance Enhancement, a section of the journal Frontiers in Sports and Active Living

Received: *21 July 2020*
Accepted: *27 January 2021*
Published: *18 March 2021*

Citation:
Falbriard M, Soltani A and Aminian K (2021) Running Speed Estimation Using Shoe-Worn Inertial Sensors: Direct Integration, Linear, and Personalized Model. Front. Sports Act. Living 3:585809. doi: 10.3389/fspor.2021.585809

INTRODUCTION

The overground speed is the most useful metric in training and performance analysis of running. Researchers have tried for decades to understand the physiological and biomechanical adjustments occurring at different ranges of running speeds (Williams and Cavanagh, 1987; Nummela et al., 2007; Moore, 2016; Thompson, 2017). However, most of the existing studies were performed in a controlled environment (i.e., treadmill running inside a laboratory) where the runner has to adapt his gait to run at a constant speed. In overground running, change of environment, surface, slope, obstacles, and turns alter the gait and the running speed. Many studies have discussed the

biomechanical adaptations associated with running on a treadmill vs. running overground (Van Hooren et al., 2019). While standard motion capture (i.e., stereophotogrammetry and force plate) offers accurate measurements in laboratories, the recent emergence of wearable systems is paving the shift toward studies carried overground and in real-world conditions (Benson et al., 2018).

The real-world estimation of the overground speed is generally obtained using a body-worn Global Navigation Satellite System (GNSS). Although these systems provide accurate and reliable measurement of the locomotion speed (Terrier et al., 2000; Witte and Wilson, 2004), they suffer from several limitations: (1) their high power consumption restricts their duration of use in portable devices, (2) the communication between the receiver and the satellite is not always guaranteed (e.g., indoor, near high buildings), and (3) the measurement accuracy decrease during rapid changes of speed and position (Varley et al., 2012; Rawstorn et al., 2014). As a solution to the latter limitation, systems based on the data fusion of body-worn inertial and GNSS sensors have been proposed to monitor sports activities (Brodie et al., 2008; Waegli and Skaloud, 2009; Zihajehzadeh et al., 2015). However, to address the issue of power consumption and communication losses, IMU-based systems must be able to estimate the speed without or with very limited input from a GNSS device.

Several methods have been proposed to estimate the walking speed using IMUs attached to different body-segments (Miyazaki, 1997; Aminian et al., 2002; Zijlstra and Hof, 2003; Sabatini et al., 2005; Hu et al., 2013; Salarian et al., 2013). One solution would be to extend and adapt these methods to running. However, these methods often relied on walking models or on the estimation of step length, which cannot be directly applied to running because of the aerial phases, where accelerometers are erroneous. Other studies have used machine learning techniques to estimate the walking speed but did not validate the results for running (Zihajehzadeh and Park, 2016; Fasel et al., 2017).

To the authors' knowledge, few studies proposed an accurate ambulatory method, based on body-worn IMUs, to estimate the overground speed of running, and even less did so for instantaneous speed estimation. Two studies used a similar method (integration of the acceleration signal) to calculate the velocity of the shank (Yang et al., 2011) and foot (Chew et al., 2017) segments. However, the error of the system was computed over multiple strides, in a small range of speeds, and for level treadmill running. As mentioned previously, the velocity estimated from the integration of segment acceleration has limitations, particularly when the flight phase varies in a wide range or when various slopes are experienced as it is the case in overground running. Another study (Hausswirth et al., 2009) compared in-lab a commercialized speed estimation device with the speed of a treadmill and reported a relatively low accuracy considering that the system required a subject-specific calibration. Subject-specific neural networks were also devised to assess the running speed in free-living conditions using only triaxial accelerometric measurements, but the model needed a calibration/learning phase for each runner and was validated for the mean speed using few trials (Herren et al., 1999). One study, however, exploited the personalized calibration and proposed a model based solely on the contact time (De Ruiter et al., 2016). Although the authors obtained a low root-mean-square error (<3%), these results were not instantaneous estimations but rather the average speed over bouts of 125 meters. Besides, a more recent study (Soltani et al., 2019) based on wrist-worn inertial sensors suggested that better results could be achieved by including more features to the model.

The objective of the current study was three-fold: first, we aimed to extend an existing walking algorithm based on strapdown integration of foot acceleration and show its limitation for running speed estimation. Then we proposed a new linear model to predict the running speed at each step and in real-world condition, based on relevant features extracted from feet acceleration and angular velocity. Finally, we investigated how personalization improved the performances of the system using additional data, such as occasional GNSS inputs. We compared each method to the GNSS speed, considered as the ground truth, obtained during outdoor measurements of overground running, at different speeds and slopes.

MATERIALS AND METHODS

Protocol and Instrumentation

Thirty-three healthy and active participants [18 males (age: 38 ± 9 y.o.; size: 180 ± 7 cm; weight: 76 ± 9 kg), 15 females (age: 36 ± 10 y.o.; size: 165 ± 7 cm; weight: 59 ± 7 kg)] without any symptomatic musculoskeletal injuries participated to this study. The measurements were performed in real-world conditions with sections of uphill, downhill, and level running. We asked the participants to run the same circuit three times, once at self-adjusted normal, fast, and slow speeds (**Figure 1A**). The periods of rest and the walking bouts, in between the running segments, were manually removed from the analysis. The local ethics committee approved the present protocol, and we conducted the measurements in agreement with the declaration of Helsinki.

Each participant was equipped with two time-synchronized sensors (Physilog 4, Gait Up, Switzerland) strapped on the dorsum of the shoe. Each sensor included a triaxial accelerometer, a triaxial gyroscope, and a barometer. The barometer was sampled at 50 Hz. Acceleration (±16 g) and angular velocity (±2,000 deg/s) were recorded at 500 Hz and were calibrated according to Ferraris et al. (1955) before each measurement session. Furthermore, a GNSS receiver (CAMM8Q, u-blox, CH) with an external active antenna (ANN-MS, u-blox, CH) was mounted on the head using Velcro attached to a cap. GNSS was used as a reference system for the estimation of the running speed. The GNSS receiver was set to pedestrian mode with a sampling frequency of 10 Hz. With such a configuration, the datasheet of the manufacturer reported a median error of 0.05 m/s for instantaneous speed estimation. MATLAB software (R2018b, MathWorks, Natick, MA USA) was used for all the data processing steps without the need for publicly available libraries.

Estimation of Reference GNSS Speed

The reference speed obtained from the GNSS receiver was processed according to Soltani et al. (2019) and in two steps

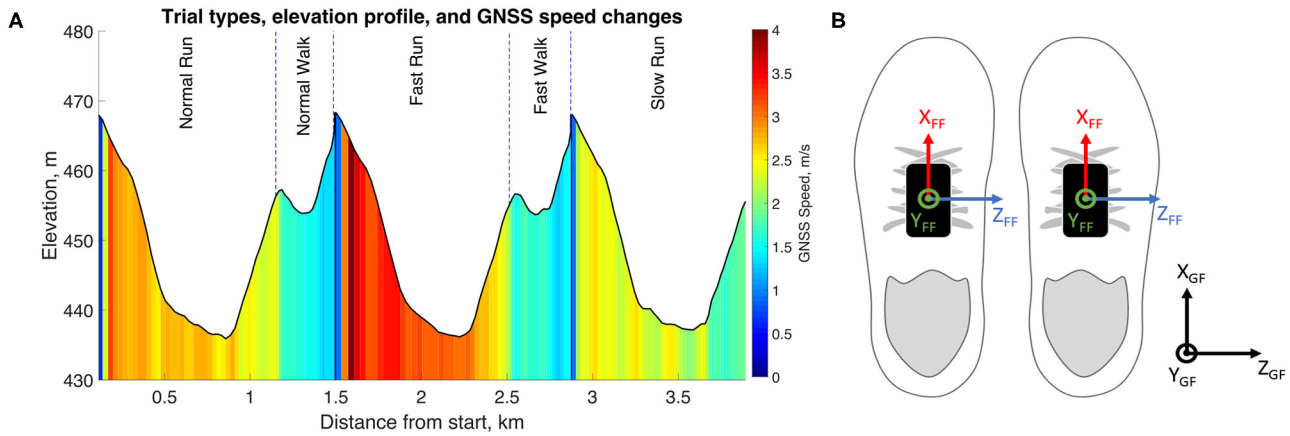

FIGURE 1 | (A) The elevation and speed of the running circuit. This figure was adapted from Soltani et al. (2019). **(B)** The definition of the foot functional frame (FF) and global frame (GF) used in this study.

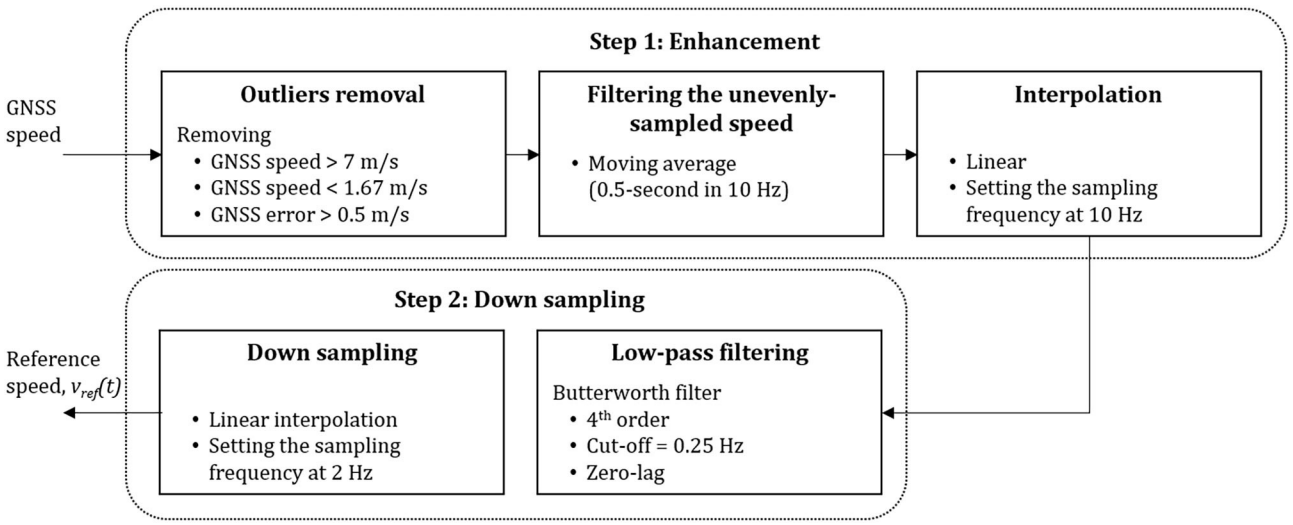

FIGURE 2 | Pre-processing steps applied to the GNNS measurements of speed to obtain the reference speed estimation. This figure was adapted from Soltani et al. (2019).

(**Figure 2**). First, we enhanced the signal by removing the outliers that did not correspond to running; hence, we removed all recorded speed samples outside of the 5–20 km/h range. Moreover, the GNSS receiver provided an estimation of the accuracy of each observation; hence we discarded any data-point with an error higher than 0.15 m/s. This process retrieved an unevenly sampled reference speed signal. We applied a moving average of 0.5-s width (in 10 Hz), followed by linear interpolation to obtain an equally-spaced time series at 10 Hz. In the second step, the signal was down-sampled to provide the reference speed (v_{ref}), after a fourth-order low-pass Butterworth filter with the cut-off frequency at 0.25 Hz to reduce the noise.

Speed Estimation Based on Direct Integration of Foot Acceleration

In this section, we describe the sequence of transformations that we applied on the IMU and barometer data to extract the gait features. The whole process can be summarized in four tasks: pre-processing, temporal analysis, spatial analysis, and foot speed estimation (**Figure 3**).

Pre-processing

First, a 4th-order low-pass Butterworth filter (Fc = 50 Hz) was applied on the raw acceleration ($a(t)$) and angular velocity ($\omega(t)$) signals to reduce the noise. Then the IMU signals were aligned with the foot segment by computing the rotation matrix that transforms the data recorded in the technical frame of the sensors into the functional frame (FF) of the foot (**Figure 1B**). For this purpose, we used the measurements of level normal walking (**Figure 1A**) and a previously reported calibration method (Falbriard et al., 2018). This process aligned the y-axis of the IMU with the vertical axis of the foot, pointing upward, the z-axis to the mediolateral axis, pointing to the right side of the subject, and the x-axis to the longitudinal axis, pointing toward the forefoot.

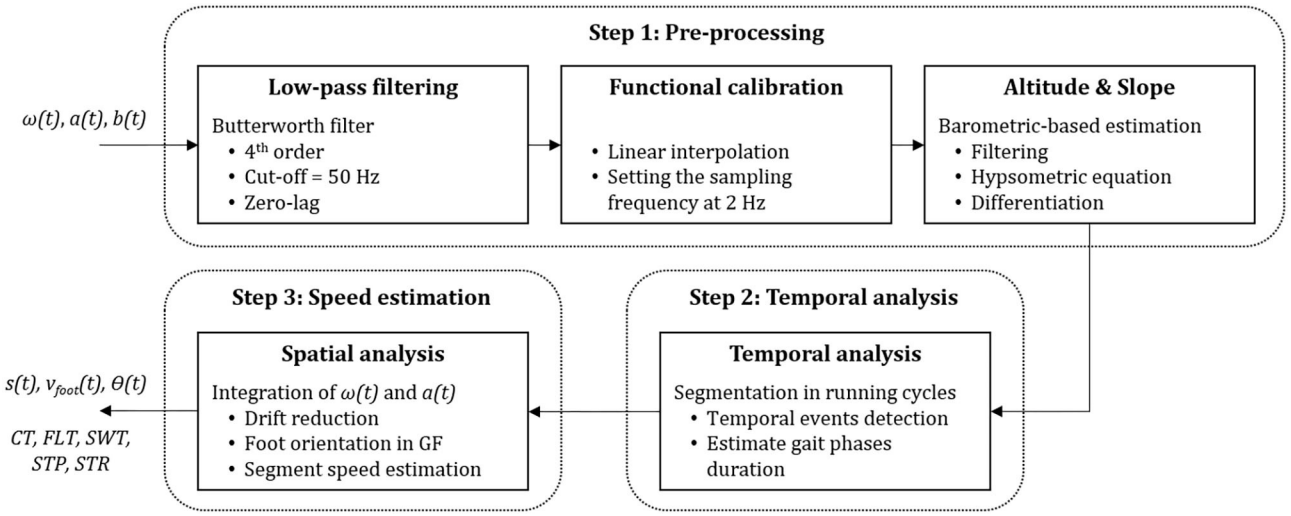

FIGURE 3 | Steps performed on the IMU acceleration *a(t)*, angular velocity $\omega(t)$, and barometric pressure *b(t)* measurements. The outputs were later used for feature extraction; the slope *s(t)*, the speed of the foot $v_{foot}(t)$, the pitch angle $\theta(t)$, contact time *CT*, flight time *FLT*, swing phase duration *SWT*, step duration *STP* and stride duration *STR*.

Throughout this paper, if not mentioned otherwise, the data are reported in the functional frame of the foot.

The last phase in pre-processing was estimating the overground slope. As the mechanics of running differ between level, uphill, and downhill running (Vernillo et al., 2017), we assumed that the elevation difference between successive steps would be a relevant input for the model. Therefore, the barometric pressure was converted by the hypsometric equation to the altitude signal (Bolanakis, 2017) smoothed by applying a 4-s moving average filter and down-sampled to 1 Hz time-series. The slope ($s(t)$) was defined as the altitude difference between two samples spaced by 5 s, by assuming that changes of altitude shorter than 5 s would not have a significant effect on the running speed.

Temporal Analysis

Temporal events detection was performed as described in Falbriard et al. (2018) by segmenting the race into mid-swing to mid-swing cycles and detecting of several temporal events within each cycle. Mid-swings were detected as the positive peaks observed on the pitch axis (FF z-axis) of the angular velocity measurements. Moreover, we improved the robustness of the peak detection algorithm by applying the YIN auto-correlation method (De Cheveigne and Kawahara, 2002) over a 10-s sliding window (5-s overlap) to obtain an approximation of the cadence and set an adequate minimum time difference between two peaks. The initial contact event (IC), defined as the moment when the foot initiates contact with the ground at landing, and terminal contact (TC), defined as the instant when the toes leave the ground during the pushing phase, were then detected within each cycle using the two minimums of the pitch angular velocity. Moreover, we defined the event MinRot as the time-point where the norm of the angular velocity ($||\omega(t)||$) is minimum within the stance phase (i.e., between IC and TC).

Spatial Analysis and Foot Speed Estimation

This process aimed to measure the orientation of the foot in the global frame (GF), remove the Earth's gravitational acceleration from the recorded acceleration, and integrate the corrected acceleration to obtain the speed of the foot. In GF, the x-axis was in the running direction, the z-axis corresponds to the axis perpendicular to the ground surface, and the y-axis was defined by the cross-product of the z and x-axes (**Figure 1B**). Using a previously validated technique (Falbriard et al., 2020), foot orientation was obtained in GF, and foot acceleration in FF was expressed in GF and the gravitational acceleration ($g = [0\ 0\ 9.81]$ m/s^2) removed. The resulting acceleration (in GF) was integrated using a trapezoidal rule to get a first estimate of the speed of the foot. We considered the speed of the foot to be zero during the stance phase and, therefore, estimated and removed the integration drift by linearly resetting the speed between MinRot and TC of each stance phase. Note that we preferred MinRot to the IC for drift resting since MinRot corresponds to the time sample when the foot is the closest to a static state, reportedly used as the integration limits in walking gait analysis (Mariani et al., 2010). We finally applied the inverse of the quaternions mentioned above to get the drift-corrected speed of the foot segments ($v_{foot}(t)$) in the FF.

Development of a Linear Model for Speed Prediction

Feature Extraction, Linearization, and Outliers Removal

First, we extracted several parameters (p_j) for each step, which were later used as inputs for the speed estimation model. As several studies reported on the association between the changes in the duration of the gait phases and the running speed (Högberg, 1952; Saito et al., 1974; Nummela et al., 2007), we computed the

TABLE 1 | List of the features extracted for each stride on the continuous acceleration $a(t)$, angular velocity $\omega(t)$, speed $v_{foot}(t)$, and slope $s(t)$.

Type	Feature	Description
Intensity	mean_<T>_<C>	Mean value
	std_<T>_<C>	Standard deviation
	med_<T>_<C>	Median
	iqr_<T>_<C>	Interquartile range
	max_<T>_<C>	Maximum
	rms_<T>_<C>	Root-mean-square
Shape	kurt_<T>_<C>	Kurtosis
	skew_<T>_<C>	Skewness
Compression	arm1_<T>_<C>	First coefficient of the auto-regressive model of order 3
	arm2_<T>_<C>	Second coefficient of the auto-regressive model of order 3
	arm3_<T>_<C>	Third coefficient of the auto-regressive model of order 3

In the name of the feature, variables <T> and <C> correspond to the label of the signal and the channel, respectively. Hence <T> must be replaced by a, ω, v_{foot}, or s while <C> must be replaced by x, y, z, or norm.

ground contact time (CT), the flight time (FLT), the swing time (SWT), the step duration (STP), and the stride duration (STR) for each step i, where i = 1…N, and N is the total number of steps (Equations 1–5).

$$CT_i = TC_i - IC_i \quad (1)$$

$$FLT_i = IC_{i+1} - TC_i \quad (2)$$

$$SWT_i = IC_{i+2} - TC_i \quad (3)$$

$$STP_i = IC_{i+1} - IC_i \quad (4)$$

$$STR_i = IC_{i+2} - IC_i \quad (5)$$

As a few strides suffered from misdetections, outliers were removed according to (1) a valid stride must last between 0.37 and 2.5 s, and (2) the flight phase (FLT) must be >0.

Pitch angle (θ) at the IC was extracted as the angle between the longitudinal axis of the foot (FF x-axis) and the ground surface (x and y-axis in GF). A positive pitch angle corresponds to a rear-foot landing (i.e., talus region lower than the toes) and a negative pitch angle to a forefoot strike.

We also extracted several statistics from the acceleration $a(t)$, the angular velocity $\omega(t)$, the foot speed $v_{foot}(t)$, and the slope $s(t)$ time-series. Moreover, since $a(t)$, $\omega(t)$, and $v_{foot}(t)$ were 3-dimensional signals, these statistics were computed for each axis (i.e., x, y, and z) and the norm of the signal. Note that the features were captured on the signals of a single stride (i.e., between IC_i and IC_{i+2}, where i = 1…N) before applying the statistical functions. We opted for a stride-based segmentation instead of the step-based segmentation because a stride corresponds to one period of gait and, therefore, is more likely to capture the complete pattern of a cycle. Besides, the list of selected features (**Table 1**) aimed to collect information in the intensity of the signal (e.g., mean, STD, RMS), the shape of its distribution (e.g., skewness, kurtosis) and its shape in a compressed format (e.g., coefficient of the auto-regressive model). Moreover, as the temporal parameters (Equations 1–5) already hold relevant periodic information, we did not consider features in the frequency domain.

Before proceeding to the selection of the best features, we visualized the relation between the reference speed $v_{ref}(t)$ and the features individually. Based on our observations, we identified three functions that improved the linear relationship between the reference speed and some of the input features; $f_1(p) = p^2$, $f_2(p) = p^3$, and $f_3(p) = 1/p$. The functions f_1, f_2, and f_3 were applied to all the features, and the results added to the list of features. Finally, we also included several anthropometric parameters to the collection of features, such as the size, weight, gender, and age of the participants.

Data Set Configuration

We divided the data into three subsets: validation, training, and testing sets. The participants were randomly distributed into the three subsets. It is important to note that all the steps of a single individual were attributed to only one of the subsets; this removed the performance bias associated with the models trained and tested on measurements originating from the same subjects (Halilaj et al., 2018). **Figure 4** shows the data from each set with different colors and illustrates their functions.

We used the 10 subjects (30%) from the validation set for feature selection (in orange in **Figure 4**), and the 23 remaining participants (70%) were used interchangeably for training (in blue in **Figure 4**) and testing (in green in **Figure 4**) of the model according to the leave-one-subject-out cross-validation method. We emphasize on the fact that the validation set was not included in the evaluation of the model and served exclusively for feature selection. We distinguished the development set from the other sets to lessen the risks of overfitting and preferred a leave-one-subject-out approach for the assessment of the model's performance due to the relatively low number of individuals present in this study. Moreover, such a method allowed us to identify potential outliers in the participants and later find collections of subjects with similar biases.

The leave-one-subject-out cross-validation method functioned as followed: we trained the model using the data from 22 subjects (training set) and tested on the data from one individual (testing set). We then repeated this process, such that each participant appeared once in the testing set.

Automatic Feature Selection

Here, we selected the features (P_{auto}) to minimize the mean-square error (MSE) of the speed estimation model using the ordinary least squares method. The leave-one-subject-out method was applied with 11 subjects for training and one subject to evaluate the error of the predictions (**Figure 4**). The automatic feature selection process started with an empty set of inputs and sequentially added the parameters p_j or their transform (f_1, f_2, f_3), which minimized the average MSE among all the subjects. This method is known as the forward stepwise selection process and has proven to be reliable on large feature space (John et al., 1994; Kohavi and John, 1997). The algorithm stopped including new parameters if the gain in the average MSE was lower than

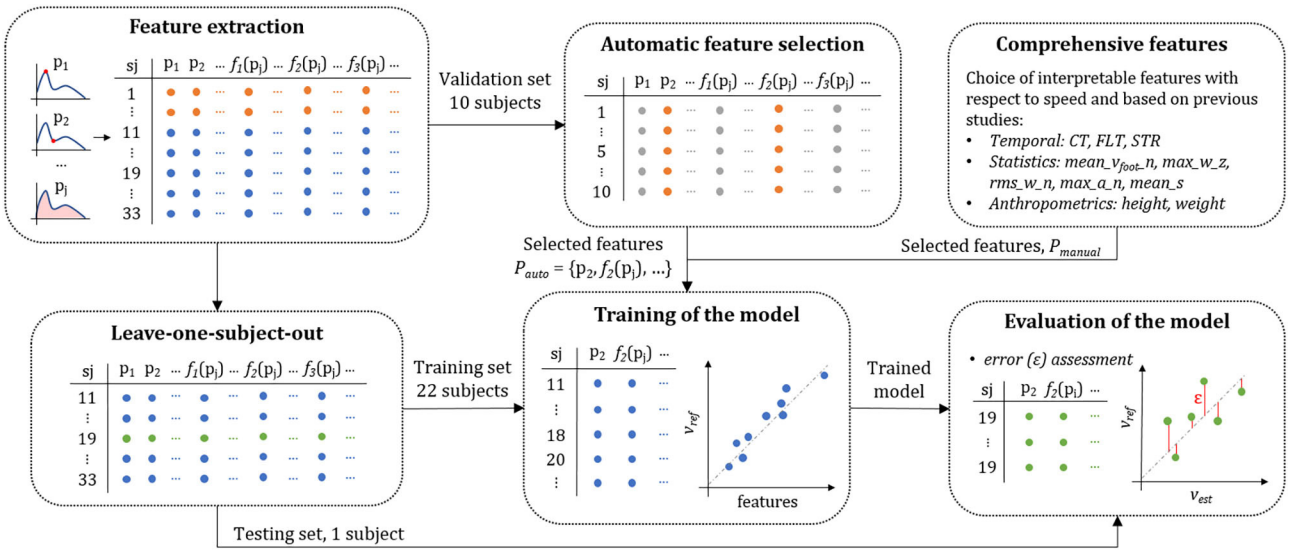

FIGURE 4 | Schematic representation of the data repartition into the validation (blue), training (orange), and testing (green) set. The validation set was used for feature selection, the training set to train the coefficients of the linear model, and the testing set to evaluate the performance of the predictions. The features are represented as p_j and the linearization function as $f_1(p_j)$, $f_2(p_j)$, and $f_3(p_j)$.

1% of the previous MSE recorded. We deliberately set a low 1% criterion to obtain a possibly unnecessary large number of inputs knowing that the model is trained using the LASSO method (Tibshirani, 1996) with shrinkage of the redundant features. To ensure that the features contributed equally to the MSE estimation, we rescaled the inputs using a robust z-score normalization method (Jain et al., 2005); after normalization, the feature's mean was equal to zero, and median absolute deviation equal to one (less sensitive to outliers than the variance of one).

Comprehensive Selected Features

Although a supervised and automatic feature selection method may retrieve the subset with the best prediction performance on a given set of parameters, the results are sometimes difficult to interpret. Hence it is generally recommended also to evaluate the performance of a comprehensive set of features selected based on their biomechanical relevance (Halilaj et al., 2018). Based on the findings of previous research in running, we defined a list of features (P_{manual}) known to be affected by variations in the running speed. As for the automatic selection of features, we willingly selected a large number of input features, potentially intercorrelated, knowing that optional inputs will be discarded later in the training stage. In summary, comprehensive features included the following:

- Anthropometric features: the height because taller individuals are likely to have longer step length, thus higher speed, than shorter individuals with similar flight times.
- Temporal features: the CT, FLT, and STR contain relevant information about the stride frequency and were shown to decrease with an increase in the running speed (Saito et al., 1974; Nummela et al., 2007; Chapman et al., 2012).
- Speed and spatial features: the average speed of the foot (*mean_v$_{foot}$_norm*) obtained with a direct integration; the maximum angular velocity of the foot in the sagittal plane (*max_ω_z*) assuming faster swing involves higher speed; the RMS value of the angular velocity norm (*rms_ω_norm*) since higher speed should result in higher dynamic movements; the maximum of the acceleration norm (*max_a_norm*) as it was demonstrated in previous studies that tibial peak accelerations increased with faster-running velocities (Sheerin et al., 2019); and the average slope (*mean_s*) since uphill and downhill may affect the running speed.

Training and Testing of the Model

The linear model was trained and tested with the leave-one-subject-out cross-validation method. For each individual, the performance of the speed prediction was evaluated with the model's coefficients trained on 22 other subjects. This approach was preferred to a traditional split of the data into two datasets (e.g., 70% training and 30% testing repartition) due to the restricted number of subjects available after the feature selection phase. Besides, the leave-one-subject-out procedure allowed us to detect potential outliers in the participants and, therefore, possibly identify the sources of poor estimation results.

The least-squares regression coefficients were trained using the LASSO method (Tibshirani, 1996), with scaled inputs to have zero mean and a variance of one, and equally distributed the observations' weights at the initialization stage. To limit the risks of overfitting, we selected the model with the smallest number of inputs, if any new input would improve the MSE by <2%.

Since we observed some disparity in the dataset (the steps between 2.5 and 4 m/s were over-represented), we used a random under-sampling (RUS) method to deal with the issue of class

imbalance (Pes, 2020). This process started by dividing the range of reference speeds into five equally spaced groups, from 1.4 to 2.2 m/s, 2.2 to 3 m/s, 3 to 3.8 m/s, 3.8 to 4.6 m/s, and 4.6 to 5.4 m/s. We then randomly selected the same number of steps from each group based on the group with the least number of steps (i.e., down-sampling of the majority). We repeated this process ten times, generating ten versions of the under-sampled data set and used these subsets independently. In other words, we trained and tested the model 10 times for each individual.

Finally, we investigated the changes in the speed prediction when input features were averaged over consecutive steps. Instead of using a single step granularity for running speed, averaging over several steps might conceivably improve the precision (i.e., random error) of the model. We tested this approach on an even number of steps (i.e., 2, 4, 6, 8, and 10), for it equally includes the sensor's information from both feet. In order to avoid grouping non-consecutive steps, we applied this averaging process before under-sampling the inputs.

Personalized Model

Running Speed Estimation Algorithm

Recently, online personalization methods have emerged in the field of human movement analysis. For instance, such an approach demonstrated significant improvement in speed estimation performances (Soltani et al., 2019). The objective is to personalize a generic speed estimation model based on the sporadic reference data obtained from a GNSS device. We describe the online-learning procedure used in this study in the following; we define n as the observation (or sample) index used for the personalization where each sample corresponds to one stride. Therefore, if we have M samples (i.e., strides) for the personalization, then $n \in \{1, 2, 3, \ldots, M\}$.

Let's Q be the number features in each stride. We defined p_n as the feature vector and sl_n as the reference stride length for the n-th stride according to Equations (6, 7). Here, $p_j[n]$ is a symbolic name for the j-th feature of the n-th stride. Moreover, $v_{ref}[n]$ is the GNSS speed of the n-th stride.

$$p_n = \left[1\, p_1[n]\, p_2[n] \ldots p_Q[n]\right] \tag{6}$$

$$sl_n = v_{ref}[n] \times \frac{1}{STR_n} \tag{7}$$

For p_n we used the selected features in P_{manual} or P_{auto} based on results obtained in the linear model. We first modeled the stride length through Recursive Least Square (RLS) and then multiplied that by the stride frequency to obtain the running speed. The RLS is a real-time and computationally effective online learning method, which does not need to have or store all the training data from the beginning of training.

Let P_n and SL_n be the feature matrix and the vector of actual stride length defined in Equations (8, 9), respectively.

$$P_n = \begin{bmatrix} p_1 \\ \vdots \\ p_n \end{bmatrix} \tag{8}$$

$$SL_n = \begin{bmatrix} sl_1 \\ \vdots \\ sl_n \end{bmatrix} \tag{9}$$

Using the RLS approach, SL_n can be modeled as in Equation 10, where β_n is the coefficient of the model trained using n observations. If P_{n-1} and β_{n-1} are the feature matrix and model coefficients estimated using *n-1* samples, then once we obtain a new sample (p_n and sl_n) for the personalization, β_n can be recursively estimated through Equation (10).

$$\beta_n = \beta_{n-1} + D_n p_n \left(sl_n - p_n^T \beta_{n-1}\right) \tag{10}$$

Where D_n, known as the dispersion matrix, itself, is recursively estimated by having only D_{n-1} (i.e., the dispersion matrix estimated using *n-1* samples) and the new personalization data (i.e. p_n and sl_n) according to Equation (11). Here, K_n is defined as Equation (12).

$$D_n = D_{n-1}\left(I - p_n \left(I + K_n\right)^{-1} p_n^T D_{n-1}\right) \tag{11}$$

$$K_n = p_n^T D_{n-1} p_n \tag{12}$$

For each individual, ten strides from the training set were used to initialize the recursion process of the RLS.

Cross-Validation

The data set was organized differently for the personalization process to consider the gait style of each individual and minimize the training data from GNSS. Data from each individual was divided into bouts of 10 strides, and half of these bouts were assigned randomly to the training set and the other half to the testing set of that same individual. Consequently, we trained and evaluated the models for each individual separately, using the uniquely the data from that same individual.

Statistical Analysis

We evaluated the performance of the model by computing the error on the training and testing sets. We did so going from a single step to a ten-steps resolution according to the configuration of the inputs. For each of the RUS iteration, the intra-subject accuracy (or bias) and precision were estimated using the mean and standard deviation, respectively. The normality of the speed error was tested using the Lilliefors test, and in the case of non-normal distribution, the mean was replaced by the median and standard deviation by the Inter-Quartile Range (IQR). To better understand the performance of the system, the intra-subject RMS error was calculated, and the Pearson correlation coefficient was used to assess the linear dependence of the predictions. Since we used the leave-one-subject-out method for training and testing, the results were reported by computing the mean, the standard deviation, the minimum and the maximum on the intra-subject biases,

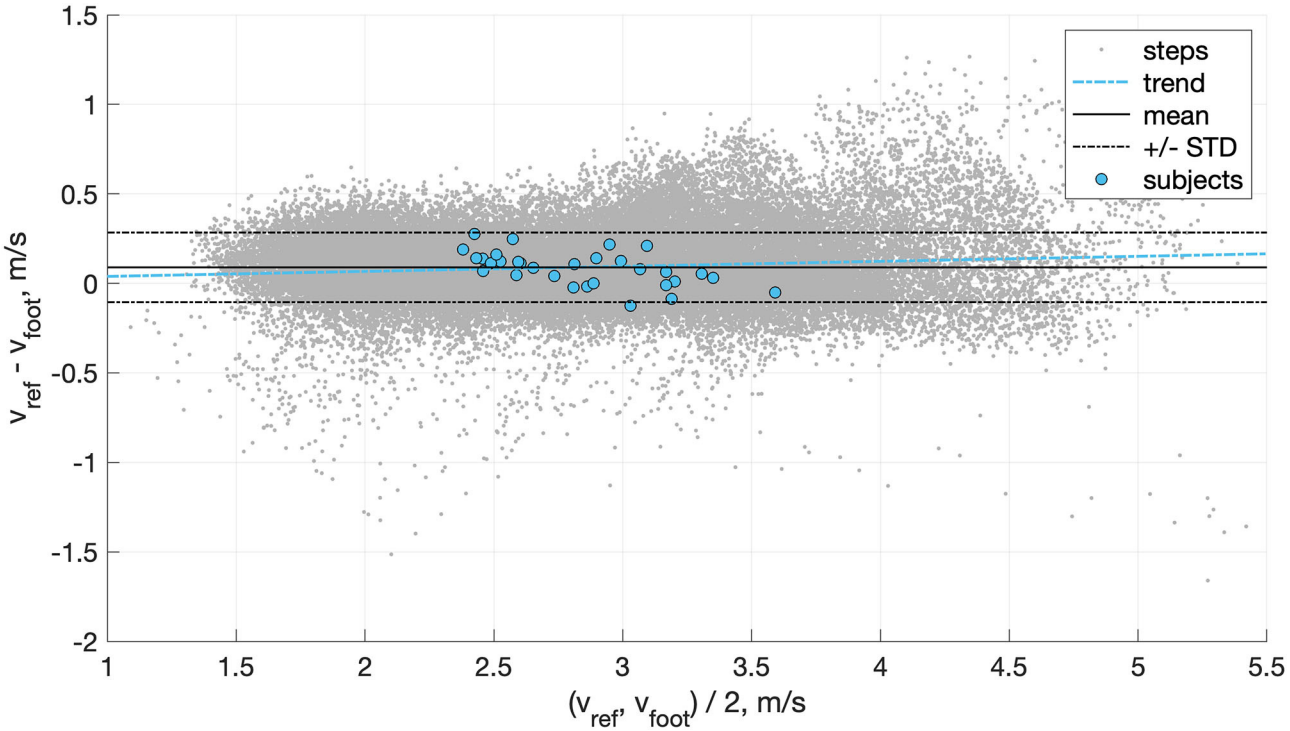

FIGURE 5 | Bland-Altman plot of the agreement between the direct speed estimation method (v_{foot}) and the GNSS reference (v_{ref}). The error was estimated with a granularity of one step.

precision, RMS error, and correlation coefficients. Agreement between the reference GNSS speed and the estimated speed was illustrated with Bland & Altman plots (Bland and Altman, 1986). Furthermore, to evaluate the distribution of the errors and possible overfitting, we used the cumulative distribution function (CDF) of step absolute error for both training and testing sets.

RESULTS

Direct Speed Estimation

Two subjects were excluded from the data set; because of the poor quality of the GNSS measurements or because of an improper fixation of the IMU on the shoe and high Signal to Noise Ratio (SNR) of the kinematic data. Since it required no learning, the direct speed estimation method was performed on the 63'435 steps available in this study. We observed an inter-subject mean ± STD (min, max) of 0.08 ± 0.10 (−0.12, 0.27) m/s for the bias, 0.16 ± 0.04 (0.08, 0.25) m/s for the precision, 0.20 ± 0.06 (0.08, 0.34) for the RMSE. The relation between the speed estimation error and the overground velocity is presented in **Figure 5**, and the effect of the slope in **Figure 6**.

Automatic Feature Selection

In total, we used the 20'084 strides of the validation set to select 28 features out of the 668 features available. The feature selection process stopped at average Mean Square Error (MSE) of 0.0057 m/s (**Figure 7**), which corresponded to a 1.12% improvement compared to the previous step with 27 features. The selection process was repeated 100 times (i.e., 10 times for each of the 10 subjects) and led to the set of features presented in **Table 2**.

Out of the 28 features selected, 16 (57%) resulted from one of the three linearization functions (f_1, f_2, f_3), one feature from the temporal analysis (STR), one from the orientation estimation (θ). The other features are statistics extracted from the different time series [i.e., acceleration $a(t)$, angular velocity $\omega(t)$, the velocity of the foot segment $v_{foot}(t)$, and the slope $s(t)$].

Linear Model

In total, 43'351 steps were used to train and test the linear model. Due to the subdivision of the data associated with the leave-one-subject-out method, we used, for each individual, an average ± STD (min, max) of 41'287 ± 188 (41'032, 41'642) steps for training and 2'064 ± 188 (1'709, 2'319) steps for testing.

When the P_{auto} feature set was used for training, the LASSO method always favored the same 7 inputs ($P_{auto,best}$) among the 28 features previously selected (**Table 2**):

$$\begin{aligned} P_{\text{auto,best}} = [&\text{mean\_a\_norm}, f_1(\text{mean\_s}), f_3(\text{STR}), f_2(\text{median\_}\omega\text{\_z}),\\ &\text{max\_}v_{\text{foot}}\text{\_norm}, f_1(\text{mean\_}v_{\text{foot}}\text{\_y}),\\ &f_3(\text{median\_}\omega\text{\_norm})] \end{aligned}$$

In comparison, with P_{manual} the LASSO method selected 4 inputs ($P_{manual,best}$):

$$P_{\text{manual,best}} = [\text{rms\_}\omega\text{\_norm}, \text{mean\_}v_{\text{foot}}\text{\_norm}, \text{mean\_s}, \text{CT}].$$

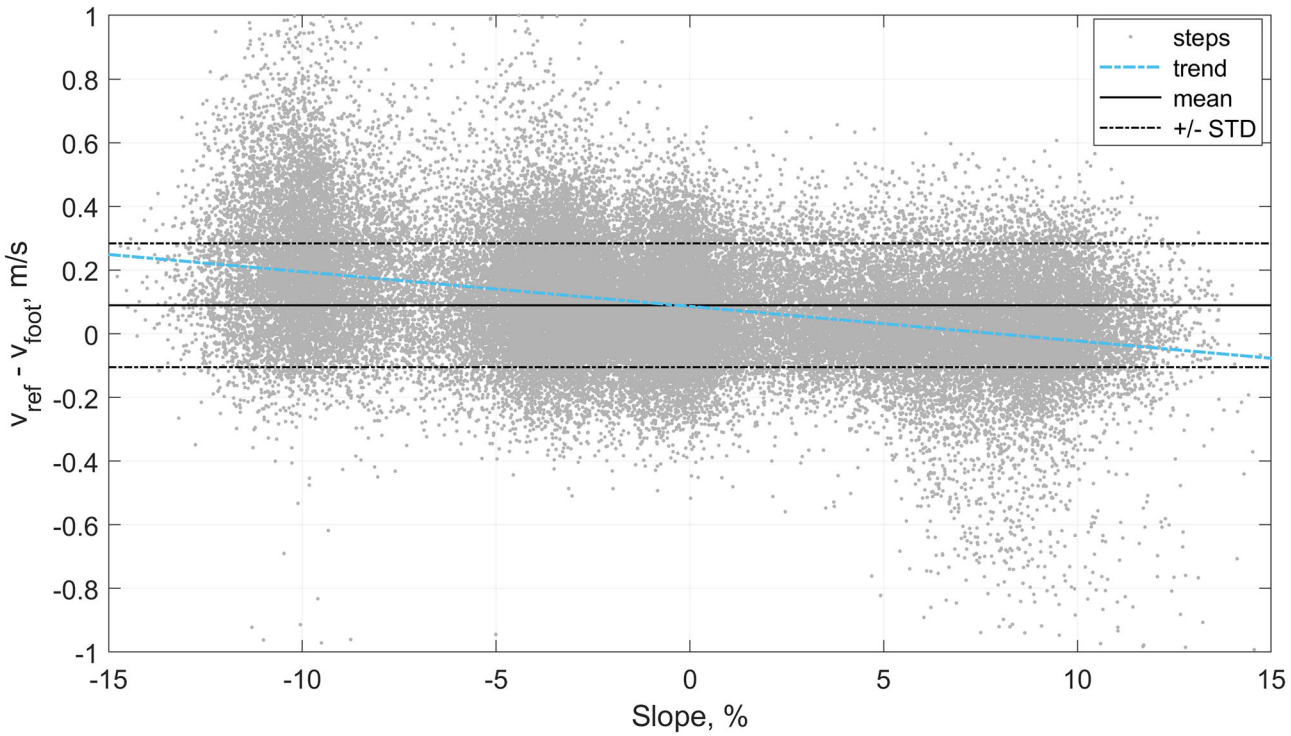

FIGURE 6 | The step by step error of the direct speed estimation method (v_{foot}) in relation to the slope of the ground surface.

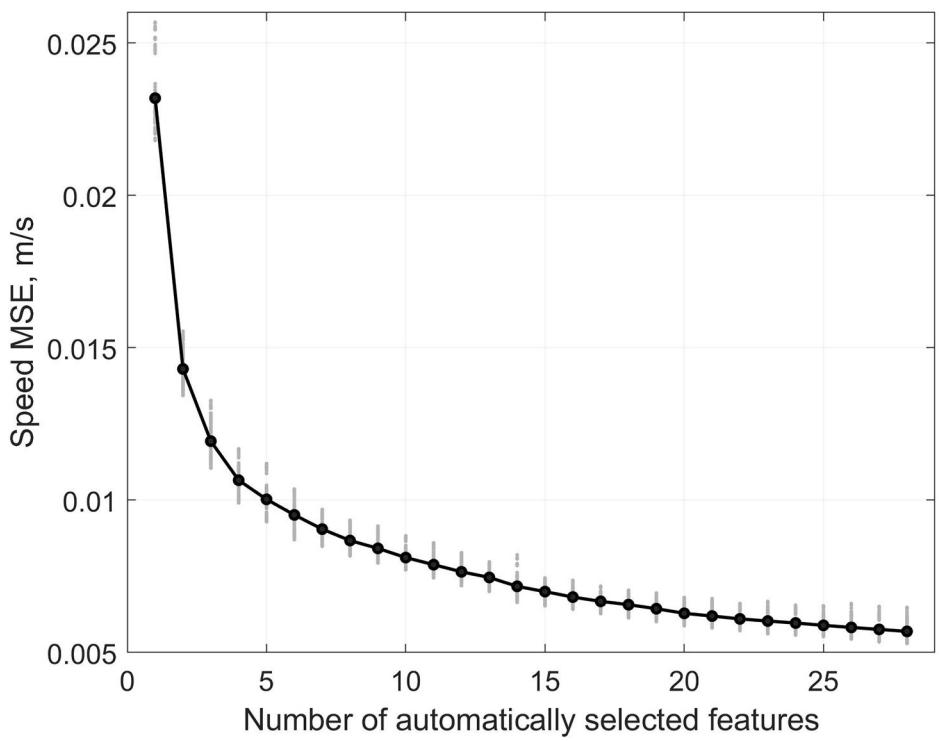

FIGURE 7 | Mean Square Error (MSE) of the speed estimation during the forward stepwise selection process. In gray, the MSE of each subject and blue the inter-subject average.

The performances of the linear predictor over the testing set are shown in **Table 3**; the inter-subject mean, STD, minimum, and maximum are presented for the bias, the precision, the RMSE, and the correlation coefficients. The results of the running speed estimation are presented for single-step resolution and also where the inputs were averaged over 2, 4, 6, 8, and 10 steps before being used by the linear model.

In comparison, when we used a moving average (four steps) on the output of the speed estimation model (i.e., not the inputs as in **Table 3**), then we obtained an inter-subject mean ± STD (min, max) bias of 0.00 ± 0.10 (−0.17, 0.17) m/s, precision of 0.13 ± 0.05 (0.06, 0.23) m/s, RMSE of 0.14 ± 0.05 (0.08, 0.28) m/s, and correlation coefficients of 0.985 ± 0.010 (0.956, 0.997). The agreement between the speed estimation using $P_{auto,best}$ (v_{est}) and the reference GNSS system is presented for each stride (gray dots) and each individual (blue circles) in **Figure 8**.

Figure 9A shows the CDF of the speed estimation error for each subject (gray lines) and the subjects aggregated (blue line). In total, 56% of the recorded steps have an error below 0.1 m/s and 86% below 0.2 m/s. Finally, as illustration of overground measurement of speed over a various range of self-adjusted speed, the speed obtained with the reference GNSS system was compared for a typical subject with the speed estimation at step level (v_{est},1), and the estimation when averaged over four steps (v_{est},4) in **Figure 9B**.

TABLE 2 | The ordered list of the features automatically selected by the forward stepwise selection algorithm.

#	Label	*f(p)*	#	Label	*f(p)*
1	*mean_a_norm*	-	15	*mean_v_{foot}_y*	p^2
2	*mean_v_{foot}_norm*	-	16	*median_ω_norm*	p^{-1}
3	*iqr_a_norm*	-	17	*median_ω_x*	-
4	*θ*	-	18	*skew_v_{foot}_norm*	-
5	*mean_s*	p^2	19	*iqr_v_{foot}_norm*	p^{-1}
6	*STR*	p^{-1}	20	*max_v_{foot}_y*	p^{-1}
7	*median_a_x*	p^3	21	*mean_ω_y*	-
8	*median_ω_z*	p^3	22	*rms_a_x*	p^3
9	*max_v_{foot}_norm*	-	23	*median_v_{foot}_x*	-
10	*median_a_y*	p^3	24	*std_a_norm*	p^{-1}
11	*mean_v_{foot}_x*	p^2	25	*skew_ω_norm*	-
12	*skew_v_{foot}_y*	p^{-1}	26	*skew_ω_z*	p^2
13	*median_v_{foot}_y*	-	27	*std_a_x*	p^{-1}
14	*std_ω_z*	-	28	*arm3_v_{foot}_y*	p^{-1}

Personalization

We used the features in P_{manual} to train and test the personalized model since the results of the generic model show little differences between $P_{auto,best}$ and $P_{manual,best}$, and because, with P_{manual}, we could include the 10 subjects from the validation set in the training and testing process without any risk of overfitting. For each subject, the training samples (i.e., half of the data of the subject, randomly selected) were fed one-by-one to the RLS, and the speed was estimated with the complete test set of the subject. **Figure 10** shows this process for the first 150 strides used for personalization of the model; the solid line and the shaded area represents the inter-subject mean and standard deviation of the RMSE, respectively. Also, the evaluation error for the first 10 strides is not displayed in **Figure 10**; these strides were used to initialize the RLS algorithm.

In total, we used 1,139 ± 149 strides for training and 1,132 ± 149 strides for testing for each individual. **Table 4** reports the bias, precision, and RMSE of the personalized model. **Figure 11** also shows the Bland-Altman plot of the personalized model where the mean and standard deviation of the error is displayed by the dark and dotted lines, respectively. Moreover, the Spearman's test showed a high correlation of 0.97 between the estimated and the reference values of running speed.

TABLE 3 | Inter-subject mean, STD, minimum, and maximum of the system's bias, precision, Root-Mean-Square error (RMSE), and the linear correlation coefficient (R).

Features	Steps	Bias (m/s)				Precision (m/s)				RMSE (m/s)				R			
		mean	STD	min	max	mean	STD	min	max	mean	STD	min	max	mean	STD	min	max
$P_{auto,best}$	1	0.00	0.10	−0.17	0.17	0.14	0.05	0.08	0.24	0.16	0.05	0.10	0.28	0.985	0.010	0.956	0.997
	2	0.00	0.11	−0.17	0.18	0.13	0.05	0.06	0.23	0.14	0.05	0.08	0.27	0.989	0.009	0.957	0.998
	4	0.00	0.11	−0.17	0.19	0.12	0.06	0.05	0.24	0.12	0.05	0.07	0.24	0.990	0.009	0.961	0.998
	6	0.00	0.11	−0.17	0.18	0.11	0.05	0.05	0.23	0.12	0.04	0.06	0.21	0.990	0.009	0.952	0.999
	8	0.00	0.11	−0.18	0.19	0.11	0.05	0.05	0.23	0.12	0.05	0.06	0.23	0.991	0.009	0.952	0.999
	10	0.00	0.11	−0.17	0.19	0.11	0.05	0.05	0.23	0.11	0.04	0.06	0.23	0.992	0.008	0.965	0.999
$P_{manual,best}$	1	0.00	0.11	−0.22	0.17	0.15	0.06	0.09	0.29	0.18	0.07	0.11	0.37	0.983	0.009	0.961	0.997
	2	0.00	0.11	−0.23	0.18	0.13	0.06	0.07	0.26	0.15	0.06	0.09	0.29	0.988	0.008	0.963	0.997
	4	0.00	0.11	−0.23	0.20	0.12	0.06	0.06	0.26	0.14	0.06	0.08	0.24	0.989	0.009	0.959	0.998
	6	0.00	0.12	−0.23	0.19	0.12	0.06	0.06	0.24	0.13	0.06	0.06	0.24	0.990	0.009	0.956	0.999
	8	0.00	0.12	−0.23	0.20	0.11	0.06	0.05	0.24	0.13	0.06	0.06	0.24	0.991	0.009	0.944	0.999
	10	0.00	0.12	−0.24	0.20	0.11	0.06	0.05	0.24	0.12	0.06	0.06	0.24	0.991	0.008	0.964	0.999

The results are presented for each configuration of inputs ($P_{auto,best}$ and $P_{manual,best}$).

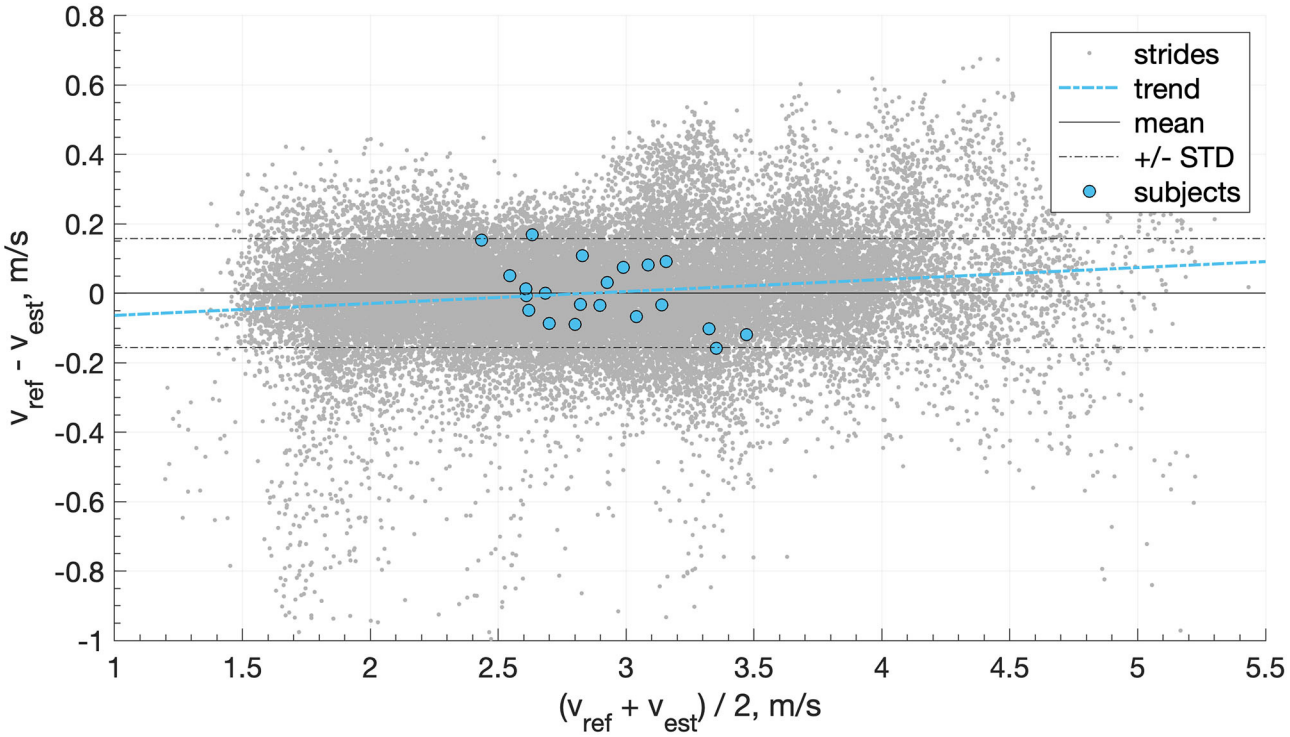

FIGURE 8 | Bland-Altman plot of the speed estimation (v_{est}) obtained with the features automatically selected ($P_{auto,best}$) and compared with the reference GNSS speed (v_{ref}). The gray dots represent the steps, the blue circle the average results of each subject, the solid black line the mean of the steps, the dashed black lines the STD of the steps, and the dashed blue line the linear trend of the steps.

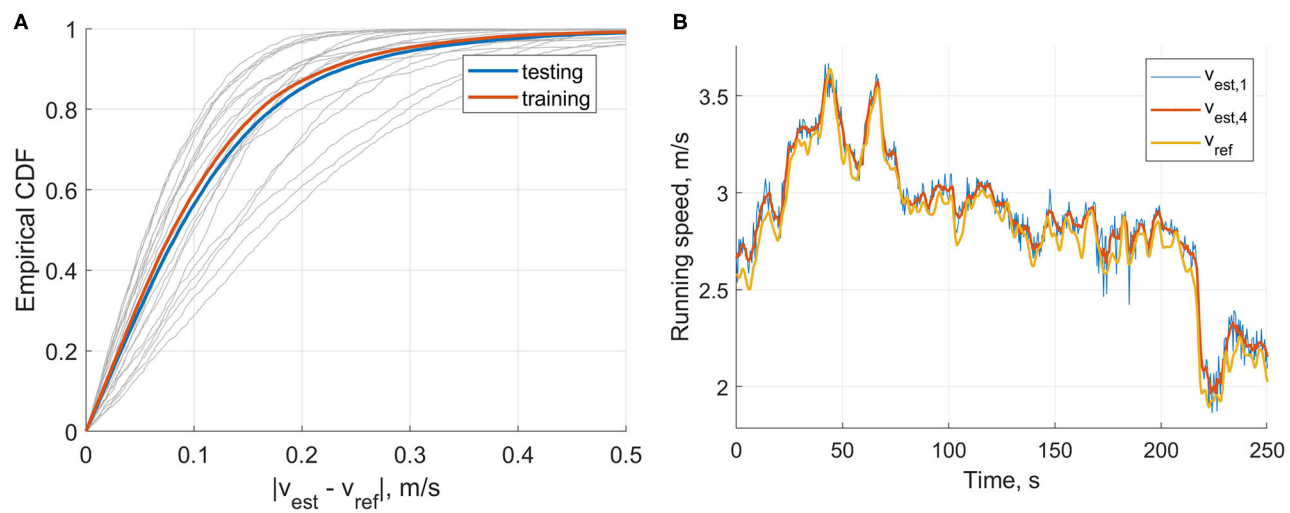

FIGURE 9 | (A) The Cumulative Density Function (CDF) of the speed estimation error of each step ($|v_{ref} - v_{est}|$). The speed was estimated using the automatically selected inputs ($P_{auto,best}$). The gray curves represent the CDF of each individual in the testing set, the blue line the inter-subject CDF of the testing set, and the orange line the inter-subject CDF of the training set. **(B)** Comparison between the speed estimation of each step ($v_{est,1}$), the speed estimation averaged over four steps ($v_{est,4}$), and the reference GNSS speed (v_{ref}).

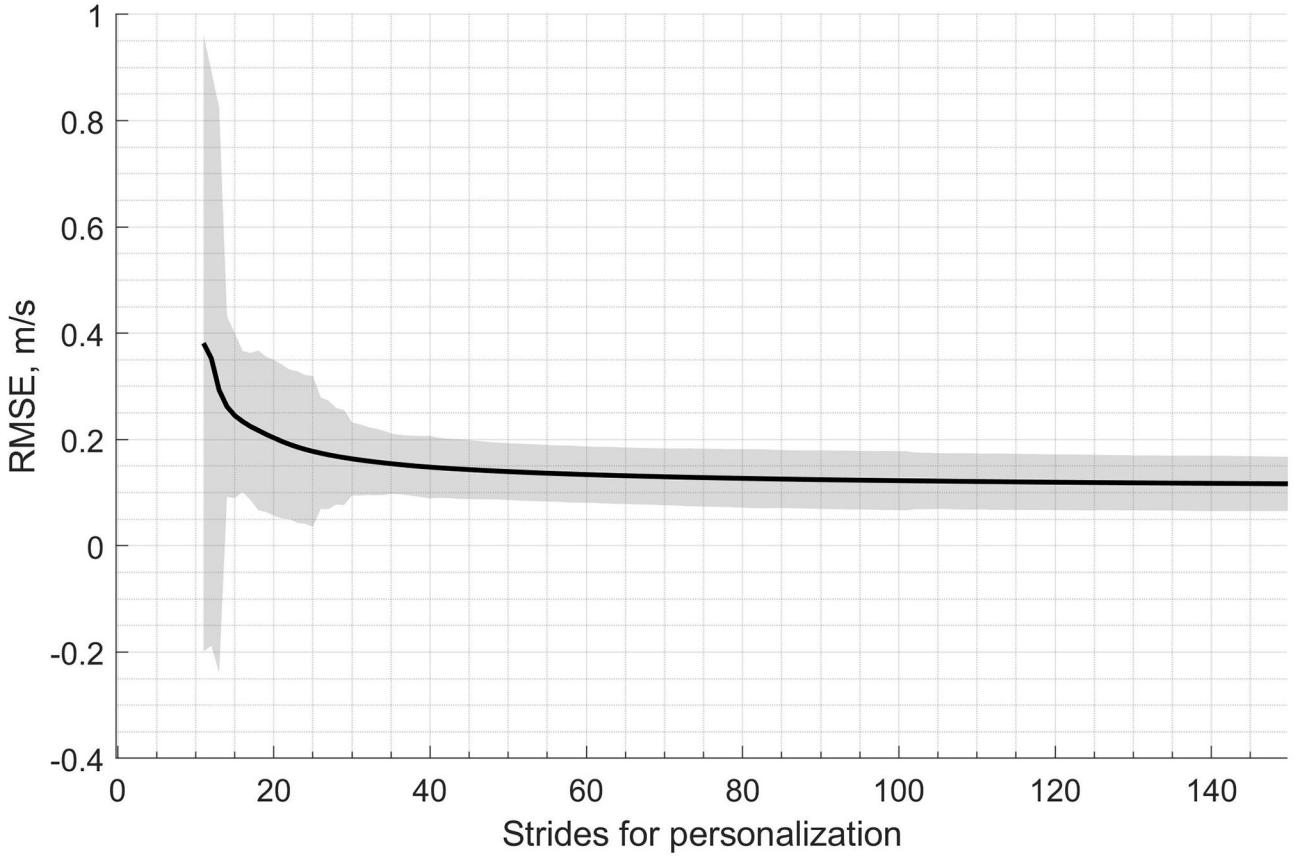

FIGURE 10 | Evolution of the RMSE error during the personalization of the speed model. Here, the solid line and the shaded area represent, respectively, the inter-subject mean and standard deviation of the RMSE. The x-axis corresponds to the number of strides used for the personalization. Note that, for a better visualization of the error evolution, the figure is zoomed only on the first 150 samples used for personalization.

TABLE 4 | Inter–subject median and Inter-Quartile Range (IQR) of bias, precision, and RMSE of the personalized model.

Bias (m/s)		Precision (m/s)		RMSE (m/s)	
median	**IQR**	**median**	**IQR**	**median**	**IQR**
0.00	0.01	0.09	0.03	0.09	0.06

DISCUSSION

In this study, we proposed three methods to estimate overground running speed using feet worn sensors. First, we estimated the overground speed using solely the velocity of the foot obtained through the direct integration of the acceleration. We evaluated this direct method to test our hypothesis that the accelerometer fails to provide the correct value during the flight phase due to the combination of rotational and translational accelerations. Nevertheless, the velocity of the foot, with other relevant features, was selected as the input of the second method based on a linear model to predict the running speed. Thanks to an exhaustive features selection procedure and cross-validation approach, the model predicted the running speed with better accuracy. Finally, we assumed that the running technique varies among individuals, but that it should be well-correlated with individual gait features. Therefore, we showed that the performance of running speed could be improved using an online-personalization method with sporadic access to some GNSS data. It is important to note that the same method could be extended to less complicated instrumentation (e.g., a stopwatch over a fixed distance).

The speed estimation result for the method based on v_{foot} only confirmed our hypothesis that the direct integration of the acceleration, as proposed for walking, cannot be generalized to running due to the presence of aerial phases. The inter-individual mean bias (0.08 m/s) we observed indicates that the direct integration method underestimates the speed during the phase of flight. This underestimation confirms the inexact measure of the translational movement by the accelerometer during the flight phase. Moreover, the trend displayed in the Bland-Altmann plot (**Figure 5**) indicates that the system underestimates the velocity more at faster speeds. This observation is coherent with our hypothesis; the higher the speed, the greater the distance covered during the phase of flight (i.e., longer step length) (Nummela et al., 2007). Slope also seems to be a confounding factor of the error (**Figure 6**), with higher errors obtained during downhill running. In conclusion, v_{foot} itself does not characterize the speed

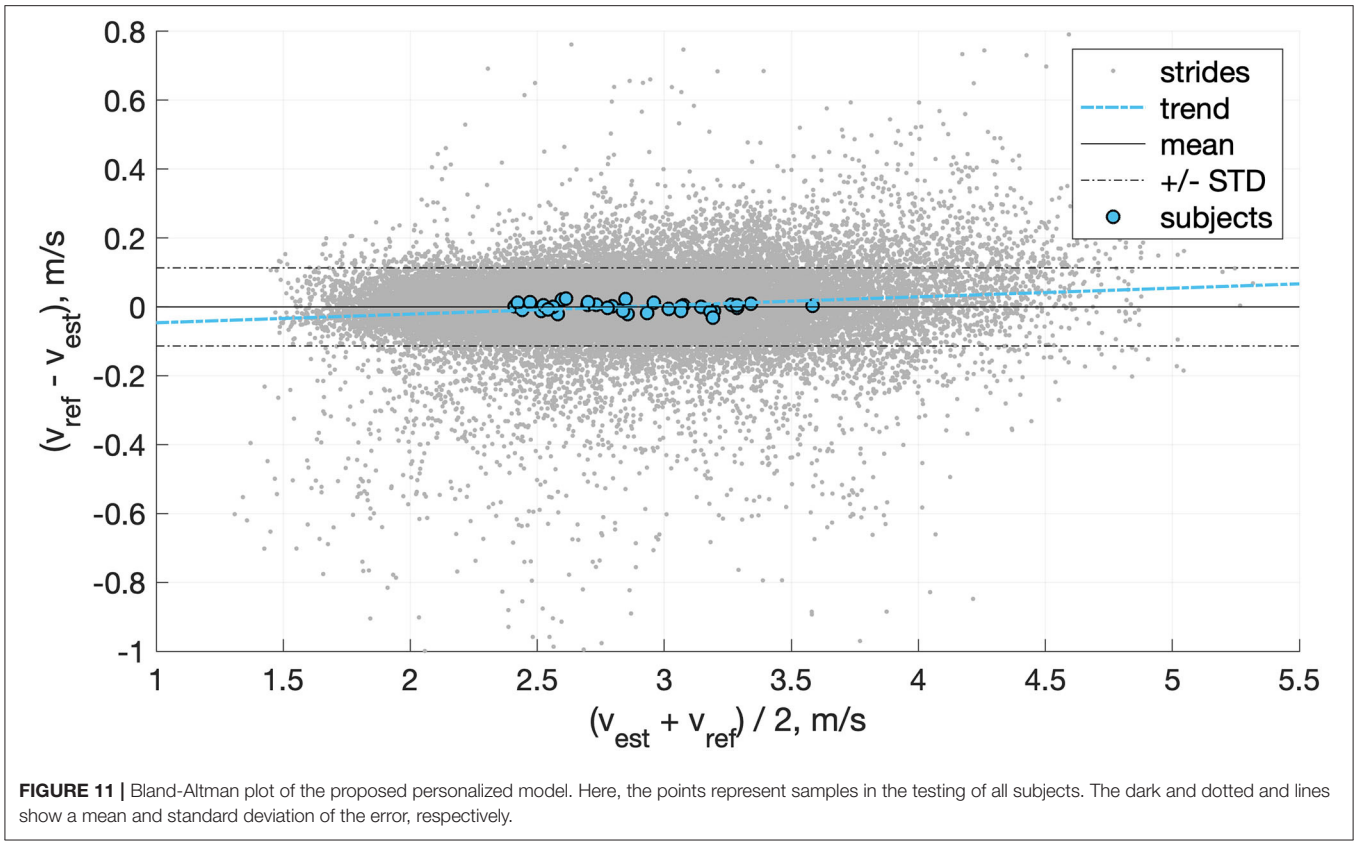

FIGURE 11 | Bland-Altman plot of the proposed personalized model. Here, the points represent samples in the testing of all subjects. The dark and dotted and lines show a mean and standard deviation of the error, respectively.

of the subject as it cannot measure the distance covered during the period of the flight, but v_{foot} was a good proxy for speed and was one of the main features for speed prediction based on the linear model.

The selection of relevant features in the linear model was a crucial phase. Feature selection was carried over 20'084 steps and aimed to retrieve the most relevant features among the 668 variables available. Although we used a high-dimensional feature space, the curse of dimensionality issue did not apply as we used approximately 30 times more observations for feature selection. The results of the feature selection process show that the cost function (i.e., MSE) decreased quickly with the first few inputs and then stabilized as additional features were included (**Figure 7**). We set the stopping criteria intentionally low (i.e., 1% improvement in the MSE), knowing that the LASSO method used for training the model would ignore the inputs with redundant information. Interestingly, several of the features manually selected (P_{manual}) were among the first to be selected by the automatic process (P_{auto}); however, using different linearization functions (**Table 2**).

The linear model required inputs parameters from the temporal and spatial domain, as well as overground slopes. Hence a precise estimation of related parameters is paramount to optimize the precision of the speed estimation. The methods used to obtain these parameters should always be carefully reported and, ideally, previously validated. Interestingly, the model did not select the FLY parameter and instead favored the inverse of the stride duration (i.e., the stride frequency); hence none of the features selected required a bipedal configuration of the sensors allowing us to use the model with a single foot-worn IMU in the future. Also, none of the anthropometric parameters was necessary for the estimation of the running speed. This result is somewhat surprising, as we expected the height to be an essential input.

Apart from its computation time greediness, one reported issue of the forward selection algorithm is that decisions made early in the process cannot be changed, therefore potentially affecting its performance when the inputs are correlated (Derksen and Keselman, 1992). Although we observed some correlation in the inputs, we presumed that the two-fold selection process (i.e., stepwise selection and LASSO) would not be significantly affected by that matter. Moreover, the linearization of the feature-space was an essential component of this study. We selected f_1, f_2, and f_3 functions based on visual inspection of the data, and out of the 28 pre-selected features, 16 (57%) resulted from these linearization functions.

Although the performance of the automatically selected set of features ($P_{auto,best}$) performed slightly better than the comprehensive set of features ($P_{manual,best}$), the differences remain in the order of a few centimeters per second (**Table 3**). Indeed, the estimations based on $P_{auto,best}$, with a granularity of 1, over-performed the ones using $P_{manual,best}$ by 0.01 m/s in the inter-subjects STD of the bias, 0.01 m/s in average precision, and display a slightly lower RMSE. These differences are relatively

little since several elements in $P_{manual,best}$ were among the most relevant features selected by the LASSO regression method in $P_{auto,best}$, or at least were highly correlated. The results also show that averaging the inputs over several steps had a moderate effect on the performance of the system; it reduced the random error of the system with mean precision values consistently decreasing from 0.14 m/s for the step level estimation to 0.11 m/s when the granularity decreased to 10 steps. Also, when the output of step level estimated speed was averaged over four steps, the precision slightly improved (0.13 ± 0.05 m/s). Hence, whether the inputs or the outputs are averaged does not seem to affect the performances of the model.

Overall, the linear method showed good prediction results across a wide range of speed and slope, observed in real-world conditions (**Figure 9B**). It principally removed the mean bias of the method based on v_{foot} only and slightly improved the precision. The Bland-Altmann plot in **Figure 8** shows a good agreement between the linear model and the reference GNSS system. The linear trend of the error (dashed blue line) is almost horizontal ($y = 0.0034x+0.098$), which suggests that the running speed has little effect on the error. These results support the usage of the RUS technique on the training data; the model ensured that all the ranges of speeds observed were equally represented. Although procedures more sophisticated than the RUS method have been proposed, they do not always provide a clear advantage in the results (Japkowicz, 2000). Moreover, the CDF curves of the training and testing sets do not indicate clear overfitting of the training data (**Figure 9A**) as the training set attains better performance than the testing set, but these are within an acceptable range.

It seems challenging to reduce further the STD of the bias using such a linear model since it depends on the inter-subject differences as it has previously been reported that individuals use different spatiotemporal adaptations at similar speeds. For instance, previous studies have shown that the relationship between stride frequency and stride length was specific to each subject (Saito et al., 1974; Nummela et al., 2007). These limitations were also encountered by previous studies that aimed to estimate the running speed based on body-worn inertial sensors. In Yang et al. (2011), the authors used a shank-worn IMU to measure the velocity of the shank and compared it with the speed of a motored treadmill. The study was conducted at five predefined speeds (2.5, 2.75, 3, 3.25, 3.54 m/s), with seven participants, and the error was calculated as the difference between the average estimated speed over 30 strides and the constant speed of the treadmill (i.e., the bias). The results show inter-trial mean and STD of the bias of 0.11 ± 0.03 m/s at 2.5 m/s, 0.10 ± 0.03 m/s at 2.75 m/s, 0.08 ± 0.02 m/s at 3 and 3.25 m/s, and 0.09 ± 0.02 at 3.5 m/s. The biases reported in Yang et al. (2011) are in range with those obtained in our study. However, the measurements were performed on a leveled treadmill at a discrete and limited number of running speeds, and the results were averaged over 30 strides (i.e., 60 steps). By considering the foot and shank as a single rigid body, the authors in Chew et al. (2017) used foot-worn inertial sensors with ten participants and a similar approach as in Yang et al. (2011). Based on the errors reported at each speed (8, 9, 10, 11 km/h), our method outperformed the one proposed in Chew et al. (2017). Aiming to evaluate the accuracy and the repeatability of a commercialized foot-worn running assessment system (RS800sd, Polar, Kempele, Finland), the authors in Hausswirth et al. (2009) performed 30-s measurements at multiple speeds (from 12 to 18 km/h) and compared the speed estimations with the speed of the treadmill. Even though the commercialized system required a subject-specific calibration, the reported mean $\pm$ STD bias of -0.03 ± 0.14 m/s indicates a slightly less accurate estimation of the running speed than the method proposed in this study. In a study (Herren et al., 1999) conducted in outdoor conditions, the authors explored whether triaxial accelerometric measurements can be combined with subject-specific neural networks to assess speed and incline of running accurately. The authors reported an RMSE of 0.12 m/s for average speed the whole running trial which is similar to our linear model estimations when the inputs are averaged at least four steps.

In a recent effort to reduce the inter-subject differences in the bias, researchers in De Ruiter et al. (2016) proposed a personalized speed estimation model based solely on the measurement of the contact time (CT). They obtained the CT using shoe-worn inertial sensors and conducted the measurements on an outdoor 2 km long tarmac. First, they personalized a model ($speed = \alpha CT^d$) for each of the 14 participants based on the average speed over several bouts of 125 meters. Then, they compared the personalized estimation results with those obtained with a stopwatch over a fixed 120-meters distance ($N = 35$ bouts) and reported a median RMSE of 2.9 and 2.1% (two runs). In comparison, our linear model method obtained a mean RMSE of 5.1% at step level estimation, and the personalized method a median RMSE of 3.1 %. This slightly higher RMSE in our study is partly reflecting the variety of slopes in our measurements in comparison to the level running in De Ruiter et al. (2016).

A recent study (Soltani et al., 2019) proposed a real-world speed estimation method based on wrist-worn inertial sensors. The authors obtained a median [IQR] (Inter-Quantile Range) bias of −0.02 [−0.2, 0.18] m/s and precision of 0.31 [0.26, 0.39] m/s for the non-personalized method. These results improved using a personalization technique similar to this study, with 0.00 [−0.01, 0.02] and 0.18 [0.14, 0.23] for the bias and precision, respectively. Hence, for both the personalized and non-personalized methods, this study out-performed the wrist-based estimation of the running speed.

The linear model is accurate for "average people" (i.e., individuals with typical running patterns), and individuals with an atypical running technique will give rise to higher speed estimation errors (**Figure 8**). In comparison, the personalized model adapts to the movements of each individual; thus, it ensures a bounded error for "average" and "atypical" individuals (**Figure 11**).

The proposed personalization demonstrates significant improvements in the performance of the real-world running speed estimation. As reported in **Table 4**, the personalization process improved the IQR of the bias by at least a factor of 10 and the median precision by roughly 30% by employing approximately 35 times less training data than

the non-personalized linear model. The personalized model bypasses the bias caused by the intrinsic variation of individuals during real-world running. This observation is best characterized by **Figure 10**, which demonstrates the relatively fast convergence of the proposed RLS-based personalization; after roughly 50 strides, the model stabilized. As a consequence, the personalized model does not require continuous GNSS value to be updated. Once a good performance is reached, GNSS switch to off to save batteries. Moreover, the proposed personalized method is based on an online learning technique that does not require a database; hence it saves time and energy. It allows real-time speed estimation, computationally optimized, and does not need to store training data.

CONCLUSION

In this study, we proposed and evaluated three different methods for real-world speed estimation in running: direct speed estimation, training based linear model, and a personalized model. The direct estimation of the foot velocity confirmed the hypothesis that accelerometers inaccurately measure the translational motion of an individual during the flight phase; therefore, techniques developed for walking analysis cannot be generalized to running. We evaluated the linear model for two sets of features: automatically selected (i.e., optimized) or manually selected (i.e., comprehensive features). The model performed best when we averaged its output over a few steps and showed that 4 steps (i.e., two left strides and two right strides) provided an acceptable trade-off between performance (bias: 0.00 $\pm$ 0.11 m/s; precision: 0.12 $\pm$ 0.06 m/s) and time-resolution. The personalized method tested in this study, used an online-learning technique based on recursive least-squares to personalize the speed estimations for each individual. Our results indicate that such an approach primarily helps to reduce the inter-subject bias (0.01 m/s) but also improves the average random error by more than 30%.

Based on the results of this study, we recommend using the linear model for speed estimation when the recordings of other accurate devices are temporarily unavailable and personalized the model when these recordings are available. For instance, the system can be used as a complement to a GNSS device experiencing sparse communication, either due to a reduced transmission bandwidth (e.g., indoor running, city centers) or because of electrical power limitations (e.g., low power systems).

DATA AVAILABILITY STATEMENT

The raw data supporting the conclusions of this article will be made available by the authors, without undue reservation.

ETHICS STATEMENT

The studies involving human participants were reviewed and approved by EPFL's Human Research Ethics Committee. The patients/participants provided their written informed consent to participate in this study.

AUTHOR CONTRIBUTIONS

MF, AS, and KA conceptualized the study design and contributed to the analysis and interpretation of the data. AS conducted the data collection. MF and AS designed the algorithms and KA supervised the study. MF drafted the manuscript, all other authors revised it critically. All authors approved the final version, and agreed to be accountable for all aspects of this work.

FUNDING

This study was supported by the Swiss CTI grant no. 18730.2 PFNM-NM.

ACKNOWLEDGMENTS

We thank M. Ziqi Zhao for his participation in the data analysis of the personalized model and all participants who took part in our measurements.

REFERENCES

Aminian, K., Najafi, B., Büla, C., Leyvraz, P. F., and Robert, P. (2002). Spatio-temporal parameters of gait measured by an ambulatory system using miniature gyroscopes. *J. Biomech.* 35, 689–699. doi: 10.1016/S0021-9290(02)00008-8

Benson, L. C., Clermont, C. A., Bošnjak, E., and Ferber, R. (2018). The use of wearable devices for walking and running gait analysis outside of the lab: a systematic review. *Gait Posture* 63, 124–138. doi: 10.1016/j.gaitpost.2018.04.047

Bland, J. M., and Altman, D. G. (1986). Statistical methods for assessing agreement between two methods of clinical measurement. *Lancet* 327, 307–310. doi: 10.1016/S0140-6736(86)90837-8

Bolanakis, D. E. (2017). *MEMS Barometers Toward Vertical Position Detection: Background Theory, System Prototyping, and Measurement Analysis*. Ioánnina: Morgan & Claypool Publishers. doi: 10.2200/s00769ed1v01y201704mec003

Brodie, M., Walmsley, A., and Page, W. (2008). Fusion motion capture: a prototype system using inertial measurement units and GPS for the biomechanical analysis of ski racing. *Sport. Technol.* 1, 17–28. doi: 10.1002/jst.6

Chapman, R. F., Laymon, A. S., Wilhite, D. P., McKenzie, J. M., Tanner, D., a., et al. (2012). Ground contact time as an indicator of metabolic cost in elite distance runners. *Med. Sci. Sports Exerc.* 44, 917–925. doi: 10.1249/MSS.0b013e3182400520

Chew, D.-K., Ngoh, K. J.-H., Gouwanda, D., and Gopalai, A. A. (2017). Estimating running spatial and temporal parameters using an inertial sensor. *Sport. Eng.* 21, 115–122. doi: 10.1007/s12283-017-0255-9

De Cheveign,é, A., and Kawahara, H. (2002). YIN, a fundamental frequency estimator for speech and music. *J. Acoust. Soc. Am.* 111, 1917–1930. doi: 10.1121/1.1458024

De Ruiter, C. J., Van Oeveren, B., Francke, A., Zijlstra, P., and Van Dieen, J. H. (2016). Running speed can be predicted from foot contact time during outdoor over ground running. *PLoS ONE* 11:e0163023. doi: 10.1371/journal.pone.0163023

Derksen, S., and Keselman, H. J. (1992). Backward, forward and stepwise automated subset selection algorithms: frequency of obtaining authentic and noise variables. *Br. J. Math. Stat. Psychol.* 45, 265–282. doi: 10.1111/j.2044-8317.1992.tb00992.x

Falbriard, M., Meyer, F., Mariani, B., Millet, G. P., and Aminian, K. (2018). Accurate estimation of running temporal parameters using foot-worn inertial sensors. *Front. Physiol.* 9, 1–10. doi: 10.3389/fphys.2018.00610

Falbriard, M., Meyer, F., Mariani, B., Millet, G. P., and Aminian, K. (2020). Drift-Free Foot Orientation Estimation in Running Using Wearable IMU. *Front. Bioeng. Biotechnol.* 8:65. doi: 10.3389/fbioe.2020.00065

Fasel, B., Duc, C., Dadashi, F., Bardyn, F., Savary, M., Farine, P. A., et al. (2017). A wrist sensor and algorithm to determine instantaneous walking cadence and speed in daily life walking. *Med. Biol. Eng. Comput.* 55, 1773–1785. doi: 10.1007/s11517-017-1621-2

Ferraris, F., Grimaldi, U., and Parvis, M. (1955). Procedure for effortless in-field calibration of three-axial rate gyro and accelerometers. *Sens. Mater.* 7, 331–330.

Halilaj, E., Rajagopal, A., Fiterau, M., Hicks, J. L., Hastie, T. J., and Delp, S. L. (2018). Machine learning in human movement biomechanics: best practices, common pitfalls, and new opportunities. *J. Biomech.* 81, 1–11. doi: 10.1016/j.jbiomech.2018.09.009

Hausswirth, C., Le Meur, Y., Couturier, A., Bernard, T., and Brisswalter, J. (2009). Accuracy and repeatability of the polar RS800sd to evaluate stride rate and running speed. *Int. J. Sports Med.* 30, 354–359. doi: 10.1055/s-0028-1105936

Herren, R., Sparti, A., Aminian, K., and Schutz, Y. (1999). The prediction of speed and incline in outdoor running in humans using accelerometry. *Med. Sci. Sports Exerc.* 31, 1053–1059. doi: 10.1097/00005768-199907000-00020

Högberg, P. (1952). Length of stride, stride frequency, "flight" period and maximum distance between the feet during running with different speeds. *Arbeitsphysiologie* 14, 431–436. doi: 10.1007/BF00934422

Hu, J. S., Sun, K. C., and Cheng, C. Y. (2013). A kinematic human-walking model for the normal-gait-speed estimation using tri-axial acceleration signals at waist location. *IEEE Trans. Biomed. Eng.* 60, 2271–2279. doi: 10.1109/TBME.2013.2252345

Jain, A., Nandakumar, K., and Ross, A. (2005). Score normalization in multimodal biometric systems. *Pattern Recognit.* 38, 2270–2285. doi: 10.1016/j.patcog.2005.01.012

Japkowicz, N. (2000). "The class imbalance problem: significance and strategies," in *Proceedings of the International Conference on Artificial Intelligence, 2000* (Las Vegas, NV), 111–117.

John, G. H., Kohavi, R., and Pfleger, K. (1994). "Irrelevant Features and the Subset Selection Problem," in *Machine Learning Proceedings 1994* (New Brunswick, NJ: Rutgers University), 121–129. doi: 10.1016/b978-1-55860-335-6.50023-4

Kohavi, R., and John, G. H. (1997). Wrappers for feature subset selection. *Artif. Intell.* 97, 273–324. doi: 10.1016/s0004-3702(97)00043-x

Mariani, B., Hoskovec, C., Rochat, S., Büla, C., Penders, J., and Aminian, K. (2010). 3D gait assessment in young and elderly subjects using foot-worn inertial sensors. *J. Biomech.* 43, 2999–3006. doi: 10.1016/j.jbiomech.2010.07.003

Miyazaki, S. (1997). Long-term unrestrained measurement of stride length and walking velocity utilizing a piezoelectric gyroscope. *IEEE Trans. Biomed. Eng.* 44, 753–759. doi: 10.1109/10.605434

Moore, I. S. (2016). Is there an economical running technique? A review of modifiable biomechanical factors affecting running economy. *Sport. Med.* 46, 793–807. doi: 10.1007/s40279-016-0474-4

Nummela, A., Keränen, T., and Mikkelsson, L. O. (2007). Factors related to top running speed and economy. *Int. J. Sports Med.* 28, 655–661. doi: 10.1055/s-2007-964896

Pes, B. (2020). Learning from high-dimensional biomedical datasets: the issue of class imbalance. *IEEE Access* 8, 13527–13540. doi: 10.1109/ACCESS.2020.2966296

Rawstorn, J. C., Maddison, R., Ali, A., Foskett, A., and Gant, N. (2014). Rapid directional change degrades GPS distance measurement validity during intermittent intensity running. *PLoS ONE* 9:e93693. doi: 10.1371/journal.pone.0093693

Sabatini, A. M., Martelloni, C., Scapellato, S., and Cavallo, F. (2005). Assessment of walking features from foot inertial sensing. *IEEE Trans. Biomed. Eng.* 52, 486–494. doi: 10.1109/TBME.2004.840727

Saito, M., Kobayashi, K., Miyashita, M., and Hoshikawa, T. (1974). "Temporal patterns in running," in *Biomechanics IV* (London: Palgrave), 106–111. doi: 10.1007/978-1-349-02612-8_15

Salarian, A., Burkhard, P. R., Vingerhoets, F. J. G., Jolles, B. M., and Aminian, K. (2013). A novel approach to reducing number of sensing units for wearable gait analysis systems. *IEEE Trans. Biomed. Eng.* 60, 72–77. doi: 10.1109/TBME.2012.2223465

Sheerin, K. R., Reid, D., and Besier, T. F. (2019). The measurement of tibial acceleration in runners—A review of the factors that can affect tibial acceleration during running and evidence-based guidelines for its use. *Gait Posture* 67, 12–24. doi: 10.1016/j.gaitpost.2018.09.017

Soltani, A., Dejnabadi, H., Savary, M., and Aminian, K. (2019). Real-world gait speed estimation using wrist sensor: a personalized approach. *IEEE J. Biomed. Heal. Informatics* 2194, 1–1. doi: 10.1109/jbhi.2019.2914940

Terrier, P., Ladetto, Q., Merminod, B., and Schutz, Y. (2000). High-precision satellite positioning system as a new tool to study the biomechanics of human locomotion. *J. Biomech.* 33, 1717–1722. doi: 10.1016/S0021-9290(00)00133-0

Thompson, M. A. (2017). Physiological and biomechanical mechanisms of distance specific human running performance. *Integr. Comp. Biol.* 57, 293–300. doi: 10.1093/icb/icx069

Tibshirani, R. (1996). Regression Shrinkage and Selection Via the Lasso. *J. R. Stat. Soc. Ser. B* 58, 267–288. doi: 10.1111/j.2517-6161.1996.tb02080.x

Van Hooren, B., Fuller, J. T., Buckley, J. D., Miller, J. R., Sewell, K., Rao, G., et al. (2019). Is motorized treadmill running biomechanically comparable to overground running? A systematic review and meta-analysis of cross-over studies. *Sport. Med.* doi: 10.1007/s40279-019-01237-z

Varley, M. C., Fairweather, I. H., and Aughey, R. J. (2012). Validity and reliability of GPS for measuring instantaneous velocity during acceleration, deceleration, and constant motion. *J. Sports Sci.* 30, 121–127. doi: 10.1080/02640414.2011.627941

Vernillo, G., Giandolini, M., Edwards, W. B., Morin, J.-B., Samozino, P., Horvais, N., et al. (2017). Biomechanics and physiology of uphill and downhill running. *Sport. Med.* 47, 615–629. doi: 10.1007/s40279-016-0605-y

Waegli, A., and Skaloud, J. (2009). Optimization of two GPS/MEMS-IMU integration strategies with application to sports. *GPS Solut.* 13, 315–326. doi: 10.1007/s10291-009-0124-5

Williams, K. R., and Cavanagh, P. R. (1987). Relationship between distance running mechanics, running economy, and performance. *J. Appl. Physiol.* 63, 1236–1245. doi: 10.1152/jappl.1987.63.3.1236

Witte, T. H., and Wilson, A. M. (2004). Accuracy of non-differential GPS for the determination of speed over ground. *J. Biomech.* 37, 1891–1898. doi: 10.1016/j.jbiomech.2004.02.031

Yang, S., Mohr, C., and Li, Q. (2011). Ambulatory running speed estimation using an inertial sensor. *Gait Posture* 34, 462–466. doi: 10.1016/j.gaitpost.2011.06.019

Zihajehzadeh, S., Loh, D., Lee, T. J., Hoskinson, R., and Park, E. J. (2015). A cascaded Kalman filter-based GPS/MEMS-IMU integration for sports applications. *Meas. J. Int. Meas. Confed.* 73, 200–210. doi: 10.1016/j.measurement.2015.05.023

Zihajehzadeh, S., and Park, E. J. (2016). Regression model-based walking speed estimation using wrist-worn inertial sensor. *PLoS ONE* 11:e0165211. doi: 10.1371/journal.pone.0165211

Zijlstra, W., and Hof, A. L. (2003). Assessment of spatio-temporal gait parameters from trunk accelerations during human walking. *Gait Posture* 18, 1–10. doi: 10.1016/S0966-6362(02)00190-X

Conflict of Interest: The authors declare that the research was conducted in the absence of any commercial or financial relationships that could be construed as a potential conflict of interest.

frontiers in Sports and Active Living

ORIGINAL RESEARCH
published: 22 April 2021
doi: 10.3389/fspor.2021.653173

Effect of Advanced Shoe Technology on the Evolution of Road Race Times in Male and Female Elite Runners

Stéphane Bermon[1,2]*, *Frédéric Garrandes*[1], *Andras Szabo*[3], *Imre Berkovics*[3] and *Paolo Emilio Adami*[1,4]

[1] Health and Science Department, World Athletics, Manoco City, Monaco, [2] Laboratoire Motricité Humaine Expertise Sport Santé, Université Côte d'Azur, Nice, France, [3] Elite Limited, Budapest, Hungary, [4] Department of Movement, Human and Health Sciences, University of Rome "Foro Italico," Rome, Italy

The influence of advanced footwear technology (thickness of light midsole foam and rigid plate) on distance running performances was analyzed during an 8-year period. Analysis of variance was used to measure effects of time, gender, shoe technology, and East African origin on male and female top 20 or top 100 seasonal best times in 10-kilometer races, half-marathons, and marathons. In both genders and three distance-running events, seasonal best times significantly decreased from 2017, which coincided with the introduction of the advanced footwear technology in distance running. This performance improvement was of similar magnitude in both East African and non-East African elite runners. In female elite athletes, the magnitudes (from 1.7 to 2.3%) of the decrease in seasonal best times between 2016 and 2019 were significantly higher than in their male counterparts (from 0.6 to 1.5%). Analyses of variance confirmed that the adoption of the advanced footwear technology significantly improved the top 20 seasonal best times in female half marathons and marathons and male marathons, with the improvements being more pronounced in females and in long-distance running events. The adoption of this new shoe technology improved female marathon time by ∼2 min and 10 s, which represents a significant increase in performance (1.7%).

Keywords: athletics, footwear, gender, marathon, performance

OPEN ACCESS

Edited by:
Brian Hanley,
Leeds Beckett University,
United Kingdom

Reviewed by:
Luca Paolo Ardigò,
University of Verona, Italy
Jordan Santos-Concejero,
University of the Basque Country, Spain

***Correspondence:**
Stéphane Bermon
stephane.bermon@worldathletics.org

Specialty section:
This article was submitted to Elite Sports and Performance Enhancement, a section of the journal Frontiers in Sports and Active Living

Received: *13 January 2021*
Accepted: *10 February 2021*
Published: *22 April 2021*

Citation:
Bermon S, Garrandes F, Szabo A, Berkovics I and Adami PE (2021) Effect of Advanced Shoe Technology on the Evolution of Road Race Times in Male and Female Elite Runners. Front. Sports Act. Living 3:653173. doi: 10.3389/fspor.2021.653173

INTRODUCTION

In 2017, Nike officially presented its Nike® Vaporfly 4% shoes. The release was associated with a large and worldwide advertising campaign that received a lot of attention because the manufacturer claimed that this new model of distance running shoes represented a breakthrough in the distance running shoe technology that could improve running time by 4% (Hoogkamer et al., 2018). This advanced footwear technology (AFT) relies on the combination of a very thick and light midsole made of polyamide block elastomer and the embedding within the midsole layers of a long and rigid carbon plate. What was initially considered as a marketing maneuver by the manufacturer quickly turned to a possible game changer in the world of distance running performance. Although several theories (Nigg et al., 2020b; Cigoja et al., 2021; Muniz-Pardos et al., 2021) have been proposed to understand the mechanisms behind these performance benefits, no definitive explanation has been provided so far. A large-scale statistical analysis published in 2018 (Quealy and Katz, 2018), based on results from 280,000 marathons and 215,000 half-marathons run, revealed that this AFT was likely responsible for a 3–4% decrease in race times in these distances. Although these statistics are

based on large numbers, the authors acknowledged some limitations in their study as it was based on athletes' self-declaration on an app dedicated to tracking running and cycling activities and did not specifically address elite distance runners. Moreover, the male and female half-marathon and marathon world records were all broken in 2018 and 2019 by Ethiopian and Kenyan athletes using AFT (Hoogkamer et al., 2017). Altogether, these facts fueled the controversy about the performance advantage (Muniz-Pardos et al., 2021), which some believe contradicts World Athletics' technical rule 143, paragraph 5.2, which states (World Athletics, 2020) that "athletes may compete barefoot or with footwear on one or both feet. The purpose of shoes for competition is to give protection and stability to the feet and a firm grip on the ground. They must not give athletes any unfair assistance or advantage. Any type of shoe must be reasonably available to all in the spirit of the universality of athletics.…" Therefore, the purpose of this exploratory study is to analyze elite male and female runners' official race results recorded between 2012 and 2019 in the 10-kilometer, half-marathon and marathon races. We tested the hypotheses that after 2017, elite runners will show relative decreases in race times such as those observed in sub-elite and club runners and that such decreases will be explained by the adoption of AFT by elite distance runners.

METHODS AND MATERIALS

The evolution of elite male and female distance runner race times between 2012 and 2019 (included) were assessed in three different road race events: the 10 kilometers (10 km), half-marathon, and marathon. For each of the 8 years studied, top 20 and top 100 individual seasonal (yearly) best performances for both genders were used for the purpose of statistical analysis. Competition results not validated by World Athletics or obtained from athletes disqualified because of anti-doping rules violations committed during the competition considered were excluded from the analysis. Results were obtained from World Athletics' official database. On the basis of declared citizenship, federation information on transfer of allegiance, and biographies, athletes from Djibouti, Ethiopia, Eritrea, Kenya, Rwanda, Uganda, Somalia, and Tanzania were grouped in an "East African" group, whereas the other athletes formed the "non-East African" group. For each gender and each event, the evolution of the top 20 and top 100 individual seasonal best times was explored with a one-way ANOVA (year) or two-way ANOVA (year*ethnic group or year*gender) and, when appropriate, Bonferroni-corrected for multiple-comparison *post-hoc* tests and Cohen's *d*. As the AFT was available early 2017, we searched when this technology was adopted by each of the top 20 male and female athletes in the three events between 2017 and 2019. As this search was performed from analysis of media content, photos, and footage of athletes in competition, it was impossible to perform it for the top 100 seasonal best times. We assumed that contracted athletes always competed with an unmodified model of shoes provided by his/her partner manufacturer. With this information, the effects of the adoption of AFT, gender, and running events on the top 20 seasonal best times were explored with one-, two-, or three-way ANOVA and, when appropriate, Bonferroni-corrected for multiple-comparison *post-hoc* tests. When the same athletes achieved performances between 2016 and 2019, with and without the AFT, their results were compared by using a paired t test after a normality check with the Shapiro-Wilk test. Descriptive statistics are presented with the mean and standard deviation. Statistical significance was considered to be indicated by a p-value < 0.05. Statistical analyses were performed using the JASP 0.13.1 free statistical software.

RESULTS

Top 100 Seasonal Best Times

The evolution of the top 100 male and female seasonal best times in the three events we have discussed is presented in **Table 1**. In both genders—and for the three distance running events—a decrease of mean seasonal best times was observed from 2017, with the lowest race times being recorded in 2019. The effect of time was significantly different between males and females—$F_{(1,7)} = 6.53$, 10.69, 8.60, $p < 0.001$—in the 10-km, half-marathon, and marathon top 100 seasonal best times, respectively. When we pooled the three distance running events, non-East African athletes represented on average 13% (range: 5–32%) and 28% (range: 12–44%) of the studied male and female populations, respectively. In all distance running events, the evolution of the top 100 seasonal best times followed a similar pattern across the years among East African and non-East African male ($F = 0.49$, $p = 0.94$) and female ($F = 0.58$, $p = 0.88$) athletes. As shown in **Table 1**, female athletes demonstrated larger decreases in race times between 2016 and 2019 than their male counterparts.

Top 20 Seasonal Best Times

The evolution of the top 20 male and female seasonal best times in the three events is presented in **Table 2**. Our analysis showed that the AFT was adopted by a limited number of runners in 2017 when this technology had only been released. However, in 2018 and especially in 2019, many seasonal best times (the top 20) were achieved by athletes running with the AFT. In 2019, 55–95% of elite male and 45–80% of female runners used advanced footwear technology in 10 km, half-marathon, and marathon races. During the period studied, when gender and events results were pooled, the adoption of the AFT showed a significant performance-enhancing effect ($F = 120.3$, $p < 0.001$). This improvement of seasonal best times was more important in female athletes ($F = 17.9$, $p < 0.001$) and in longer distance running events ($F = 31.03$, $p < 0.001$; see **Table 3**). In half-marathon and marathon races, we were able to identify small numbers of athletes who competed in the same event within the 2016–2019 period with and without the AFT. All athletes (except male half-marathon runners) significantly improved their seasonal best times when using the AFT (**Table 4**).

TABLE 1 | Evolution of top 100 male and female seasonal best times in the 10 km, half-marathon, and marathon races.

	Year								
	2012	**2013**	**2014**	**2015**	**2016**	**2017**	**2018**	**2019**	$F_{(7,792)}$, p-values
Male events									
10 km [min:s]	28:13.8 (00:14.7)	28:07.4 (00:14.7)	28:14.3 (00:16.9)	28:14.1 (00:16.4)	28:19.2 (00:17.8)	28:13.4 (00:19.2)	28:07.9 (00:23.6)*** †	27:59.8 (00:22.3)*** ‡	10.36, $p < 0.001$
Half Marathon [h:min:s]	01:00:33.8 (00:43.0)	01:00:38.7 (00:37.1)	01:00:21.7 (00:39.0)	01:00:14.9 (00:28.9)	01:00:31.9 (00:42.1)	01:00:18.5 (00:37.3)	01:00:07.0 (00:34.6)*** †	01:00:05.3 (00:37.5)*** †	10.85, $p < 0.001$
Marathon [h:min:s]	02:06:58.4 (01:12.4)	02:07:33.0 (01:22.5)	02:07:19.1 (01:18.4)	02:07:42.5 (01:08.0)	02:07:42.1 (01:34.9)	02:07:27.9 (01:22.4)	02:06:54.1 (01:28.5)*** †	02:06:07.2 (01:20.4)*** ‡	15.70, $p < 0.001$
Female events									
10 km [min:s]	32:15.1 (00:28.6)	32:17.5 (00:26.0)	32:09.4 (00:26.5)	32:12.2 (00:29.0)	32:15.5 (00:33.2)	32:00.0 (00:38.0)	31:57.3 (00:33.1)*** †	31:39.4 (00:36.2)*** ‡	16.75 $p < 0.001$
Half-Marathon [h:min:s]	01:09:40.2 (00:01:15.2)	01:09:25.8 (01:11.2)	01:09:26.9 (01:00.7)	01:09:31.7 (01:07.9)	01:09:17.6 (01:20.3)	01:08:42.9 (01:25.2)	01:08:19.3 (01:23.3)*** †	01:08:05.1 (01:16.3)*** ‡	23.05 $p < 0.001$
Marathon [h:min:s]	02:24:58.2 (02:31.8)	02:25:54.6 (02:14.6)	02:26:27.8 (02:24.9)	02:25:32.4 (02:14.2)	02:25:40.3 (02:08.9)	02:25:05.8 (02:32.7)	02:23:46.7 (02:23.1)*** ‡	02:22:45.4 (02:14.9)*** ‡	26.55 $p < 0.001$

*Results are presented as mean (standard deviation). *** Different than 2016 race time: $p < 0.001$. †Cohen's $d > 0.5$ (medium effect size). ‡Cohen's $d > 0.8$ (large effect size).*

TABLE 2 | Evolution of top 20 male and female seasonal best times in the 10 km, half-marathon, and marathon races.

	Year								
	2012	**2013**	**2014**	**2015**	**2016**	**2017**	**2018**	**2019**	$F_{(7,\ 152)}$, p-values
Male events									
10 km [min:s]	27:50.6 (00:08.9)	27:43.1 (00:07.4)	27:45.9 (00:11.3)	27:48.1 (00:07.0)	27:49.9 (00:9.6)	27:44.8 (00:16.1)	27:30.7 (00:14.5)*** †	27:24.3 (00:16.4)*** †	12.76, $p < 0.001$
Half Marathon [h:min:s]	59:23.3 (00:18.7)	59:39.5 (00:27.0)	59:21.7 (00:15.1)	59:30.1 (00:10.6)	59:27.7 (00:15.3)	59:20.6 (00:17.6)	59:11.8 (00:18.2)	59:07.7 (00:20.2)* †	6.03, $p < 0.001$
Marathon [h:min:s]	02:05:02.1 (00:28.7)	02:05:16.3 (00:58.7)	02:05:14.3 (01:03.2)	02:05:56.0 (00:38.7)	02:05:08.0 (01:06.2)	02:05:20.9 (00:49.4)	02:04:33.0 (00:51.8)	02:03:59.5 (00:57.6)** †	8.48, $p < 0.001$
Female events									
10 km [min:s]	31:29.7 (00:21.4)	31:38.1 (00:28.5)	31:26.0 (00:19.9)	31:25.3 (00:25.9)	31:23.1 (00:23.9)	30:59.7 (00:28.9)	31:05.3 (00:21.8)	30:41.3 (00:24.4)*** †	11.82, $p < 0.001$
Half-Marathon [h:min:s]	01:07:46.0 (00:33.0)	01:07:32.6 (00:42.1)	01:07:59.3 (00:53.9)	01:07:42.7 (01:00.0)	01:07:10.2 (00:45.8)	01:06:26.8 (00:51.2)	01:06:09.6 (00:43.7)** †	01:06:03.2 (00:23.4)*** †	20.97, $p < 0.001$
Marathon [h:min:s]	02:20:49.0 (01:10.5)	02:22:31.1 (01:13.9)	02:22:30.9 (01:35.4)	02:22:15.4 (01:27.1)	02:22:30.9 (01:12.3)	02:20:57.4 (01:26.1)* †	02:20:00.3 (01:13.6)*** †	02:19:18.2 (01:38.3)*** †	17.02, $p<0.001$

*Results are presented as mean (standard deviation). *Different than 2016 race time: $p < 0.05$, **Different than 2016 race time: $p < 0.01$. ***Different than 2016 race time: $p < 0.001$. †Cohen's $d > 0.8$ (large effect size).*

DISCUSSION

The main result from this retrospective study is a significant decrease in elite athletes' seasonal bests times in 10 km, half marathon and marathon races for both genders from 2017. This change coincides with the release of the AFT and its adoption by elite athletes, and it has itself been identified as a factor improving seasonal best times. A decrease of seasonal bests has been found at the highest elite (top 20) and elite (top 100) levels. The reported decreases in race times observed from 2016 (female marathon) and 2017 (all others) is unlikely to be explained by a decennial trend since performances were rather steady between 2012 and 2016 in both genders and in the three distances. The fact that the top 20 seasonal best times do not always reflect performances of the same people from year to year is a limitation of the present study. Indeed, in view of the duration of the period studied and the high "turn-over rate" of East African elite-level athletes in road running events, it was almost impossible to set up a large enough dataset on which a robust repeated-measures analysis of variance could be conducted. However, our complementary analysis conducted on limited numbers of half-marathon and marathon runners for whom we had seasonal best times achieved with and without the AFT tend to confirm the results reported for top 20 and

TABLE 3 | Effects of the advanced footwear technology on top 20 male and female seasonal best times in 10 km, half marathon, and marathon.

	No AFT	AFT	*t*, *p*-values	Cohen's *d*
Male events				
10 km [min:s]	27:44.7 (00:13.6) $n = 130$	27:30.7 (00:14.8)$n = 28$	4.85, $p < 0.001$	1.01
Half-Marathon [h:min:s]	59:24.8 (00:19.5) $n = 140$	59:09.2 (00:21.2)$n = 20$	3.32, $p < 0.01$	0.79
Marathon [h:min:s]	02:05:18.3 (00:53.6) $n = 123$	02:04:15.4 (01:09.3)$n = 37$	6.06, $p < 0.001$	1.14
Female events				
10 km [min:s]	31:18.4 (00:30.1) $n = 136$	31:01.3 (00:23.8)$n = 23$	2.58, $p < 0.05$	0.58
Half Marathon [h:min:s]	01:07:15.9 (01:02.2) $n = 135$	01:06:14.5 (00:29.4)$n = 25$	4.83, $p < 0.001$	1.05
Marathon [h:min:s]	02:21:49.9 (01:34.9) $n = 124$	02:19:39.4 (01:30.6)$n = 35$	7.25, $p < 0.001$	1.39

Results are presented as mean (standard deviation).
AFT, advanced footwear technology.

TABLE 4 | Comparison of male and female seasonal best times in half-marathon and marathon races in a subgroup of top 20 athletes who competed without and with the AFT between 2016 and 2019.

	Without AFT	With AFT	*t*, *p*-values	Cohen's *d*
Male events				
Half-Marathon [h:min:s]$n = 7$	59:08.4 (00:23.4)	59:00.3 (00:26.6)	0.61, NS	/
Marathon [h:min:s]$n = 8$	02:05:07.4 (01:20.6)	02:03:25.6 (01:09.9)	2.70, $p < 0.05$	1.35
Female events				
Half Marathon [h:min:s]$n = 6$	01:07:04.2 (00:41.4)	01:05:55.4 (00:30.0)	3.29, $p < 0.01$	1.90
Marathon [h:min:s]$n = 6$	02:21:56.5 (01:06.7)	02:18:55.9 (02:55.9)	2.35, $p < 0.05$	1.36

Results are presented as mean (standard deviation).
AFT, advanced footwear technology.

top 100 groups as well as the performance-enhancing effect of the AFT.

Low marathon race times observed in male and female runners in 2012 are an unexpected result. This could be explained by a larger number of competitors abusing performance enhancing drugs in that year. In 2012, the International Association of Athletics Federations (IAAF now World Athletics) was indeed already running a solid in-competition testing program complemented by an athlete biological passport program (Saugy et al., 2014), but this new generation of anti-doping programs was in its early phases and improved over time. Interestingly, the top 1,000 seasonal best times in male and female marathon runners show (results not presented) that even sub-elite or high-level club runners achieved good results in 2012, making the doping hypothesis less likely. An alternative explanation may be related to environmental race conditions. NASA's Goddard Institute for Space Studies (NASA, 2020) reported that, on a global level, 2012 was cooler than the seven following years. As high air temperature and relative humidity are known to limit endurance performance (Maughan, 2010), slightly cooler conditions encountered in 2012, could have facilitated achievement of better results in marathon competitions. Missing or unavailable data on weather for most races considered is a limiting factor in our study. However, the fact that seasonal best times recorded during the 8-year period were obtained from more than 200 different races organized in the spring and fall of both hemispheres makes it very unlikely that thermal stress accounts for the observed improvement in road race performances.

While looking for evidence of AFT adoption in the top 20 runners, we noted that some of them later committed anti-doping rules violations and subsequently served a period of ineligibility. Although such cheating behavior could represent a bias, we believe that it is unlikely to explain the observed performance improvements after 2017. Indeed, information obtained from the Athletics Integrity Unit website (Athletics Integrity Unit, 2020), shows that adverse passport findings and blood doping cases have not been reported to be more frequent in the period 2017–2019, compared with 2012–2016.

As shown in **Tables 1**, **2**, the year 2017 was a turning point in the road running industry with the first release by a shoe manufacturer of a model of distance running shoe that benefited from an AFT incorporating both an increased thickness of a new midsole light foam and a rigid plate along the shoe (Nigg et al., 2020a). The present study is a retrospective observational study from which a possible causality link between the availability of this AFT and distance running performances in top 20 seasonal best times can be derived. Moreover, the market release of AFT and its progressive adoption by elite distance runners coincided with the observed significant trend in improved performances. An alternative explanation to our main finding would be a possible overrepresentation of East African runners at the highest level of endurance competition. Indeed, East African runners have dominated distance running in athletics for almost two

decades (Tucker et al., 2013). Although our demographic data suggest such a trend in female athletes, this hypothesis can be discarded since non-East African elite male and female distance runners, while less numerous than East African runners, also significantly improved their performances from 2017.

The magnitude of seasonal best-time decreases was larger in elite females when compared with elite male runners. This phenomenon is also observed in the top 100 statistical analyses. Indeed, between 2016 and 2019, female race times decreased by 1.9, 1.7, and 2.0% in the 10 km, half-marathon, and marathon respectively, whereas these decreases were calculated at 1.1, 0.7, and 1.2% in male runners. In the consideration of top 20 seasonal bests, where the effect of AFT could be tested and quantified, the adoption of this new shoe technology improved female marathon time by ∼2 min and 10 s. Such a 1.7% increase in performance is remarkable at the elite level. For purposes of comparison only, Malm et al. (2016) reported an average 3% performance increase after blood doping. The top 20 male and top 20 female runners adopted the AFT to a similar extent between 2017 and 2019. However, the race time decrease observed between 2016 and 2019 always appeared to be larger for females than for males. This would suggest that this technology benefits female athletes more than males. As women, when compared with men, show greater fatigue resistance, greater substrate efficiency, and lower energetic demands during endurance events (Hunter, 2016; Tiller et al., 2021), the female lower body mass and/or a smaller shoes sizes could represent a possible explanation for this gender difference. It could be hypothesized that smaller shoe size is associated with a shorter but stiffer rigid plate in the AFT (Hoogkamer et al., 2017), and/or a higher midsole thickness/body mass ratio, facilitating a higher percentage of energy return in female runners (Hoogkamer et al., 2018).

Although highly significant at this competition level, the magnitude of elite runners' race time decrease reported in this study is lower than the average 3.4% change of running velocity calculated by Hoogkamer et al. (2018) in male sub-elite runners in their comparison of AFT with classical footwear. In their study, the authors measured energy costs of running 5 min at 14, 16, and 18 km/h, and concluded that the percentage of savings was similar at the three velocities. These experimental conditions (only applied to male subjects) are somewhat different from real race conditions, where higher velocities are maintained from approximately 28 min (10 km) to 145 min (marathon). During this extended time, the energy cost of running may progressively increase, due to slow component increases in oxygen uptake kinetics (Jones et al., 2011) and muscle damage (Assumpcao Cde et al., 2013). The magnitude of elite runners' race time decreases reported in this study is also lower than the ∼4% reported in club and sub-elite runners (Quealy and Katz, 2018).

CONCLUSIONS

The present study showed that top 20 and top 100 seasonal best times in 10 km, half-marathons, and marathons significantly decreased from 2017. Adoption of the advanced footwear technology has been identified as a factor contributing to these observed changes. The magnitude of this relative change was higher in female than in male elite athletes and was more pronounced in marathons than in 10 km road races. Although very relevant at an elite level, it appears that the magnitude of elite runners' race time changes observed between 2016 and 2019 is lower than race time changes reported in club or sub-elite distance runners.

DATA AVAILABILITY STATEMENT

The race results raw data supporting the conclusions of this article will be made available by the authors, without undue reservation.

AUTHOR CONTRIBUTIONS

SB, FG, AS, IB, and PA contributed to the conception or design of the work, drafted the manuscript, and critically revised the manuscript. All gave final approval and agreed to be accountable for all aspects of work, ensuring integrity and accuracy.

ACKNOWLEDGMENTS

We thank Professor Andrew Grundstein from the Department of Geography, University of Georgia (USA), and Thomas Capdevielle from the Athletics Integrity Unit (Principality of Monaco) who advised the authors on the climatologic and anti-doping parts of the manuscript, respectively.

REFERENCES

Assumpcao Cde, O., Lima, L. C., Oliveira, F. B., Greco, C. C., and Denadai, B. S. (2013). Exercise-induced muscle damage and running economy in humans. *Sci. World J.* 2013:189149. doi: 10.1155/2013/189149

Athletics Integrity Unit (2020). *Global List of Ineligible Persons*. Available online at: https://www.athleticsintegrity.org/disciplinary-process/global-list-of-ineligible-persons/p2?order-by=infractionDate1andsort=asc (accessed October 05, 2020).

Cigoja, S., Fletcher, J. R., Esposito, M., Stefanyshyn, D. J., and Nigg, B. M. (2021). Increasing the midsole bending stiffness of shoes alters gastrocnemius medialis muscle function during running. *Sci. Rep.* 11:749. doi: 10.1038/s41598-020-80791-3

Hoogkamer, W., Kipp, S., Frank, J. H., Farina, E. M., Luo, G., and Kram, R. (2018). A comparison of the energetic cost of running in marathon racing shoes. *Sports Med.* 48, 1009–1019. doi: 10.1007/s40279-017-0811-2

Hoogkamer, W., Kram, R., and Arellano, C. J. (2017). How biomechanical improvements in running economy could break the 2-hour marathon barrier. *Sports Med.* 47, 1739–1750. doi: 10.1007/s40279-017-0708-0

Hunter, S. K. (2016). The relevance of sex differences in performance fatigability. *Med. Sci. Sports Exerc.* 48, 2247–2256. doi: 10.1249/MSS.0000000000000928

Jones, A. M., Grassi, B., Christensen, P. M., Krustrup, P., Bangsbo, J., and Poole, D. C. (2011). Slow component of VO2 kinetics: mechanistic bases and practical applications. *Med. Sci. Sports Exerc.* 43, 2046–2062. doi: 10.1249/MSS.0b013e31821fcfc1

Malm, C. B., Khoo, N. S., Granlund, I., Lindstedt, E., and Hult, A. (2016). Autologous doping with cryopreserved red blood cells - effects on physical

performance and detection by multivariate statistics. *PLoS ONE* 11:e0156157. doi: 10.1371/journal.pone.0156157

Maughan, R. J. (2010). Distance running in hot environments: a thermal challenge to the elite runner. *Scand. J. Med. Sci. Sports* 20, 95–102. doi: 10.1111/j.1600-0838.2010.01214.x

Muniz-Pardos, B., Sutehall, S., Angeloudis, K., Guppy, F. M., Bosch, A., and Pitsiladis, Y. (2021). Recent improvements in marathon run times are likely technological, not physiological. *Sports Med*. 13, 1–8. doi: 10.1007/s40279-020-01420-7

NASA (2020). *Goddard Institute for Space Studies*. Available online at: https://climate.nasa.gov/vital-signs/global-temperature/ (accessed July 05, 2020).

Nigg, B. M., Cigoja, S., and Nigg, S. R. (2020a). Effects of running shoe construction on performance in long distance running. *Footwear Sci*. 12, 133–138. doi: 10.1080/19424280.2020.1778799

Nigg, B. M., Cigoja, S., and Nigg, S. R. (2020b). Teeter-totter effect: a new mechanism to understand shoe-related improvements in long-distance running. *Br. J. Sports. Med*. 7:bjsports-2020-102550. doi: 10.1136/bjsports-2020-102550

Quealy, K., and Katz, J. (2018, July 18). Nike says its $250 running shoes will make you run much faster. what if that's actually true. *New York Times*, 18.

Saugy, M., Lundby, C., and Robinson, N. (2014). Monitoring of biological markers indicative of doping: the athlete biological passport. *Br. J. Sports Med*. 48, 827–832. doi: 10.1136/bjsports-2014-093512

Tiller, N. B., Elliott-Sale, K. J., Knechtle, B., Wilson, P. B., Roberts, J. D., and Millet, G. Y. (2021). Do sex differences in physiology confer a female advantage in ultra-endurance sport? *Sports Med*. doi: 10.1007/s40279-020-01417-2. [Epub ahead of print].

Tucker, R., Santos-Concejero, J., and Collins, M. (2013). The genetic basis for elite running performance. *Br. J. Sports Med*. 47, 545–549. doi: 10.1136/bjsports-2013-092408

World Athletics (2020). *World Athletics technical Rules 2020*. Available online at: https://www.worldathletics.org/about-iaaf/documents/book-of-rules (accessed July 05, 2020).

Conflict of Interest: AS and IB were employed by the company Elite Ltd, Budapest.

The remaining authors declare that the research was conducted in the absence of any commercial or financial relationships that could be construed as a potential conflict of interest.

frontiers in Sports and Active Living

ORIGINAL RESEARCH
published: 21 June 2021
doi: 10.3389/fspor.2021.689341

Assessment of Sprint Parameters in Top Speed Interval in 100 m Sprint—A Pilot Study Under Field Conditions

Thomas Seidl[1]*, *Tiago Guedes Russomanno*[2], *Michael Stöckl*[3] and *Martin Lames*[1]

[1] Chair for Performance Analysis and Computer Science in Sports, Faculty for Health and Sport Sciences, Technical University of Munich, Munich, Germany, [2] Laboratory for Teaching Computer Science Applied to Physical Education and Sport, Faculty of Physical Education, University of Brasilia, Brasilia, Brazil, [3] Institute of Sport Science, University of Vienna, Vienna, Austria

Improving performances in sprinting requires feedback on sprint parameters such as step length and step time. However, these parameters from the top speed interval (TSI) are difficult to collect in a competition setting. Recent advances in tracking technology allows to provide positional data with high spatio-temporal resolution. This pilot study, therefore, aims to automatically obtain general sprint parameters, parameters characterizing, and derived from TSI from raw speed. In addition, we propose a method for obtaining the intra-cyclic speed amplitude in TSI. We analyzed 32 100 m-sprints of 7 male and 9 female athletes (18.9 ± 2.8 years; 100 m PB 10.55–12.41 s, respectively, 12.18–13.31 s). Spatio-temporal data was collected with a radio-based position detection system (RedFIR, Fraunhofer Institute, Germany). A general velocity curve was fitted to the overall speed curve (v_{base}), TSI (upper quintile of v_{base} values) was determined and a cosine term was added to v_{base} within TSI (v_{cycle}) to capture the cyclic nature of speed. This allowed to derive TSI parameters including TSI amplitude from the fitted parameters of the cosine term. Results showed good approximation for v_{base} (error: 5.0 ± 1.0%) and for v_{cycle} (2.0 ± 1.0%). For validation we compared spatio-temporal TSI parameters to criterion values from laser measurement (speed) and optoelectric systems (step time and step length) showing acceptable RMSEs for mean speed (0.08 m/s), for step time (0.004 s), and for step length (0.03 m). Top speed interval amplitude showed a significant difference between males (mean: 1.41 m/s) and females (mean: 0.71 m/s) and correlations showed its independence from other sprint parameters. Gender comparisons for validation revealed the expected differences. This pilot study investigated the feasibility of estimating sprint parameters from high-quality tracking data. The proposed method is independent of the data source and allows to automatically obtain general sprint parameters and TSI parameters, including TSI amplitude assessed here for the first time in a competition-like setting.

Keywords: sprint performance analysis, radio-based tracking, speed curve, top speed interval, intra-cyclic speed amplitude

OPEN ACCESS

Edited by:
Brian Hanley,
Leeds Beckett University,
United Kingdom

Reviewed by:
Ian Bezodis,
Cardiff Metropolitan University,
United Kingdom
Paul Anthony Jones,
University of Salford, United Kingdom

***Correspondence:**
Thomas Seidl
thomas.seidl@sg.tum.de

Specialty section:
This article was submitted to Elite Sports and Performance Enhancement, a section of the journal Frontiers in Sports and Active Living

Received: *31 March 2021*
Accepted: *19 May 2021*
Published: *21 June 2021*

Citation:
Seidl T, Russomanno TG, Stöckl M and Lames M (2021) Assessment of Sprint Parameters in Top Speed Interval in 100 m Sprint—A Pilot Study Under Field Conditions. Front. Sports Act. Living 3:689341. doi: 10.3389/fspor.2021.689341

INTRODUCTION

Improving performances in sprinting requires feedback on central sprint parameters ideally obtained in training as well as in competition. The 100 m-sprint can be divided into three main phases: acceleration phase, maximum velocity phase, and deceleration phase (Jones et al., 2009; Ae, 2017). In each phase, sprint parameters, such as split times, step length, step time, and ground contact time have been studied to improve the understanding of sprint performances and, subsequently, improve sprint performance based on those variables during training and competition (Moravec et al., 1988; Ae et al., 1992; Coh et al., 2001; Hunter et al., 2004; di Prampero et al., 2005; Morin et al., 2012; Colyer et al., 2018).

Since early velocity-time curve models proposed by Hill (1927) to very recent papers (Nagahara et al., 2018a, 2020; Bezodis et al., 2019; Morin et al., 2019; Ruiter and Van Dieen, 2019; von Lieres und Wilkau et al., 2020) research has focused on kinematic parameters of sprinting with a remarkable increase of papers analyzing the current world record of Usain Bolt in 2009 (9.58 s) (Beneke and Taylor, 2010; Taylor and Beneke, 2012; Krzysztof and Mero, 2013). However, there are still open questions such as the optimum relationship between step length and step time (Hunter et al., 2004; Bezodis et al., 2008; Debaere et al., 2013; Schubert et al., 2014).

Research has mostly investigated the first acceleration phase of the run (Nagahara et al., 2018a; Bezodis et al., 2019) typically trying to understand the step-to-step relations during acceleration based on ground reaction forces (Hunter et al., 2005; Rabita et al., 2015; Colyer et al., 2018; Nagahara et al., 2018a) and characteristic body angles by high-precision 3D kinematics (Manzer et al., 2016; Mattes et al., 2021).

The reason for the focus on this phase in sprint research may be found in the demanding methods of assessment employed (Mero, 1988; Nagahara et al., 2014a, 2019, 2020; Willwacher et al., 2016; Bezodis et al., 2019), which are typically, with only few exceptions (Nagahara et al., 2018a; Mattes et al., 2021), available only in laboratory settings. As it is a well-established fact that top speed is reached in 100 m-sprint only after around 40 m of maximum acceleration effort (Krzysztof and Mero, 2013; Healy et al., 2019), it is comprehensible that comparatively fewer studies exist which examined the maximum velocity phase or the final part of the acceleration phase. On the other hand, there is clear evidence that the maximum velocity phase is decisive for sprinting performance. Correlations between top speed and 100 m time are typically very high: $r = 0.98$ (Fuchs and Lames, 1990), $r = 0.96$ (Ryu et al., 2012), and $r = 0.97$ (Saito et al., 2008), making feedback on sprint parameters during this interval highly desirable.

Assessing sprint parameters in the maximum velocity phase in field settings either lack the necessary spatial or temporal resolution like timing gates, laser measurements, or manual video annotation (Brüggemann et al., 1999; Ferro et al., 2001; Graubner and Nixdorf, 2011; Krzysztof and Mero, 2013) or require an extensive instrumental setup such as motion capture systems or force plates applied at competitive and training tracks (Hunter et al., 2004; Park, 2011; Walker et al., 2019; Nagahara et al., 2020; Mattes et al., 2021). Hence, there are no satisfactory solutions for assessing sprint parameters in maximum velocity phase on a routine basis in competition and training.

However, due to the development of new tracking technologies with high spatial and temporal resolution (Sathyan et al., 2012; Seidl et al., 2016, 2017), like the radio-based tracking system RedFIR, (Grün et al., 2011) the analysis of sprint parameters in field settings has come into reach. As tracking systems are designed for routine analyses on training and competition sites they represent an excellent prospect for innovative contributions to sprint analysis and training.

Thus, the aims of the present study are two-fold. First, it aims at investigating the feasibility of using radio-based position detection for extracting sprint performance parameters including information on the maximum velocity phase in a field setting. Second, it proposes a data-driven method for obtaining the Top Speed Interval (TSI) and to derive TSI-specific sprint parameters including the intra-cyclic speed TSI amplitude, reported here for the first time. In addition, for validation the precision of the tracking data in this study and of the derived sprint parameters is explored, and comparisons between male and female sprinters as well as inter-correlations between sprint parameters are reported.

METHODS

Sample and Data Acquisition

We conducted our experiments in an official track and field stadium (Nuremberg, Germany), where a RedFIR radio-based tracking system (Fraunhofer Research Institute, Nuremberg, Germany) is installed. The RedFIR Real-Time Locating System (Grün et al., 2011) is based on time-of-flight measurements. Small transmitters (61 mm × 38 mm × 7 mm, 15 g) work with a sampling rate of 200Hz. **Figure 1** shows the attachment of transmitters on the athletes' backs in a pocket of a compression shirt. For a more detailed description of the RedFIR system and the generated data streams see Grün et al. (2011), Mutschler et al. (2013), and Seidl et al. (2017).

Sixteen U20 athletes of regional and national level from surrounding clubs (age: 18.9 ± 2.8 years; IAAF points: 796 ± 146; specialization in 100 m) performed 32 100 m-sprints in total. Their personal bests ranged from 10.55 to 12.41 s (11.64 ± 0.68 s) for seven male and from 12.18 to 13.31 s (12.72 ± 0.43 s) for nine female sprinters, respectively. Each athlete performed two sprints in a competition-like setting after a 20 min warm-up that was chosen individually. Athletes rested at least 15 min between trials.

The study has been approved by the ethical committee of Technical University Munich and subjects gave informed consent.

Data Analysis

A general assumption of this study is that there is an extended TSI in 100 m-sprint, where the sprinter runs at an almost constant, near-to-maximum or maximum speed. Further, it is assumed that running coordination is more or less stable in this interval (Brüggemann et al., 1999). We propose as operational definition of TSI as the upper quintile of all speed values over the full 100 m.

FIGURE 1 | Transmitter placement on the athletes. Transmitters were placed inside a specially designed pocket.

Based on these assumptions, we propose the following procedure to derive TSI parameters from raw tracking data that will be described in detail below:

(1) Fit a basic speed model $v_{base}(t)$ for 100 m sprint to raw speed data,
(2) Extract TSI,
(3) Fit a cyclic speed model to this interval to obtain TSI sprint parameters.

Basic Speed Model for Sprint Running

We start by applying a general sprint model that was proposed by Fuchs and Lames (1990), which is similar to one proposed by Arsac and Locatelli (2002), to obtain a *smooth* speed curve from raw speed data. In this model, running speed is perceived as the superposition of an acceleration and deceleration/fatigue process. Both processes are given by exponential growth functions:

$$v_{base}(t) = A\left(1 - e^{-\lambda t}\right) + B\left(1 - e^{\mu t}\right),$$

where A and B are weights for the corresponding acceleration/deceleration and λ, μ growth/decline rates, respectively.

Of course, any other smoothing method could be used as basic speed model if it validly describes the speed curve without the within-step velocity fluctuations (Bezodis et al., 2012). Applying the method from Fuchs and Lames (1990) allows for calculating the following sprint parameters: *maximum velocity* $v_{\max}$, *start acceleration* a_{start} and *speed endurance* v_{endu} given by the following equations:

$$v_{\max} = v_{base}(t_{\max}),\ t_{\max} = \begin{cases} \frac{\ln\left(\frac{A\lambda}{B\mu}\right)}{\lambda+\mu}, & B > 0 \\ t_{100}, & B = 0 \end{cases}$$

$$v_{endu} = \frac{v_{base}(t_{100})}{v_{\max}},$$

$$a_{start} = a(0) = A\lambda - B\mu$$

where $a(t)$ is the *acceleration* [derivation of $v_{base}(t)$]

$$a(t; A, B, \lambda, \mu) = A\lambda e^{-\lambda t} - B\mu e^{\mu t}$$

and t_{100} is the time for 100 m obtained from tracking data. *Speed endurance* v_{endu} is a measure of the ability of athletes to maintain their top speed and is calculated relative to top speed $v_{\max}$. Hence, v_{endu} will be 1 if top speed is maintained until the finish line (Bompa and Bompa, 1999). An example of raw data and fitted base model is depicted in **Figure 2A**.

Extract TSI

Sprint steps in the TSI are supposed to show a stable (top speed) coordination pattern (Brüggemann and Rühl, 1990). We define TSI to be the time interval when athletes are running at a speed within the top quintile of their speed distribution over the full 100 m track, as shown in **Figure 2B**:

$$TSI := \{t \mid v \geq Q_4,\ v \in v_{base}\},$$

where Q_4 is the lower border of the top quintile of speed values from function v_{base}. This threshold was chosen by convention to make sure TSI contains "enough" cycles for a stable parameter estimation in the next step and still meeting the requirement of constant coordination patterns.

TSI Parameters

To capture the cyclic structure of the speed within TSI we propose a cosine function added to v_{base}. The model function for TSI then is:

$$v_{cycle}(t) = a^{*}\cos\left(2\pi/bt + c\right) + v_{base}(t),$$

where $2\pi/b$ estimates *top speed step time*. Analogously, we obtain *top speed step length* by performing the calculations in the distance domain instead of time domain. c is an offset/shift parameter and $v_{base}(t)$ corresponds to the function value of the base speed model during TSI. a is the amplitude of the cosine, i.e., 2a is the *intra-cyclic top speed amplitude* which is defined as the maximum speed difference between two consecutive ground contacts in the TSI (**Figure 2C**).

Sprint time is measured by the tracking system (sprint time tracking) thus not including reaction time. A summary of obtained variables is shown in **Table 1**.

For each run, we fitted the curves v_{base} and v_{cycle} by solving the respective least squares optimization problem (Levenberg, 1944; Marquardt, 1963). Data analysis has been done using Python 3.7 and scipy package.

Validation of RedFIR for Estimating TSI Sprint Parameters

The RedFIR system as such has been validated before in a sprint-specific study (Seidl et al., 2017). To assess the validity of derived top speed parameters based on the proposed method we conducted additional validation experiments in the same location by simultaneously recording 100 m-sprints with RedFIR and criterion systems for horizontal speed (Laveg −13 runs) and step parameters (OptoGait −23 runs).

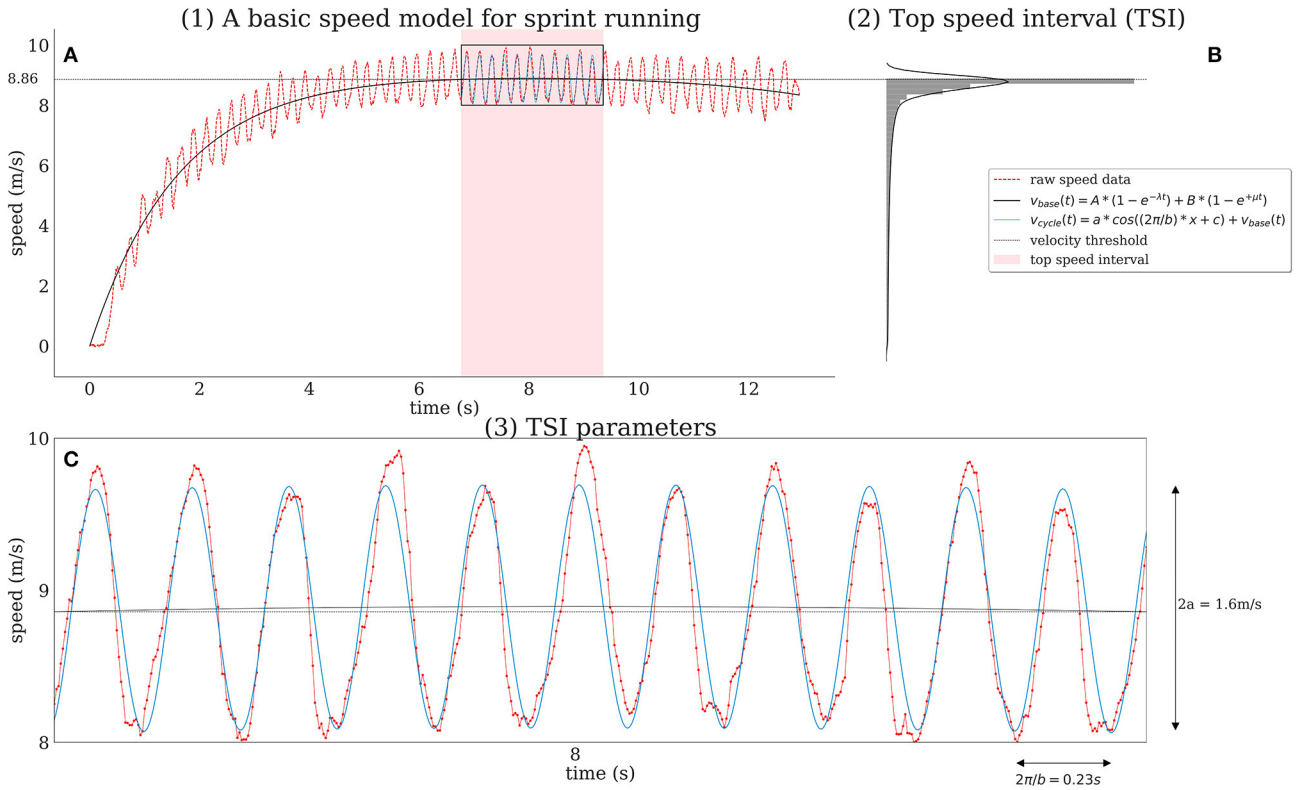

FIGURE 2 | An overview of the three-step modeling process is shown for a sample run of a male sprinter. We start by fitting the basic speed model proposed by (Fuchs and Lames, 1990) **(A)**—application to raw data (red dotted line) yields a smooth speed curve (solid black line) and provides estimates for maximum speed, maximum acceleration, and speed endurance. We then obtain a run-specific Top Speed Interval [TSI, light red shaded area in **(A)**] which corresponds to the time period when running speed is within the top 20% percentile of an athlete's running speed for the given run **(B)**. Its calculation is based on the modeled speed (solid black line) rather than the raw speed data (dotted red line) and the corresponding velocity threshold (dotted black line, here: 8.86 m/s). Within the TSI we obtain intra-cyclic parameters (amplitude, step time, and step length) by fitting a cosine model (blue solid line) to raw speed data **(C)**.

A Laveg laser (Jenoptik, Germany; 100 Hz) was positioned 13 m behind the starting line and an operator aimed the laser on the spot on the back between the shoulder blades where the RedFIR transmitter was located. The Laveg system is known to provide accurate and reliable estimates for displacement and speed (Harrison et al., 2005). Criterion speed was derived from Laveg distance data by fitting a fifth-order polynomial to positions and analytical differentiation afterwards (Bezodis et al., 2012). For each run the location of TSI was estimated based on our method on RedFIR data, yielding start and end locations of TSI on the 100 m track, e.g., (54 m, 73 m). We then calculated the mean speed based on Laveg speed at the same section of the track and compared it to the results obtained by RedFIR.

Simultaneously, a photoelectric measurement system OptoGait (Microgate, Bolzano, Italy/OJ) was placed to cover the second half of the 100 m track (50–100 m) providing step-by-step estimates for step length and step time. The OptoGait system is comprised of 1 m modules, which can be attached to each other to cover a larger distance. Each bar was 100 × 8 cm and contained 96 light diodes that were located 3 mm above floor level and approximately 1 cm apart. Lienhard et al. (2013) reported 95% limits of agreement of 1.0–1.8 cm for step length, 0.007–0.023 s for cycle time for older adults walking. Although we are using the OptoGait system as a criterion for analyzing sprint parameters obtained from young sprinters we deem this system to be a valid choice as our approach only provides mean values for step length and step time within TSI. OptoGait is often used as criterion system for evaluation studies in sprinting (Gindre et al., 2016; Schmidt et al., 2016). For more details on the validation setting see Seidl et al. (2017). Mean step length and step time estimates within the TSI based on RedFIR data were compared to criterion measurements captured by the OptoGait system.

Statistical Analysis

All statistical analyses were performed in SPSS, Version 25.0 (SPSS, Inc., Chicago, IL, USA). The level of significance was set at $p = 0.05$ and descriptive results were expressed as mean ± *SD*. Variables were checked for normality using the Kolmogorov-Smirnov and Shapiro-Wilk's test. For normally distributed parameters a *t*-test for independent samples was used to investigate differences between male and females. For variables TSI start location, TSI end location, TSI amplitude,

TABLE 1 | Overview for automatically derived parameters.

Parameters	Unit	Definition	Source
Sprint time	(s)	Sprint time measured by the RedFIR system (no reaction time)	Tracking system
Max. speed	(m/s)	Maximum speed derived from v_base(t)	v_base
Start acceleration	(m/s^2)	Maximum acceleration derived from v_base(t)	v_base
Speed endurance	(%)	Speed endurance derived from v_base(t)	v_base
Top speed start location	(m)	Start position in running direction (m) of the top speed interval based on threshold obtained by top quintile of speed distribution for the run	v_base
Top speed end location	(m)	End position in running direction (m) of the top speed interval based on threshold obtained by top quintile of speed distribution for the run	v_base
Top speed length	(m)	Distance covered (m) within top speed interval based on threshold obtained by top quintile of speed distribution for the run	v_base
Top speed start time	(s)	Start time (s) of the top speed interval based on threshold obtained by top quintile of speed distribution for the run	v_base
Top speed end time	(s)	End time (s) of the top speed interval based on threshold obtained by top quintile of speed distribution for the run	v_base
Top speed duration	(s)	Duration (s) of the top speed interval based on threshold obtained by top quintile of speed distribution for the run	v_base
Top speed step time	(s)	Mean step time during top speed interval	v_cycle
Top speed step length	(m)	Mean step length during top speed interval derived	v_cycle
Top speed amplitude	(m/s)	Peak-to-peak amplitude of intracyclic speed during top speed interval	v_cycle
Normalized top speed amplitude	(%)	Peak-to-peak amplitude of intracyclic speed during top speed interval—normalized by maximum speed	v_cycle

Units, definitions, and source for each parameter is shown. E.g., maximum speed is derived from v_{base} (t) whereas TSI amplitude is derived from v_{cycle} (t).

and normalized TSI amplitude non-normal distribution were observed and, hence, Mann-Whitney's U-test was used.

Effect size was calculated and classified according to Cohen's classification of effect sizes into small ($d \leq 0.2$), moderate ($d \leq 0.5$), and large ($d \geq 0.8$) effects (Cohen, 1988).

The relationships between sprint parameters (independent variables) and sprint time (dependent variable) were investigated by calculating Spearman correlations coefficients (small effect <0.3; medium <0.5; large >0.5). Reliability of sprint variables was assessed calculating intra-class correlation coefficients (ICC, two-way mixed methods, single measurements, absolute agreement). ICC coefficients were classified according to Koo and Li (2016) into poor (ICC $\leq$ 0.5), moderate (ICC $\leq$ 0.75), good (ICC $\leq$ 0.9), and excellent (ICC > 0.9).

RESULTS

Validation of TSI Parameters

Mean speed differences (RedFIR—criterion) within TSI were −0.03 m/s whereas RMSE was 0.08 m/s (1.05%). Errors for mean step time (step length) were −0.001 s (0.001 m) showing a slight underestimation of the RedFIR system with a RMSE for step time of 0.004 s (1.67%) and 0.03 m (1.43%) for step length showing a slight overestimation, respectively. Top speed parameter estimates for mean speed, mean step length, mean step time for the radio-based tracking, and criterion systems are shown in **Table 2**. Bland-Altman plots are shown in the **Supplementary Material**.

Results for TSI Parameters

The method was successfully applied to all 32 trials and giving RMSE as percentage of maximum speed showed a good fit for v_{base} (t) (5.0 ± 1.0%) as well as for v_{cycle} (t) (2.0 ± 1.0%).

A graphical description of the best male and female performance is given in **Figure 3**. It shows the clear cyclical structure of running speed and its rather constant pattern in TSI allowing for fitting our cyclic TSI-speed model. The faster male runner reaches TSI later with a short duration but at a higher maximum speed compared to the female sprinter. Within TSI both show the same step time (0.23 s) but different TSI speed amplitude (1.39 vs. 0.73 m/s).

Table 3 shows descriptive statistics for TSI parameters. Reliability tests for TSI parameters showed good to excellent reliability except for speed endurance, TSI start and end time, top speed distance, TSI start, and end location.

Comparison of TSI parameters between male and female sprinters showed significant differences for maximum speed, TSI start location, and TSI end location. For females mean TSI speed amplitudes were 0.71 m/s, which corresponds to 8.42% of respective maximum speed. For males we even found TSI speed amplitudes of 1.31 m/s (13.88% of max speed). Top speed interval speed amplitudes of male runners were, on average, 0.60 m/s (5.4%) larger than for females ($U = 245$, $p < 0.001$, $d = 0.8$). This

TABLE 2 | Validation results when comparing TSI mean speed, TSI mean step time, and TSI mean step length derived from ther RedFIR system to criterion measurements for speed (Laveg laser), step time (OptoGait), and step length (OptoGait).

		Criterion*				RedFIR				Differences (RedFIR – Criterion)					
Parameter	***n***	**Mean**	**Std**	**Min**	**Max**	**Mean**	**Std**	**Min**	**Max**	**Mean**	**Mean abs**	**Percentage abs**	**RMSE**	**Percentage RMSE**	**loa**	**Percentage loa**
Mean speed (TSI) (m/s)	14	7.700	0.560	7.010	8.930	7.660	0.580	6.990	8.960	−0.040	0.060	0.010	0.085	0.011	[−0.19, 0.10]	[−0.02, 0.01]
Mean step time (TSI) (s)	23	0.250	0.010	0.229	0.273	0.249	0.008	0.236	0.262	−0.001	0.003	0.012	0.004	0.017	[−0.05, 0.06]	[−0.03, 0.03]
Mean step length (TSI) (m)	23	1.954	0.150	1.630	2.230	1.955	0.150	1.660	2.220	0.001	0.020	0.012	0.027	0.014	[−0.01, 0.01]	[−0.04, 0.03]

All variables are captured with a percentage RMSE of <2%.

**Laveg for speed/OptoGait for step time and step length.*

was also the case for TSI amplitude normalized with maximum speed ($U = 227$, $p < 0.001$, $d = 0.67$).

Table 4 shows correlations between sprint parameters for male and female sprinters that give an insight into the respective structures of sprinting performance.

There were several significant correlations concerning TSI and other sprint parameters, e.g., TSI start and end location correlated significantly with speed endurance (male: $r = 0.824$, $p < 0.01$; $r = 0.829$, $p < 0.01$; female: $r = 0.834$, $p < 0.01$; $r = 0.864$, $p < 0.01$). TSI time parameters and location parameters showed similar results.

Top speed amplitude (absolute and % of max speed) did not show a significant correlation to any other sprint parameter (exception TSI step length in females: $r = 0.575$, $p < 0.05$) indicating that it is a sprint parameter independent of all other sprint determinants.

DISCUSSION

The study was in first place aiming at investigating the appropriateness of radar-based position detection as a routine instrument for obtaining sprint parameters in competition and training. This is motivated by our perception that especially for sprint parameters related to the TSI there is a considerable lack of routine diagnostics of sprint parameters despite the decisive importance of TSI for the 100 m-sprint.

The measurement device, the RedFIR system, was validated for our study in comparison to laser-based speed measurements and step length and step time obtained from Optogait. Regrettably, there was a mismatch between Optogait measurement interval (50–100 m) and TSI (start typically <50 m). Nevertheless, the deviations of RedFIR-based measurements were acceptable (speed: 1.05%, step time: 1.67%, step length: 1.43%). In addition, a direct validation of the TSI speed amplitude for example with a high precision, marker based optical tracking system would be desirable.

The suggested model for identifying TSI is solely based on investigating the horizontal speed distribution of the full 100 m sprint. This circumvents the need for estimating the COM from a full body model (von Lieres und Wilkau et al., 2020) and/or the analysis of consecutive step characteristics derived from motion capture data (Nagahara et al., 2014a). We used the upper quintile of the overall speed values obtained. This threshold implies though, that the speed curve enters and leaves TSI only with a small speed slope thus leading to a lack of reproducibility (ICC for TSI start and end location/time between 0.336 and 0.518). Maybe a lower threshold could cure this but one would have to be still sure, that the important assumption of a stable top speed running pattern is not violated. Thus, it would be beneficial to investigate the optimal percentile for defining the TSI in subsequent studies.

The procedure of identifying TSI parameters is quite straightforward. The regression fitting errors for v_{base} (5.0 ± 1.0%) and v_{cycle} (2.0 ± 1.0%) were acceptable.

The suggested method for obtaining TSI sprint parameters fits a cyclic sprint speed model to each sprint step in TSI. As a

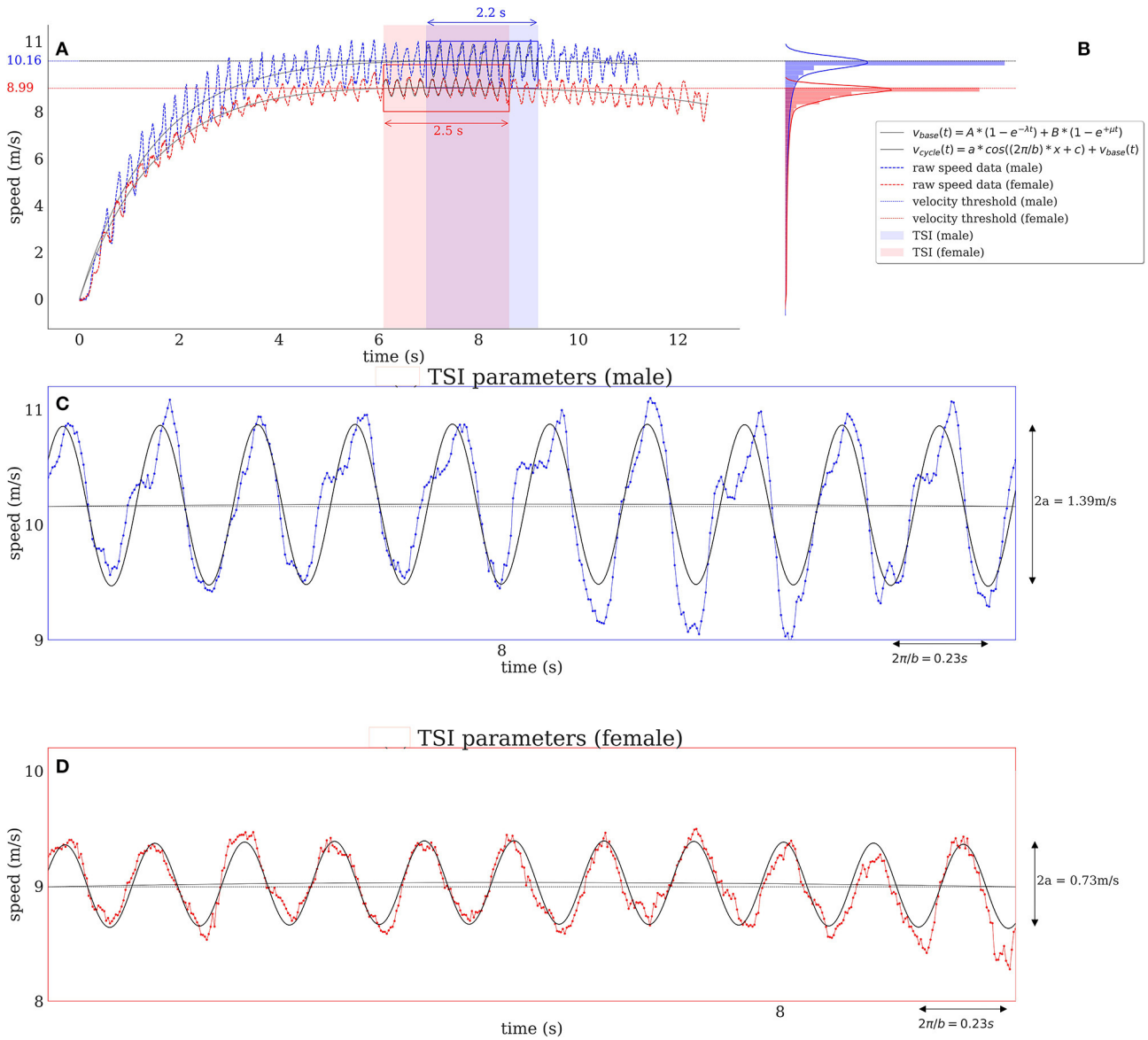

FIGURE 3 | Comparison for two runs performed by female (red) and male (blue) athletes. Panel **(A)** shows raw speed (dotted line) and fitted v_{base} (t) which allows to estimate TSI start and end time for each run individually by estimating a run-specific speed threshold based on the observed speed distribution **(B)**. Zoomed views of TSI are shown for a male **(C)** and a female runner **(D)**. Within TSI we obtain TSI step time (which is the same for both runners −0.23 s) and TSI amplitude which is larger for the male runner (1.39 vs. 0.73 m/s).

"by-product" an estimation of the intra-cyclic speed amplitude in TSI is obtained. To the best of the authors' knowledge this is the first time this parameter is explicitly reported when calculating sprint parameters for TSI. This is somewhat surprising, because there is some evidence that TSI speed amplitudes do exists. If only positional data with a sufficiently high frequency (≥200 Hz) and high spatial accuracy are available, intra-cyclic speed variations are readily observed for example when tracking sprinters with a laser device, e.g., in the documentation of Usain Bolt's world record these cyclic patterns are obviously present (Graubner and Nixdorf, 2011).

Coh et al. (2018) report a similar phenomenon in their analysis of a 100 m event at Zagreb in 2011 (including Usain Bolt running 9.85 s). They examined the ground contacts in his fastest 20 m interval (70–90 m) and found a minimal speed of 11.13 m/s and a maximum of 12.04 m/s at toe-off resulting in an intra-contact speed amplitude for the horizontal displacement of COM of 0.91 m/s (this corresponds to 7.5% standardized amplitude). Notwithstanding some criticism on the applied methodology (2D-kinematics from 100 Hz videos with pixel resolution of 720 × 576) and the fact that this is intra-contact speed, these results are evidence for intra-step speed variation.

TABLE 3 | Descriptive statistics for sprint time and obtained sprint parameter values for 18 female and 14 male runs.

	Male				Female				*t*-test			Reliability ICC
	Mean	Std	Min	Max	Mean	Std	Min	Max	*t*-Values	*p*-Values	Effect size	
Sprint time (s)	11.93	0.56	11.21	12.67	13.08	0.44	12.34	14.11	6.47	$p < 0.001$	2.22	0.963
Max. speed (m/s)	9.44	0.50	8.86	10.18	8.47	0.35	7.88	9.03	−6.23	$p < 0.001$	2.26	0.990
Start acceleration (m/s^2)	6.29	0.55	5.39	7.32	5.84	0.44	4.92	6.57	−2.56	$p < 0.016$	0.90	0.851
Speed endurance (%)	93.11	3.23	88.07	98.54	91.06	3.69	84.01	97.99	−1.65	$p < 0.109$	0.59	0.190
Top speed start location (m)	47.94	4.82	43.01	59.06	43.08	4.51	36.17	57.08	210.00	$p < 0.001$	0.56	0.440$^+$
Top speed end location (m)	68.64	4.80	63.53	79.39	63.92	4.70	57.69	78.63	203.00	$p < 0.003$	0.51	0.416$^+$
Top speed length (m)	20.69	0.66	19.96	22.27	20.84	0.68	19.73	22.04	0.60	$p < 0.552$	0.21	0.336
Top speed start time (s)	6.52	0.60	5.76	7.93	6.47	0.59	5.54	8.11	−0.25	$p < 0.802$	0.09	0.424
Top speed end time (s)	8.72	0.65	7.83	10.18	8.93	0.61	8.12	10.55	0.94	$p < 0.357$	0.33	0.518
Top speed duration (s)	2.20	0.13	2.01	2.41	2.47	0.12	2.30	2.68	5.83	$p < 0.001$	2.07	0.903
Top speed step time (s)	0.23	0.01	0.22	0.24	0.24	0.01	0.22	0.26	1.51	$p < 0.141$	0.54	0.914
Top speed step length (m)	2.10	0.09	1.99	2.21	2.00	0.09	1.80	2.14	−2.97	$p < 0.006$	1.06	0.865
Top speed amplitude (m/s)	1.31	0.31	0.82	1.77	0.71	0.11	0.51	0.91	245.00	$p < 0.001$	0.80	0.976
Normalized top speed amplitude (%)	13.88	3.18	8.93	18.27	8.42	1.25	6.26	10.40	227.00	$p < 0.001$	0.67	0.970

Sprint time was measured by the RedFIR system. Maximum speed, maximum acceleration and speed endurance are obtained by $v_{base}(t)$ whereas amplitude, step length and step time are obtained by $v_{base}(t)$. Results of t-tests/Mann-Whitney (t-value, p-value and effect size d).
$^+$Mann Whitney U-test.

Also, there is a considerable body of studies on horizontal braking and acceleration impulses during ground contact in sprinting (Nagahara et al., 2014b, 2018a,b). These are large braking and accelerating impulses and only the small difference between them may be used for propulsion. These impulses impact on the whole body and must give rise to cyclic intra-step speed variation, although to the best of our knowledge this consequence was not mentioned in the quoted papers.

It must be assumed, though, that the absolute values for intra-cyclic speed amplitudes depend on the body part of sensor fixation. Linke et al. (2018) report significant differences between measurements of running kinematics taken from center of shoulders like in our study and center of pelvis, with the latter representing center of mass better. It is not yet well-understood how braking and acceleration impulses from ground contact of sprinters propagate through the body giving rise to intra-cyclic speed variations. Theoretically, there is constant speed within flight time and the only changes of speed may be induced in contact time. Nevertheless, properties of the human body (body segments with non-rigid connections) may care for "dampening" of the net ground reaction forces in higher body locations, e.g., center of mass, and center of shoulders, where our sensors were placed. The goodness-of-fit results of the cosine-wave model and the qualitative shape of within-cycle speed support this notion, but as mentioned there is reason to assume that TSI amplitude is specific to the investigated body part, e.g., center of shoulders (examined here) or center of pelvis or even center of mass.

The absolute values for the amplitude of the cyclic component in sprint speed in TSI for the center of shoulders are quite high (mean females: 0.71 m/s; 8.42% of maximum speed; mean males 1.31 m/s; 13.88%). This means, within one step a sprinter is exposed to considerable accelerations and decelerations. The question that suggests itself is why these are hardly perceived and reported by the athletes. A first speculation could take into account that, because there are braking and acceleration impulses in normal gait also, we have learnt by assimilation (Piaget and Inhelder, 1967) and habituation (Hinde, 1970) in early childhood to ignore this irrelevant sensor input. Thus, even a top-level sprinter might adhere to a perception of constant running speed.

Nevertheless, it might turn out that intra-cyclic amplitude will become a valuable parameter for sprint diagnostics. Coh et al. (2018) make a low braking force responsible for Usain Bolt's high sprinting speed. This would correspond to a smaller TSI amplitude, although there should be a mechanical lower limit for it. It may be expected that there is an individual optimum for TSI amplitude as too large values should be too energy demanding and too small ones do not allow generating sufficient propulsion forces.

Descriptive statistics and gender comparisons allow a deeper understanding of TSI. Female sprinters stay a significantly longer time in TSI due to reaching it earlier and due to mostly leaving it later. There are no significant differences in the length of TSI; female sprinters reach and leave it after significantly shorter distances. It must be mentioned that this study was designed as a technical feasibility study and not for gender comparisons.

The same holds for the correlations reported in this research. These were mainly included to show the construct validation of the performance structure of the 100 m sprint. The inter-correlations between the sprint parameters confirm the decisive role of maximum speed for the 100 m performance with $r = -0.912$ male/-0.864 female. Maximum speed itself is influenced negatively by the duration and end time (not for females) of TSI as well as acceleration at start.

The TSI parameters for location correlate with sprint endurance: the farther TSI is down the way the smaller the loss of speed toward the end. The same holds for the temporal onset and offset of TSI. Step time and step length in TSI show low to moderate correlations with other sprint parameters for the male athletes, whereas for female athletes we find significant relationships to other TSI parameters as well as to maximum

TABLE 4 | Correlation Matrix separately for male (lower triangular matrix, white) and females (upper triangular matrix, gray).

	Male													
	Sprint time (s)	**Max. speed (m/s)**	**Start acceleration (m/s^2)**	**Speed endurance (%)**	**Top speed start location (m)**	**Top speed end location (m)**	**Top speed length (m)**	**Top speed start time (s)**	**Top speed end time (s)**	**Top speed duration (s)**	**Top speed step time (s)**	**Top speed step length (m)**	**Top speed amplitude (m/s)**	**Normalized top speed amplitude (%)**
Sprint time (s)	1.000	−0.912**	−0.798**	0.138	0.125	0.116	−0.218	0.420	0.695**	0.808**	0.218	0.323	−0.248	0.090
Max. speed (m/s)	−0.864**	1.000	0.749**	−0.121	−0.073	−0.068	0.279	−0.402	−0.682**	−0.795**	−0.073	−0.121	0.169	−0.156
Start acceleration (m/s^2)	−0.176	0.083	1.000	0.090	−0.182	−0.152	0.367	−0.429	−0.609*	−0.570*	−0.068	0.108	0.196	−0.059
Speed endurance (%)	−0.265	0.014	−0.465	1.000	0.824**	0.829**	0.134	0.732**	0.629*	0.073	−0.521	−0.160	−0.103	−0.042
Top speed start location (m)	−0.408	0.355	−0.659**	0.834**	1.000	0.987**	0.103	0.881**	0.706**	0.011	−0.459	−0.415	−0.143	−0.077
Top speed end location (m)	−0.378	0.316	−0.612**	0.864**	0.969**	1.000	0.204	0.868**	0.715**	0.075	−0.455	−0.393	−0.103	−0.046
Top speed length (m)	−0.076	−0.018	0.148	0.340	0.153	0.317	1.000	0.002	−0.009	0.289	0.332	−0.020	−0.011	0.033
Top speed start time (s)	−0.073	0.009	−0.827**	0.839**	0.904**	0.892**	0.112	1.000	0.915**	0.267	−0.363	−0.354	−0.314	−0.160
Top speed end time (s)	0.067	−0.195	−0.764**	0.849**	0.786**	0.809**	0.278	0.941**	1.000	0.593*	−0.233	−0.156	−0.295	−0.044
Top speed duration (s)	0.623**	−0.782**	0.028	0.202	−0.177	−0.059	0.596**	0.069	0.327	1.000	0.374	0.242	−0.123	0.218
Top speed step time (s)	0.033	−0.093	−0.434	0.230	0.255	0.207	−0.181	0.402	0.411	0.102	1.000	0.516	−0.182	−0.420
Top speed step length (m)	−0.557*	0.710**	−0.412	0.230	0.589*	0.498*	−0.183	0.428	0.233	−0.606**	0.501*	1.000	−0.182	−0.156
Top speed amplitude (m/s)	−0.163	0.371	−0.189	−0.102	0.232	0.108	−0.321	0.180	0.015	−0.443	0.259	0.575*	1.000	0.912**
Normalized top speed amplitude (%)	0.038	0.192	−0.121	−0.284	0.022	0.106	−0.424	0.035	−0.100	−0.356	0.259	0.416	0.959**	1.000

Sprint time corresponds to the time it took an athlete to cover the distance between start and finish and was obtained directly from the tracking system. For male athletes top speed step length shows significant correlations with top speed step time (r = 0.50), maximum speed (r = 0.71), TSI amplitude (r = 0.58), top speed duration, top speed start location (r = 0.59), top speed end location (r = 0.50), sprint time tracking (r = −0.56) and sprint time stopwatch (r = −0.57) In contrast, for females top speed step length is not correlated with other sprint variables.

** $p < 0.05$, ** $p < 0.01$.*

speed. The correlation between step length and time is moderate ($r = 0.516$ male/0.501 female). This could be explained by a combination of step length and time that constitutes an individually optimal relation. This relation is determined by individual muscular and anthropometric properties (Salo et al., 2011; Van Oeveren et al., 2019).

Finally, there were no significant correlations found for the intra-cyclic speed amplitude for the male athletes and only with top speed step length for female athletes. This could mean that the top speed amplitude constitutes a rather independent dimension of sprint performance impacting maximum speed with $r = 0.370$ (male only 0.169).

The aims of the study were to demonstrate that employing sensor-based position detection allows for comprehensive sprint diagnostics in competition and training settings. It must be mentioned that the sprint parameters obtained do not rely on the specific technological platform, here the RedFIR system. Instead, any platform providing sufficiently accurate high frequency position data from sprinters may be used. The increasing market for sensor-based position detection in sports, mostly powered by the demand of professional team sports, will make appropriate systems much more available in the future.

As it is a well-known fact that top speed is decisive for the overall performance in 100 m-sprint, a method assessing sprint parameters like TSI step length and step time are of high relevance. The newly introduced parameter TSI amplitude also bears potential for improving the theoretical understanding as well as training in top level sprint athletes.

DATA AVAILABILITY STATEMENT

The datasets presented in this article are not publicly available. Requests to access the datasets should be directed to martin.lames@tum.de.

ETHICS STATEMENT

The studies involving human participants were reviewed and approved by Technical University of Munich. Written informed consent from the participants' legal guardian/next of kin was not required to participate in this study in accordance with the national legislation and the institutional requirements.

AUTHOR CONTRIBUTIONS

All authors listed have made a substantial, direct and intellectual contribution to the work, and approved it for publication.

FUNDING

This work was funded by the Federal Institute for Sports Science (BISp) under grant ZMVI4-071503/16-18.

ACKNOWLEDGMENTS

The authors would like to thank the Fraunhofer Institute for Integrated Circuits for providing us with the radio-based tracking data and for their valuable input throughout the course of this project.

SUPPLEMENTARY MATERIAL

The Supplementary Material for this article can be found online at: https://www.frontiersin.org/articles/10.3389/fspor.2021.689341/full#supplementary-material

Supplementary Figure 1 | Bland-Altman plots for TSI speed vs. Laveg (left), TSI step length (middle), and TSI step time vs. OptoGait, respectively. Systematic differences (solid line) and 95% limits of agreement (dashed lines) are shown.

REFERENCES

Ae, M. (2017). "Sprint running: running at maximum speed," in *Handbook of Human Motion*, eds B. Müller, S. I. Wolf, G.-P. Brueggemann, Z. Deng, A. McIntosh, F. Miller, and W. S. Selbie (Cham: Springer International Publishing), 1–29. doi: 10.1007/978-3-319-30808-1_119-1

Ae, M., Ito, A., and Suzuki, M. (1992). The men's 100 meters. *New Stud. Athlet.* 7, 47–52.

Arsac, L. M., and Locatelli, E. (2002). Modeling the energetics of 100-m running by using speed curves of world champions. *J. Appl. Physiol.* 92, 1781–1788. doi: 10.1152/japplphysiol.00754.2001

Beneke, R., and Taylor, M. J. (2010). What gives Bolt the edge - A.V. Hill knew it already! *J. Biomech.* 43, 2241–2243. doi: 10.1016/j.jbiomech.2010.04.011

Bezodis, I. N., Salo, A. I. T., and Kerwin, D. G. (2008). "A longitudinal case study of step characteristics in a world class sprint athlete," in *Proceedings of the XXVI International Conference on Biomechanics in Sports,* eds Y.-H. Kwon, J. Shim, J. K. Shim, and I. S. Shin (Paju-si: Rainbow Books), 537–540.

Bezodis, N. E., Salo, A., and Trewartha, G. (2012). Measurement error in estimates of sprint velocity from a laser displacement measurement device. *Int. J. Sports Med.* 33, 439–444. doi: 10.1055/s-0031-1301313

Bezodis, N. E., Willwacher, S., and Salo, A. I. T. (2019). The biomechanics of the track and field sprint start: a narrative review. *Sports Med.* 49, 1345–1364. doi: 10.1007/s40279-019-01138-1

Bompa, T. O., and Bompa, T. O. (1999). *Periodization: Theory and Methodology of Training*. Champaign, IL: Human Kinetics.

Brüggemann, G. P., Koszewski, and, D., Müller, H., and Foundation, I. A. (1999). *Biomechanical Research Project, Athens 1997: Final Report*. Meyer and Meyer Sport.

Brüggemann, G. P., and Rühl, J. K. (eds.) (1990). *Techniques in Athletics: Conference Proceedings*. Köln: Strauß.

Coh, M., Hébert-Losier, K., Štuhec, S., Babić, V., and Supej, M. (2018). Kinematics of Usain Bolt's maximal sprint velocity. *Kinesiology* 50, 100–101. doi: 10.26582/k.50.2.10

Coh, M., Milanovic, and, D., and Kampmiller, T. (2001). Morphologic and kinematic characteristics of elite sprinters. *Coll. Antropol.* 25, 605–610.

Cohen, J. (1988). *Statistical Power Analysis for the Behavioral Sciences*. New York, NY: Routledge.

Colyer, S. L., Nagahara, R., and Salo, A. I. T. (2018). Kinetic demands of sprinting shift across the acceleration phase: novel analysis of entire force waveforms. *Scand. J. Med. Sci. Sports* 28, 1784–1792. doi: 10.1111/sms.13093

Debaere, S., Jonkers, I., and Delecluse, C. (2013). The contribution of step characteristics to sprint running performance in high-level male and female athletes. *J. Strength Cond. Res.* 27, 116–124. doi: 10.1519/JSC.0b013e31825183ef

di Prampero, P. E., Fusi, S., Sepulcri, L., Morin, J. B., Belli, A., and Antonutto, G. (2005). Sprint running: a new energetic approach. *J. Exp. Biol.* 208(Pt 14), 2809–2816. doi: 10.1242/jeb.01700

Ferro, A., Pagola, I., Ferreruela, M., Martin, A., and Rocandio, V. (2001). Biomechanical analysis of the 7th World Championships in Athletics Seville 1999. *New Stud. Athlet.* 16, 25–60.

Fuchs, P., and Lames, M. (1990). Mathematische modellierung des wettkampfverhaltens im sprint. *Leistungssport* 20, 35–41.

Gindre, C., Lussiana, T., Hebert-Losier, K., and Morin, J. B. (2016). Reliability and validity of the Myotest® for measuring running stride kinematics. *J. Sports Sci.* 34, 664–670. doi: 10.1080/02640414.2015.1068436

Graubner, R., and Nixdorf, E. (2011). Biomechanical analysis of the sprint and hurdles events at the 2009 IAAF World Championships in Athletics. *New Stud. Athlet.* 26, 19–53. doi: 10.1097/JSM.0b013e318191c8e7

Grün, T., Franke, N., Wolf, D., Witt, N., and Eidloth, A. (2011). "A real-time tracking system for football match and training analysis," in Microelectronic *Systems*, eds A. Heuberger, G. Elst, and R. Hanke (Berlin; Heidelberg: Springer), 199–212. doi: 10.1007/978-3-642-23071-4_19

Harrison, A. J., Jensen, R. L., and Donoghue, O. (2005). A comparison of laser and video techniques for determining displacement and velocity during running. *Measur. Phys. Educ. Exerc. Sci.* 9, 219–231. doi: 10.1207/s15327841mpee0904_2

Healy, R., Kenny, I. C., and Harrison, A. J. (2019). Profiling elite male 100-m sprint performance: the role of maximum velocity and relative acceleration. *J. Sport Health Sci*. doi: 10.1016/j.jshs.2019.10.002

Hill, A. V. (1927). *Muscular Movement in Man: The Factors Governing Speed and Recovery from Fatigue*. New York, NY: McGraw-Hill Book Company.

Hinde, R. (1970). *Behavioral Habituation*. New York, NY: Cambridge Univ. Press.

Hunter, J. P., Marshall, R. N., and McNair, P. J. (2004). Interaction of step length and step rate during sprint running. *Med. Sci. Sports Exerc.* 36, 261–271. doi: 10.1249/01.MSS.0000113664.15777.53

Hunter, J. P., Marshall, R. N., and McNair, P. J. (2005). Relationships between ground reaction force impulse and kinematics of sprint-running acceleration. *J. Appl. Biomech.* 21, 31–43. doi: 10.1123/jab.21.1.31

Jones, R., Bezodis, and, I., and Thompson, A. (2009). Coaching sprinting: expert coaches' perception of race phases and technical constructs. *Int. J. Sports Sci. Coach.* 4, 385–396. doi: 10.1260/174795409789623964

Koo, T., and Li, M. (2016). A guideline of selecting and reporting intraclass correlation coefficients for reliability research. *J. Chiropract. Med.* 15, 155–163. doi: 10.1016/j.jcm.2016.02.012

Krzysztof, M., and Mero, A. (2013). A kinematics analysis of three best 100 m performances ever. *J. Hum. Kinet.* 36, 149–160. doi: 10.2478/hukin-2013-0015

Levenberg, K. (1944). A method for the solution of certain non linear problems in least squares. *Q. Appl. Mathemat.* 2, 164–168. doi: 10.1090/qam/10666

Lienhard, K., Schneider, D., and Maffiuletti, N. A. (2013). Validity of the Optogait photoelectric system for the assessment of spatiotemporal gait parameters. *Med. Eng. Phys.* 35, 500–504. doi: 10.1016/j.medengphy.2012.06.015

Linke, D., Link, D., and Lames, M. (2018). Validation of electronic performance and tracking systems EPTS under field conditions. *PLoS ONE* 13:e0199519. doi: 10.1371/journal.pone.0199519

Manzer, S., Mattes, K., and Holländer, K. (2016). Kinematic analysis of sprinting pickup acceleration versus maximum sprinting speed. *J. Biol. Exerc.* 12, 55–67. doi: 10.4127/jbe.2016.0109

Marquardt, D. W. (1963). An algorithm for least-squares estimation of nonlinear parameters. *J. Soc. Indus. Appl. Mathemat.* 11, 431–441. doi: 10.1137/0111030

Mattes, K., Wolff, S., and Alizadeh, S. (2021). Kinematic stride characteristics of maximal sprint running of elite sprinters-verification of the "Swing-Pull Technique". *J. Hum. Kinet.* 77, 15–24. doi: 10.2478/hukin-2021-0008

Mero, A. (1988). Force-time characteristics and running velocity of male sprinters during the acceleration phase of sprinting. *Res. Q. Exerc. Sport* 59, 94–98. doi: 10.1080/02701367.1988.10605484

Moravec, P., Ruzicka, J., Susanka, P., Dostal, E., Kodejs, M., and Nosek, M. (1988). The 1987 International Athletic Foundation/IAAF scientific project report: time analysis of ihe 100 metres events at the II World Championships in Athletics. *New Stud. Athlet.* 3, 61–96.

Morin, J. B., Bourdin, M., Edouard, P., Peyrot, N., Samozino, P., and Lacour, J. R. (2012). Mechanical determinants of 100-m sprint running performance. *Eur. J. Appl. Physiol.* 112, 3921–3930. doi: 10.1007/s00421-012-2379-8

Morin, J. B., Samozino, P., Murata, M., Cross, M. R., and Nagahara, R. (2019). A simple method for computing sprint acceleration kinetics from running velocity data: replication study with improved design. *J. Biomech.* 94, 82–87. doi: 10.1016/j.jbiomech.2019.07.020

Mutschler, C., Ziekow, H., and Jerzak, Z. (2013). "The DEBS 2013 grand challenge," in *Proceedings of the 7th ACM International Conference on Distributed Event-Based Systems* (Arlington, TX: ACM), 289–294. doi: 10.1145/2488222.2488283

Nagahara, R., Kanehisa, H., and Fukunaga, T. (2020). Ground reaction force across the transition during sprint acceleration. *Scand. J. Med. Sci. Sports* 30, 450–461. doi: 10.1111/sms.13596

Nagahara, R., Kanehisa, H., Matsuo, A., and Fukunaga, T. (2019). Are peak ground reaction forces related to better sprint acceleration performance? *Sports Biomech.* 20, 360–369. doi: 10.1080/14763141.2018.1560494

Nagahara, R., Matsubayashi, T., Matsuo, A., and Zushi, K. (2014a). Kinematics of transition during human accelerated sprinting. *Biol. Open* 3, 689–699. doi: 10.1242/bio.20148284

Nagahara, R., Mizutani, M., Matsuo, A., Kanehisa, H., and Fukunaga, T. (2018a). Association of sprint performance with ground reaction forces during acceleration and maximal speed phases in a single sprint. *J. Appl. Biomech.* 34, 104–110. doi: 10.1123/jab.2016-0356

Nagahara, R., Mizutani, M., Matsuo, A., Kanehisa, H., and Fukunaga, T. (2018b). Step-to-step spatiotemporal variables and ground reaction forces of intra-individual fastest sprinting in a single session. *J. Sports Sci.* 36, 1392–1401. doi: 10.1080/02640414.2017.1389101

Nagahara, R., Naito, H., Morin, J. B., and Zushi, K. (2014b). Association of acceleration with spatiotemporal variables in maximal sprinting. *Int. J. Sports Med.* 35, 755–761. doi: 10.1055/s-0033-1363252

Park, S. (2011). *Biomechanics Research Project in the IAAF World Championships*. Daegu 2011.

Piaget, J., and Inhelder, B. (1967). *La Psychologie de L'enfant*. Presses Universitaires de France.

Rabita, G., Dorel, S., Slawinski, J., Sàez-de-Villarreal, E., Couturier, A., Samozino, P., et al. (2015). Sprint mechanics in world-class athletes: a new insight into the limits of human locomotion. *Scand. J. Med. Sci. Sports* 25, 583–594. doi: 10.1111/sms.12389

Ruiter, C., and Van Dieen, J. (2019). Stride and step length obtained with inertial measurement units during maximal sprint acceleration. *Sports* 7:202. doi: 10.3390/sports7090202

Ryu, J.-S., Yoon, S., Park, S.-K., Kim, T., Yoo, S.-H., Lee, G.-s., et al. (2012). "Sprinting speed of elite sprinters at the world championships," in *30th Annual Conference of Biomechanics in Sports* (Melbourne, VIC).

Saito, Y., Nagahara, R., Ae, M., and Matsuo, A. (2008). "Evaluation of speed change in 100 m sprint running," in *26 International Conference on Biomechanics in Sport*s (Seoul).

Salo, A., Bezodis, I., Batterham, A., and Kerwin, D. (2011). Elite sprinting: are athletes individually step-frequency or step-length reliant? *Med. Sci. Sports Exerc.* 43, 1055–1062. doi: 10.1249/MSS.0b013e318201f6f8

Sathyan, T., Shuttleworth, R., Hedley, M., and Davids, K. (2012). Validity and reliability of a radio positioning system for tracking athletes in indoor and outdoor team sports. *Behav. Res. Methods* 44, 1108–1114. doi: 10.3758/s13428-012-0192-2

Schmidt, M., Rheinländer, C., Nolte, K. F., Wille, S., Wehn, N., and Jaitner, T. (2016). IMU-based determination of stance duration during sprinting. *Proc. Eng.* 147, 747–752. doi: 10.1016/j.proeng.2016.06.330

Schubert, A. G., Kempf, J., and Heiderscheit, B. C. (2014). Influence of stride frequency and length on running mechanics: a systematic review. *Sports Health* 6, 210–217. doi: 10.1177/1941738113508544

Seidl, T., Czyz, T., Spandler, D., Franke, N., and Lochmann, M. (2016). Validation of football's velocity provided by a radio-based tracking system. *Proc. Eng.* 147, 584–589. doi: 10.1016/j.proeng.2016.06.244

Seidl, T., Linke, D., and Lames, M. (2017). Estimation and validation of spatio-temporal parameters for sprint running using a radio-based tracking system. *J. Biomech.* 65, 89–95. doi: 10.1016/j.jbiomech.2017.10.003

Taylor, M. J. D., and Beneke, R. (2012). Spring mass characteristics of the fastest men on earth. *Int. J. Sports Med.* 33, 667–670. doi: 10.1055/s-0032-1306283

Van Oeveren, B. T., De Ruiter, C. J., Hoozemans, M. J. M., Beek, P. J., and Van Dieën, J. H. (2019). Inter-individual differences in stride frequencies during running obtained from wearable data. *J. Sports Sci.* 37, 1996–2006. doi: 10.1080/02640414.2019.1614137

von Lieres und Wilkau, H. C., Irwin, G., Bezodis, N. E., Simpson, S., and Bezodis, I. N. (2020). Phase analysis in maximal sprinting: an investigation of step-to-step technical changes between the initial acceleration, transition and maximal velocity phases. *Sports Biomech.* 19, 141–156. doi: 10.1080/14763141.2018.1473479

Walker, J., Tucker, C. B., Paradisis, G. P., Bezodis, I., Bissas, A., and Merlino, S. (2019). *Biomechanical Report for the IAAF World Indoor Championships 2018: 60 Metres Men*. Birmingham: International Association of Athletics Federations.

Willwacher, S., Kurz, M., Menne, C., Schrödter, E., and Brüggemann, G.-P. (2016). Biomechanical response to altered footwear longitudinal bending stiffness in the early acceleration phase of sprinting. *Footwear Sci.* 8, 99–108. doi: 10.1080/19424280.2016.1144653

Conflict of Interest: The authors declare that the research was conducted in the absence of any commercial or financial relationships that could be construed as a potential conflict of interest.

frontiers in Sports and Active Living

ORIGINAL RESEARCH
published: 29 June 2021
doi: 10.3389/fspor.2021.682401

Runners Adapt Different Lower-Limb Movement Patterns With Respect to Different Speeds and Downhill Slopes

David Sundström[1]*, *Markus Kurz*[1] and *Glenn Björklund*[2]

[1] Sports Tech Research Centre, Department of Quality Management and Mechanical Engineering, Mid Sweden University, Östersund, Sweden, [2] Swedish Winter Sport Research Centre, Department of Health Sciences, Mid Sweden University, Östersund, Sweden

The aim of this study was to investigate the influence of slope and speed on lower-limb kinematics and energy cost of running. Six well-trained runners (VO_{2max} 72 ± 6 mL·kg^{-1}·min^{-1}) were recruited for the study and performed (1) VO_{2max} and energy cost tests and (2) an experimental running protocol at two speeds, 12 km·h^{-1} and a speed corresponding to 80% of VO_{2max} (V80, 15.8 ± 1.3 km·h^{-1}) on three different slopes (0°, −5°, and −10°), totaling six 5-min workload conditions. The workload conditions were randomly ordered and performed continuously. The tests lasted 30 min in total. All testing was performed on a large treadmill (3 × 5 m) that offered control over both speed and slope. Three-dimensional kinematic data of the right lower limb were captured during the experimental running protocol using eight infrared cameras with a sampling frequency of 150 Hz. Running kinematics were calculated using a lower body model and inverse kinematics approach. The generic model contained three, one, and two degrees of freedom at the hip, knee, and ankle joints, respectively. Oxygen uptake was measured throughout the experimental protocol. Maximum hip extension and flexion during the stance phase increased due to higher speed ($p < 0.01$ and $p < 0.01$, respectively). Knee extension at the touchdown and maximal knee flexion in the stance phase both increased on steeper downhill slopes (both $p < 0.05$). Ground contact time (GCT) decreased as the speed increased ($p < 0.01$) but was unaffected by slope ($p = 0.73$). Runners modified their hip movement pattern in the sagittal plane in response to changes in speed, whereas they altered their knee movement pattern during the touchdown and stance phases in response to changes in slope. While energy cost of running was unaffected by speed alone ($p = 0.379$), a shift in energy cost was observed for different speeds as the downhill gradient increased ($p < 0.001$). Energy cost was lower at V80 than 12 km·h^{-1} on a −5° slope but worse on a −10° slope. This indicates that higher speeds are more efficient on moderate downhill slopes (−5°), while lower speeds are more efficient on steeper downhill slopes (−10°).

Keywords: biomechanics, gait analysis, gradient, motion analysis, running technique, work economy

OPEN ACCESS

Edited by:
Brian Hanley,
Leeds Beckett University,
United Kingdom

Reviewed by:
Tyler Brown,
Boise State University, United States
Alexandre J. M. Rambaud,
Université Jean Monnet, France

***Correspondence:**
David Sundström
david.sundstrom@miun.se

Specialty section:
This article was submitted to Elite Sports and Performance Enhancement, a section of the journal Frontiers in Sports and Active Living

Received: *18 March 2021*
Accepted: *03 June 2021*
Published: *29 June 2021*

Citation:
Sundström D, Kurz M and Björklund G (2021) Runners Adapt Different Lower-Limb Movement Patterns With Respect to Different Speeds and Downhill Slopes. Front. Sports Act. Living 3:682401. doi: 10.3389/fspor.2021.682401

INTRODUCTION

Running is one of the most popular physical activities, both recreationally and competitively. It is also a fundamental part of human locomotion and has been investigated in numerous studies (Cavanagh and Lafortune, 1980; Cavanagh and Kram, 1985; Staab et al., 1992; Anderson, 1996; Townshend et al., 2010; Kasmer et al., 2013). Competitive running includes many disciplines, categorized by distance or duration, in combination with various terrain and course surfaces. As in any locomotive endurance sport, long-distance running performance is determined by the athlete's maximum aerobic power (VO_{2max}), lactate threshold, and work economy (Joyner, 1991; Joyner and Coyle, 2008). Several studies have investigated various biomechanical aspects of work economy in running (i.e., energy cost of running; Tartaruga et al., 2012; Santos-Concejero et al., 2014a, 2017).

Studies on the influence of foot-strike patterns on marathon performance show the dominance of the heel-strike pattern, irrespective of a runner's location on a course or the final race result (Kasmer et al., 2013). Although the heel-strike pattern is the dominant foot-strike pattern at all performance levels, there is a greater percentage of fore-foot runners among the fastest runners in level-terrain races (Hasegawa et al., 2007). 2D video recordings assessed this distribution of foot-strike patterns; however, no information of the inter- or intraindividual reliability is presented for the method itself. Furthermore, none of these studies include spatiotemporal stride characteristics nor angles of the lower extremities that could possibly explain differences in foot-strike patterns.

The benefit of an optimal foot-strike pattern is that it decreases the braking forces acting on the foot at the ground contact. These braking forces inherently counteract the propulsive forces that move the body in a forward running direction. Interestingly, the effect of foot-strike patterns on energy cost of running is not clear (Moore, 2016). One major reason for the uncertainty is the position of the lower limbs in relation to foot and possibly ankle flexibility. If the foot is placed too far in front of the hip, a runner is, by definition, over striding, which increases braking force (Lieberman et al., 2015). To decrease the risk of over striding, a runner should increase stride frequency (SF) with a concomitant decrease in stride length (SL). This may explain why an increase in SF decreases energy cost (Hunter and Smith, 2007; de Ruiter et al., 2014) at a given submaximal speed.

Overall performance on hilly and undulating trail-running courses is related to both uphill and downhill running ability. However, in trail running, which includes hilly terrain and sustained downhill sections with rocky and root-covered surfaces, downhill running ability seems to be more important to performance than uphill running ability (Kay, 2014). The results of Kay (2014) also showed that the fastest runners on these types of trail-running courses overall also excelled on the downhill sections. However, no analysis or explanation is presented as to why or how these runners achieved higher speeds of descent. Moreover, previous studies of downhill running show that oxygen uptake drops at a −5% gradient (approximately−3°) or steeper, despite speed increasing and runners performing at the maximal effort (Staab et al., 1992; Born et al., 2017). Therefore, it is reasonable to assume that biomechanics is a constraint on running speed and that this becomes more severe on steeper downhill slopes. Hence, lower-limb dynamics ought to be highly important to describe downhill running performance. Running on an instrumented treadmill at 3.0 $m \cdot s^{-1}$ shows that braking force peaks (parallel ground reaction forces) and braking impulses increase on steeper downhill slopes (Gottschall and Kram, 2005). Nevertheless, the study by Gottschall and Kram (2005) does not present any data to explain if and how running kinematics are altered to achieve higher braking forces on steeper downhill slopes. However, Buczek and Cavanagh (1990) showed that greater downhill slope was associated with greater knee flexion. Moreover, Khassetarash et al. (2020) showed that greater speed was associated with a greater hip angle range of motion, at both level and downhill slopes.

On level terrain, Lieberman et al. (2015) showed that the horizontal position difference between the ankle and hip at touchdown increases with greater speed. Nonetheless, neither Gottschall and Kram (2005) nor Lieberman et al. (2015) investigated near-race speed of high-performance athletes. Therefore, the aim of this study was to investigate the influence of downhill slope (0° to −10°) and speed (12 $km \cdot h^{-1}$ and speed at 80% of VO_{2max}) on lower-limb kinematics and energy cost when running close to race pace. Hence, we hypothesized that (a) Increased running speed will have a negative effect on energy cost of running compared to slower running speed on the same slope; (b) increased downhill slope is associated with greater knee flexion; and (c) increased running speed is associated with greater range of motion in the hip joint.

METHODS

Participants

Six well-trained male runners (VO_{2max}: 72 ± 6 $mL \cdot kg^{-1} \cdot min^{-1}$, body mass: 71 ± 8 kg, body height: 178 ± 6 cm) were recruited for the study. They were all used to trail running in hilly terrain, including downhill, although their preferable running discipline varied between road running, trail running, and orienteering, including off-trail running. The participants were informed of the aim, procedures, and risks of the tests before giving their informed written consent to participate in the study. The regional ethical review board in Umeå, Sweden, preapproved the research techniques and experimental protocol (#2017/140-31), which conformed to the Declaration of Helsinki.

General Design

The overall study comprised of two parts: the pretests and the experimental tests. The pretests included basic anthropometric measurements as well as submaximal and maximal treadmill-running protocols to determine participants' energy cost of running and VO_{2max}. The experimental tests included a 30-min treadmill protocol to assess lower-limb kinematics and energy cost in level and downhill running.

Pretests

Anthropometric measurements, including body height (cm) and body mass (kg), were conducted using a measuring tape and precision scale (SECA, Hamburg, Germany), respectively. The runners started the test with a 10-min warm-up on a motorized treadmill (Rodby Innovation AB, Vänge, Sweden) at a self-selected speed. Their energy cost (expressed as $J \cdot kg^{-1} \cdot m^{-1}$) was estimated using the Weir equation (Weir, 1949) and by measuring their steady-state oxygen uptake (VO_2) during the final minute of a 5-min running period at 16 $km \cdot h^{-1}$. VO_2 and respiratory exchange ratio (RER) were measured using the ergospirometry system Moxus Metabolic Cart (AEI Technologies, Pittsburg, PA, United States). To be accepted as a valid energy cost estimate, VO_2 data had to meet the criterion of RER <1.00, indicating purely aerobic exercise. In addition to oxygen cost of running (VO_2), we calculated the energy cost of running because it accounts for the different metabolic substrate mixtures when running at submaximal speeds and is more sensitive to changes in speed than oxygen cost (Fletcher et al., 2009). Maximal oxygen uptake (VO_{2max}) was assessed during a ramp test, starting at 16 $km \cdot h^{-1}$ on a level running surface followed by a stepwise increase in slope of 1°/min until voluntary exhaustion. To confirm that the maximal effort was achieved, two criteria had to be satisfied: a rating of perceived exertion on the Borg scale >18 directly after completing the ramp test and RER >1.15. Runners breathed through a mouthpiece while wearing a nose clip to secure all expired air flowed through the ergospirometry system. The O_2 and CO_2 sensors were calibrated using two-component high-precision gases ($\%O_2 = 15.99$, $\%CO_2 = 4.5$ and $\%O_2 = 21.00$, $\%CO_2 = 0.03$, respectively), i.e., two-point calibration. The volume transducer was calibrated using a 3-L syringe (Hans Rudolph) for low, medium, and high flow rates. At all times during the use of the treadmill, a suspended safety harness connected to an emergency stop triggered by their bodyweight secured the participants.

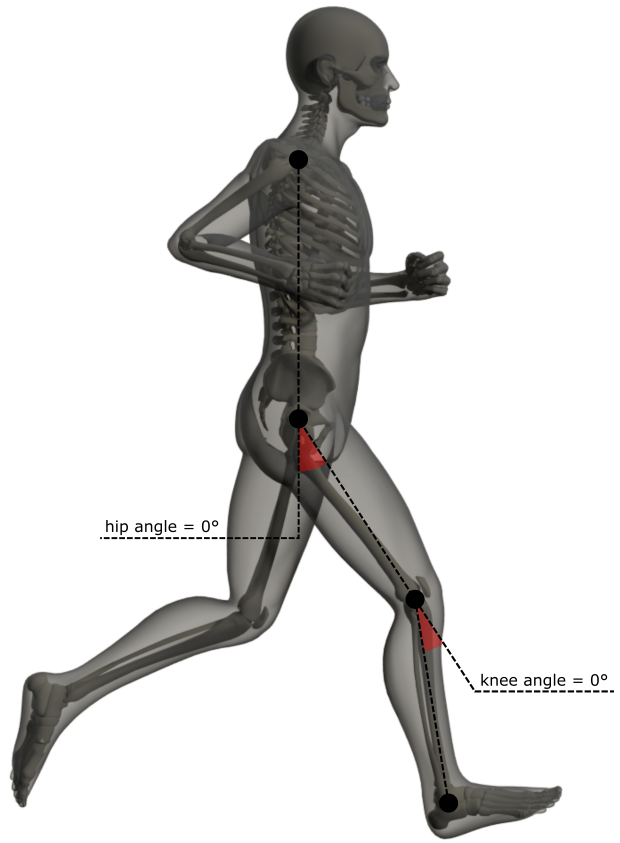

FIGURE 1 | Lower-limb kinematic angles. Areas shaded red indicate the angles analyzed (sagittal plane of the hip and knee joint, respectively). Filled black circles closest to the red areas represent the joint center of the hip and knee. Dashed lines indicate 0° for the angles.

Experimental Tests

Test Protocol

The runners started the test with a 15-min warm-up at a self-selected speed on the same treadmill as used for the pretests. During the warm-up, the runners were familiarized with the three different slopes that would be used in the experimental testing (0°, −5°, and −10°). They then performed a treadmill running test at each of the three slopes, 0°, −5°, and −10°, at two different speeds, a baseline speed of 12 $km \cdot h^{-1}$ and 80% of the speed at which they achieved their VO_{2max} for level running (V80). V80 is close to race pace but still reliable to calculate the energy cost of running (RER <1.0) (Shaw et al., 2014). The participants ran each of the six slope–speed conditions for 5 min, a total running duration of 30 min. The experimental conditions were run in a randomized order to control any confounding factors, i.e., learning effect, and there were no pauses between the experimental conditions. Measurements of VO_2 and energy cost of running were taken as previously described for the pretests.

Kinematics

Eight infrared cameras (Qualisys AB, Göteborg, Sweden, 300/301), evenly distributed around the treadmill (measurement volume: 2.0 × 2.0 × 2.0 m) and set to a capture frequency of 150 Hz, captured three-dimensional kinematic data of a full-body marker set consisting of 77 markers. For the present study, we only analyzed the pelvis and right lower limb (Karamanidis et al., 2003). Markers were attached to the following bony landmarks: both spina iliaca anterior superiors, both spina iliaca posterior superiors, lateral and medial femoral epicondyles, lateral and medial malleolus, most prominent point of the tuber calcanei, head of the first and fifth metatarsal bones, and top of the hallux. Furthermore, two rigid-plate marker clusters, each containing four markers, were mounted to the thigh and shank using hook-and-loop fasteners. For every speed–slope combination, we measured five trials. The measurements took place at the last 15 s of each minute during the 5-min efforts. On average, 89 ± 15 steps were then extracted and analyzed with respect to hip and knee angle in the sagittal plane for every participant and experimental condition.

Data Analysis

Cardiorespiratory data were analyzed in Excel 2013 (Microsoft Office, v15.0). All data synchronization was performed in MATLAB R2016a (The MathWorks, Inc., Natick, MA, United States).

TABLE 1 | Spatiotemporal variables on level and downhill running ($n = 6$).

	0°	−5°	−10°	*F*-values, *P*-values, and effect size (η^2_G)
GCT (s)				
12 km·h^{-1}	0.262 ± 0.023	0.260 ± 0.032	0.259 ± 0.037	[a]$F_{(1,5)} = 28.1$, $p = 0.003$, $\eta^2_G = 0.312$
80% of VO_{2max}	0.221 ± 0.025*	0.222 ± 0.023*	0.230 ± 0.025*	[b]$F_{(2,10)} = 0.3$, $p = 0.714$, $\eta^2_G = 0.002$
				[c]$F_{(2,10)} = 5.3$, $p = 0.027$, $\eta^2_G = 0.009$
SL (m)				
12 km·h^{-1}	2.50 ± 0.15	2.66 ± 0.21	2.66 ± 0.20†#	[a]$F_{(1,5)} = 27.5$, $p = 0.003$, $\eta^2_G = 0.689$
80% of VO_{2max}	3.30 ± 0.50*	3.33 ± 0.22*	3.68 ± 0.40*†#	[b]$F_{(2,10)} = 9.3$, $p = 0.005$, $\eta^2_G = 0.139$
				[c]$F_{(2,10)} = 1.3$, $p = 0.180$, $\eta^2_G = 0.065$
SF (min^{-1})				
12 km·h^{-1}	80.3 ± 4.9	75.6 ± 5.8	75.6 ± 5.3†	[a]$F_{(1,5)} = 0.1$, $p = 0.755$, $\eta^2_G = 0.001$
80% of VO_{2max}	80.9 ± 7.1	79.5 ± 5.5	72.2 ± 6.0†	[b]$F_{(2,10)} = 11.9$, $p = 0.002$, $\eta^2_G = 0.210$
				[c]$F_{(2,10)} = 1.4$, $p = 0.282$, $\eta^2_G = 0.075$

The values are presented as means ± SD. GCT, ground contact time; SL; stride length; SF; stride frequency.
A factorial ANOVA for repeated measurement was used to compare the speed and slope with a Bonferroni post-hoc test.
[a]*Factorial ANOVA for repeated measurement of speed (2).*
[b]*Factorial ANOVA for repeated measurement of slope (3).*
[C]*Interaction effect between speed and slope (2 × 3).*
**Statistically different from 12 km·h^{-1}.*
† Statistically different from 0°.
 # Statistically different from −5°.

Hip and knee angles (**Figure 1**) were calculated using OpenSim 4.1 (Delp et al., 2007; Seth et al., 2018). We used a lower-body model (Gait2392_Simbody) with three, one, and two degrees of freedom in the hip, knee, and ankle joints, respectively. The generic models were scaled to each participant's mass and the position of the markers placed at their bony landmarks (scaling markers). OpenSim uses an inverse kinematic approach to calculate joint angles, and the kinematic data were filtered using a third-order zero-phase low-pass Butterworth filter with a cutoff frequency of 20 Hz.

We calculated gait events (i.e., touchdown and toe off) using kinematic algorithms (Fellin et al., 2010; Handsaker et al., 2016, respectively) and normalized the parameters with respect to the stance phase. Ground contact time (GCT) and SF were calculated using these gait events together with the treadmill speed, while SL was calculated according to Cavanagh and Williams (1982).

Statistical Analyses

All data were checked for normal distribution using Shapiro–Wilk tests and assumption of homogeneity of variance *via* Levene's test. The data were processed and further analyzed using *jamovi* (version 1.2 [Computer Software]. Retrieved from https://www.jamovi.org) and MATLAB R2016a (The MathWorks, Inc., Natick, MA, United States). Two-way factorial ANOVA with repeated measures (speed × slope) was applied to test global differences for dependent variables as kinematic (hip-, knee-flexion extension), spatiotemporal (GCT, SL, SF), and cardiorespiratory (relative and absolute VO_2, J·kg^{-1}·m^{-1}). For all ANOVAs, data were controlled for type one errors using Mauchly's sphericity test and, if violated, the Greenhouse–Geisser-corrected *F*-values were used. If there were global significances in the ANOVA, a further Bonferroni *post-hoc* analysis was performed. Generalized eta-squared (η^2_G) was used to determine the effect size for the ANOVA. The thresholds for interpreting the effect size were small: $\eta^2_G > 0.02$; medium: $\eta^2_G > 0.13$; and large: $\eta^2_G > 0.26$ (Bakeman, 2005). A paired Student's *t*-test was used to compare the differences in speed between 12 km·h^{-1} and V80 with Cohen's *d* as an effect size. Data are presented as mean ± SD or a 95% confidence interval (95% CI). The significance level was set to $\alpha = 0.05$ a priori.

RESULTS

The speed at V80 of 15.8 ± 1.3 km·h^{-1} was considerably faster than the low-speed condition of 12 ± 0.0 km·h^{-1} ($p < 0.001$, 95% CI 2.45–5.24, $d = 2.89$).

Spatiotemporal Parameters

Table 1 shows the changes in spatiotemporal parameters for the two different speeds and three different slopes. GCT was shorter at V80 compared with 12 km·h^{-1} throughout, independent of slope, as shown by the large effect size (**Table 1**). There was an interaction effect for speed and slope ($p = 0.003$; **Table 1**), while slope did not affect GCT ($p = 0.714$; **Table 1**). SL increased due to the faster running speed ($p = 0.003$) (large η^2_G: large) (**Table 1**) and further increased with a steeper slope, from −5° to −10° ($p = 0.047$), at V80 (η^2_G: medium) (**Table 1**). There was an overall decrease in SF for both running speeds when the steepness of the slope increased from 0° to −10° ($p = 0.002$) (η^2_G: medium) (**Table 1**).

Hip and Knee Angles

Table 2 displays the hip and knee angles for the speed and slope conditions studied. During stance, maximal hip flexion and extension increased at V80 compared to 12 km·h^{-1} regardless of the slope ($p = 0.007$) (both η^2_G: medium) (**Table 2**). Maximal

TABLE 2 | Hip and knee angles on level and downhill running ($n = 6$).

	0°	−5°	−10°	*F*-values, *P*-values, and effect size (η^2_G)
Hip max (°)				
12 km·h^{-1}	24.2 ± 3.2	24.7 ± 4.9	22.0 ± 3.7	[a]$F_{(1,5)} = 19.5$, $p = 0.007$, $\eta^2_G = 0.168$
80% of VO_{2max}	26.7 ± 4.2*	27.1 ± 3.5*	27.2 ± 4.5*	[b]$F_{(2,10)} = 1.3$, $p = 0.309$, $\eta^2_G = 0.021$
				[c]$F_{(2,10)} = 1.5$, $p = 0.261$, $\eta^2_G = 0.029$
Hip min (°)				
12 km·h^{-1}	−18.9 ± 3.9	−19.6 ± 4.7	−19.6 ± 5.2	[a]$F_{(1,5)} = 11.6$, $p = 0.019$, $\eta^2_G = 0.147$
80% of VO_{2max}	−23.1 ± 2.9*	−22.0 ± 4.3*	−23.4 ± 5.9*	[b]$F_{(2,10)} = 0.2$, $p = 0.821$, $\eta^2_G = 0.005$
				[c]$F_{(2,10)} = 1.5$, $p = 0.269$, $\eta^2_G = 0.008$
Knee max (°)				
12 km·h^{-1}	50.3 ± 3.9	50.9 ± 4.5	53.5 ± 3.6†#	[a]$F_{(1,5)} = 2.3$, $p = 0.193$, $\eta^2_G = 0.007$
80% of VO_{2max}	51.5 ± 4.0	51.5 ± 4.4	53.5 ± 3.3†#	[b]$F_{(2,10)} = 12.0$, $p = 0.002$, $\eta^2_G = 0.090$
				[c]$F_{(2,10)} = 2.8$, $p = 0.111$, $\eta^2_G = 0.005$
Knee TD (°)				
12 km·h^{-1}	20.6 ± 3.8	16.7 ± 4.2†	15.4 ± 5.7†	[a]$F_{(1,5)} = 0.3$, $p = 0.632$, $\eta^2_G = 0.003$
80% of VO_{2max}	21.6 ± 4.2	16.5 ± 3.4†	13.4 ± 4.2†	[b]$F_{(2,10)} = 34.0$, $p < 0.001$, $\eta^2_G = 0.334$
				[c]$F_{(2,10)} = 3.4$, $p = 0.077$, $\eta^2_G = 0.026$

The values are presented as means ± SD. Hip max, maximum hip flexion; HIP min, maximum hip extension; Knee max, maximum knee flexion; Knee TD, knee flexion at touchdown. A factorial ANOVA for repeated measurement was used to compare the speed and slope with a Bonferroni post-hoc test.

[a]*Factorial ANOVA for repeated measurement of speed (2).*

[b]*Factorial ANOVA for repeated measurement of slope (3).*

[C]*Interaction effect between speed and slope (2 × 3).*

[*]*Statistically different from 12 km·h^{-1}.*

[†]*Statistically different from 0°.*

[#]*Statistically different from −5°.*

knee flexion during stance was greater at a −10° slope compared with both 0° ($p = 0.004$) and −5° ($p = 0.008$) (both η^2_G: medium) (**Table 2**). There was a small but non-significant interaction effect for speed and slope on knee flexion at touchdown ($p = 0.077$) (η^2_G: small) (**Table 2**). Knee flexion at touchdown decreased with increases in the steepness of the decline slope ($p < 0.001$) (η^2_G: large) (**Table 2**).

Cardiorespiratory Parameters

Relative VO_2 (mL·kg^{-1}·min^{-1}) increased at faster speeds [$F_{(1,5)} = 27.8$, $p = 0.003$, $\eta^2_G = 0.637$: large] but decreased during running on steeper downhill slopes [$F_{(2,10)} = 87.9$, $p < 0.001$, $\eta^2_G = 0.761$: large; **Figure 2A**]. There was a medium interaction effect for speed and slope [$F_{(2,10)} = 7.9$, $p = 0.009$, $\eta^2_G = 0.167$: medium] that is explained by the higher relative VO_2 at V80 compared with 12 km·h^{-1} at slopes of 0° and −10°, but not at −5° (**Figure 2A**). Absolute VO_2 (L·min^{-1}) was greater at V80 than 12 km·h^{-1} [$F_{(1,5)} = 24.4$, $p = 0.004$, $\eta^2_G = 0.367$: large] but decreased with a change in slope of 0° to −5° [$F_{(2,10} = 61.6$, $p < 0.001$, $\eta^2_G = 0.506$: large]. However, absolute VO_2 did not decrease further between −5° and −10° slopes ($p = 0.123$). There was a small interaction effect for speed and slope that is explained by the higher absolute VO_2 at V80 compared with 12 km·h^{-1} on a slope of 0° and −10° but not −5° [$F_{(2,10)} = 8.8$, $p = 0.006$, $\eta^2_G = 0.063$: small]. Energy cost of running (J·kg^{-1}·m^{-1}) remained unchanged between the two speeds [$F_{(1,5)} = 0.9$, $p = 0.379$, $\eta^2_G = 0.023$: small] but improved with a steeper downhill slope [$F_{(2,10)} = 90.1$, $p < 0.001$, $\eta^2_G = 0.826$: large; **Figure 2B**]. Energy cost of running showed no interaction effect for speed × slope [$F_{(2,10)} = 3.5$, $p = 0.071$, $\eta^2_G = 0.096$: small; **Figure 2B**].

DISCUSSION

The main finding of the study is a shift in the energy cost of running, not only due to changes in downhill slope but speed as well. This shift seems to imply that energy savings at steep declines as compared to level running are greater at 12 km·h^{-1} than at a speed equivalent to 80% of the runner's VO_{2max} (V80). This supports hypothesis (a).

Minetti et al. (2002) derived a fifth-order polynomial relationship between energy cost of running and gradient, showing that the downhill gradient of minimal energy cost is close to −20% (equal to a slope angle of −11.3°). However, the energy cost of running in that study was measured at slower speeds than are typical in races (∼10–11 km·h^{-1} in the gradient range 0 to −20%) and the polynomial relationship does not account for differences in speed. Moreover, their study investigates neither the effect of speed nor the interaction effect of gradient and speed on energy cost. Although we did not find any significant interaction effect of slope and speed on energy cost of running, the results do show an interaction effect for slope and speed on relative VO_2. On a moderate downhill slope of −5°, the energy cost of running was higher at 12 km·h^{-1} than at V80. On the steeper downhill slope of −10°, the relationship was reversed, and the energy cost of running was higher at V80 compared with 12 km·h^{-1}. Although this was not significant, it indicates that speed, not just slope, may alter the energy cost of downhill

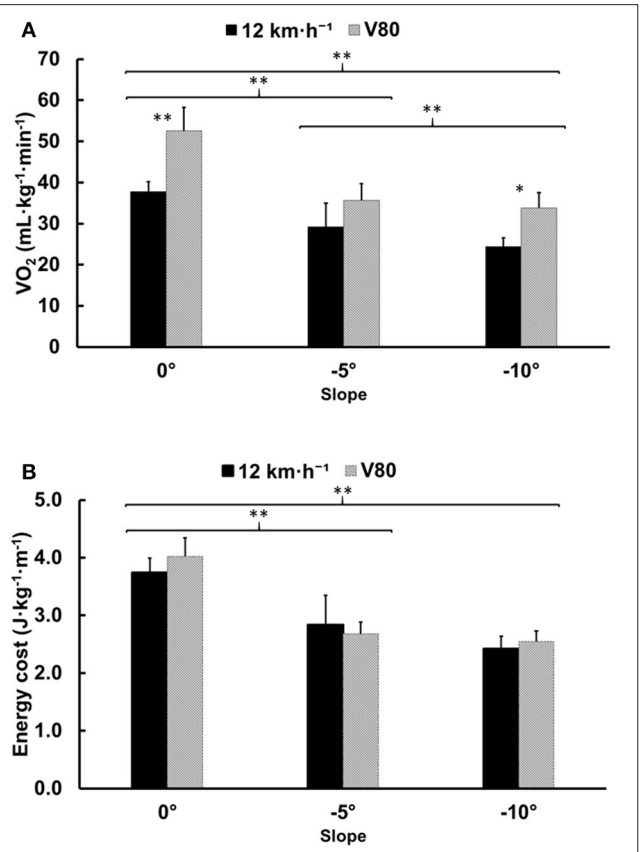

FIGURE 2 | (A) Relative oxygen uptake (mL·kg^{-1}·min^{-1}) for 0°, −5°, and −10° slopes. **(B)** Energy cost of running for 0°, −5°, and −10° slopes expressed as joules relative to body mass per meter (J·kg^{-1}·m^{-1}). Running speeds of 12 km·h^{-1} and 80% of VO_{2max} are illustrated using black and gray bars, respectively. Brackets illustrate the differences between slopes, while * or ** above the bars indicate differences between speeds (*$p < 0.05$ and **$p < 0.01$). The values given are mean ± SD.

running, especially on steep slopes. The current experimental evidence suggest that minimal energy cost occurs with flatter slopes as individuals run at faster speeds.

Gottschall and Kram (2005) found that the parallel breaking force impulse increases linearly with steeper decline gradients, while the parallel propulsive force impulse decreased exponentially at an ever-decreasing rate in relation to the downhill gradient. According to Gottschall and Kram (2005), this may be why running becomes more metabolically costly beyond a −20% gradient. In accordance with this, Vernillo et al. (2020) found higher propulsive force impulse and higher step frequency at 4.17 m·s^{-1} than at 2.50 and 3.33 m·s^{-1} on a −10° slope. Another possible explanation is less pronounced elastic energy storage and release in downhill running compared with level (Snyder et al., 2012). At faster speeds, due to insufficient muscle contraction velocity, the parallel braking impulse may increase and thus require an increased parallel propulsive force impulse. Moreover, the greater propulsive force demanded requires muscle contractions of greater force. These high-force contractions recruit additional fast-twitch muscle fibers that are less energy efficient (Coyle et al., 1992). Both these mechanisms may explain the shift in downhill slope of minimal energy cost toward less-steep slopes. Furthermore, higher energy cost of running at high speed on steep descents may be explained by the greater range of motion in the knee observed in the present study, since this is known to be associated with higher knee power absorption during the stance phase (DeVita et al., 2008).

In accordance with Park et al. (2019), the present study showed that knee flexion increased with steeper downhill slope, and therefore, we accept hypothesis (b). Seki et al. (2020) showed similar results between level and downhill running for maximal hip extension (level: 167° ± 13 vs. downhill: 168° ± 13). Additionally, in accordance with Khassetarash et al. (2020), the present study displayed that hip angle range of motion increased with running speed, and therefore, hypothesis (c) is accepted. The increased hip angle range of motion at higher speeds is also associated with an increase in SL. SL at V80 further increased at a slope between −5° and −10°, which could, partly, be explained by the corresponding increase in knee angle extension at touchdown (20.6° ± 3.8 vs. 16.7° ± 4.2 vs. 15.4° ± 5.7). This running technique adaption, often called over striding, may also be responsible for the greater energy cost of running at high speeds on steep descents mentioned above. Over striding at high speeds on steep descents may also be a strategy to reduce work demand on the hip flexor and extensor muscles while managing speed and avoiding uncontrolled acceleration. Supporting this hypothesis, DeVita et al. (2008) found that the lever arm of the ground reaction force is greater in uphill running than in downhill, suggesting that downhill running does not exert more strain on the hip muscles than uphill running, despite the lower magnitude of ground reaction force in uphill running. This might be why Park et al. (2019) did not find increased joint power in the hip joint on downhill slopes.

The increased range of motion of the knee in steep downhill compared with level running, as observed in the present study, could be explained by the increased knee extension at touchdown. Increased range of motion in the knee and greater knee extension at touchdown (Buczek and Cavanagh, 1990: 24.6 ± 3 vs. 17.0 ± 4.2) on steeper downhill slopes are both consistent with previous findings on downhill running (Buczek and Cavanagh, 1990; Mizrahi et al., 2001). Furthermore, Vernillo et al. (2020) found a slope × speed interaction effect for peak ground reaction forces in the normal direction with the highest values at 4.17 m·s^{-1} and −10°, together with an increase in breaking impulse for the same slope–speed combination, which could be explained by over striding. However, we cannot analyze nor confirm those kinetic findings and the effect of over striding, because we did not measure ground reaction forces, in the present study.

Pacing strategy is an important consideration, especially in long-distance races. Given the tendency for higher energy costs in high-speed steep downhill running (V80, −10°) compared with slower speeds (12 km·h^{-1}, −10°), a wise strategy may be to reduce speed on steep downhill slopes to retain metabolic energy. This is in contrast with the common regime of pacing strategy in endurance sports that favors an even work rate and therefore high-speed descents and slow-speed ascents. Another argument in support of the slow-speed steep downhill running strategy is

the increased muscle damage caused by prolonged high-impact eccentric exercise, such as downhill running (Sargeant and Dolan, 1987). In the present study, GCT decreased at faster running speeds consistently across all slopes, but we found no effect of slope on GCT. Moreover, GCT at 12 km·h^{-1} was in line with previously reported GCT in outdoor downhill running (Björklund et al., 2019). In the literature, there are equivocal findings presented regarding the relationship between GCT and running economy (i.e., energy cost or oxygen cost of running). Several studies found no association between GCT and running economy (Heise and Martin, 2001; Kyröläinen et al., 2001; Støren et al., 2011), while some found that longer GCT correlates with better running economy (Di Michele and Merni, 2014), and others found that shorter GCT correlates with better running economy (Nummela et al., 2007; Santos-Concejero et al., 2014b).

The speed at 80% of VO_{2max} (V80) of 15.8 ± 1.3 km·h^{-1} is close to the most commonly used reference speed of 16 km·h^{-1} when assessing oxygen cost of running (Barnes and Kilding, 2015). The mean value of VO_2 at V80 in level running of 52.5 ml·kg^{-1} · min^{-1} is in line with the values reported for highly trained male runners (mean: 50.6, range: 40.5–66.8 ml·kg^{-1} · min^{-1}) (Conley and Krahenbuhl, 1980; Daniels and Daniels, 1992; Morgan et al., 1994; Saunders et al., 2004). Moreover, the mean value of VO_2 at 12 km·h^{-1} in level running of 37.7 ml·kg^{-1} · min^{-1} is in line with the values reported for moderately trained male runners (mean: 40.7, range: 37.4–48.1 mL·kg^{-1} · min^{-1}) (Johnson et al., 1997; Spurrs et al., 2003; Støren et al., 2008; Berryman et al., 2010; Mikkola et al., 2011).

Study limitations include the low number of participants ($n = 6$). Despite the low number of participants, the effects for the measured variables were estimated to be reasonably large according to the sample size calculation using a power of 0.8 with an alpha at 0.05. Nevertheless, the generalization of the study results should be related to runners that are used to run on trails and undulating terrain. The surface itself do pose a constraint on the applicability of the current study results in trail running. Therefore, future studies may investigate the validity of these indoor treadmill-running findings for in-field trail running on ever-changing surfaces. Furthermore, the steepest slope (−10°) might have not been steep enough to see the full effect of how speed influences the running economy at various slopes. However, according to previous studies using slower speeds, the slope used in the current study was estimated to be a turning point where the energy cost of running is minimal. The additional measurements of ground reaction forces in future studies could provide more insight into how joint moments are changing with respect to different speeds and slopes in treadmill running.

CONCLUSION

The results of this study show that runners modify their hip movement pattern in the sagittal plane during the stance phase with changes in speed, whereas they alter their knee movement pattern during the touchdown and stance phases with respect to the slope. Therefore, runners competing in hilly races may benefit from training programs that include running on race-specific slopes at race speed. We also observed that running economy was better at moderate speeds than near-race speed on steep downhill slopes (−10°), while the reverse was true on less-steep declines (−5°). This implies that pacing schemes for different race distances have to be taken into consideration during preparation, e.g., low-speed steep descents to retain metabolic energy in long-distance races.

DATA AVAILABILITY STATEMENT

The raw data supporting the conclusions of this article will be made available by the authors, without undue reservation.

ETHICS STATEMENT

The studies involving human participants were reviewed and approved by the regional ethical review board in Umeå, Sweden. The patients/participants provided their written informed consent to participate in this study.

AUTHOR CONTRIBUTIONS

DS and GB designed the study and performed the experiments. DS, GB, and MK performed the data analysis, interpreted the results, revised the manuscript, approved the final version, and agreed to be accountable for all aspects of the study. DS wrote the first draft. All authors contributed to the article and approved the submitted version.

FUNDING

This study was supported financially by the European Regional Development Fund of the European Union.

ACKNOWLEDGMENTS

We would like to thank Jonas Danvind, Anna Bjerkefors, and Johanna Rosén for performing kinematic measurements during the experimental protocol of the study. We also thank Juan Alonso for performing anthropometric measurements, Jonathan Frank for taking part in the data analysis, and Per Skoglund for mounting equipment in the laboratory; they are greatly appreciated. We would also like to thank all the runners for their enthusiastic contribution to the study.

REFERENCES

Anderson, T. (1996). Biomechanics and running economy. *Sports Med.* 22, 76–89. doi: 10.2165/00007256-199622020-00003

Bakeman, R. (2005). Recommended effect size statistics for repeated measures designs. *Behav. Res. Methods* 37, 379–384. doi: 10.3758/BF03192707

Barnes, K. R., and Kilding, A. E. (2015). Running economy: measurement, norms, and determining factors. *Sports Med. Open* 1:8. doi: 10.1186/s40798-015-0007-y

Berryman, N., Maurel, D. B., and Bosquet, L. (2010). Effect of plyometric vs. dynamic weight training on the energy cost of running. *J. Strength Cond. Res.* 24, 1818–1825. doi: 10.1519/JSC.0b013e3181 def1f5

Björklund, G., Swarén, M., Born, D. P., and Stöggl, T. (2019). Biomechanical adaptations and performance indicators in short trail running. *Front. Physiol.* 10:506. doi: 10.3389/fphys.2019.00506

Born, D. P., Stöggl, T., Swarén, M., and Björklund, G. (2017). Near-infrared spectroscopy: more accurate than heart rate for monitoring intensity in running in hilly terrain. *Int. J. Sports Physiol. Perform.* 12, 440–447. doi: 10.1123/ijspp.2016-0101

Buczek, F. L., and Cavanagh, P. R. (1990). Stance phase knee and ankle kinematics and kinetics during level and downhill running. *Med. Sci. Sports Exerc.* 22, 669–677. doi: 10.1249/00005768-199010000-00019

Cavanagh, P. R., and Kram, R. (1985). Mechanical and muscular factors affecting the efficiency of human movement. *Med. Sci. Sports Exerc.* 17, 326–331. doi: 10.1249/00005768-198506000-00005

Cavanagh, P. R., and Lafortune, M. A. (1980). Ground reaction forces in distance running. *J. Biomech.* 13, 397–406. doi: 10.1016/0021-9290(80)90033-0

Cavanagh, P. R., and Williams, K. R. (1982). The effect of stride length variation on oxygen uptake during distance running. *Med. Sci. Sports Exerc.* 14, 30–35. doi: 10.1249/00005768-198201000-00006

Conley, D. L., and Krahenbuhl, G. S. (1980). Running economy and distance running performance of highly trained athletes. *Med. Sci. Sports Exerc.* 12, 357–360. doi: 10.1249/00005768-198025000-00010

Coyle, E. F., Sidossis, L. S., Horowitz, J. F., and Beltz, J. D. (1992). Cycling efficiency is related to the percentage of type I muscle fibers. *Med. Sci. Sports Exerc.* 24, 782–788. doi: 10.1249/00005768-199207000-00008

Daniels, J., and Daniels, N. (1992). Running economy of elite male and elite female runners. *Med. Sci. Sports Exerc.* 24, 483–489. doi: 10.1249/00005768-199204000-00015

de Ruiter, C. J., Verdijk, P. W., Werker, W., Zuidema, M. J., and De Haan, A. (2014). Stride frequency in relation to oxygen consumption in experienced and novice runners. *Eur. J. Sport Sci.* 14, 251–258. doi: 10.1080/17461391.2013.783627

Delp, S. L., Anderson, F. C., Arnold, A. S., Loan, P., Habib, A., John, C. T., et al. (2007). OpenSim: open-source software to create and analyze dynamic simulations of movement. *IEEE Trans. Biomed. Eng.* 54, 1940–1950. doi: 10.1109/TBME.2007.901024

DeVita, P., Janshen, L., Rider, P., Solnik, S., and Hortobágyi, T. (2008). Muscle work is biased toward energy generation over dissipation in non-level running. *J. Biomech.* 41, 3354–3359. doi: 10.1016/j.jbiomech.2008.09.024

Di Michele, R., and Merni, F. (2014). The concurrent effects of strike pattern and ground-contact time on running economy. *J. Sci. Med. Sport* 17, 414–418. doi: 10.1016/j.jsams.2013.05.012

Fellin, R. E., Rose, W. C., Royer, T. D., and Davis, I. S. (2010). Comparison of methods for kinematic identification of footstrike and toe-off during overground and treadmill running. *J. Sports Sci. Med.* 13, 646–650. doi: 10.1016/j.jsams.2010.03.006

Fletcher, J. R., Esau, S. P., and Macintosh, B. R. (2009). Economy of running: beyond the measurement of oxygen uptake. *J. Appl. Physiol.* 107, 1918–1922. doi: 10.1152/japplphysiol.00307.2009

Gottschall, J. S., and Kram, R. (2005). Ground reaction forces during downhill and uphill running. *J. Biomech.* 38, 445–452. doi: 10.1016/j.jbiomech.2004.04.023

Handsaker, J. C., Forrester, S. E., Folland, J. P., Black, M. I., and Allen, S. J. (2016), A kinematic algorithm to identify gait events during running at different speeds and with different footstrike types. *J. Biomech.* 49, 4128–4133. doi: 10.1016/j.jbiomech.2016.10.013

Hasegawa, H., Yamauchi, T., and Kraemer, W. J. (2007). Foot strike patterns of runners at the 15-km point during an elite-level half marathon. *J. Strength Cond. Res.* 21, 888–893. doi: 10.1519/00124278-200708000-00040

Heise, G. D., and Martin, P. E. (2001). Are variations in running economy in humans associated with ground reaction force characteristics? *Eur. J. Appl. Physiol.* 84, 438–442. doi: 10.1007/s004210100394

Hunter, I., and Smith, G. A. (2007). Preferred and optimal stride frequency, stiffness and economy: changes with fatigue during a 1-h high-intensity run. *Eur. J. Appl. Physiol.* 100, 653–661. doi: 10.1007/s00421-007-0456-1

Johnson, R. E., Quinn, T. J., Kertzer, R., and Vroman, N. B. (1997). Strength training in female distance runners: impact on running economy. *J. Strength Condit. Res.* 11, 224–229. doi: 10.1519/00124278-199711000-00004

Joyner, M. J. (1991). Modeling: optimal marathon performance on the basis of physiological factors. *J. Appl. Physiol.* 70, 683–687. doi: 10.1152/jappl.1991.70.2.683

Joyner, M. J., and Coyle, E. F. (2008). Endurance exercise performance: the physiology of champions. *J. Physiol.* 586, 35–44. doi: 10.1113/jphysiol.2007.143834

Karamanidis, K., Arampatzis, A., and Brüggemann, G.-P. (2003). Symmetry and reproducibility of kinematic parameters during various running techniques. *Med. Sci. Sports Exerc.* 35, 1009–1016. doi: 10.1249/01.MSS.0000069337.49567.F0

Kasmer, M. E., Liu, X. C., Roberts, K. G., and Valadao, J. M. (2013). Foot-strike pattern and performance in a marathon. *Int. J. Sports Physiol. Perform.* 8, 286–292. doi: 10.1123/ijspp.8.3.286

Kay, A. (2014). Importance of descending skill for performance in fell races: a statistical analysis of race results. *J. Quant. Anal. Sports* 10, 173–181. doi: 10.1515/jqas-2013-0075

Khassetarash, A., Vernillo, G., Martinez, A., Baggaley, M., Giandolini, M., Horvais, N., et al. (2020). Biomechanics of graded running: part II-Joint kinematics and kinetics. *Scand. J. Med. Sci. Sports* 30, 1642–1654. doi: 10.1111/sms.13735

Kyröläinen, H., Belli, A., and Komi, P. V. (2001). Biomechanical factors affecting running economy. *Med. Sci. Sports Exerc.* 33, 1330–1337. doi: 10.1097/00005768-200108000-00014

Lieberman, D. E., Warrener, A. G., Wang, J., and Castillo, E. R. (2015). Effects of stride frequency and foot position at landing on braking force, hip torque, impact peak force and the metabolic cost of running in humans. *J. Exp. Biol.* 218, 3406–3414. doi: 10.1242/jeb.125500

Mikkola, J., Vesterinen, V., Taipale, R., Capostagno, B., Häkkinen, K., and Nummela, A. (2011). Effect of resistance training regimens on treadmill running and neuromuscular performance in recreational endurance runners. *J. Sports Sci.* 29, 1359–1371. doi: 10.1080/02640414.2011.589467

Minetti, A. E., Moia, C., Roi, G. S., Susta, D., and Ferretti, G. (2002). Energy cost of walking and running at extreme uphill and downhill slopes. *J. Appl. Physiol.* 93, 1039–1046. doi: 10.1152/japplphysiol.01177.2001

Mizrahi, J., Verbitsky, O., and Isakov, E. (2001). Fatigue-induced changes in decline running. *Clin. Biomech.* 16, 207–212. doi: 10.1016/S0268-0033(00)00091-7

Moore, I. S. (2016). Is there an economical running technique? A review of modifiable biomechanical factors affecting running economy. *Sports Med.* 46, 793–807. doi: 10.1007/s40279-016-0474-4

Morgan, D. W., Craib, M. W., Krahenbuhl, G. S., Woodall, K., Jordan, S., Filarski, K., et al. (1994). Daily variability in running economy among well-trained male and female distance runners. *Res. Q. Exerc. Sport* 65, 72–77. doi: 10.1080/02701367.1994.10762210

Nummela, A., Keränen, T., and Mikkelsson, L. O. (2007). Factors related to top running speed and economy. *Int. J. Sports Med.* 28, 655–661. doi: 10.1055/s-2007-964896

Park, S.-K., Jeon, H.-M., Lam, W.-K., Stefanyshyn, D., and Ryu, J. (2019). The effects of downhill slope on kinematics and kinetics of the lower extremity joints during running. *Gait Posture* 68, 181–186. doi: 10.1016/j.gaitpost.2018.11.007

Santos-Concejero, J., Tam, N., Coetzee, D. R., Oliván, J., Noakes, T. D., and Tucker, R. (2017). Are gait characteristics and ground reaction forces related to energy cost of running in elite Kenyan runners? *J. Sports Sci.* 35, 531–538. doi: 10.1080/02640414.2016.1175655

Santos-Concejero, J., Tam, N., Granados, C., Irazusta, J., Bidaurrazaga-Letona, I., Zabala-Lili, J., et al. (2014a). Interaction effects of stride angle and strike pattern on running economy. *Int. J. Sports Med.* 35, 1118–1123. doi: 10.1055/s-0034-1372640

Santos-Concejero, J., Tam, N., Granados, C., Irazusta, J., Bidaurrazaga-Letona, I., Zabala-Lili, J., et al. (2014b). Stride angle as a novel indicator of running economy in well-trained runners. *J. Strength Cond. Res.* 28, 1889–1895. doi: 10.1519/JSC.0000000000000325

Sargeant, A. J., and Dolan, P. (1987). Human muscle function following prolonged eccentric exercise. *Eur. J. Appl. Physiol. Occup. Physiol.* 56, 704–711. doi: 10.1007/BF00424814

Saunders, P. U., Pyne, D. B., Telford, R. D., and Hawley, J. A. (2004). Reliability and variability of running economy in elite distance runners. *Med. Sci. Sports Exerc.* 36, 1972–1976. doi: 10.1249/01.MSS.0000145468.17329.9F

Seki, K., Kyrolainen, H., Sugimoto, K., and Enomoto, Y. (2020). Biomechanical factors affecting energy cost during running utilising different slopes. *J. Sports Sci.* 38, 6–12. doi: 10.1080/02640414.2019.1676527

Seth, A., Hicks, J. L., Uchida, T. K., Habib, A., Dembia, C. L., Dunne, J. J., et al. (2018). OpenSim: Simulating musculoskeletal dynamics and neuromuscular control to study human and animal movement. *PLoS Comput. Biol*. 14:e1006223. doi: 10.1371/journal.pcbi.1006223

Shaw, A. J., Ingham, S. A., and Folland, J. P. (2014). The valid measurement of running economy in runners. *Med. Sci. Sports Exerc*. 46, 1968–1973. doi: 10.1249/MSS.0000000000000311

Snyder, K. L., Kram, R., and Gottschall, J. S. (2012). The role of elastic energy storage and recovery in downhill and uphill running. *J. Exp. Biol.* 215, 2283–2287. doi: 10.1242/jeb.066332

Spurrs, R. W., Murphy, A. J., and Watsford, M. L. (2003). The effect of plyometric training on distance running performance. *Eur. J. Appl. Physiol.* 89, 1–7. doi: 10.1007/s00421-002-0741-y

Staab, J. S., Agnew, J. W., and Siconolfi, S. F. (1992). Metabolic and performance responses to uphill and downhill running in distance runners. *Med. Sci. Sports Exerc.* 24, 124–127. doi: 10.1249/00005768-199201000-00020

Støren, Ø., Helgerud, J., and Hoff, J. (2011). Running stride peak forces inversely determine running economy in elite runners. *J. Strength Cond. Res.* 25, 117–123. doi: 10.1519/JSC.0b013e3181b62c8a

Støren, O., Helgerud, J., Støa, E. M., and Hoff, J. (2008). Maximal strength training improves running economy in distance runners. *Med. Sci. Sports Exerc.* 40, 1087–1092. doi: 10.1249/MSS.0b013e318168da2f

Tartaruga, M. P., Brisswalter, J., Peyré-Tartaruga, L. A., Ávila, A. O. V., Alberton, C. L., Coertjens, M., et al. (2012). The relationship between running economy and biomechanical variables in distance runners. *Res. Q. Exerc. Sport* 83, 367–375. doi: 10.1080/02701367.2012.10599870

Townshend, A. D., Worringham, C. J., and Stewart, I. B. (2010). Spontaneous pacing during overground hill running. *Med. Sci. Sports Exerc.* 42, 160–169. doi: 10.1249/MSS.0b013e3181af21e2

Vernillo, G., Martinez, A., Baggaley, M., Khassetarash, A., Giandolini, M., Horvais, N., et al. (2020). Biomechanics of graded running: part I - stride parameters, external forces, muscle activations. *Scand. J. Med. Sci. Sports* 30, 1632–1641. doi: 10.1111/sms.13708

Weir, J. B. (1949). New methods for calculating metabolic rate with special reference to protein metabolism. *J. Physiol.* 109, 1–9. doi: 10.1113/jphysiol.1949.sp004363

Conflict of Interest: The authors declare that the research was conducted in the absence of any commercial or financial relationships that could be construed as a potential conflict of interest.

frontiers in Sports and Active Living

BRIEF RESEARCH REPORT
published: 08 July 2021
doi: 10.3389/fspor.2021.704308

Biomechanics of World-Class Men and Women Hurdlers

Brian Hanley[1]*, *Josh Walker*[1], *Giorgos P. Paradisis*[2], *Stéphane Merlino*[3] and *Athanassios Bissas*[1,4,5]

[1] Carnegie School of Sport, Leeds Beckett University, Leeds, United Kingdom, [2] Athletics Sector, School of Physical Education and Sport Science, National and Kapodistrian University of Athens, Athens, Greece, [3] International Relations and Development Department, World Athletics, Monte Carlo, Monaco, [4] Athletics Biomechanics, Leeds, United Kingdom, [5] School of Sport and Exercise, University of Gloucestershire, Gloucester, United Kingdom

The sprint hurdle events require athletes to cross ten hurdles between the start and finish line. The height of the hurdles, and the distances between them, differ for men and women, possibly resulting in technical differences. The aim of this study was to provide a kinematic comparison of in-competition hurdle technique for world-class men and women hurdlers. Video data were collected for the 16 finalists in the 100 m and 110 m hurdles events at the 2017 IAAF World Championships using four high-speed cameras (150 Hz), focusing on the sixth hurdle for the men and fifth for the women. Center of mass (CM) position, joint angles, step lengths and clearance times were compared between sexes at key events before, during and after hurdle clearance. The hurdle height was ∼7% higher for men when calculated as a proportion of stature ($p < 0.001$). This discrepancy in relative hurdle height provided women with a kinematic and mechanical advantage over men as they took off farther from the hurdle (relative to hurdle height) ($p < 0.001$), leading to a lower and more efficient flight parabola. Women were also able to maintain longer relative step lengths after hurdle clearance and showed minimal vertical oscillation of the CM in the stance phases before and after the hurdle compared with men. The lower relative hurdle heights in the women's event provide a less demanding task, and thus these findings present preliminary evidence to those coaches who advocate revising the women's hurdle heights in competition.

Keywords: coaching, elite-standard athletes, kinematics, speed, track and field

OPEN ACCESS

Edited by:
Ryu Nagahara, National Institute of Fitness and Sports in Kanoya, Japan

Reviewed by:
Roland Van Den Tillaar, Nord University, Norway
Jasper Verheul, University of Birmingham, United Kingdom

***Correspondence:**
Brian Hanley
b.hanley@leedsbeckett.ac.uk

Specialty section:
This article was submitted to Elite Sports and Performance Enhancement, a section of the journal Frontiers in Sports and Active Living

Received: *02 May 2021*
Accepted: *15 June 2021*
Published: *08 July 2021*

Citation:
Hanley B, Walker J, Paradisis GP, Merlino S and Bissas A (2021) Biomechanics of World-Class Men and Women Hurdlers. Front. Sports Act. Living 3:704308. doi: 10.3389/fspor.2021.704308

INTRODUCTION

The hurdle events are part of the track and field athletics program at the Olympic Games and all other outdoor major championships. The athletes must cross ten obstacles at set distances, making the event highly technical as the hurdlers try to minimize contact with each barrier while maintaining forward velocity. The sprint hurdle races are held over 100 m for women and 110 m for men, where the women's hurdles are 0.838 m (2'9") high and the men's hurdles are 1.067 m (3'6") high. The distance between hurdles in the women's race is 8.50 m, with a 13.00 m approach run and a 10.50 m run-out to the finish; in the men's race the distance between hurdles is 9.14 m, with a 13.72 m approach run and a 14.02 m run-out (World Athletics, 2019). The closeness of the first hurdle to the start line results in a different start technique from that used by sprinters (Bezodis et al., 2019) and, although it is the fastest athlete over the total race distance who wins, the height and distance between the hurdles has a profound effect on the running speeds achieved,

with hurdlers not reaching peak speeds until the run-out (Graubner and Nixdorf, 2011). This restriction on speed is not only apparent when crossing the hurdle itself but when recovering speed after clearing it, and in preparing for the next hurdle (McDonald and Dapena, 1991). An analysis of the steps taken after landing from the hurdle clearance would therefore assist coaches to develop a better understanding of the interaction between hurdle clearance and its effect on subsequent steps.

After landing from the hurdle step, athletes take three steps between the hurdles, which comprise the landing, recovery and preparatory steps (McDonald and Dapena, 1991; González-Frutos et al., 2019) (**Figure 1**). Given that these steps' lengths are limited, coaches have recommended approximate lengths for these distances (and the hurdle step) so that athletes maintain forward velocity. For example, in his "model technique" for the men's 110 m hurdles, Tidow (1991) advocated a hurdle step length of ∼3.50 m for men, consisting of 2.10–2.20 m before the hurdle and 1.30–1.40 m after it. The ratio used is therefore approximately 60:40 (Čoh et al., 2020), and Salo et al. (1997) similarly recommended a long take-off distance as it allows for a lower flight parabola and better maintenance of horizontal velocity. Because velocity cannot be recovered until ground contact, Salo et al. (1997) stated that the relatively short landing distance after the hurdle helps the athlete to bring the lead leg (the first leg over the hurdle) down more rapidly, which could affect the joint angles at the knee and ankle. This landing component of hurdle step technique is important to develop correctly (Čoh, 2003) as the hurdler must avoid the large horizontal braking impulses that accrue from the foot landing too far in front of the whole body center of mass (CM) (McLean, 1994). Regarding step lengths between the women's hurdles, Hücklekemkes (1990) suggested distances of 1.65, 1.95 and 1.85 m for the landing, recovery and preparatory steps, respectively, based on coaching expertise. In an analysis of hurdlers using three-dimensional (3D) videography (50 Hz), McDonald and Dapena (1991) found that the absolute landing and recovery step lengths differed little between national-standard men and women (by 0.03 and 0.08 m, respectively), but whether these similar values are found in world-class athletes has not been studied. Furthermore, a 3D study using a higher sampling rate would allow for greater precision in identifying specific events such as take-off and touchdown, which can give a more accurate assessment of kinematic and spatiotemporal aspects of hurdling performance, such as step lengths and clearance time. Given that much of the previous recommendations on hurdling have been based on coaches' observations, small sample sizes, or non-elite athletes, a novel analysis of World Championship finalists will provide robust evidence regarding spatiotemporal and kinematic recommendations for elite-standard men's and women's hurdling.

Although coaches have suggested approximate step measurements for athletes to take (e.g., Hücklekemkes, 1990), the length of any steps can depend greatly on athlete stature and thus their step length. Being taller can help clear the hurdle but also hinder a naturally long step length in the three steps between hurdles. It is noteworthy that although the men's hurdle is 27% higher than the women's, the distance between hurdles is only 8% longer for men, and previous case study research has suggested that crossing the barriers is less disruptive to horizontal velocity in the women's event (Čoh, 2003; Čoh et al., 2019). Indeed, coaching literature has previously suggested that, because the men's hurdle is much higher as a proportion of their mean stature, the women's hurdles are too low for modern athletes (Etcheverry, 1993; Stein, 2000); however, there is nonetheless coaching evidence from individual athletes that better hurdling technique (seen in faster clearance times) can differentiate race performance in world-class women hurdlers (Bedini, 2016). Given the differences between men's and women's hurdling in terms of hurdle heights and positioning, a novel study on world-class athletes analyzed in the ecological setting of a major championship final will aid coaches' understanding of key elements of sprint hurdling and any sex-based differences that should be considered in practical terms, including whether there should be an increase in women' hurdle height. The aim of this observational study was to analyze spatiotemporal factors, comprising CM position before, over and after the hurdle, clearance times, step lengths and knee and ankle joint angles, in world-class men's and women's hurdling.

MATERIALS AND METHODS

Research Approval

Data were collected as part of the London 2017 World Championships Biomechanics Research Project (Pollitt et al., 2018a,b). The use of those data for this study was approved by the IAAF (since renamed World Athletics), who own and control the data, and locally the study was reviewed and approved by Carnegie School of Sport Research Ethics Committee. The participants provided their written informed consent to participate in this study. The study was conducted in accordance with the recognized ethical standards of the Declaration of Helsinki.

Participants

The eight finalists from the men's 110 m hurdles (age: 27 ± 3; stature: 1.87 ± 0.05 m) and the eight finalists from the women's 100 m hurdles (age: 27 ± 3; stature: 1.68 ± 0.04 m) were analyzed in this study. Athletes' dates of birth and finishing times were obtained from the open-access World Athletics website (World Athletics, 2021) for competitors in both races, whereas their statures were obtained from Matthews (2017).

Data Collection

All data were collected using four Sony PXW-FS7 high-speed cameras (150 Hz; shutter speed: 1/1250 s; ISO: 2000-4000; FHD: 1920 × 1080 px). Cameras were stationary and positioned along the home straight to focus on the sixth and fifth hurdle for the men's and women's event, respectively. These hurdles were analyzed because the allocated camera positions necessitated the analysis of the mid-section of the track (a hurdle position with 50.58 m and 53.00 m remaining for men and women, respectively). A calibration procedure was carried out before and after each event using a rigid cuboid calibration frame (3.044 m^3) that comprised 24 control points. The frame was

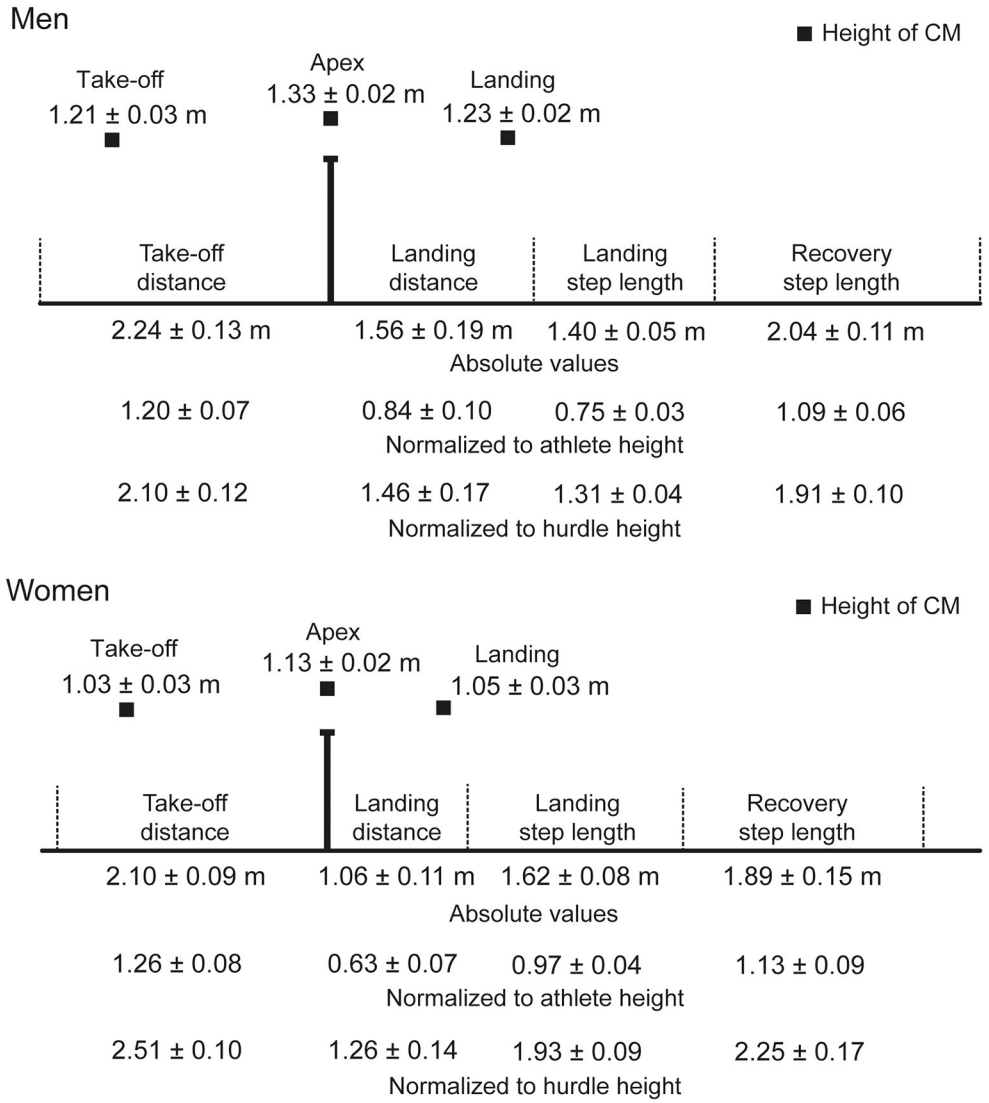

FIGURE 1 | Visual representation of the take-off and landing distances, landing and recovery step lengths, and the height of the CM at take-off and landing. The barrier is shown as the athletes would approach it running from left to right. The diagram is approximately to scale, with separate diagrams for men and women. The mean values (± SD) are shown as absolute values and, for the distances, as normalized to athlete and hurdle height.

positioned in six specific, predefined locations along and across the track to ensure an accurate definition of a volume covering the area around the hurdle for all eight lanes. This approach produced a large number of non-coplanar control points per calibrated volume and facilitated the construction of bi-lane local coordinate systems, which were then combined into a global coordinate system.

Data Analysis

The collected video files were imported into SIMI Motion (version 9.2.2, Simi Reality Motion Systems GmbH, Germany) and manually digitized by a single experienced operator to obtain whole-body spatiotemporal and kinematic data. An event synchronization technique (synchronization of four critical instants: take-off foot initial contact, take-off foot toe-off, landing foot initial contact and landing foot toe-off) was applied to synchronize the two-dimensional coordinates from each camera. Each file was first digitized frame-by-frame and, upon completion, adjustments were made using the points-over-frame method (Bahamonde and Stevens, 2006). The digitizing process was centered upon critical events (e.g., touchdown, take-off), and identified 17 key anatomical locations (head, shoulder, elbow, wrist, metacarpophalangeal, hip, knee, ankle, and metatarsophalangeal joint centers). The reliability of the digitizing process conducted has been documented previously (Bezodis et al., 2019). The Direct Linear Transformation (DLT) algorithm (Abdel-Aziz et al., 2015) was used to reconstruct the 3D coordinates of each anatomical location from individual

camera's x- and y-image coordinates. de Leva's (1996) body segment parameter models were used to obtain data for the CM.

Several spatiotemporal and kinematic variables were obtained from the digitized files. Before the hurdle, take-off distance was defined as the horizontal distance from the metatarsophalangeal joint (representing the part of the foot nearest the ground) at take-off to the base of the hurdle. Distance and height of the CM were defined as the horizontal and vertical positions of the CM relative to the metatarsophalangeal joint, respectively, for touchdown and take-off before and after the hurdle clearance. After hurdle clearance, landing distance was defined as the horizontal distance from the metatarsophalangeal joint to the hurdle. Landing step length was defined as the horizontal distance covered (from touchdown to contralateral touchdown) by the first step after hurdle clearance, and recovery step length was similarly defined for the following step. These variables were computed as absolute values, relative to each athlete's stature and to the height of the hurdle. The knee angle was a sagittal plane angle defined by the three points of the hip, knee and ankle joint centers. The ankle joint was a sagittal plane angle defined by the three points of the knee, ankle and metatarsophalangeal joint centers.

Statistics

Results are reported as individual values or as means ± one standard deviation (SD). All statistical analyses were carried out using SPSS Statistics 26 (IBM SPSS, Inc., Chicago, IL). Independent samples *t*-tests were used to compare differences between men and women athletes for all variables; significance was set at $p < 0.05$ (Field, 2009). Additionally, Cohen's *d* (Cohen, 1988) was used as an effect size to determine the magnitude of the differences between groups with interpretation thresholds of 0.2 (small), 0.5 (medium), 0.8 (large), 1.2 (very large), and 2.0 (huge).

RESULTS

The mean finishing time in the men's race was 13.27 s (± 0.12), whereas it was 12.76 s (± 0.14) in the women's race. The men were taller than the women ($p < 0.001$, $d = 3.95$), and the barrier height for men was greater when normalized to stature (57.1 ± 1.6%) than the women's hurdle height was for them (49.9% ± 1.3) ($p < 0.001$, $d = 4.89$). Mean hurdle step length was 3.80 m (± 0.13) in the men's race and 3.16 m (± 0.11) in the women's event. The clearance time for men (0.33 ± 0.02 s) was longer than for women (0.28 ± 0.02 s) ($p < 0.001$, $d = 3.00$). In the men's event, the take-off distance was ∼59% of total hurdle step length, whereas for women it was 66% (**Figure 1**). In absolute terms, the men's take-off distance was longer by 0.14 m ($p = 0.032$, $d = 1.19$), but the women's take-off distance was longer when normalized for hurdle height ($p < 0.001$, $d = 3.64$). The height of the CM at take-off was higher in men both in absolute terms ($p < 0.001$, $d = 5.92$) (**Figure 2**) and normalized to stature (men: 0.65 ± 0.01; women: 0.61 ± 0.01; $p < 0.001$, $d = 2.81$) (**Figure 3**), but was higher in women when normalized to hurdle height (men: 1.13 ± 0.03; women: 1.23 ± 0.03; $p < 0.001$, $d = 3.18$) (**Figure 4**). The height of the CM increased in men by 0.16 m (± 0.03) from touchdown to toe-off during the stance phase before the hurdle, and in women by 0.12 m (± 0.01) (**Figure 2**). Men's clearance heights (flight parabola apex) were higher by 0.20 m ($p < 0.001$, $d = 11.26$) (**Figure 1**), which was also higher normalized to stature (men: 0.71 ± 0.02; women: 0.67 ± 0.02; $p = 0.001$, $d = 2.08$), but lower relative to hurdle height (men: 1.25 ± 0.01; women: 1.35 ± 0.02; $p < 0.001$, $d = 4.94$).

Men's landing distances after clearing the hurdle were longer than women's as absolute values and when normalized to stature and hurdle height (**Figure 1**) (all $p \leq 0.022$, $d \geq 1.31$). The height of the CM was higher in men at touchdown by 0.18 m (**Figure 2**) ($p < 0.001$, $d = 7.14$), which was also higher than in women when normalized to stature (men: 0.66 ± 0.02; women: 0.62 ± 0.02; $p = 0.004$, $d = 2.00$) (**Figure 3**) but lower when normalized to hurdle height (men: 1.15 ± 0.02; women: 1.25 ± 0.03; $p < 0.001$, $d = 3.60$) (**Figure 4**). The height of the CM decreased from touchdown to toe-off during the landing contact phase in men by 0.09 m (± 0.01) and in women by 0.05 m (± 0.02) (**Figure 2**). The knee angle at touchdown was 166° (± 10) in men, greater than that found in women (156° ± 9) ($p = 0.037$, $d = 1.15$); there was no difference in ankle angle (men: 130° ± 11; women: 126° ± 7).

The landing step was the only step longer in women when expressed in absolute values ($p < 0.001$, $d = 3.51$) (**Figure 1**). Men had longer recovery steps in absolute values ($p = 0.032$, $d = 1.19$) but these were longer in women when normalized to hurdle height ($p < 0.001$, $d = 2.41$), but not stature. Although not directly measured, knowing the set distance between hurdles and these other step lengths indicate that the men's preparatory step length was approximately 1.90 m, whereas the women's was 1.83 m.

DISCUSSION

The aim of this observational study was to analyze spatiotemporal factors, comprising CM position before, over and after the hurdle, clearance times, step lengths and knee and ankle joint angles, in world-class men's and women's hurdling. Amongst the finalists in the 2017 World Championships, the men's hurdle height corresponded to 57.1% of their mean stature, whereas the women's hurdle corresponded to only 49.9% of theirs. As a result, spatiotemporal aspects of the hurdle step were different between men and women, even when taking stature into account. This included the height of the CM during the stance phase during both the preparation for take-off before the hurdle, its flight apex, and when landing after it. When normalized to hurdle height, men's CMs travel closer to the top of the hurdle whereas women are relatively higher, meaning that women have a larger margin for error during clearance. Indeed, women deliberately trying to cross the hurdle lower could require more effort and loss of speed. By contrast, men adopt a technique that minimizes their already high parabola. For example, the men had higher CM positions relative to stature at both initial contact and toe-off before and after clearance, meaning that women do not need to raise their CM as much to clear the hurdle, and the easier maintenance of horizontal speed allows women to have relatively longer step lengths during both landing and recovery steps. This difference becomes more apparent when

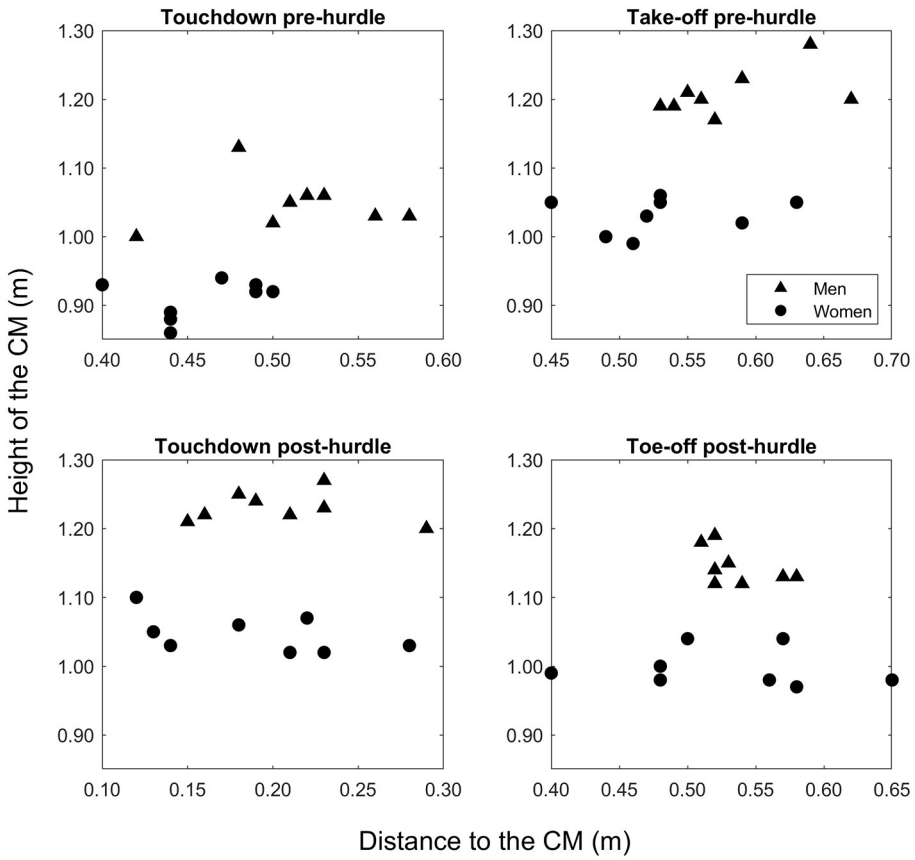

FIGURE 2 | Absolute values for the height of the CM for each man and woman at touchdown and toe-off in the stance phases pre- and post-hurdle.

comparing the CM heights expressed relative to hurdle height, where women's CM values are much higher than the hurdle height compared with men. The ratio of take-off to landing distance during the hurdle step for men was 59:41, practically identical to what was recommended by Tidow (1991), whereas for women it was 66:34. Given that longer take-off distances allow for lower flight parabolas and better maintenance of horizontal velocity (Salo et al., 1997), it is clear that a lower relative hurdle height means that women require less effort to project the body upward and maintaining velocity is less disrupted (Čoh, 2003; Čoh et al., 2019), resulting in an overall less demanding task with more horizontal running and less demand for applying ground reaction forces. Indeed, the technical difference between national-standard and elite-standard women hurdlers over 60 m is less than in the same groups amongst men (González-Frutos et al., 2019). In coaching literature, Etcheverry (1993) and Stein (2000) have both advocated an increase in women's hurdle height to 0.914 m (3'0"). Such an increase in height would represent 54.5% of the mean stature of the women analyzed in this study, still lower than the men's relative height but presenting a more similar challenge.

Clearing the hurdles is easier if the take-off position of the CM is higher, and men's relatively higher take-off and touchdown positions during the hurdle step require a greater raise of their CM during the take-off stance phase and a greater drop in CM position during the landing stance phase, respectively. Overall, this means that men's CM positions fluctuate more during the stance phases at either end of the hurdle step; however, when normalizing the same variables for hurdle height there is no difference between men and women. It seems that when absolute and stature-normalized values are used, men's CM positions fluctuate more vertically than women to complete the task, with corresponding effects on step lengths and clearance time. When these fluctuations are compared based on hurdle height, the two groups appear equal because men sacrifice all other mechanics to adjust to the hurdle's height, and the height of the women's hurdle does not need specific tuning but instead allows a smoother flow between both initial contact and toe-off both before and after the hurdle. Men's higher position at landing was achieved by adopting a more extended knee at touchdown, and the drop in the CM position to toe-off in this stance phase requires considerable leg strength to avoid too great a lowering of the CM before the landing step. Given the landing leg's important role in reducing landing distance to avoid unnecessarily large braking forces and to recover forward velocity (McLean, 1994; Salo et al., 1997), coaches are advised to develop lower leg strength in supporting the body on landing in all hurdlers, but possibly more so for men, via an additional focus on eccentric knee extensor

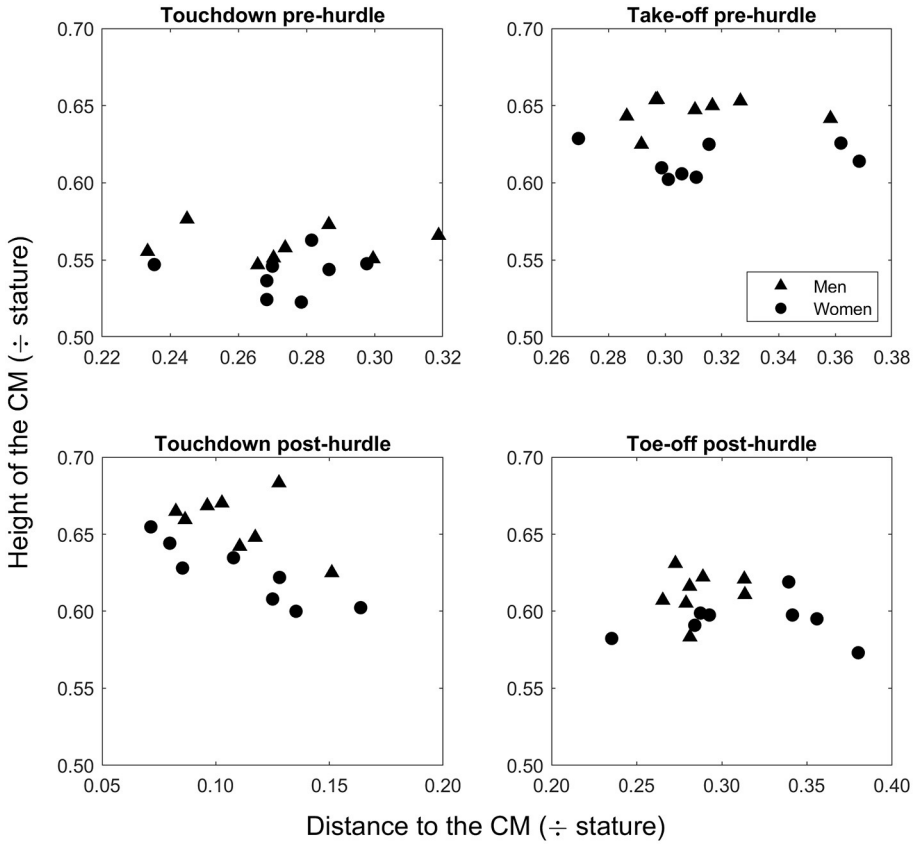

FIGURE 3 | Stature-normalized values for the height of the CM for each man and woman at touchdown and toe-off in the stance phases pre- and post-hurdle.

strength to allow for higher knee stiffness and a more extended knee at landing.

The height of the hurdle does not just affect how men and women cross it differently, but also has a profound effect on the sex-based differences in step lengths between the hurdles. All distances (apart from landing distance, which is a more passive distance, i.e., landing from the hurdle) are longer for women in relative terms, with the landing step length longer in women even when expressed in absolute terms. This means (in particular when normalizing for stature) a more distance-optimal forward movement for women, in that they cover more distance per step for their stature compared with men. This is not the case when considering, for example, the 100 m finals from the same 2017 World Championships where the mean stature-normalized step length for men was 1.21, whereas for women it was 1.19 (Bissas et al., 2018a,b). Accordingly, during late stance propulsion in the pre-hurdle contact phase, ending with take-off, women propel their bodies forward more with respect to their height; it is possible to therefore assume that women are more efficient with regard to force production and energy consumption, and could explain why women hurdlers are not trained to produce as much horizontal force as women sprinters (Stavridis et al., 2019). Indeed, if women traveled the same relative distance as men for the landing and recovery step lengths, this would have meant traveling on average (using the group mean) 3.08 m for these two steps compared with the measured 3.51 m. As this would have implications in all subsequent steps before the next hurdle, the current hurdle height therefore provides women with a "kinematic" and perhaps mechanical advantage (which might be measured in future studies using kinetic analyses). Therefore, the hurdle height not only affects the clearance phase but also the steps between the hurdles and energy requirements, and raising the women's hurdle height would have a consequent effect on these elements of the race. There is thus ecological evidence to support coaches' historical recommendations that the women's hurdle height be raised to 0.914 m. However, it should be noted that it is not essential that men's and women's events are "equivalent", and that there would be considerable effects on the training methods and technical requirements of women hurdlers, including those who compete in the heptathlon, where the 100 m hurdles is the first of the seven events. Nonetheless, the findings of the present study provide a scientific basis for revising the hurdle heights currently used to increase similarity between men and women's hurdling events. Few studies have been conducted in laboratory conditions to measure relevant kinetic variables such as impulse and braking forces, but future studies of this nature could inform coaching practice in concert with the kinematic

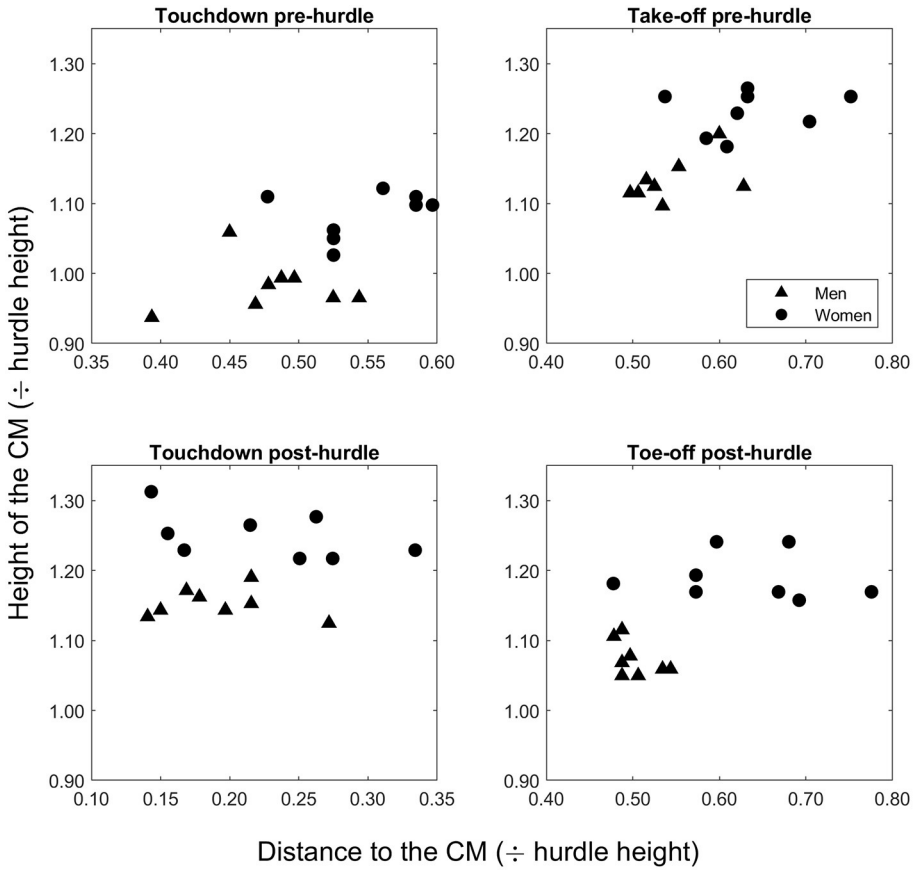

FIGURE 4 | Hurdle height-normalized values for the height of the CM for each man and woman at touchdown and toe-off in the stance phases pre- and post-hurdle.

and spatiotemporal findings from this study of the world's best hurdlers.

The main strength of this novel study is that the data are of world-class hurdlers competing in World Championship finals, and therefore the research has high ecological validity. Additionally, the competitors analyzed were the largest group of elite-standard hurdlers ever studied, and mean that the results can be used by coaches as a model of excellence. For example, we found the absolute distances for the hurdle step, landing step, recovery step and preparatory step (estimated) to be 3.80, 1.40, 2.04 and 1.90 m for men, and 3.16, 1.62, 1.89 and 1.83 m for women, similar to those value predicted by coaches (e.g., Hücklekemkes, 1990). However, the nature of the event's structure means that the sample was limited to eight athletes in each race, and recording performances in competition was constrained to analyzing the kinematics of one mid-race hurdle clearance only, meaning that our analyses will apply mostly to those hurdles where running speed is relatively constant (i.e., from the third hurdle to the ninth) (Pollitt et al., 2018a,b). The clearance of the first hurdle, in particular, could be quite different given slower running speeds, with fatigue also potentially affecting clearance of the last hurdle. Additionally, the clearance of the last hurdle could differ from the others as the athletes no longer need concern themselves with preparing for a step pattern that must accommodate the approach to a hurdle. Nonetheless, by focusing all recording on a single hurdle clearance meant that the four cameras used for 3D analysis provided extensive coverage of the hurdling motion and successive steps, and by using high-definition high-speed cameras, it was possible to obtain a precision of analysis not used before in outdoor competition (e.g., McDonald and Dapena, 1991). Future biomechanical studies at world-class competitions that focus on other sections of the race, such as hurdles earlier or later in the race, would complement these findings and provide more information to coaches on key factors in hurdling success.

CONCLUSIONS

In summary, this was the first study to analyze hurdling kinematics in a group of world-class athletes within the highly ecological setting of a World Championships. The men's hurdle was about 7% higher relative to their stature than the women's hurdle was for them, resulting in a more energy-costly vertical

displacement of the CM in men not only over the hurdle but also during the take-off and landing stance phases. The relatively higher hurdle of the men's event also required a more extended knee upon landing, and emphasized the landing leg's role in supporting the body effectively regarding moving into the subsequent landing step. Women were also able to take off farther from the hurdle in relative terms, meaning a less demanding task and affecting the step lengths achieved between the hurdles. Overall, the lower hurdle heights for women, relative to stature, provide them with a kinematic and potentially mechanical advantage over the men.

DATA AVAILABILITY STATEMENT

The raw data supporting the conclusions of this article will be made available by the authors, without undue reservation.

ETHICS STATEMENT

The studies involving human participants were reviewed and approved by Carnegie School of Sport Research Ethics Committee, Leeds Beckett University. The patients/participants provided their written informed consent to participate in this study.

AUTHOR CONTRIBUTIONS

BH, JW, and AB performed data collection. JW, GP and AB processed the data. BH and JW created the figures. All authors conceptualized and designed the study, wrote the manuscript, interpreted the results of the research, edited, critically revised, and approved the final version for submission.

FUNDING

The data collection and initial data analysis were supported by funding provided by the IAAF/World Athletics as part of a wider development/education project; however, the nature of the data is purely descriptive and not associated with any governing body, commercial sector, or product. The results of the present study do not constitute endorsement by World Athletics.

REFERENCES

Abdel-Aziz, Y. I., Karara, H. M., and Hauck, M. (2015). Direct linear transformation from comparator coordinates into space coordinates in close range photogrammetry. *Photogramm. Eng. Remote Sens.* 81:103–107. doi: 10.14358/PERS.81.2.103

Bahamonde, R. E., and Stevens, R. R. (2006). "Comparison of two methods of manual digitization on accuracy and time of completion," in *Proceedings of the XXIV International Symposium on Biomechanics in Sports*, eds H. Schwameder, G. Strutzenberger, V. Fastenbauer, S. Lindinger and E. Müller. Salzburg: Universität Salzburg, 650–653. Available online at: https://ojs.ub.uni-konstanz.de/cpa/article/view/207/167 (accessed July 17, 2006).

Bedini, R. (2016). Technical ability in the women's 100m hurdles. *New Stud. Athlet.* 31, 117–132.

Bezodis, I. N., Brazil, A., von Lieres und Wilkau, H. C., Wood, M., Paradisis, G. P., Hanley, B., et al. (2019). World-class male sprinters and high hurdlers have similar start and initial acceleration techniques. *Front. Sports Act. Living* 1:23. doi: 10.3389/fspor.2019.00023

Bissas, A., Walker, J., Tucker, C., Paradisis, G., and Merlino, S. (2018a). "Biomechanical report for the IAAF world championships London 2017: 100m men's," in *2017 IAAF World Championships Biomechanics Research Project, July 2018, London*. Monte Carlo: IAAF. Available online at: https://www.worldathletics.org/about-iaaf/documents/research-centre (accessed July 15–24, 2022).

Bissas, A., Walker, J., Tucker, C., Paradisis, G., and Merlino, S. (2018b). "Biomechanical report for the IAAF world championships London 2017: 100m women's," in *2017 IAAF World Championships Biomechanics Research Project, July 2018, London*. Monte Carlo: IAAF. Available online at: https://www.worldathletics.org/about-iaaf/documents/research-centre (accessed July 15–24, 2022).

Čoh, M. (2003). Biomechanical analysis of Colin Jackson's hurdle clearance technique. *New Stud. Athlet.* 18, 37–45.

Čoh, M., Bončina, N., Štuhec, S., and Mackala, K. (2020). Comparative biomechanical analysis of the hurdle clearance technique of Colin Jackson and Dayron Robles: key studies. *Appl. Sci.* 10:3302. doi: 10.3390/app10093302

Čoh, M., Zvan, M., Bončina, N., and Štuhec, S. (2019). Biomechanical model of hurdle clearance in 100m hurdle races: a case study. *J. Anthropol. Sport Phys. Educ.* 3, 3–6. doi: 10.26773/jaspe.191001

Cohen, J. (1988). *Statistical Power Analysis for the Behavioural Sciences, 2nd Edn*. Hillsdale, NJ: Lawrence Erlbaum.

de Leva, P. (1996). Adjustments to Zatsiorsky-Seluyanov's segment inertia parameters. *J. Biomech.* 29, 1223–1230. doi: 10.1016/0021-9290(95)00178-6

Etcheverry, S. G. (1993). A proposal to change the women's hurdles events. *New Stud. Athlet.* 8, 23–26.

Field, A. P. (2009). *Discovering Statistics Using SPSS, 4th Edn*. London: Sage.

González-Frutos, P., Veiga, S., Mallo, J., and Navarro, E. (2019). Spatiotemporal comparisons between elite and high-level 60 m hurdlers. *Front. Psychol.* 10:2525. doi: 10.3389/fpsyg.2019.02525

Graubner, R., and Nixdorf, E. (2011). Biomechanical analysis of the sprint and hurdles events at the 2009 IAAF world championships in athletics. *New Stud. Athlet.* 26, 19–53. doi: 10.1097/JSM.0b013e318191c8e7

Hücklekemkes, J. (1990). Model technique analysis sheets for the hurdles. Part VI: the women's 100 metres hurdles. *New Stud. Athlet.* 5, 33–58.

Matthews, P. (2017). *Athletics 2017: The International Track and Field Annual*. New York, NY: SportsBooks Ltd.

McDonald, C., and Dapena, J. (1991). Linear kinematics of the men's 110-m and women's 100-m hurdles races. *Med. Sci. Sports Exerc.* 23, 1382–1391. doi: 10.1249/00005768-199112000-00010

McLean, B. (1994). The biomechanics of hurdling: force plate analysis to assess hurdling technique. *New Stud. Athlet.* 9, 55–58.

Pollitt, L., Walker, J., Bissas, A., and Merlino, S. (2018a). "Biomechanical report for the IAAF world championships London 2017: 110 m hurdles men's," in *2017 IAAF World Championships Biomechanics Research Project, July 2018, London*. Monte Carlo: IAAF. Available online at: https://www.worldathletics.org/about-iaaf/documents/research-centre (accessed July 15–24, 2022).

Pollitt, L., Walker, J., Bissas, A., and Merlino, S. (2018b). "Biomechanical report for the IAAF world championships London 2017: 100 m hurdles women's," in *2017 IAAF World Championships Biomechanics Research Project, July 2018, London*. Monte Carlo: IAAF. Available online at: https://www.worldathletics.org/about-iaaf/documents/research-centre (accessed July 15–24, 2022).

Salo, A., Grimshaw, P., and Marar, L. (1997). 3-D biomechanical analysis of sprint hurdles at different competitive levels. *Med. Sci. Sports Exerc.* 29, 231–237.

Stavridis, I., Smilios, I., Tsopanidou, A., Economou, T., and Paradisis, G. (2019). Differences in the force velocity mechanical profile and the effectiveness of force

application during sprint-acceleration between sprinters and hurdlers. *Front. Sports Act. Living* 1:26. doi: 10.3389/fspor.2019.00026

Stein, N. (2000). Reflections on a change in the height of the hurdles in the women's sprint hurdles event. *New Stud. Athlet.* 15, 15–19.

Tidow, G. (1991). Model technique analysis sheets for the hurdles. Part VII: high hurdles. *New Stud. Athlet.* 6, 51–66.

World Athletics (2019). *C2.1 – Technical Rules*. Monte Carlo: World Athletics.

World Athletics (2021). *Timetable/Results*. Available online at: https://www.worldathletics.org/competitions/world-athletics-championships/iaaf-world-championships-london-2017-7093740/timetable/bydiscipline (accessed March 29, 2021).

Conflict of Interest: The authors declare that the research was conducted in the absence of any commercial or financial relationships that could be construed as a potential conflict of interest.

frontiers in Sports and Active Living

ORIGINAL RESEARCH
published: 09 July 2021
doi: 10.3389/fspor.2021.702743

New Text

The Role of Upper Body Biomechanics in Elite Racewalkers

Helen J. Gravestock[1,2], *Catherine B. Tucker*[2] *and Brian Hanley*[2]*

[1] School of Health Sciences, Birmingham City University, Birmingham, United Kingdom, [2] Carnegie School of Sport, Leeds Beckett University, Leeds, United Kingdom

The aim of this study was to analyze the link between the upper and lower body during racewalking. Fifteen male and 16 female racewalkers were recorded in a laboratory as they racewalked at speeds equivalent to their 20-km personal records [men: 1:23:12 (±2:45); women: 1:34:18 (±5:15)]; a single representative trial was chosen from each athlete for analysis and averaged data analyzed. Spatial variables (e.g., stride length) were normalized to stature and referred to as ratios. None of the peak upper body joint angles were associated with speed ($p < 0.05$) and there were no correlations between pelvic motion and speed, but a medium relationship was observed between peak pelvic external rotation (right pelvis rotated backwards) and stride length ratio ($r = 0.37$). Greater peak shoulder extension was associated with lower stride frequencies ($r = -0.47$) and longer swing times ($r = 0.41$), whereas peak elbow flexion had medium associations with flight time ($r = -0.44$). Latissimus dorsi was the most active muscle at toe-off during peak shoulder flexion; by contrast, pectoralis major increased in activity just before initial contact, concurrent with peak shoulder extension. Consistent but relatively low rectus abdominis and external oblique activation was present throughout the stride, but increased in preparation for initial contact during late swing. The movements of the pelvic girdle were important for optimizing spatiotemporal variables, showing that this exaggerated movement allows for greater stride lengths. Racewalkers should note however that a larger range of shoulder swing movements was found to be associated with lower stride frequency, and smaller elbow angles with increased flight time, which could be indicative of faster walking but can also lead to visible loss of contact. Coaches should remember that racewalking is an endurance event and development of resistance to fatigue might be more important than strength development.

Keywords: coaching, elite-standard athletes, endurance, kinematics, track and field

OPEN ACCESS

Edited by:
Franck Brocherie, Institut national du sport, de l'expertise et de la performance (INSEP), France

Reviewed by:
Gaspare Pavei, University of Milan, Italy
Koji Hoga-Miura, Japan Sport Council, Japan

***Correspondence:**
Brian Hanley
b.hanley@leedsbeckett.ac.uk

Specialty section:
This article was submitted to Elite Sports and Performance Enhancement, a section of the journal Frontiers in Sports and Active Living

Received: *29 April 2021*
Accepted: *21 June 2021*
Published: *09 July 2021*

Citation:
Gravestock HJ, Tucker CB and Hanley B (2021) The Role of Upper Body Biomechanics in Elite Racewalkers. Front. Sports Act. Living 3:702743. doi: 10.3389/fspor.2021.702743

INTRODUCTION

Racewalking is a technical event with its own unique gait pattern, determined by the athletes' attempts to maximize speed and to adhere to World Athletics Rule 54.2 (previously known as Rule 230.2). This rule states that racewalking is a progression of steps with no visible (to the human eye) loss of contact with the ground and that the athlete's advancing leg must be straightened from first contact with the ground until the vertical upright position (World Athletics, 2019). Although the upper body is not directly affected by Rule 54.2, it nonetheless functions to counterbalance the angular momentum of the lower body during racewalking (Hoga-Miura et al., 2016) and therefore the upper body might adopt particular movements to accommodate the rule. One major function of

the arms' movements during normal walking and running is to counteract moments of the swinging legs around the vertical axis (Herr and Popovic, 2008; Pontzer et al., 2009), and this action is also considered by several coaches to be of particular importance in racewalking (Hopkins, 1981; Villa, 1990). Racewalking coaching literature has long recommended an emphasis on arm movements (e.g., considerable shoulder hyperextension at ipsilateral initial contact) (Payne and Payne, 1981; Drake, 2003), and indeed the vigorous arm swing in racewalking is accompanied by a transverse rotation of the thorax in an opposite direction to the pelvis, with thorax rotation in racewalking about double that of normal walking (Murray et al., 1983; Pavei and La Torre, 2016). Laboratory-based studies have found large transverse plane motions that generate torsion within the trunk (Pavei and La Torre, 2016) that coaches have long believed counteract the exaggerated movements of the pelvis (Hopkins, 1978), which themselves are emphasized to try to increase stride length (Knicker and Loch, 1990). However, whether the movements of the upper body, including the pelvis, have an effect on key spatiotemporal variables has not been fully established in racewalking to date.

Because the stance knee cannot flex until after the torso has passed over the foot, there is a profound effect on the contribution of the other joints during stance (Hanley and Bissas, 2017) as the lower limb becomes a rigid lever about which the upper body rotates, possibly affecting the path of the center of mass (CM). Similar to normal walking and running, it has been suggested that racewalkers improve mechanical efficiency by decreasing vertical displacement during walking (Murray et al., 1983). Cairns et al. (1986) reported the CM trajectory to be absent or diminished when racewalking because pelvic motions in the frontal plane (pelvic obliquity) reduce vertical CM movement and thereby increase efficiency. Because of pelvic obliquity, the hip is in the highest position over the center of the support leg and lowest when over the swinging leg (Pavei et al., 2014) and, in their small-scale study, Murray et al. (1983) noted the S-shape vertebral column reverses as weight is shifted between stance phases. This motion was proposed to help maintain a smooth vertical trajectory of the CM during racewalking (Murray et al., 1983; Cairns et al., 1986) under the old rules where the knee did not have to be straightened until the vertical upright position. More recently, Pavei et al. (2017) and Pavei et al. (2019) showed instead that the CM trajectory is closer to running than walking. The understanding of thorax motion in coaches would therefore benefit from further detailed analysis conducted in a laboratory using optoelectronics.

The magnitude of thorax torsion reported previously (Pavei and La Torre, 2016) suggests core abdominal muscles are important in racewalking, although the few studies of muscle activity using electromyography (EMG) in racewalking have focused on the lower limbs (Hanley and Bissas, 2013; Padulo et al., 2013; Cronin et al., 2016; Gomez-Ezeiza et al., 2019), with only one study of upper body muscle activity conducted before the current rule was introduced in 1995, and on a limited sample of two national-standard men (Murray et al., 1983). In competition, exaggerated upper body movements have indeed been found in kinematic studies of world-class racewalkers (Hanley et al., 2011, 2013), but the three-dimensional (3D) data analyzed were collected at 50 Hz and might not accurately describe movement in elite racewalking. Furthermore, these field-based studies used joint centers only to measure pelvic and thorax movements, and thus a novel 3D study using multiple markers and a higher sampling rate can provide more accurate information about how world-class racewalkers achieve their unique gait (Cazzola et al., 2016; Pavei and La Torre, 2016). In addition, the analysis of activity in key upper body muscles using EMG can explain their contribution to racewalking and provide a rationale for including specific training for these muscles (or muscle groups) within a strength and conditioning program.

Racewalk coaches have long emphasized arm movements and exaggerated pelvic and thoracic movements in trying to improve racewalking performances (Hopkins, 1981; Villa, 1990; Drake, 2003). However, the scientific rationale of these coaching recommendations for the upper body are not clearly established under the current rules for racewalking. Furthermore, it is not clear whether upper body movements influence racewalking speed and other key spatiotemporal measures that contribute to racewalking speed. Therefore, this study will make an original contribution to the literature by analyzing upper body kinematics with synchronized muscle activity patterns for both elite men and women racewalkers. Such information will impact coaches and athletes in informing training strategies and identify what kinematic movements are important for achieving high racewalking speeds and abiding by completion racewalking rules. Therefore, the aim of this study was to analyze the link between the upper and lower body movements during racewalking. This was achieved through a detailed biomechanical analysis on a large sample of elite standard men and women racewalkers using precise 3D motion capture and EMG to analyze the whole body during the entire gait cycle.

MATERIALS AND METHODS

Research Approval

All human subjects were treated in accordance with established ethical standards. The protocol was approved by the Carnegie School of Sport Research Ethics Committee. All subjects gave written informed consent in accordance with the Declaration of Helsinki. The subjects were provided with Participant Information Sheets, and in accordance with the Carnegie School of Sport Research Ethics Committee's policies for use of human subjects in research, all subjects were informed of the benefits and possible risks associated with participation and informed of their right to withdraw at any time.

Participants

Thirty-one racewalkers of 15 different nationalities volunteered for the study. Fifteen participants were men (age: 26 $\pm$ 5 years; stature: 1.78 $\pm$ 0.04 m; body mass: 64.7 $\pm$ 4.9 kg) and 16 were women (age: 28 $\pm$ 6 years; stature: 1.66 $\pm$ 0.08 m; body mass: 55.3 $\pm$ 9.4 kg). The sample included two IAAF World Championship medalists, a European Champion, a European Championship silver medalist, a World U20 Champion, a Commonwealth Games silver medalist, 13 other athletes who had competed at

the Olympic Games and/or World Championships, two who had the Olympic qualifying time and three who had competed at the World U20 Championships or European Championships. The mean 20 km personal record time (h:min:s) for the men was 1:23:12 (±2:45), whereas for the women it was 1:34:18 (±5:15).

Data Collection

Each participant visited the laboratory on a single occasion. Participants wore tight fitting clothing and their usual training shoes. Having performed several familiarization trials before testing, the participants racewalked along a 45-m indoor track in the biomechanics laboratory at race pace (**Figure 1**); a minimum of six acceptable trials were recorded, defined as the athlete achieving the target speed (±5%), clean foot contacts on at least one force plate, and with no visible evidence of targeting or breaching of racewalk competition rules (one of the study authors, who was present during all data collection, is a qualified racewalking judge). There was at least a 30-s rest period between trials.

Each trial involved the participants racewalking multiple times across three successively positioned force plates (9287BA, Kistler Instruments Ltd., Winterthur). The force plates sampled at 1000 Hz and were 900 mm long and 600 mm wide [natural frequency ≈ 750 Hz (x-, y-), ≈ 520 Hz (z-); linearity < ±0.5% full scale output; cross talk < ±1.5%; hysteresis <0.5% full scale output]. The force plates were covered with a synthetic athletic surface to make them flush with the rest of the track and ensure ecological validity (Bezodis et al., 2008). Force plate voltages were recorded through Qualisys Track Manager Software (QTM) (v2.17, Qualisys, Gothenburg). Each participant's racewalking pace was recorded using double photocell timing gates (Microgate, Witty, Bolzano) placed 4 m apart and positioned around the force plates. Kinematic data were simultaneously recorded using a 12-camera optoelectronic motion analysis system (Oqus 7, Qualisys, Gothenburg) operating at 250 Hz. A configuration of 70 reflective markers and marker clusters were placed on anatomical landmarks and segments to describe participants' segment kinematics (**Table 1**). The capture volume was calibrated according to the manufacturer's instructions. Given that a large capture volume was used, an error of <2 mm for the dynamic calibration was accepted. The mean calibration error from all testing sessions was 1.45 ± 0.23 mm.

Surface EMG was recorded with eight wireless sensors (Delsys Trigno, Delsys Inc, USA), sampling at 1926 Hz. The EMG sensors had four silver 5 × 1 mm bar contacts with an inter-electrode distance of 10 mm. Raw signals were measured at a bandwidth of 20–450 Hz using a differential amplifier. The common mode rejection ratio (CMRR) was ≤−80 dB at 60 Hz and input

TABLE 1 | Description of the segments used for kinematic analysis.

Segment	Description
Head	Bilateral markers on front and back of head
Thorax	Bilateral markers on acromion process, C7 spinous process, T7 spinous process, suprasternal notch, xiphoid process
Pelvis	Bilateral markers on ASIS and PSIS
Right and left upper arm	Acromion process, three-marker tracking cluster, humeral lateral, and medial epicondyles
Right and left forearm	Humeral lateral and medial epicondyles, three-marker tracking cluster, radial and ulnar styloid processes
Right and left hand	Radial and ulnar styloid processes, marker on center of dorsal aspect of hand
Right and left thigh	Greater trochanter, medial and lateral femoral epicondyles, four-marker tracking cluster
Right and left shank	Medial and lateral femoral epicondyles, four-marker tracking cluster, medial and lateral malleoli
Right and left foot	Medial and lateral malleoli, first and second metatarsal heads
Right and left forefoot	Calcaneus, first and fifth metatarsal heads

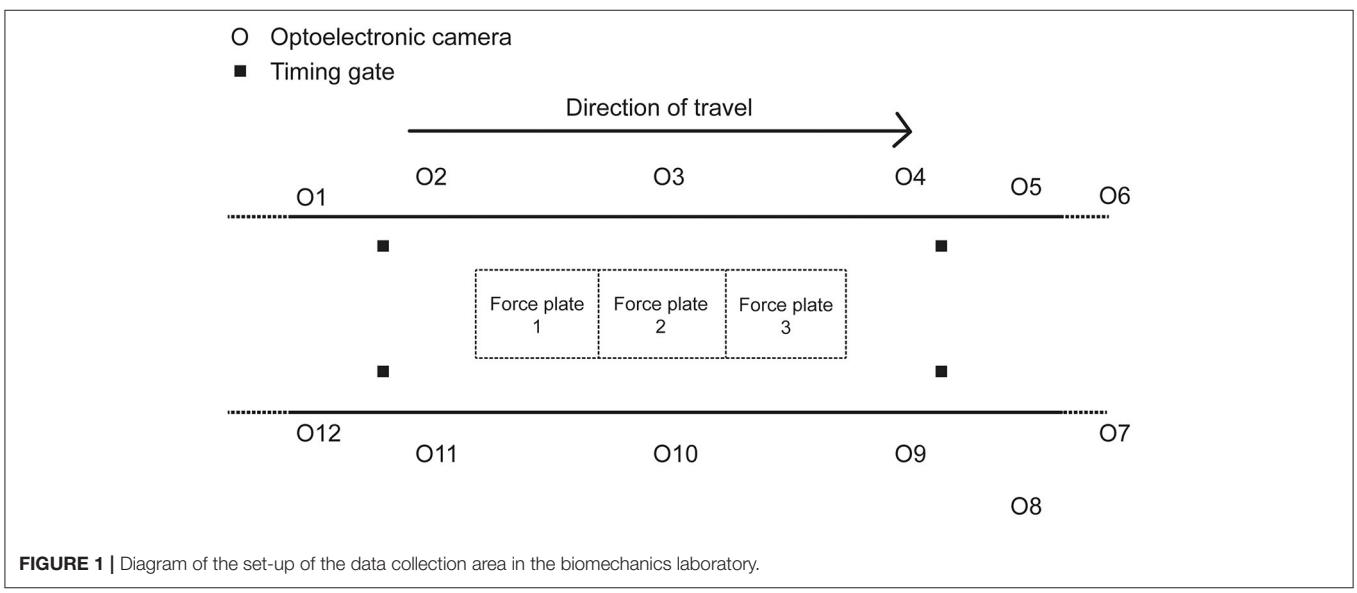

FIGURE 1 | Diagram of the set-up of the data collection area in the biomechanics laboratory.

impedance was <10 Ω. Baseline noise was <750 μV root mean square (RMS), and effective signal gain was 909 V/V ± 5%. The EMG sensors were attached to the right side only and were positioned in the direction of the muscle fibers (Clarys and Cabri, 1993). Before placing the EMG sensors, the skin surface was prepared by shaving (if necessary), lightly abrading and cleaning with an isopropyl alcohol swab. EMG sensors were placed on the biceps brachii, middle deltoid, pectoralis major, latissimus dorsi, trapezius middle fibers, trapezius lower fibers, rectus abdominis and external oblique. These muscles were selected based on previous research that analyzed upper body muscle contributions in normal walking (Goudriaan et al., 2014). The EMG sensors were positioned in line with the Surface Electromyography for the Non-Invasive Assessment of Muscles (SENIAM) guidelines (Hermens et al., 2000). Simultaneous data capture of all systems was initiated using a trigger module (Delsys Inc., USA). Data from the optoelectronic system and force plates were recorded through QTM (v. 2.17, Qualisys, Gothenburg). EMG data were stored in EMGworks Acquisition software for post-processing.

Data Analysis

3D kinematic marker trajectories from the motion trials were labeled from which Automatic Identification of Markers (AIM) models were generated (Qualisys, Gothenburg) (Rodger et al., 2013). Gap filling was completed when fewer than 10 consecutive frames were missing in the trajectory. Gait events were identified using the force plate data (O'Connor et al., 2007; Zeni et al., 2008); the vertical component of the ground reaction force (GRF) was used to determine the timing of each gait event. The instant of initial contact occurred when the vertical GRF exceeded three standard deviations (SD) above force plate noise (Addison and Lieberman, 2015), which itself was calculated from the first 50 samples of unloaded data for each trial. The mean threshold found using this method was 5 N (±5). Where gait events occurred without force plate contact, the vertical velocity of the calcaneus marker was used. The vertical velocity of this marker was found to have a characteristic shape, repeated in each gait cycle. By locating the relevant vertical velocity value of the heel marker at the time instant defined by vertical GRF data, the subsequent gait event could be identified using this velocity value validated from the gold standard event identification method. A similar principle was used by O'Connor et al. (2007) who used foot CM velocity in an algorithm to identify gait events.

Kinematic data were exported to Visual3D (V6 x64, C-Motion Inc., Maryland) using a custom-made Project Automation Framework (Qualisys, Gothenburg). Data from the static and tracking markers in a standing trial were used to develop a six degrees of freedom (6DOF) 3D whole-body kinematic model in Visual3D. All body segment parameter values were estimated from total body mass using regression analysis conducted by Dempster (1955). The center of gravity location and moments of inertia for each segment was calculated using the Hanavan (1964) mathematical model, an approach that has been validated through comparisons using experimental data (Hanavan, 1964). Shoulder, elbow, thorax, pelvis, hip, knee, ankle, ankle, and forefoot angles were calculated based on the Cardan angle rotation order of XYZ. Kinematic data were filtered using a fourth-order zero-lag low pass Butterworth digital filter. Residual analysis was carried out to determine the optimal cut-off frequency (Winter, 2005); the results showed an optimal cut-off frequency ranging from 11.1 to 12.8 Hz so it was decided to use 12 Hz as the cut-off frequency.

EMG data were filtered using the in-built hardware bandpass filter (20–450 Hz). Signal bandwidth was 430 Hz where the slopes of the lower (20 ± 5 Hz) and upper (450 ± 50 Hz) cut-offs were >40 dB/dec and >80 dB/dec, respectively. EMG data were processed in EMGworks analysis software (v.4.2.7 Analysis, Delsys, Massachusetts). To remove the effects of any offset, the mean was removed from each raw EMG reading for each of the eight muscles (Chuang and Acker, 2019). Data were cropped in the time domain to the same gait events as the kinematic data. An RMS calculation was applied with a moving window size of 50 ms and overlap of 25 ms with zero padding (Hanley and Bissas, 2013). A cubic spline was used to smooth and interpolate the data to 101 points. Similar to the kinematic data, the stance phase data were interpolated to 51 points, and the swing phase data interpolated to 50 points to ensure toe-off visually occurred at 50% of the gait cycle. This process was adopted to visualize the two different phases in the right leg, rather than to state categorically the relative duration of each phase; note that flight time occurs when both legs are in swing: one in early swing, and the other in late swing, and will therefore occur near the start and end of each cycle.

For each participant, at least six good trials were collected at race pace (i.e., equivalent to their season's best performance), and one successful trial was selected for analysis. A successful trial was defined using the same criteria during data collection with the additional conditions of good tracking data with minimal marker drop out, and one whole gait cycle (i.e., one single stride) for the right side recorded within the capture volume. Spatiotemporal variables were computed using the initial contact and toe-off gait events. Both spatiotemporal and joint angle variables were calculated using Visual3D. Stride length was defined as the perpendicular anteroposterior distance between subsequent right foot initial contacts. Stride length was also expressed as a percentage of the participants' statures, as this is the easiest method of normalization for coaches given difficulties in accurately measuring leg length, and referred to as stride length ratio. Foot ahead and foot behind distances were defined as the anteroposterior distances between the whole body CM and the foot segment CM at initial contact and toe-off, respectively. Flight distance, which is a component of stride length, was defined as the anteroposterior travel distance of the whole body CM during any flight phase (Hunter et al., 2004). Stride width was defined as the mediolateral distance from the proximal end position of the foot (the toes) at initial contact to the toes of the contralateral foot at the subsequent initial contact. As with stride length, these distances were also expressed as a proportion of stature, and referred to as ratios. Stance time and swing time were calculated as the time between right initial contact to right toe-off and right toe-off to right initial contact, respectively. Flight time was calculated as the time between right foot toe-off and left foot initial contact. Stride frequency (Hz) was calculated as the reciprocal of stride time.

Joint angle maxima and minima were calculated over the gait cycle with the timings of these events determined. Joint angle time series data have been presented with the percentage of gait cycle for each of the major upper and lower body joints for the predominant planes of motion. An additional angle, the forefoot angle, was calculated at the foot to monitor the sagittal plane angle at the metatarsophalangeal joints. This angle was included as during the contact phase the foot rolls forward around the forefoot leaving the tip of the toe as the last contact point. Movement of the forefoot toward the tibia in the sagittal plane was considered plantarflexion. Pelvic and thorax internal rotation described rotation of the right side of the body forwards (in the direction of hip flexion), whereas external rotation described rotation of the right side backwards (in the direction of hip hyperextension).

Statistics

Results are reported as means ±1 SD. Density ridgeline plots display the relative timing of key joint actions during the gait cycle and were interpreted in a similar way to a smoothed histogram. In effect, ridgeline plots are partially overlapping line plots that resemble a mountain range, and are considered useful for visualizing changes in distributions over time (Wilke, 2017). The height of each curve represents the frequency of each event in the gait cycle (%); the width of each curve along the x-axis denoted the time window at which the joint reached maximum or minimum values. For the smoothed appearance, a kernel density estimate was used to produce the shaded probability density functions. This estimate was based on the probability density function of each variable using a 3.6 bandwidth. Density ridgeline plots were produced in R (Version 1.1463, Rstudio Inc., Boston, MA) using ggridges library (Wilke, 2017). Spatiotemporal group means with associated SD were also calculated. Pearson's product moment correlation coefficient (r) was used to find associations between spatiotemporal, minimum, and maximum joint angle data. A confidence level of 5% was set. Significant correlations were considered to be small ($r = 0.10$–0.29), medium ($r = 0.30$–0.49) or large ($r \geq 0.50$) (Cohen, 1992). All statistical analyses were conducted using SPSS Statistics 19, Release Version 25.0.0 (IBM SPSS, Inc., 2010, Chicago, IL). EMG data were presented with appropriate joint kinematics with respect to the gait cycle; this involved finding the maximum value for each individual (in V) and expressing each value in the sequence as a percentage of the maximum. These percentage data were then averaged across all participants.

RESULTS

None of the normalized (ratio) variables differed between sexes, and consequently the means, SDs and ranges for men and women have been combined for the purposes of description and analysis and are presented in **Table 2**. To put some of the results below into context, notable significant associations were found between speed and stride length ratio ($r = 0.65$) and stride frequency ($r = 0.67$), between flight time and flight distance ratio ($r = 0.71$), and between flight time and stride length ratio ($r = 0.52$); it should be noted that flight distance will contribute to overall stride length, but also that this individual component of stride length is important in racewalking speed.

TABLE 2 | Group mean ± SD data for spatiotemporal variables for men, women, and all athletes (combined data).

Variable	Men	Women	All athletes
Speed (m/s)	3.99 ± 0.29	3.60 ± 0.35	3.79 ± 0.38
Stride length (m)	2.41 ± 0.14	2.22 ± 0.14	2.31 ± 0.17
Stride length ratio (%)	136 ± 7.0	134 ± 6.3	135 ± 7
Stride frequency (Hz)	1.65 ± 0.08	1.63 ± 0.15	1.64 ± 0.12
Foot ahead (m)	0.36 ± 0.03	0.33 ± 0.03	0.34 ± 0.03
Foot ahead ratio (%)	19.9 ± 1.0	19.6 ± 1.6	19.7 ± 1.4
Foot behind (m)	0.47 ± 0.03	0.44 ± 0.04	0.45 ± 0.04
Foot behind ratio (%)	26.5 ± 2.0	26.3 ± 1.7	26.4 ± 1.7
Flight distance (m)	0.21 ± 0.05	0.18 ± 0.06	0.19 ± 0.05
Flight distance ratio (%)	11.8 ± 2.6	10.9 ± 3.4	11.3 ± 3.4
Flight time (s)	0.049 ± 0.010	0.048 ± 0.020	0.048 ± 0.016
Stance time (s)	0.254 ± 0.020	0.266 ± 0.041	0.260 ± 0.032
Swing time (s)	0.351 ± 0.015	0.354 ± 0.027	0.353 ± 0.021
Stride width (m)	0.05 ± 0.03	0.05 ± 0.02	0.05 ± 0.03

Peak shoulder flexion occurred just before ipsilateral toe-off, approximately at the same time as peak thorax internal rotation, pelvic external rotation, hip extension, and forefoot plantarflexion (**Figure 2**). Peak movements in the opposite direction (shoulder extension, thorax external rotation, pelvic internal rotation) occurred just before ipsilateral initial contact during late swing; greater peak shoulder extension was associated with lower stride frequencies and longer swing times, whereas peak shoulder flexion was correlated with foot behind ratio (**Table 3**). Peak shoulder adduction occurred during early swing to assist its extension movement; similarly, peak shoulder abduction occurred during shoulder flexion (**Figures 2**, **3**). Forefoot dorsiflexion occurred at midstance, at roughly the same time as peak knee extension (or hyperextension), hip adduction, pelvic obliquity (right side up) and thorax obliquity (right side down) (**Figure 2**). Their opposing movements (knee flexion, hip abduction, pelvic obliquity (right side down) and thorax obliquity (right side up) occurred during midswing. Peak ankle plantarflexion occurred immediately after toe-off, although peak ankle dorsiflexion varied more within the group (**Figure 2**); for most athletes it occurred just before initial contact (**Figure 3**). The timing of many other kinematic measures, such as anterior and posterior pelvic tilt, hip rotation and thorax flexion/extension, was also more varied across the group of athletes, as shown by the spread across the x-axis in **Figure 2** and by the SD clouds in **Figure 3**. None of the peak upper body joint positions were associated with speed, although pelvic external rotation was negatively correlated with stride length ratio and foot behind ratio (**Table 3**), and stride width was positively correlated with pelvic internal rotation, hip abduction and hip internal rotation and negatively with hip external rotation.

Regarding the shoulder muscles, latissimus dorsi was the most active muscle at toe-off (**Figure 4**) when the shoulder

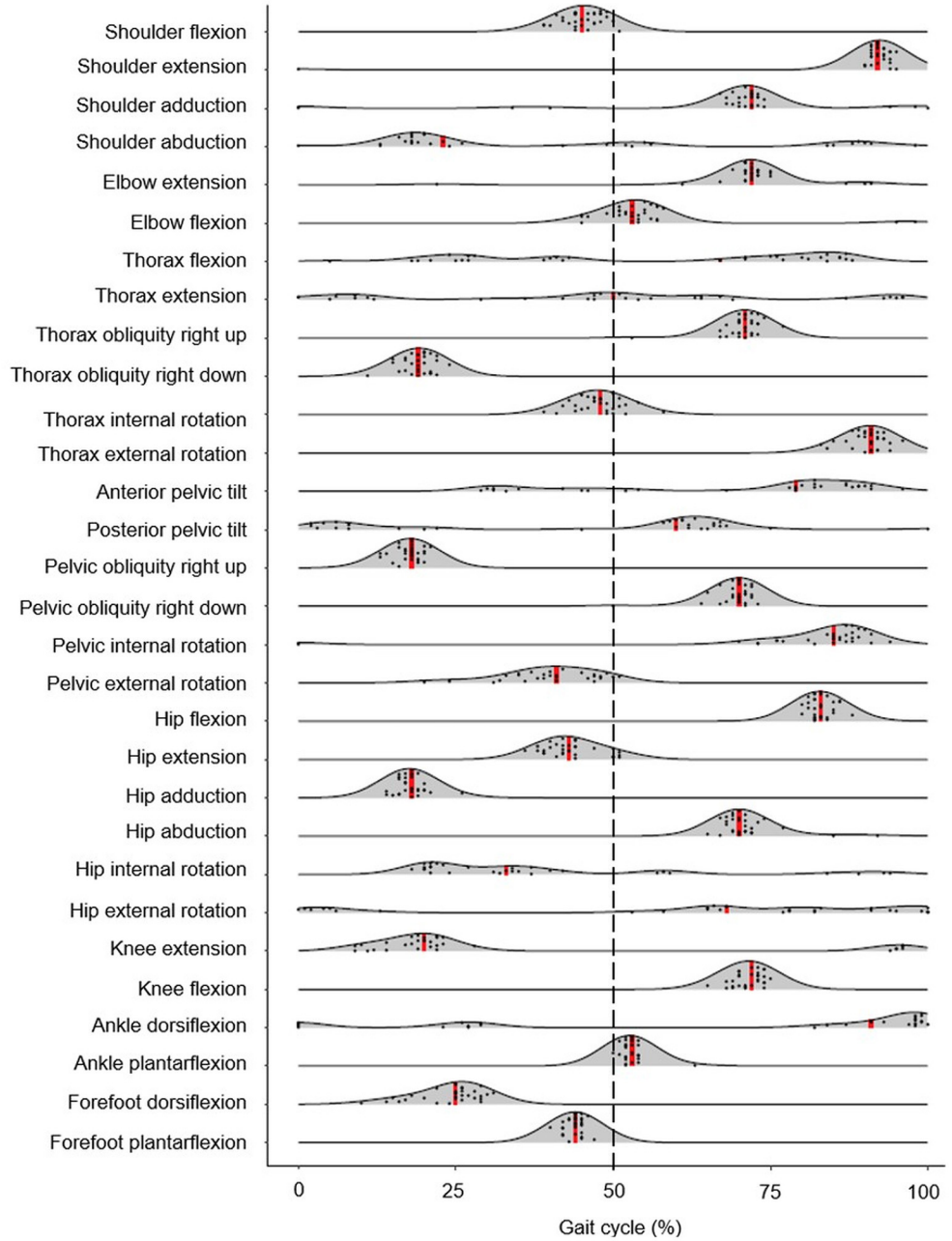

FIGURE 2 | Density ridgeline plot of the timing of each joint angle peak during the gait cycle. Individual variation is dotted, and median values are represented by red vertical lines. The dashed vertical line represents gait cycle division between stance (from 0 to 50%) and swing (from 51 to 100%).

was at peak flexion. By contrast, the pectoralis major trace in **Figure 4** shows an increase in activity just before and after initial contact, when the shoulder was at peak extension. Biceps brachii, also an elbow muscle, shows a bimodal pattern of two peaks that occur during the first part of the stance phase and terminal swing phase, when the elbow was flexed least (**Figure 4**). These periods of the gait cycle fall just after and before initial contact, where the shoulder flexion-extension moves out of phase with hip flexion-extension (**Figure 3**). The elbow was found to be most flexed near toe-off when the shoulder is also in peak flexion, positioned in front of the body (**Figure 3**). Peak elbow flexion was correlated with flight time ($r = -0.44$). With regard to the trapezius muscle, the middle fibers peak near the middle of the stance phase (∼23% of gait cycle) and the lower fibers peak near terminal stance and toe-off (∼36% of gait cycle) (**Figure 4**).

Middle deltoid muscle activation shows one burst of activity at about 30% of the gait cycle (**Figure 4**), after the shoulder

TABLE 3 | Relationships (*r*) between spatiotemporal variables and upper body minimum and maximum joint angles.

Peak joint position	Stride length ratio	Stride frequency	Foot behind ratio	Stance time	Swing time	Stride width
Shoulder extension	0.01	−0.47**	−0.05	0.32	0.41*	0.20
Shoulder flexion	0.30	0.06	0.40*	−0.01	−0.10	0.05
Pelvic obliquity right down	−0.02	−0.26	0.39*	0.33	0.07	0.24
Pelvic obliquity right up	−0.06	−0.32	0.31	0.39*	0.13	0.22
Pelvic external rotation	0.37*	−0.16	0.44*	0.09	0.11	0.07
Pelvic internal rotation	−0.11	0.05	0.06	0.17	−0.29	0.38*
Hip adduction	0.10	0.05	−0.06	−0.16	0.05	−0.30
Hip abduction	−0.01	−0.30	0.37*	0.39*	0.06	0.53**
Hip external rotation	0.32	−0.19	0.30	0.09	0.23	0.45*
Hip internal rotation	0.18	−0.35	0.35	0.26	0.31	0.49**

Correlations were significant at $p < 0.05$ (*) and $p < 0.01$ (**). All values are presented as magnitudes (no associated direction) to make interpretation simpler.

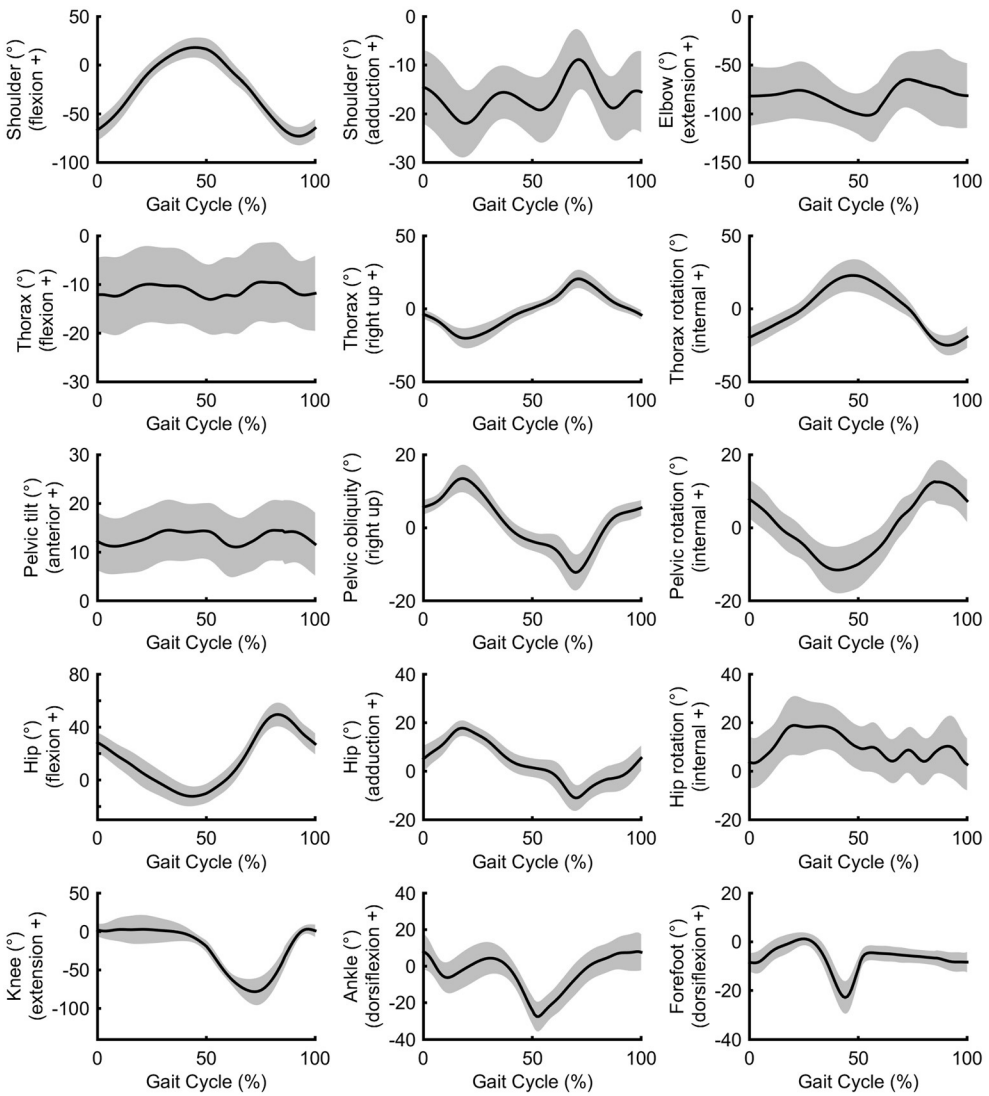

FIGURE 3 | Group mean (± SD) upper and lower body joint angle kinematics.

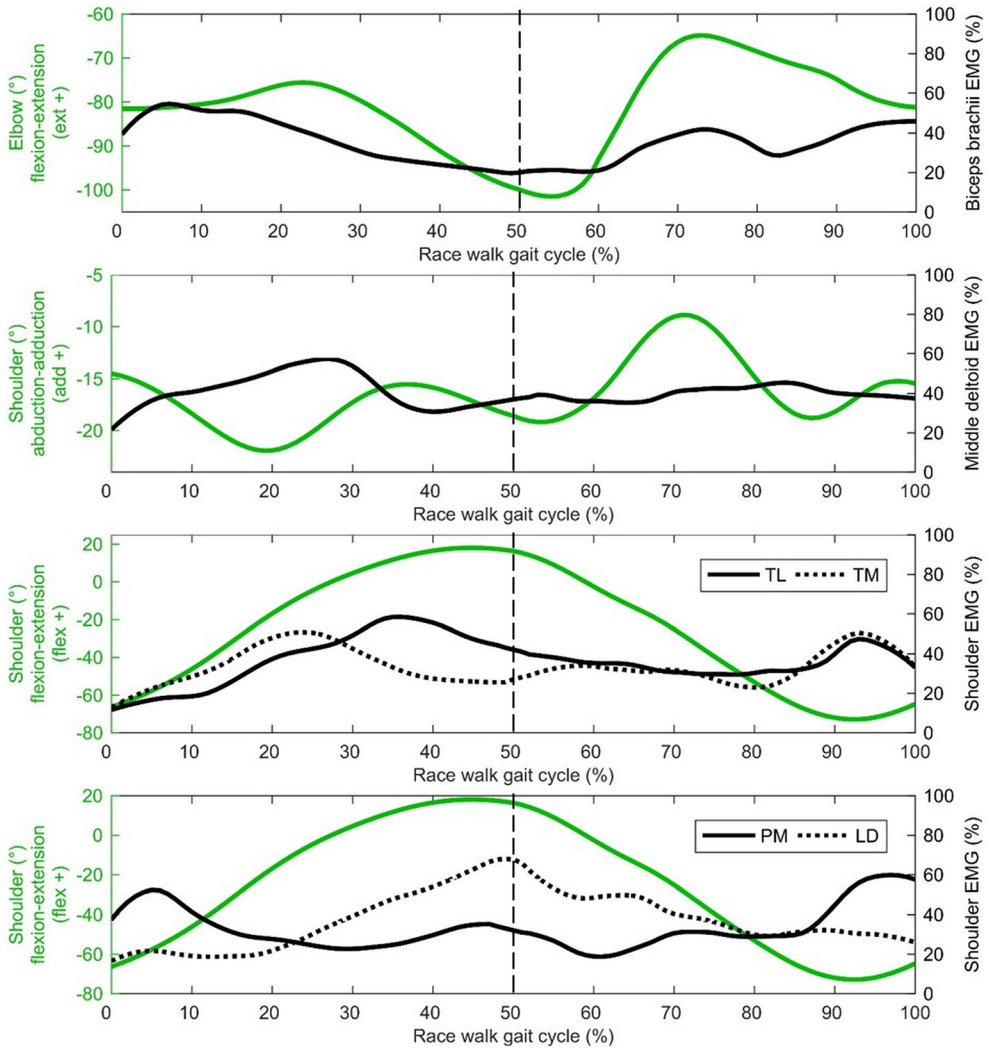

FIGURE 4 | Shoulder and elbow group mean joint angle kinematics (green) presented with EMG activity (black) on the secondary axis [biceps brachii, middle deltoid, trapezius lower (TL), trapezius middle (TM dotted), pectoralis major (PM), latissimus dorsi (LM dotted)]. The dashed vertical line represents gait cycle division between stance (from 0 to 50%) and swing (from 50 to 100%).

has returned from its most abducted position in the gait cycle and adducts to a more neutral position that is maintained for most of the gait cycle (**Figure 3**). Rectus abdominis has been presented with thorax flexion-extension in **Figure 5**, which shows muscle activity patterns of the upper body during the gait cycle. Both thorax flexion and extension had no clear peak that was consistent across the group of athletes (**Figure 2**), most likely because the angle changed little during the stride (**Figure 3**). The activation magnitude of rectus abdominis fluctuates between 32 and 52% of the gait cycle. Slightly increased rectus abdominis activity occurs at 20%, 40%, and then again between 70 and 90% of the gait cycle. Similar to rectus abdominis, consistent external oblique activation is present throughout the gait cycle that is relatively low but increased in preparation for initial contact during terminal swing (**Figure 5**).

DISCUSSION

The aim of this study was to analyze the link between the upper and lower body movements during racewalking. The inclusion of spatiotemporal variables is important given that there is a specific rule defining the motion, and therefore any interpretation of the role of upper body movement should take these into account. Flight time is of particular interest to racewalkers and coaches given that World Athletics Rule 54.2 states that no visible loss of contact should occur. Each participant incurred a flight phase to some extent, and as the group's mean flight time was 0.048 s, the racewalkers in this study were thus individually below or only just above the detectable threshold of 0.045 s (Hanley et al., 2019). Longer flight times were associated with stride length ratio and flight distance ratio, which in normal running would be of benefit

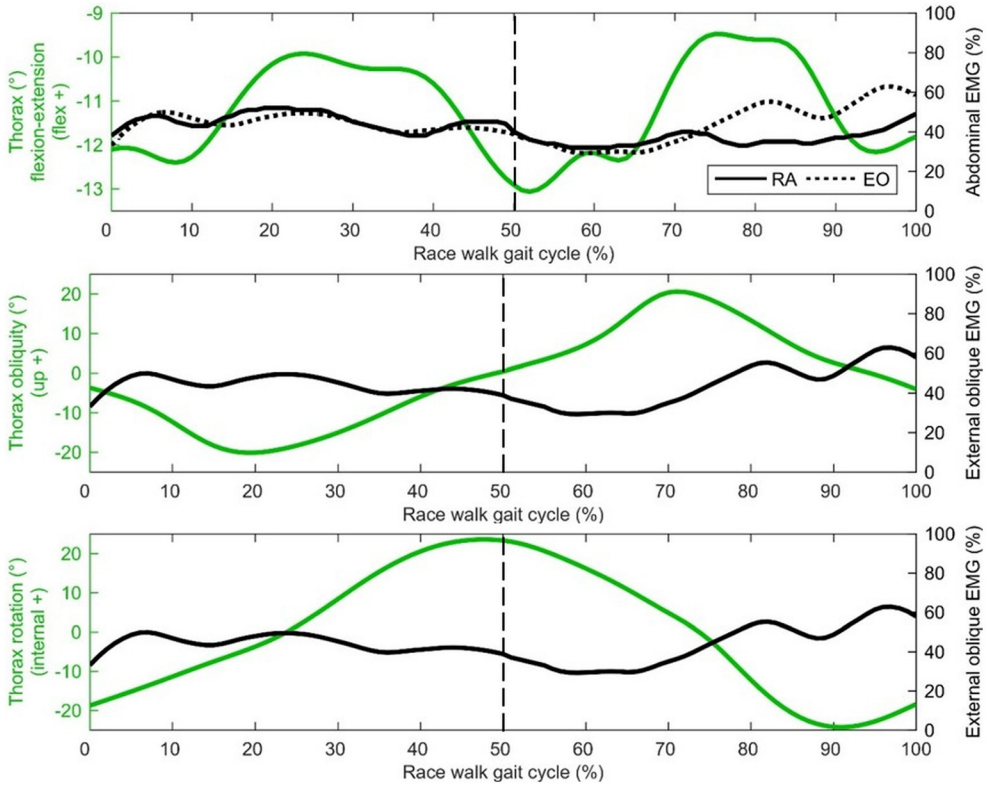

FIGURE 5 | Thorax group mean joint angle kinematics (green) presented with EMG activity (black) on the secondary axis [rectus abdominis (RA), external oblique (EO dotted)]. The dashed vertical line represents gait cycle division between stance (from 0 to 50%) and swing (from 50 to 100%).

but in racewalking must be restrained to avoid detection by the judges. We should note that flight distance is not separate from stride length, but one component of it, and so a reduction or absence of flight distance will reduce stride length and, most likely, speed. Because the racewalker cannot use a long flight phase to increase stride length, other movements are exaggerated to try to achieve this (Pavei and La Torre, 2016). For example, racewalkers use a greater range of pelvic rotation about the vertical axis than normal walking (Cairns et al., 1986). This theoretically helps the racewalker maintain a narrow step width to help increase step length (Murray et al., 1983), and although there were no correlations between pelvic motion and speed, a positive relationship was observed between peak pelvic external rotation and stride length ratio showing that this movement does achieve this goal in practice (Pavei and La Torre, 2016), and should continue to be encouraged by coaches. Peak external pelvic rotation occurs at toe-off, and therefore increases the foot behind distance component of stride length, and occurs at the same time as the ipsilateral shoulder's peak flexion position (in front of the body), showing that this movement helps to counterbalance the lower limb's movement (Pavei and La Torre, 2016).

In terms of shoulder musculature, peak pectoralis major activation occurred as the shoulder moved to its most hyperextended behind the body at initial contact, whereas latissimus dorsi activity peaked at toe-off, occurring as the shoulder and elbow reach peak flexion. Although we did not measure joint powers because we did not have GRF data for all strides, it is probable that these muscles were absorbing energy during these respective phases and effectively working to decelerate backward and forward arm swing in preparation for the reverse movement. The role of these muscles might therefore be one of elastic energy storage and return, and a more forced arm swing that has been recommended by coaches (e.g., Payne and Payne, 1981) does not appear to occur in practice; indeed, given that racewalking is an endurance event, it could be more important that racewalkers develop upper body musculature fatigue resistance (as in the lower limb) to maintain correct technique. Research has shown that the middle deltoid and supraspinatus have nearly equal cross sectional areas and moment arms for shoulder abduction (within 10–12% of each other), and each muscle produces a roughly equal share of the total abduction torque at the shoulder joint (Neumann, 2017). It could be that the supraspinatus had greater muscle activation during racewalking but, as it is located deep to the trapezius, is not suitable for surface EMG measurement. Nonetheless, it is clear that the shoulder muscles (acting in the sagittal and frontal planes) have important roles in racewalking to achieve fast movements, and the development of an optimal range of movement (with requisite strength and conditioning training)

that balances well the lower body is recommended. This might be particularly important with regard to restraining shoulder hyperextension during late swing given larger magnitudes were associated with reduced stride frequencies.

The middle deltoid muscle was most active during midstance as the shoulder was abducted during the forward arm swing. The middle and lower trapezius muscles were also at their most active during this phase, possibly as they function to retract and depress the shoulder girdle, corresponding with peak thorax obliquity (right down) and pelvic obliquity (right up); this combination of movements contributes to the S-shape of the vertebral column during stance that is a hallmark of racewalking (Murray et al., 1983). With regard to the counterbalancing movements of the thorax, the consistently low activation profile of the rectus abdominis is suggestive of a constant isometric action to maintain upper body posture throughout the racewalking gait cycle. It was noticeable from **Figures 2**, **3** that for many movements, there was no consistent pattern for all athletes, which was most likely because the range of motion was quite small (and peak magnitudes were therefore not that discernable). The similar lack of large peak values for the EMG data (i.e., few values close to 100%) was indicative of how athletes tended to attain peak muscle activity values at different phases of the movement. Other authors have noted very low and variable activity throughout the normal walking gait cycle (Cromwell et al., 2001; Anders et al., 2007). Previous research found no rectus abdominis activity or no clear relationship with lumbo-pelvic motion during normal walking (Mann et al., 1986; Callaghan et al., 1999), but high activity in association with initial contact in running (Mann et al., 1986). When comparing variables such as duty factor, CM energy and vertical GRF magnitude, racewalking is closer to running (Cavagna and Franzetti, 1981; Pavei et al., 2014, 2017, 2019) than to normal walking, but nonetheless the thorax kinematics in our study of racewalkers were not enough to elicit the muscle activity magnitudes observed in running (Pontzer et al., 2009). In studies where rectus abdominis muscle activity has been monitored alongside hip flexor activation, it has been noted that activity of these muscle sites is somewhat synchronized (Neumann, 2017). At slower walking speeds, Anders et al. (2007) noted similar continuous activation profiles between rectus abdominis and the external obliques, but at faster speeds a mixed phasic activation pattern was recorded.

In the present study, slightly greater external oblique activation occurred during early stance phase and terminal swing, similar to the patterns presented by Anders et al. (2007), and the rectus abdominis activation pattern noted above. With respect to thorax kinematics, the external oblique muscle activation pattern appears to follow rotation in the transverse plane, with greater activity observed with external thorax rotation. Therefore, external oblique activity is mostly isometric, with eccentric muscle actions when the thorax is high and externally rotated. Murray et al. (1983) noted increased activity of the lateral abdominal muscles was related to reversals of the extremes of the lateral trunk flexion associated with racewalking. Furthermore, the increased activity of the abdominal muscles could limit the amount of pelvic tilt, which was found to be one of the few kinematics not in excess of normal walking when racewalking (Murray et al., 1983), and which did not have a distinct timing for its peak across all athletes in the present study. Greater external oblique activation at terminal swing has also been noted in response to perturbations during normal walking (Stokes et al., 2017). From a coaching perspective, Drake (2003) suggested that a lack of core stability results in sub-optimal hip flexion-extension and is a contributing factor to illegal knee motion or visible flight phase technical errors, although our data were not conclusive in showing whether this was the case; there were no correlations between thorax movements and flight time, although the sample studied were homogenous in that they were elite athletes and typically engaged in abdominal strength exercises.

Given the relatively low percentage of muscle activation from the biceps brachii throughout the gait cycle, it would appear that little muscular action produces the cyclical flexion-extension pattern at the elbow and instead this could largely be a passive motion resulting from the angular momentum of the lower body (somewhat similar to the shoulder), albeit with some muscular work needed to overcome friction. Furthermore, biceps brachii activity is lowest when elbow flexion is greatest. It could be that the role of the biceps brachii is to maintain elbow flexion throughout the arm swing that might be compromised because of gravity, especially on the downswing where a noticeable burst of activation occurs. This activation begins as the elbow is extending relatively quickly compared with the rest of the elbow flexion-extension trace. An energy absorbing action is therefore performed by the biceps brachii to initiate the burst in activity just after 60% of the gait cycle. This action then changes to isometric, whereas elbow flexion angle remains relatively constant in preparation for initial contact between 90 and 100% of the gait cycle. This looks to continue after initial contact where muscle activation and elbow flexion is sustained from initial contact to ∼25% of the gait cycle, which could be to flex the shoulder as Murray et al. (1983) also showed a burst in biceps brachii activity immediately after initial contact that they believed initiated the forward thrust of the arm swing. Indeed, the lack of considerable differences in EMG descriptions between the present study and that of Murray et al. (1983) is indicative of how little the racewalking rule change (in 1995) affected muscle activity in the upper body. Racewalkers with smaller elbow angles in early swing when the elbow was most flexed had longer flight times, which can be beneficial for speed, but also lead to detectable flight times and maintaining a more extended position, and therefore greater arm moment of inertia, might be better. However, the mass of the forearm is so small, and as the movement of one arm is counterbalanced by the opposite movement of the contralateral arm, it is unlikely that it is the arm movement itself that causes these longer flight times; rather, the arm's movement might be symptomatic of other movements causing these actions. The arms' movements, therefore, might be a reaction rather than a cause. Indeed, the data showed that the athletes' elbows through flexion-extension while racewalking (Pavei and La Torre, 2016), rather than maintaining a set angle (e.g., of 90°) as recommended by coaches (Markham, 1989; Rogers, 2000), and this variance might help racewalkers reduce the duration of any flight phase

(which often occurs during early swing, when the elbow was most flexed).

With regard to potential limitations, it was assumed that elite racewalkers would be symmetrical as their well-trained gait has been found to show low asymmetry for the most important kinematic variables across racewalking speeds (Tucker and Hanley, 2020). All EMG data in the present study were collected for the right side only, in line with other studies that have measured muscle activity of the right lower limb in elite racewalkers (Hanley and Bissas, 2013) and normal walking and running (Saunders et al., 2005). An alternative approach might have been to pool left and right side data together. Where this method has been used, a common limitation was acknowledged in that pooling data smooths out individual participation and that these overall means cannot be perceived as a true profile of muscle activity. From a practical perspective, the number of EMG sensors available was limited to eight, and so increasing the number and different functions of muscles tested was prioritized over bilateral analysis. It is also accepted that analysis of movement in the laboratory environment might not be representative of racewalking in competition. It was also decided in this study to use the maximum EMG value within each muscle for each individual as a basis to normalize their EMG data before averaging across the group; this might have led to difficulties in establishing distinct patterns of activation. An alternative approach could have been to normalize relative to maximum voluntary contraction (MVC), but this was considered too difficult to achieve for many of the muscles analyzed given the multiplanar movements of the joints they cross. However, the value of synchronized EMG and 3D motion capture analyses to coaches and athletes was considered to outweigh the ecological validity of competition data and provide an original contribution to the knowledge base of racewalking biomechanics. Furthermore, the laboratory approach of testing each participant individually one at a time meant that greater sample sizes could be included in the analysis to better represent the movements of world-class racewalkers. We included only one stride per participant (rather than the mean of the six good trials collected) to ensure that the trial included was not affected by the averaging process across multiple trials. However, this means the total number of strides analyzed was limited to 31 (one for each participant) and this might restrict the generalizability of our results.

CONCLUSIONS

This was the first study to analyze the effect of upper body movements on spatiotemporal variables and the activity of relevant muscles in elite racewalkers. The movements of the pelvic girdle were the most important in terms of optimizing key spatiotemporal variables, which is unsurprising given it articulates with the femur and functions as an origin for many lower limb muscles. Pelvic rotation was associated with longer foot behind ratio and hence stride length ratio, showing that this exaggerated movement in racewalking does compensate to some extent for restrained stride lengths, and should continue to be encouraged by racewalk coaches. As with all bipedal gaits, the arms have a purpose in balancing the lower limb's movements, although there was little evidence to support coaching recommendations that these should be particularly exaggerated. Indeed, elite racewalkers should be mindful of the elbow and shoulder movements used during arm swing: a larger range of shoulder swing movements was found to be associated with lower stride frequency, which could either indicate a shoulder motion that drives a longer stride time, or a lower stride frequency that allows for a longer shoulder swing. In either case, such a movement can be beneficial to some extent but can also lead to visible loss of contact. When taken into consideration with the kinematic data, it is clear that the shoulder muscles mostly absorb energy when racewalking; therefore, completing arm exercises within a training program is encouraged. Other muscle actions, such as those of the abdominal muscles, had few distinct peaks and might therefore function isometrically to restrain excessive thorax movements. Although a comprehensive strength and conditioning program is recommended for racewalkers, coaches should bear in mind that it is an endurance event and resistance to fatigue might be more important than strength.

DATA AVAILABILITY STATEMENT

The raw data supporting the conclusions of this article will be made available by the authors, without undue reservation.

ETHICS STATEMENT

The studies involving human participants were reviewed and approved by Carnegie School of Sport Research Ethics Committee. The patients/participants provided their written informed consent to participate in this study.

AUTHOR CONTRIBUTIONS

HG conducted the data collection and analyses and created the figures and tables. All authors conceptualized and designed the study, wrote the manuscript, edited, critically revised, and approved the final version for submission.

ACKNOWLEDGMENTS

The authors would like to thank Prof. Athanassios Bissas for his contribution to the development of the study.

REFERENCES

Addison, B. J., and Lieberman, D. E. (2015). Tradeoffs between impact loading rate, vertical impulse and effective mass for walkers and heel strike runners wearing footwear of varying stiffness. *J. Biomech.* 48, 1318–1324. doi: 10.1016/j.jbiomech.2015.01.029

Anders, C., Wagner, H., Puta, C., Grassme, R., Petrovitch, A., and Scholle, H. C. (2007). Trunk muscle activation patterns during walking at different

speeds. *J. Electromyogr. Kinesiol.* 17, 245–252. doi: 10.1016/j.jelekin.2006.01.002

Bezodis, I. N., Kerwin, D. G., and Salo, A. (2008). Lower-limb mechanics during the support phase of maximum-velocity sprint running. *Med. Sci. Sports Exerc.* 40, 707–715. doi: 10.1249/MSS.0b013e318162d162

Cairns, M. A., Burdette, R. G., Pisciotta, J. C., and Simon, S. R. (1986). A biomechanical analysis of racewalking gait. *Med. Sci. Sports Exerc*. 18, 446–453. doi: 10.1249/00005768-198608000-00015

Callaghan, J. P., Patla, A. E., and McGill, S. M. (1999). Low back three-dimensional joint forces, kinematics, and kinetics during walking. *Clin. Biomech.* 14, 203–216. doi: 10.1016/S0268-0033(98)00069-2

Cavagna, G. A., and Franzetti, P. (1981). Mechanics of competition walking. *J. Physiol*. 315, 243–251. doi: 10.1113/jphysiol.1981.sp013745

Cazzola, D., Pavei, G., and Preatoni, E. (2016). Can coordination variability identify performance factors and skill level in competitive sport? The case of race walking. *J. Sport Health Sci.* 5, 35–43. doi: 10.1016/j.jshs.2015.11.005

Chuang, T. D., and Acker, S. M. (2019). Comparing functional dynamic normalization methods to maximal voluntary isometric contractions for lower limb EMG from walking, cycling and running. *J. Electromyogr. Kines*. 44, 86–93. doi: 10.1016/j.jelekin.2018.11.014

Clarys, J. P., and Cabri, J. (1993). Electromyography and the study of sports movements. *J. Sports Sci*. 11, 379–448. doi: 10.1080/02640419308730010

Cohen, J. (1992). A power primer. *Psychol. Bull.* 112, 155–159. doi: 10.1037/0033-2909.112.1.155

Cromwell, R. L., Aadland-Monahan, T. K., Nelson, A. T., Stern-Sylvestre, S. M., and Seder, B. (2001). Sagittal plane analysis of head, neck, and trunk kinematics and electromyographic activity during locomotion. *J. Orthop. Sports Phys. Ther.* 31, 255–262. doi: 10.2519/jospt.2001.31.5.255

Cronin, N. J., Hanley, B., and Bissas, A. (2016). Mechanical and neural function of triceps surae in elite racewalking. *J. Appl. Physiol.* 121, 101–105. doi: 10.1152/japplphysiol.00310.2016

Dempster, W. T. (1955). *Space Requirements for the Seated Operator, Geometrical, Kinematic, and Mechanical Aspects of the Body With Special Reference to the Limbs. Technical Report (TR-55-159)*. Dayton, OH: Wright-Patterson Air Force Base. Available online at: https://deepblue.lib.umich.edu/handle/2027.42/4540 (accessed June 23, 2020).

Drake, A. (2003). Developing race walking technique. *Coach* 17, 32–36.

Gomez-Ezeiza, J., Santos-Concejero, J., Torres-Unda, J., Hanley, B., and Tam, N. (2019). Muscle activation patterns correlate with race walking economy in elite race walkers: a waveform analysis. *Int. J. Sports Physiol. Perform*. 14, 1250–1255. doi: 10.1123/ijspp.2018-0851

Goudriaan, M., Jonkers, I., van Dieen, J. H., and Bruijn, S. M. (2014). Arm swing in human walking: what is their drive? *Gait Posture* 40, 321–326. doi: 10.1016/j.gaitpost.2014.04.204

Hanavan, E. P. Jr. (1964). *A Mathematical Model of the Human Body. Technical Report (AMRL-63-102)*. Dayton, OH: Wright-Patterson Air Force Base. Available online at: https://pubmed.ncbi.nlm.nih.gov/14243640/ (accessed June 23, 2020).

Hanley, B., and Bissas, A. (2013). Analysis of lower limb internal kinetics and electromyography in elite race walking. *J. Sports Sci*. 31, 1222–1232. doi: 10.1080/02640414.2013.777763

Hanley, B., and Bissas, A. (2017). Analysis of lower limb work-energy patterns in world-class race walkers. *J. Sports Sci*. 35, 960–966. doi: 10.1080/02640414.2016.1206662

Hanley, B., Bissas, A., and Drake, A. (2011). Kinematic characteristics of elite men's and women's 20 km race walking and their variation during the race. *Sports Biomech*. 10, 110–124. doi: 10.1080/14763141.2011.569566

Hanley, B., Bissas, A., and Drake, A. (2013). Kinematic characteristics of elite men's 50 km race walking. *Eur. J. Sport Sci.* 13, 272–279. doi: 10.1080/17461391.2011.630104

Hanley, B., Tucker, C. B., and Bissas, A. (2019). Assessment of IAAF racewalk judges' ability to detect legal and non-legal technique. *Front. Sports Act. Living* 1:9. doi: 10.3389/fspor.2019.00009

Hermens, H. J., Freriks, B., Disselhorst-Klug, C., and Rau, G. (2000). Development of recommendations for SEMG sensors and sensor placement procedures. *J. Electromyogr. Kinesiol.* 10, 361–374. doi: 10.1016/S1050-6411(00)00027-4

Herr, H., and Popovic, M. (2008). Angular momentum in human walking. *J. Exp. Biol.* 211, 467–481. doi: 10.1242/jeb.008573

Hoga-Miura, K., Ae, M., Fujii, N., and Yokozawa, T. (2016). Kinetic analysis of the function of the upper body for elite race walkers during official men 20 km walking race. *J. Sports. Med. Phys. Fitness* 56, 1147–1155.

Hopkins, J. (1978). The Mexican race walkers. *Coach* 12, 10–14.

Hopkins, J. (1981). The biomechanics of race walking. *Athlet. Coach* 15, 22–26.

Hunter, J. P., Marshall, R. N., and McNair, P. J. (2004). Interaction of step length and step rate during sprint running. *Med. Sci. Sport Exerc*. 36, 261–271. doi: 10.1249/01.MSS.0000113664.15777.53

Knicker, A., and Loch, M. (1990). Race walking technique and judging—the final report to the International Athletic Foundation research project. *New Stud. Athlet*. 5(3), 25–38.

Mann, R. A., Moran, G. T., and Dougherty, S. E. (1986). Comparative electromyography of the lower extremity in jogging, running, and sprinting. *Am. J. Sports Med.* 14, 501–510. doi: 10.1177/036354658601400614

Markham, P. (1989). *Race Walking*. Birmingham: British Amateur Athletic Board.

Murray, M. P., Guten, G. N., Mollinger, L. A., and Gardner, G. M. (1983). Kinematic and electromyographic patterns of Olympic race walkers. *Am. J. Sports Med.* 11, 68–74. doi: 10.1177/036354658301100204

Neumann, D. (2017). *Kinesiology of the Musculoskeletal System: Foundations for Rehabilitation, 3rd Edn*. St Louis, MO: Elsevier.

O'Connor, C. M., Thorpe, S. K., O'Malley, M. J., and Vaughan, C. L. (2007). Automatic detection of gait events using kinematic data. *Gait Posture* 25, 469–474. doi: 10.1016/j.gaitpost.2006.05.016

Padulo, J., Annino, G., Tihanyi, J., Calcagno, G., Vando, S., Smith, L., et al. (2013). Uphill racewalking at iso-efficiency speed. *J. Strength Cond. Res.* 27, 1964–1973. doi: 10.1519/JSC.0b013e3182752d5e

Pavei, G., Cazzola, D., La Torre, A., and Minetti, A. E. (2014). The biomechanics of race walking: literature overview and new insights. *Eur. J. Sport Sci.* 14, 661–670. doi: 10.1080/17461391.2013.878755

Pavei, G., Cazzola, D., La Torre, A., and Minetti, A. E. (2019). Race walking ground reaction forces at increasing speeds: a comparison with walking and running. *Symmetry* 11:873. doi: 10.3390/sym11070873

Pavei, G., and La Torre, A. (2016). The effects of speed and performance level on race walking kinematics. *Sports Sci. Health* 12, 35–47. doi: 10.1007/s11332-015-0251-z

Pavei, G., Seminati, E., Cazzola, D., and Minetti, A. E. (2017). On the estimation accuracy of the 3D body center of mass trajectory during human locomotion: inverse vs. forward dynamics. *Front. Physiol.* 8:129. doi: 10.3389/fphys.2017.00129

Payne, A. H., and Payne, R. (1981). *The Science of Track and Field Athletics*. London: Pelham Books.

Pontzer, H., Holloway, J. H., Raichlen, D. A., and Lieberman, D. E. (2009). Control and function of arm swing in human walking and running. *J. Exp. Biol.* 212, 523–534. doi: 10.1242/jeb.024927

Rodger, M. W., Young, W. R., and Craig, C. M. (2013). Synthesis of walking sounds for alleviating gait disturbances in Parkinson's disease. *IEEE Trans. Neural Syst. Rehabil. Eng.* 22, 543–548. doi: 10.1109/TNSRE.2013.2285410

Rogers, J. L. (2000). *USA Track and Field Coaching Manual*. Champaign, IL: Human Kinetics.

Saunders, S. W., Schache, A., Rath, D., and Hodges, P. W. (2005). Changes in three dimensional lumbo-pelvic kinematics and trunk muscle activity with speed and mode of locomotion. *Clin. Biomech.* 20, 784–793. doi: 10.1016/j.clinbiomech.2005.04.004

Stokes, H. E., Thompson, J. D., and Franz, J. R. (2017). The neuromuscular origins of kinematic variability during perturbed walking. *Sci. Rep*. 7, 808–817. doi: 10.1038/s41598-017-00942-x

Tucker, C. B., and Hanley, B. (2020). Increases in speed do not change gait symmetry or variability in world-class race walkers. *J. Sports Sci*. 38, 2758–2764. doi: 10.1080/02640414.2020.1798730

Villa, F. (1990). NSA photosequences 12 and 13: race walking. *New Stud. Athlet.* 5, 63–68.

Wilke, C. O. (2017). *ggridges: ridgeline plots in'ggplot2' R package, Version 0.4.1, 1-27*. Vienna: R Foundation for Statistical Computing.

Winter, D. A. (2005). *Biomechanics and Motor Control of Human Movement, 3rd Edn*. Hoboken, NJ: John Wiley and Sons.

World Athletics (2019). *C2.1—Technical Rules*. Monte Carlo: World Athletics.

Zeni, J. A., Richards, J. G., and Higginson, J. S. (2008). Two simple methods for determining gait events during treadmill and overground walking using kinematic data. *Gait Posture* 27, 710–714. doi: 10.1016/j.gaitpost.2007.07.007

Conflict of Interest: The authors declare that the research was conducted in the absence of any commercial or financial relationships that could be construed as a potential conflict of interest.

Advantages of publishing in Frontiers

OPEN ACCESS
Articles are free to read for greatest visibility and readership

FAST PUBLICATION
Around 90 days from submission to decision

HIGH QUALITY PEER-REVIEW
Rigorous, collaborative, and constructive peer-review

TRANSPARENT PEER-REVIEW
Editors and reviewers acknowledged by name on published articles

Frontiers
Avenue du Tribunal-Fédéral 34
1005 Lausanne | Switzerland

Visit us: www.frontiersin.org
Contact us: frontiersin.org/about/contact

REPRODUCIBILITY OF RESEARCH
Support open data and methods to enhance research reproducibility

DIGITAL PUBLISHING
Articles designed for optimal readership across devices

FOLLOW US
@frontiersin

IMPACT METRICS
Advanced article metrics track visibility across digital media

EXTENSIVE PROMOTION
Marketing and promotion of impactful research

LOOP RESEARCH NETWORK
Our network increases your article's readership